AN ABSTRACT OF THE DISSERTATION OF

Jeffrey W. Krause for the degree of Doctor of Philosophy in Oceanography presented on April 18, 2008.
Title: Silicon Biogeochemistry in the Open-ocean Surface Waters: Insights from the Sargasso Sea and Equatorial Pacific

Abstract approved:

_____

David M. Nelson

Diatoms are a ubiquitous group of plankton responsible for 20-40% of oceanic primary production, and a higher fraction of organic matter export to the ocean interior. Diatoms actively transport dissolved inorganic silicon into their cells, and through the process of silicification (i.e. biogenic silica production) they build tough and intricate shells, known as frustules. With a global distribution and the ability to persist in high numerical abundances, diatoms dominate the biological cycling of Si in the oceans. The biogeochemical cycling of Si has been well studied in the coastal ocean, specifically in upwelling regions where diatoms are generally the dominant phytoplankton group. However, much less is known about the role diatoms play in the open ocean; which comprises the vast majority of the oceanic surface area. Outside of the Southern Ocean, only 11 studies (prior to 2003) directly examined surface-water Si biogeochemistry in the open ocean. Current knowledge about Si biogeochemistry in the open ocean suffers from what can only be described as gross under-sampling. This dissertation reports on the surface-water Si biogeochemistry in two open-ocean regions: the northwestern Sargasso Sea and the eastern equatorial Pacific. The three research chapters are linked by the examination of spatial or temporal variability in surface-water Si biogeochemistry. Chapters 2 and 4 examine scales of temporal variability in Si biogeochemistry in the Sargasso Sea. The results demonstrate that biogenic silica concentrations, and presumably Si biogeochemical processes, vary on

daily, seasonal, multi-year (e.g. ~3-4 years), and decadal time scales. In Chapter 3 data were gathered over a ~2.6×10^6 km^2 area (i.e. larger than the Bering Sea) in the equatorial Pacific. Within that area biogenic silica production showed little spatial or temporal variability. Additionally, the estimated contribution to new production (productivity supporting the export of organic matter to the ocean interior) by diatoms in this region was 4-10 times higher than the diatom contribution to total autotrophic biomass.

Silicon Biogeochemistry in the Open-Ocean Surface Waters: Insights from the Sargasso Sea and Equatorial Pacific

by
Jeffrey W. Krause

A DISSERATION

submitted to

Oregon State University

in partial fulfillment of
the requirement for the
degree of

Doctor of Philosophy

Presented April 18, 2008
Commencement June 15, 2008

Doctor of Philosophy dissertation of Jeffrey W. Krause presented on April 18, 2008.

APPROVED:

_____

Major Professor, representing Oceanography

_____

Dean of the College of Oceanic and Atmospheric Sciences

_____

Dean of the Graduate School

I understand that my dissertation will become part of the permanent collection of Oregon State University libraries. My signature below authorizes release of my dissertation to any reader upon request.

_____

Jeffrey W. Krause, Author

ACKNOWLEDGEMENTS

I am extremely fortunate to have a vast network of support; I take delight in mentioning individuals by name:

- Leah, you have been immensely supportive and loving during my graduate studies. Your personality and work ethic continually inspire me to strive for my goals, even those which seem too far to reach. Thank you so much for suffering the intolerable cruelty of listening to my rants about how silicon is the greatest element and diatoms are the greatest phytoplankton group. Most of all, thank you for your love. Your many personal sacrifices have allowed me to reach my goals, and I thank you with all my heart.
- Dave Nelson, you have been an amazing mentor. During my studies you have been supportive, and allowed me to find my own way. At the same time you showed eagerness to hear ideas and interpretations, and took the time to help me grasp many concepts. Thank you for exercising both genuine concern and constructiveness in your detailed feedback. Additionally, thank you for making time for me without notice; allowing short Q&A sessions to balloon into 2 or 3 hour discussions. Those dialogues have been a highlight of my graduate career, while also helping me develop the skills to have edifying and progressive scientific discussion.
- Mike Lomas, you have been like a co-advisor during my graduate career. You always made time regardless of geographic or time constraints, and you have the unique talent to open my eyes to different perspectives. While in your lab, you not only put up with my subconscious mantra "divide and conquer the bench-top and storage space," but you fostered my desire explore new methods even though I killed your diatom cultures and caused you more work. Thank you for everything.
- Ricardo Letelier, Pete Strutton, Tim Cowles, and Peter Bottomley. Ricardo and Pete, you both gave me fresh perspectives and constructive comments. Pete, you have the fastest email response time of anybody I have met! Ricardo, your support during this final year allowed me to thoroughly develop my dissertation. Tim, you stepped up and provided very detailed and useful feedback in a very short amount of time, thank you for the help. Peter, you were very straightforward and I thank you for your patience and assistance during the process.

- Erica Schaefer and Stephanie Jaeger, you two bailed for real jobs, but I am very fortunate to have shared your company for three years. Thank you for your friendships.
- Margaret Sparrow and Julie Arrington are the techs that I questioned most often. Thanks to both of you for sharing your wealth of practical knowledge.
- Kelly Benoit-Bird, Charlie Miller, Fred Prahl, and Yvette Spitz have always been there for little odds/ends, questions, and great conversation. Kelly and Charlie, I appreciate how both of you routinely checked up on me after Dave moved to France; thank you for being genuine.
- The BIOS researchers: Amanda, Deb, Jonathan, Kevin, Lilia, Rod and others have been of tremendous assistance.
- Mentors that shaped my scientific path before COAS:
  - Russ Quackenbush (King's High School) introduced me to marine science and instilled the desire to study the ocean.
  - Roland Anderson (Seattle Aquarium) introduced me to research on marine organisms.
  - Hans Jakobsen (Shannon Point Marine Center) introduced me to oceanography, and got me hooked on studying things I could not see with my eye.
  - Chris Gobler (Southampton College) solidified my desire to pursue biological oceanography. He helped prepare me for graduate work by exposing me to different methodology, and being an excellent example of work ethic.
- Last but not least, a very loving immediate family including Kristi and Bob, Kenny, Jessica and Todd. You all have been there for me since day one. Thank you for your love and support.

CONTRIBUTION OF AUTHORS

Dr. David M. Nelson (committee chair) provided invaluable discussion and critique of the manuscripts found in chapters 2 through 4. Dr. Nelson is (or will be) a co-author on all three submitted manuscripts from these chapters. Dr. Michael W. Lomas (Bermuda Institute for Ocean Sciences) has been instrumental in discussion and critique of the scientific ideas. Dr. Lomas is a co-author for submitted manuscripts in chapter 2 and 4. Dr. Mark A. Brzezinski (University of California at Santa Barbara) provided assistance in data interpretation and constructive critique; he will be a co-author for the submitted manuscript from chapter 3.

TABLE OF CONTENTS

TABLE OF CONTENTS (Continued)

TABLE OF CONTENTS (Continued)

LIST OF FIGURES

LIST OF FIGURES (Continued)

LIST OF FIGURES (Continued)

LIST OF TABLES

DEDICATED TO:

Larry & Kathleen Krause

You have provided unconditional love and support my entire life. You continuously give so much of yourselves, and I wish to extend my deepest gratitude for your personal sacrifices and investment in my life and education. I love you both with all my heart.

Silicon Biogeochemistry in the Open-ocean Surface Waters: Insights from the Sargasso Sea and Equatorial Pacific

1. Introduction

"Nature composes some of her loveliest poems for the microscope and the telescope."
Theodore Roszak (b.1933- , American Professor), Where the Wasteland Ends, 1972

1.1 Diatoms in the global ocean

Diatoms are a ubiquitous phytoplankton group in both freshwater and marine ecosystems, and play a significant role in the oceanic cycling of nutrients and organic matter. Their estimated contribution to global oceanic primary production ranges between 20 and 40% (Nelson et al. 1995, Raven and Waite 2004), and their role in biological particle export from the upper ocean is estimated to be at least as large (Michaels and Silver 1988, Honjo et al. 1995, Buesseler 1998, Boyd and Trull 2007, Honjo et al. 2008). Diatoms have a cellular requirement for silicon, which they satisfy by taking up dissolved Si from seawater. At ocean pH of ~8.1 – 8.2 orthosilicic acid ($Si(OH)_4$) is the predominant form of Si in solution, with other forms (i.e. $SiO(OH)_3^-$, $SiO(OH)_2^{2-}$, $Si_4O_6(OH)_6^{2-}$) comprising < 5% of the total (Stumm and Morgan 1996). It is theorized that diatom Si transporters have evolved to utilize orthosilicic acid ($Si(OH)_4$) as their main source of Si (Del Amo and Brzezinski 1999). Diatoms polymerize $Si(OH)_4$ intracellularly to produce hydrated amorphous silica ($SiO_2 \cdot nH_20$, referred to hereafter as biogenic silica, $bSiO_2$), which is used to build intricate shells, known as frustules (Figure 1.1, see Martin-Jézéquel et al 2000 and references therein).

Building siliceous structures is not unique to diatoms. Oceanic groups using Si for similar purposes include radiolarians, silicoflagellates, choanoflagellates, and hexactinellid sponges; additionally, there are many groups of terrestrial flora and fauna that also use Si for structural purposes (Simpson and Volcani 1981, Raven 1983, Alexandre et al. 2002, Conley 2002, De La Rocha 2003). Diatoms first appeared in the late Cretaceous (Falkowski et al. 2004) and are thus a relatively young silicifying group, as radiolarians and hexactinellid sponges appeared in the Cambrian (Siever

1991, Schubert et al. 1997, Maldonado et al. 1999, Racki and Cordey 2000, Kidder and Irwin 2001).

Diatom frustules are composed of two valves of slightly different sizes; with the terminus of the smaller valve fitting into the larger valve. To overcome the challenges to reproduction presented by a rigid siliceous frustule, diatoms have adapted to use both asexual and sexual reproduction (Figure 1.1). Each asexual cell division results in one cell of equal size to the parent while the other is smaller. Continuing this trend of would lead to a decrease in the mean population size with time. Thus, at some critical size, diatoms will reproduce sexually and develop an auxospore, which allows the cell size to be reset to that of the original parent cell.

The rate at which diatom take up $Si(OH)_4$ (this rate is often denoted as V) depends on its extracellular concentration ($[Si(OH)_4]$) in a manner describable by a hyperbolic Michaelis-Menten function (Paasche 1973):

$$V = V_{MAX} [Si(OH)_4] / (K_S + [Si(OH)_4])$$

where V_{MAX} represents the maximum uptake rate at very high $[Si(OH)_4]$ and K_S the $[Si(OH)_4]$ at which V is limited to $V_{MAX}/2$. Low $[Si(OH)_4]$ thus limits rates of Si uptake (e.g. Martin-Jézéquel et al. 2000 and references therein) and unlike other marine planktonic silicifiers, Si limitation in diatoms can dramatically impact their physiology and growth.

Harrison et al. (1977) showed a major difference in diatoms grown in Si-replete conditions versus grown at low $[Si(OH)_4]$. The Si-depleted diatoms had frustules which were noticeably (i.e. visibly) less silicified, indicating that under Si limitation diatoms can be decrease their Si per cell and survive with a less-silicified frustule. Additionally, under Si limitation the diatom species *Thalassiosira weissflogii*, *Cylindrotheca fusiformis* and *Chaetoceros simplex* have been observed to increase generation times ~2–5x versus generation times under Si-replete conditions (Brzezinski et al. 1990, Brzezinski 1992, see also Martin-Jézéquel et al. 2000 for review). This response in generation time demonstrates that diatoms also will retard growth rates in response to Si-limitation. In Si-uptake experiments, Paasche (1973) showed that K_S for *Skeletonema costatum* (the most efficient of several diatoms studied) was only ~1/4 that for *Thalassiosira decipiens* (the least efficient). These

species differences led Paasche to theorize that changes in [$Si(OH)_4$] during a diatom bloom may be a mechanism leading to species succession.

The first record of diatoms being observed was by an unknown person who communicated a paper to the Royal Society of London, which was later published in its Philosophical Transactions (Round et al. 1990). Round et al. (1990) describe:

> In 1703 an English country gentleman looked with his simple microscope at roots of the pond-weed *Lemna* and '… saw adhering to them (and sometimes separate in the water) many pretty branches, compos'd [sic] of rectangular oblongs and exact squares'. His descriptions and diagrams, which probably refer to what we now call *Tabellaria flocculosa*, are the first certain records of a diatom… He came to the conclusion that the rectangles and squares (which he saw to be 'made up of two parallelograms joyn'd [sic] longwise') were plants, which was a remarkable judgment considering that all he had for comparison were macroscopic bryophytes, vascular plants and seaweeds, none of which have anything like the precise geometry of diatoms.

Diatom physiology has been thoroughly studied since the mid-19th century when "the perfection of lenses made the critical study of diatoms possible,(and) accurate descriptions were made" (Patrick 1940). In 1896 F. Schütt proposed that both the characteristics of the living cells and the differences in frustule morphology be used as taxonomic classification criteria (Schütt 1896, see also Patrick 1940). The intricate detail and construction of the diatom frustule, even in the most diminutive parts, has inspired awe and been put to practical use in fields ranging from the arts and humanities (Figure 1.1, Fields and Kontrovitz 1980, see http://www.diatoms.co.uk) to structural and materials sciences (Hamm et al. 2003, Lopez et al. 2005). Round et al. (1990) note "With their almost indestructible shells, conveniently small size, great variety and beauty, diatoms were perfectly 'pre-adapted' to their role as the objects of scientific fashion."

Ancient diatom frustules (sedimentary diatomaceous earth, DE) have been used for many purposes in the modern world. From personal experience, DE can be used as material for students to learn the proper techniques of microscopy, and also a material for students to visualize how biological matter transforms through geological time. DE is also used in swimming pool filters, as the myriad of tiny frustules create a siliceous matrix which allows for efficient particle capture, working much like a glass

fiber filter (e.g. Golden House Organics ®, for more information see http://www.ghorganics.com/DiatomaceousEarth.html). Similarly, the micro-siliceous (glass) structure is sharp enough to harm small insects and parasites without harming the hardier systems of larger animals and humans. Thus DE has uses as an insect control alternative to harmful chemicals (see previous citation), and also in a food grade variety for humans and large animals to kill intestinal parasites (e.g., Alternative Health & Herbs Remedies ®, see http://www.herbalremedies.com/diead6oz.html).

In the last 40 years several methodological advancements beyond traditional light microscopy have led to an increased understanding of diatom physiology and ecology, and to a greater appreciation of their biogeochemical importance. Some of these advances include: the use of stable and radioisotope Si tracers (Goering et al. 1973, Nelson and Goering 1977, Tréguer et al. 1991, Brzezinski and Phillips 1997), analytical distinction between biogenic and lithogenic (i.e. mineral) particulate silica (Paasche 1973, Nelson et al. 2001), measurement of diatom-specific pigment markers (Wright and Jeffrey 1987, Bidigare and Ondrusek 1996), the use of novel fluorescent dyes (Brzezinski and Conley 1994, Shimizu et al. 2001, Leblanc and Hutchins 2005), use of microscopy without visible light sources (Almqvist et al. 2001, Gebeshuber et al. 2003, Hildebrand et al. 2006), coupling diatom ecology and gene expression (Hildebrand and Dahlin 2000, Parker and Armbrust 2005), and the field coupling of a flow cytometer and pictorial imaging systems (Sosik and Olson 2007). While these technological advancements have led to improved understanding of the linkage of diatom physiology and ecology with cycling of nutrients in the upper ocean, this is still a research area in the early stages of its development.

1.2 Regional variability in diatom ecology and biogeochemistry

Diatoms' absolute Si requirement along with their high abundances, mean that they dominate the biogeochemical cycling of Si in the ocean. Given the diatoms' impact on oceanic primary productivity and global ocean particle export, it is important to understand the coupling between the cycling of Si and C in the ocean.

The diatoms' role in the cycling of organic matter and nutrients in coastal systems has been a topic of research for several decades (e.g. Allen 1934 and

references therein, Allen 1936). Coastal diatoms are very abundant in the water column (e.g. >10,000 cells per liter, >1 μmol l^{-1} [$bSiO_2$] c.f. Allen 1936, Nelson and Goering 1978, Brzezinski et al. 1997, Leblanc and Hutchins 2005), eclipsing open-ocean diatom abundances by one to three orders of magnitude (e.g. ≤1,000 cells per liter, ≤50 nmol l^{-1} [$bSiO_2$] c.f. Hulburt et al. 1960, Nelson and Brzezinski 1997). Coastal systems tend to be areas of high turbulence and high surface nutrient concentrations, both of which generally favor diatoms over other groups (Margalef 1997). Many physiological adaptations allow diatoms to thrive in these regions, including (but not limited to): nutrient storage capabilities (Dortch 1982), high maximum growth rates (Martin-Jézéquel et al. 2000 and references therein), and rapid and/or luxury nutrient uptake (Sunda and Huntsman 1995).

Despite a firm knowledge base on the role of diatom Si cycling in coastal regions, the quantitative importance of diatoms in the large open-ocean habitats that comprise most of the ocean is far less understood. In terms of Si cycling the most studied open-ocean region, by far, is the Southern Ocean. In contrast, current knowledge of open-ocean Si cycling in other regions has been shaped by remarkably few studies (Table 1.1). For example, the subtropical mid-ocean gyres constitute and estimated ~40% of the open ocean surface area (Nelson et al. 1995), but as of 2003 knowledge of Si cycling in the upper water column of those systems had been based on only five studies (Table 1.1). The problem of under-sampling, both temporally and spatially, in the open ocean is well recognized (Dickey et al. 2001, Schiermeier 2007); however, current knowledge of Si cycling suffers from gross under-sampling, especially outside the Southern Ocean.

This dissertation reports on the standing stock, vertical and lateral distributions, production and vertical export of $bSiO_2$ in the upper water column (0 – ~150 m) of two large and biogeochemically important open-ocean habitats, the northwestern Sargasso Sea and the eastern equatorial Pacific. These areas were chosen for the knowledge gaps in Si biogeochemistry (to be addressed later) and because the opportunity to get on research ships within these areas arose. As background to understanding diatom growth and Si biogeochemistry, the next two

sections provide an overview of the physical and biogeochemical properties of the northwestern Sargasso Sea and eastern equatorial Pacific, respectively.

1.2.1 Northwestern Sargasso Sea

The Sargasso Sea refers to the subtropical gyre within the North Atlantic Ocean, getting its name from the presence of the pelagic macro-alga *Sargassum* (Figure 1.2). While the Gulf Stream forms both its western and northern boundaries, the eastern and southern boundaries are difficult to define and vary with the complex recirculation of the Gulf Stream (Figure 1.2a, see Michaels and Knap 1996 and references therein). The island of Bermuda is located in the northwestern Sargasso Sea and due to its strategic location in the North Atlantic, has been occupied for civilian and military use since the 17th century. The sea floor south of Bermuda drops off quickly to 3000 – 4000 m (Figure 1.2b). This proximity of Bermuda to a deep, open-ocean habitat is incomparable for the staging and execution of open-ocean research in the North Atlantic, with the central ocean much more readily accessible than it is from any location in the eastern shorelines of the United States, or Canada. Thus, in addition to over 300 years of military presence, Bermuda and the northwestern Sargasso Sea have been a location of scientific investigation for over a century.

Most research in the open-ocean waters surrounding Bermuda has benefited from the presence of the Bermuda Biological Station for Research (BBSR), known as the Bermuda Institute for Ocean Sciences since 2006. The station was established in 1903 by the Harvard biologist E.L. Marks and in 1926 it became incorporated in the state of New York (USA, Michaels and Knap 1996). Another research pioneer in this region was W. Beebe, a naturalist from the New York Zoological Society. Aside from publications on the flora and fauna of Bermuda (Beebe 1932) one of his most noteworthy accomplishments was a journey he shared with O. Barton (an engineer) in 1934, at which time they made a record setting half-mile decent into the open-ocean abyss near Bermuda in a crude steel sphere (Beebe 1934).

Logistically, the opportunity to stage research so close to the open ocean has been a boon for ocean scientists. Michaels and Knap (1996) list eight different multi-

year time-series studies that have been initiated at or near Bermuda for the study of ocean biogeochemistry and atmospheric chemistry (for a more thorough history on time-series studies near Bermuda see Michaels and Knap 1996 and references therein). This has made the waters around Bermuda perhaps the single most studied open-ocean habitat on Earth (see Michaels and Knap 1996 and references therein, Steinberg et al. 2001 and references therein). One of the most influential studies in upper ocean biogeochemistry in the last 50 years, Dugdale and Goering (1967), introduced the concept of new production (to be discussed in more detail below) and included some data collected near one of the time-series sites in the Sargasso Sea (Hydrostation S, which will be discussed further below). While the current body of knowledge has led to a thorough understanding of many aspects of the biogeochemistry and oceanic physics in the northwestern Sargasso Sea, it is by no means exhaustive, and new questions are constantly arising. With this in mind, I will discuss the basic character of the Sargasso Sea as it pertains to the general autotrophic community and more specifically diatoms:

The northwestern Sargasso Sea is characterized by strong thermal stratification throughout most of the year (Figure 1.3). During periods of prolonged stratification the lack of physical mixing cuts off the supply of deep, nutrient-rich water into the euphotic zone (i.e. the vertical layer where light intensities remain high enough to support net photosynthesis); this pushes the autotrophic community towards nutrient limitation (Figure 1.3). Concentrations of the macronutrients NO_3^-, NH_4^+, HPO_4^{2-} are chronically low and generally near (or below) the detection limits of conventional colorimetric analyses in Sargasso Sea surface waters, under stratified conditions (see Lipschultz 2001, Steinberg et al. 2001 and references therein); while not at detection limits, surface-layer $[Si(OH)_4]$ is typically 0.7 – 0.9 μM, among the lowest persistent surface values in the global ocean (Brzezinski and Nelson 1995). In this physical/chemical environment nutrient limitation regulates biomass; therefore, chlorophyll a concentrations (chl-a, proxy for total autotrophic biomass) are lower and generally deeper in the water column than chl-a in coastal systems (Figures 1.3, 1.4). Additionally, rates of primary and new production are low in the Sargasso Sea

compared to other oceanic regions (Eppley and Peterson 1979, Steinberg et al. 2001, Lipschultz et al. 2002).

Dugdale and Goering (1967) defined new production as the primary production, in units of nitrogen (opposed to carbon), supported by nitrogen from outside sources (predominantly NO_3^- from deep water). This is in contrast to regenerated production which is primary production fueled by nutrients recycled within the upper ocean (primarily NH_4^+ from metabolic waste and recycling pathways). Dugdale and Goering's concept is important because production which is not recycled within the euphotic zone, i.e. new production, can be utilized by higher trophic levels (e.g. fish) or transported to the deep ocean by particle export. In the Sargasso Sea the *f*-ratio (ratio of new production to total primary production) is typically ~0.10 (Eppley and Peterson 1979, Lipschultz et al. 2002). This is very low compared to coastal and upwelling systems (~0.3–0.5, Eppley and Peterson 1979); indicating that in the Sargasso Sea recycling pathways keep limiting nutrients (e.g. N) within the system through several cycles of uptake and regeneration before they are lost to the deep ocean via particle export.

During late fall and winter, thermal stratification of the upper water column begins to erode in latitudes generally >30°N. This breakdown allows for the mixing of deeper, more nutrient-rich, water closer to the surface by late winter (Figure 1.4). While the ambient plankton community thus has plenty of nutrients in the late winter, the combination low solar radiation, decreased water column temperatures, and mixing of particles to depths where little light penetrates hinders biomass accumulation. During spring the storm intensity declines and water temperatures begin to increase. As a result, the water column begins to stratify and primary producers are able to utilize the replenished nutrients in the water column and increase biomass. While this process is temporally variable from year to year, it usually happens in the spring months and is generally referred to as the spring bloom (Figure 1.4). The spring bloom seldom lasts all spring, as one or more nutrients becomes limiting, thus leading to lower phytoplankton biomass and lower primary production rates.

Over the course of an annual cycle the autotrophic community may be limited by several different nutrients, but nitrogen is currently thought of as the predominant limiting nutrient in the Sargasso Sea (Lipschultz 2001). However, phosphate concentrations ($[HPO_4^{2-}]$) and $[Si(OH)_4]$ are both chronically low in this environment and limit rates of uptake and/or biomass accumulation to a certain degree (Brzezinski and Nelson 1996, Ammerman et al. 2003). Likewise, it has been reported that dissolved iron concentrations ([Fe]) can be limiting to phytoplankton during the end of the spring bloom (Sedwick et al. 2005). But for most of the year Saharan desert dust leads to a supply of Fe that rarely limits phytoplankton growth to the extent that N or P do (see Ginoux et al. 2001, 2004).

The northwestern Sargasso Sea is the location of longest running open-ocean oceanographic time series in the world, Hydrostation S (HS). Started in 1955, the HS sampling regime has included hydrographic and chemical measurements with monthly resolution (Menzel and Ryther 1960), while also providing a ship of opportunity of additional scientific research projects (e.g. Dugdale and Goering 1967). In the 1970s the Ocean Flux Program moored sediment traps in the vicinity of HS to monitor changes in particle flux with time (e.g. Deuser 1986, Conte et al. 2001). Data from that program led to the insight of seasonality in the deep ocean, as changes in particle flux systematically alter the availability of organic matter in the deep ocean over an annual cycle. In late 1988 the US Joint Global Ocean Flux Study established the Bermuda Atlantic Time-Series Study (BATS) site to the southeast of HS, in what was believed to be a more representative open-ocean location. The BATS program has a monthly to bi-weekly (in spring only) sampling resolution and, unlike HS, has sampled for $bSiO_2$ (Brzezinski and Nelson 1995) in addition to a suite of biogeochemical measurements since 1989 (Knap et al. 1997). Data from the BATS program have led to many advances in understanding of carbon, nitrogen, phosphorus and silicon cycling in the Sargasso Sea (Nelson and Brzezinski 1997, Lipschultz 2001, Ammerman et al. 2003, Lomas and Bates 2004). In the 1990s the Bermuda Testbed Mooring instrument platform was established, allowing for much higher temporal resolution (minutes to hours) of physical and biological parameters at multiple depths (Dickey et al. 1998, 2001).

Early studies at HS measured diatom cell abundance (Hulburt et al. 1960) but methodology to link diatom abundance with Si cycling was not available. Steinberg et al. (2001) and Goericke (1998) both noted that diatoms contribute only a small proportion (<5%) of the total autotrophic biomass in the Sargasso Sea, in sharp contrast with coastal systems, where diatoms often dominate. Margalef (1997, building on his earlier work) theorized that diatoms should not dominate in systems with low turbulence and low nutrients; therefore, within the context of his theory, diatom biomass in the Sargasso Sea should be low compared to coastal systems.

Brzezinski and Nelson (1995) started the measurement of $bSiO_2$ standing stock at the BATS site in 1989 and, from mid 1991 through 1994, measured the production rate of $bSiO_2$ in the surface waters and its export flux to the ocean interior. Although the open ocean is an area of low diatom biomass, diatoms and their remains dominate the $bSiO_2$ pool. Thus $bSiO_2$ provides one proxy for diatom biomass and $bSiO_2$ production provides one measure of diatom growth and productivity. With production and flux measurements taken over a three-year period (mid 1991 through mid 1994), complemented by six years of $bSiO_2$ standing stock measurements, this early BATS Si study has provided the most comprehensive look at Si cycling with time in the upper 1000 m of a mid-ocean gyre to date (Brzezinski and Nelson, 1995, 1996, Nelson and Brzezinski, 1997).

Like their pre-BATS era predecessors, Brzezinski and Nelson (1995) reported seasonality in diatom biomass. They found that the standing stock, production rate and export rate of $bSiO_2$ were generally highest in spring and declined to minima in the fall and winter. Vertically integrated (0 – 160 m) $bSiO_2$ production rates were the lowest yet measured anywhere in the global ocean, lower even than those in the Weddell Sea under 80 – 100% ice cover (Leynaert et al. 1993, Nelson and Brzezinski 1997). Using the stable isotope ^{29}Si, Brzezinski and Nelson found that diatoms at the BATS site were taking up Si at only ~15% of their potential maximum rate. They noted that under this chronic substrate limitation rates of $Si(OH)_4$ uptake increased almost linearly with $[Si(OH)_4]$ up to ~ 6 μM. Surface-layer $[Si(OH)_4]$ in the Sargasso Sea is < 0.9 μM throughout the year (Nelson and Brzezinski, 1997) and K_S for $Si(OH)_4$ uptake by diatoms is generally low enough (1 – 5 μM) that the curvilinear

nature of the Michaelis-Menten function would be evident over the 0 – 6 μM range (e.g. Nelson and Dortch 1996). Brzezinski and Nelson's results thus showed that the rate of diatom Si uptake is chronically, and quite strongly, limited by low [$Si(OH)_4$] at the BATS site. Their results also implied that K_S for $Si(OH)_4$ uptake may be unusually high (e.g. 1 – 5 μM), since in Sargasso Sea diatoms rarely see 1 μM [$Si(OH)_4$] in the surface waters (Nelson and Brzezinski 1997 and references therein).

Although [$Si(OH)_4$] is low (< 0.9 μM) year-round, diatom blooms have been observed in the Sargasso Sea. Biogenic silica standing stocks ([$bSiO_2$]) are generally much higher at the time of the spring phytoplankton bloom (~100 nmol Si l^{-1} as opposed to < 30 nmol Si l^{-1} at most other times of year; Nelson and Brzezinski, 1997). In addition there are occasional episodes of much higher [$bSiO_2$] (up to ~600 nmol Si l^{-1}; see Chapter 4) most notably associated with eddies and other mesoscale physical features (McNeil et al. 1999, Conte et al. 2003, see also McGillicuddy et al. 2007). Additionally, large diatoms at the base of the euphotic zone have been hypothesized to be a major source of new production in this system, although their actual contribution to new production has yet to be quantified (Goldman et al. 1992, Goldman 1993, Goldman and McGillicuddy 2003).

Nelson and Brzezinski (1997) estimated annual $bSiO_2$ production at the BATS site by extrapolation of measured daily rates using the stable-isotope tracer ^{30}Si. Their estimate came to 240 mmol Si m^{-2} y^{-1}. When converted to carbon productivity using a diatom Si:C ratio of 0.15 from culture studies (Brzezinski 1985) diatoms were estimated to account for ~ 15 – 25% of the annual primary productivity in this section of the North Atlantic. Using a similar approach, Nelson and Brzezinski (1997) estimated that diatoms at the BATS site contribute ~30% of the annual organic-matter export, with values near 100% during the spring bloom. Thus, despite low biomass and low numerical abundance in this system, the diatoms' estimated role in both primary production and organic-matter export is disproportionably large.

1.2.2 Equatorial Pacific

The equatorial Pacific, like the Sargasso Sea, has a history of scientific exploration (Figure 1.5). In 1768, Captain James Cook set sail on the HMS

Endeavour on a voyage of discovery; among his 94-person crew were several scientists (Shackleton 1962). Cook's initial objective was to sail to Tahiti in order for the scientists to observe the transit of the planet Venus, but he was also intent to discover the "Great Southern Continent" that was thought to be located in the South Pacific (ibid.). Later, in September/October 1835 the HMS *Beagle* landed in the Galápagos Islands in the eastern equatorial Pacific, where the naturalist aboard, Charles Darwin, would make his famous observations. But that expedition, like Cook's, was not truly focused on the oceans. In the 1875 the HMS *Challenger* traversed the equatorial Pacific en route to Tahiti and the Hawaiian Islands. This expedition circumnavigated the globe and was the first of its type to study the physical, chemical, geological and biological characteristics of the oceans.

Research in the 20th century yielded new knowledge on the ocean environment of the equatorial Pacific, with insights into the key role this region plays in physical and biogeochemical processes at the global scale. Many studies in the equatorial Pacific were carried out within (or partially within) a ~10^7 km^2 region that has come to be called the 'Wyrtki box', an area extending from 5°N to 5°S, and from 90°W to 180° (Figure 1.5, Wyrtki 1981). In the last two decades, a wealth of new scientific data has come from the broader equatorial Pacific as the National Oceanic and Atmospheric Administration Tropical Atmosphere Ocean (TAO) array has >70 moorings between 8°S and 8°N, equally spaced over nearly all the equatorial Pacific from ~95°W to ~150°E (see Feely et al. 2006 and references therein).

The equatorial Pacific is a region where there is nearly continuous upwelling, focused at the equator. Crossing the equator changes the sign of the Coriolis parameter, with the result that the net meridional movement of surface waters in response to the predominant easterly trade winds is divergent at the equator; south of the equator surface waters are deflected ~90 degrees to the left, and north of the equator ~90 degrees to the right (Figure 1.6a). This divergence of surface water near the equator results in upwelling (Figure 1.6a). The relatively constant easterly winds over the equatorial Pacific also cause a net movement of surface water to the west, and the consequent 'piling-up' of water in the western equatorial Pacific creates a sea-level gradient (Figure 1.6b). The effect on the subsurface thermocline is opposite to the

sea-level, as the 'piled-up' water in the west forces the thermocline in that region to be deeper than in the east (Figure 1.6b). Across the equatorial Pacific basin the source depth of the upwelled water is relatively constant (e.g. Dugdale and Wilkerson 1998), with the result that wind-driven upwelling penetrates the thermocline only in the east (Figure 1.6b). In those areas where upwelling penetrates the thermocline, nutrient rich sub-thermocline water is transported into the euphotic zone, making nutrients available to the autotrophic community. The consequence of this physical forcing can be seen in the persistently high $[NO_3^-]$ and $[HPO_4^{-2}]$ in the surface waters, resulting in chl-a biomass that is higher than in the gyres to the north and south (Figure 1.7).

The high-nutrient environment allows for the development of higher biomass at the upper trophic levels. Jacquet et al. 1996 demonstrated that sperm whale kills between 1761 and 1920 were maximum in areas that are now known to have high chlorophyll located in the upwelling tongue of the equatorial Pacific (note: approximately 1665 recorded voyages during this period, with locations of where ~37000 sperm whales were taken, see Jacquet et al. (1996) and references therein for historical data sources). Jacquet et al. reported that the number of whale kills in this area was an order of magnitude more than in the north and south gyres. Another result of the capacity to support higher trophic levels is the potential for the elevated particle export (i.e. new production ≈ export production) into the deep ocean. Chavez and Barber (1987) estimated the equatorial Pacific contributes 0.8 – 1.9 Pg C $year^{-1}$ of new production (1 petagram (Pg) = 10^{15} g), which is potentially >10% of global new production. Despite being higher in biomass and primary production than the central gyres of the North and South Pacific, the equatorial Pacific is still not as productive as most coastal systems (see regional differences in Behrenfeld and Falkowski 1997).

While the equatorial Pacific is an open-ocean region of enhanced annual primary production, in comparison with the gyres, the high surface water nutrient content implies that chlorophyll and primary productivity in this region could be higher if the ambient autotrophic community were able to utilize all the available nutrients. Carbon dioxide (CO_2) is also brought towards the surface, along with macronutrients, via upwelling. The lack of high primary productivity in equatorial Pacific (compared to its potential) prevents much of the upwelled CO_2 from being

taken up photosynthetically. This CO_2 is released to the atmosphere, with the result that the eastern equatorial Pacific is the largest oceanic source of CO_2 to the atmosphere (Takahashi et al. 2002, Feely et al. 2006). The causes of this general condition of high nutrients and low chlorophyll (HNLC; Minas et al. 1986) have been debated; possible explanations include a combination of low iron availability (Martin et al. 1991, Coale et al. 1996), intense grazing pressure (Landry et al. 1997 and references therein) and low [$Si(OH)_4$] (Dugdale and Wilkerson 1998).

The geographic remoteness of most of the equatorial Pacific removes it from any prominent continental dust source. This makes the equatorial Pacific very different from the North Atlantic, which has the Sahara desert as a dust source. Thus, dissolved [Fe] is very low in the surface waters of the equatorial Pacific (Martin et al. 1991). The addition of Fe to the equatorial Pacific surface water has resulted in the enhancement of primary production rates and increases in phytoplankton biomass (e.g. chl-a), both in multi-day bottle incubations performed on deck (e.g. Martin et al. 1991) and in open-ocean fertilization experiments (e.g. Coale et al. 1996). These studies indicate that Fe limitation indeed does have a role in sustaining the HNLC condition, but whether it is the only controlling mechanism is debatable. Landry et al. (1997) presented evidence of a strong coupling between primary production and zooplankton grazing in this region (see also Latasa et al. 1997). Strong and tightly coupled zooplankton grazing would keep autotrophic biomass below levels observed in coastal systems, as any production would be rapidly cropped by grazers, thus potentially preventing the autotrophic community from utilizing all the surface macronutrients.

Ku et al. (1995) observed that $Si(OH)_4$ delivery into the surface waters of the equatorial Pacific is ~50% lower than that of NO_3^-. Using Ku et al.'s findings, Dugdale and Wilkerson (1998) developed a model suggesting that the low supply of $Si(OH)_4$ relative to NO_3^- would limit diatom production in this system; diatom Si:N is ~1:1 under nutrient-replete conditions in culture (Brzezinski, 1985), while the Si:N supply ratio in the equatorial Pacific it is ~0.5:1. $Si(OH)_4$ regeneration, via dissolution of $bSiO_2$, is generally thought to be a slower process than the regeneration of NH_4^+ from the metabolic breakdown of organic nitrogen; thus a 'silicate pump' driven by the differential regeneration of N and Si would preferentially remove Si from the

surface layer of this system (Dugdale and Wilkerson, 1998). Dugdale and Wilkerson further assumed that diatoms were the main agents of new production in the eastern equatorial Pacific; thus $Si(OH)_4$, in their view, could be the ultimate limiting nutrient for new production in this system and would sustain the HNLC condition.

On annual time scales the equatorial Pacific is assumed to operate near steady state, with only relatively minor changes in biological rates under 'normal' conditions (i.e. in the absence of El Niño, or of mesoscale nutrient injections; Landry et al. 1997 and references therein). Despite this apparent steady state, the equatorial Pacific is an area with dynamic non-steady-state physical perturbations. For example tropical instability waves (which result from the shear with the eastward-flowing northern equatorial counter current, Figure 1.6a), alter thermocline circulation between the equator and ~6°N, resulting in both convergent and divergent zones in a westward propagating vortex (Kennan and Flament 2000, Menkes et al. 2002). Observations at these zones indicate areas of both increased and decreased phytoplankton biomass; and presumably, biological rates (Archer et al. 1997, Strutton et al. 2001). Understanding of how $bSiO_2$ production might respond to such non-steady-state physical features, or perturbation of the nutrient environment via wide-scale Fe fertilizations (e.g. IronExII, Coale et al. 1996) is still almost completely lacking in field data, and has been addressed primarily by modeling studies (e.g. Chai et al. 2007). Considering the role the equatorial Pacific plays in global new production and air-sea CO_2 exchange, it is important to understand how physical perturbations enhance or depress primary production, new production, and diatom growth in the system.

The equatorial Pacific has also been observed to be prone to dramatic regime shifts associated with phase changes in the El Niño Southern Oscillation (ENSO) index. During El Niño events the easterly trade winds are weakened or, under a strong El Niño, absent; this results in a breakdown of the normal sea level gradient, causing a relative elevation of sea level in the east and a depression of sea level in the west. The onset of strong El Niño conditions (warm period) has been observed to lower biological productivity (Barber et al. 1996). Quinn et al. (1978) inferred past El Niño intensities by coupling the atmospheric Southern Oscillation Index (SOI) with many

reports of biological disturbances to fisheries and marine life off the Peruvian coast (from data sources spanning more than two centuries, 1726–1976). Later, Quinn et al. (1987) analyzed reports in five different languages dating back to the 16th century, and plotted a historical record of El Niño events from 1525 – 1987. In that study Quinn et al. showed a high intensity in both the early and late periods of each century, qualitatively inferring a 50-year oscillation. In opposition to El Niño is La Niña (cool period). La Niña intervals possess stronger easterly trade winds and thus a steeper west-east slope of the sea surface and greater upwelling intensity, and enhanced primary production over El Niño conditions (Barber et al. 1996). Currently, the understanding of the physical forcing of El Niño/La Niña events and the biogeochemical responses is an active area of research in both oceanography and the atmospheric sciences. Considering the equatorial Pacific's role in global climate (as largest oceanic source of CO_2 to the atmosphere), a mechanistic understanding of natural variation in this system (e.g. ENSO) is a critical component in climate models that aim to forecasting the effects of climate change in the next century.

While many studies have examined the biological community in the equatorial Pacific, most data sets related to diatom ecology do not include measurements pertaining to Si cycling (Chavez et al. 1990, Chavez et al. 1991, Kaczmarkska and Fryxell 1995, Bidigare and Ondrusek 1996, Archer et al. 1997, Kobayashi and Takahaski 2002). In a situation similar to that in the Sargasso Sea, only a few studies in the equatorial Pacific have reported data on Si cycling (Table 1.1). Microscopy and floristic studies have shown that >14 μm cells, mainly diatoms, generally represent ≤4% of the autotrophic biomass in the equatorial Pacific, and that diatom cell abundances are much lower than in coastal systems (Kaczmarkska and Fryxell 1995, Bidigare and Ondrusek 1996). Consistent with low diatom cell abundances, Si-focused studies observed both low [$bSiO_2$] (~50 – 100 nmol l^{-1}) and low $bSiO_2$ production rates, average ~1.5 mmol Si m^{-2} d^{-1} (Blain et al. 1997, Leynaert et al. 2001). The sampling scheme in those studies did not allow for resolution of zonal variability in the eastern equatorial Pacific region near the enhanced upwelling (see Figure 1.6b); however, meridional transect data observed a maximum in [$bSiO_2$] and $bSiO_2$ production rates between 1°S and 1°N. This was similar to the findings of

Bidigare and Ondrusek (1996) who observed that the proportion of diatom chl-a (to total chl-a) was greatest near the equator, the area of the most intense upwelling.

Maximum rates of integrated $bSiO_2$ production in the equatorial Pacific (Blain et al. 1997, Leynaert et al., 2001) were ~3x higher than maximum rates measured by Nelson and Brzezinski (1997) in the Sargasso Sea. In addition, Leynaert et al. (2001) observed higher $bSiO_2$ production rates in the daylight hours than at night, suggesting a light energy dependence or correlation for $bSiO_2$ production that has not been observed in other parts of the open ocean (e.g. Gulf Stream Warm-Core Ring, Brzezinski and Nelson 1989; Sargasso Sea, Nelson and Brzezinski 1997). Similar to the situation in the Sargasso Sea, rates of Si uptake by diatoms in the equatorial Pacific were kinetically limited by the availability of $[Si(OH)_4]$ (Leynaert et al. 2001). Leynaert et al. reported the range of ambient Si uptake was between 13 and 78% of potential maximum uptake; values below 25% indicate a high likelihood that diatom growth rates are limited by ambient $[Si(OH)_4]$ unless some other nutrient is even more strongly limiting (Martin-Jézéquel et al. 2000 and references therein).

Diatoms in the equatorial Pacific, despite their low contribution to autotrophic biomass, may be disproportionately important to new production, similar to the situation suggested for the Sargasso Sea. Dugdale et al. (2007) made size-fractioned measurements of new and regenerated production (as estimated by NH_4^+ and NO_3^- uptake) and found that *f*-ratios for cells > 5 μm are generally >0.5, whereas cells <5 μm had *f*-ratios ~0.15. The implication is that primary production carried out by large cells (e.g. diatoms) is mainly new production. While this is compelling evidence it does not necessarily imply that diatoms carry out most of the new production in the system; to support such a conclusion the absolute amount of new production carried out by diatoms and by nonsiliceous phytoplankton, integrated throughout the euphotic zone must be compared. Leynaert et al. (2001), by converting integrated $bSiO_2$ production into estimates of integrated new production, estimated that diatoms were potentially able to sustain most of the new production in this system, supporting the assumption of Dugdale and Wilkerson's (1998) model.

1.3 Knowledge gaps regarding Si cycling in the open ocean

While previous studies in both the Sargasso Sea and the equatorial Pacific have allowed for general characterization of these systems in terms of Si cycling, this description is far from exhaustive. For example, Si cycling processes in the Sargasso Sea are known to be dominated by a seasonal signal. However, less known are responses to event-scale forcing on the time scale of hours to days. For instance, research in the Bering Sea has given insight into the impact of event-scale physical phenomena on new production. Sambrotto et al. (1986) reported that during the transition from a phytoplankton bloom to a stratified, post-bloom water column, passing storms mixed the water column and penetrated a shallow pycnocline, providing nitrate which sustained new production. These storm-forced mixing events were important, contributing an estimated 37% of the spring bloom new production (Sambrotto et al. 1986). Late winter is a period in the Sargasso Sea with frequent storm events which, due to an already destabilized water column, can mix limiting nutrients into the euphotic zone. Phytoplankton production occurring in response to this forcing could potentially increase annual new production above current estimates in the Sargasso Sea. Due to physiological adaptations (e.g. nutrient storage, Dortch 1982; high maximum growth rates, Martin-Jézéquel et al. 2000 and references therein; rapid and/or luxury nutrient uptake, Sunda and Huntsman 1995), diatoms are a group that could exploit short-lived nutrient injections and significantly contribute to community new production.

Interannual variability in Si cycling in the equatorial Pacific and Sargasso Sea is also a major gap in current knowledge. Nelson and Brzezinski (1997) presented the results of three years worth of $bSiO_2$ production and export data at the BATS site, complementing six years of [$bSiO_2$] data; this is currently the longest time-series of [$bSiO_2$] data in the primary literature. Nelson and Brzezinski's study led to an understanding of the general nature of Si-cycle parameters and how they change on monthly and seasonal scales; however statistically meaningful extrapolation to inter-annual variability was not possible with their data set. Thus current knowledge about how diatom biomass changes with time in response to changing physical and/or climatic forcing has been unknown, and addressed only in modeling studies (e.g.

Mongin et al. 2003). Similarly, in the equatorial Pacific, responses to El Niño climatic oscillations have been observed (Barber et al. 1996, Latasa et al. 1997). Barber et al. (1996) invoke the argument that the differences in community biomass and production between the El Niño and La Niña phases of the Southern Oscillation are due to changes in circulation, through their effect on iron supply. Barber et al. included diatoms within this hypothesis. However, there is active debate about what nutrient limits diatom growth and productivity in the equatorial Pacific (Dugdale and Wilkerson 1998, Chai et al. 2002, Dugdale et al. 2007, Brzezinski et al. 2008). Only recently have kinetic studies of nutrient limitation in the equatorial Pacific considered both Fe and Si as potentially limiting nutrients, and examined their possible interactive effects (Brzezinski et al. 2008).

Current data sets addressing Si cycling in the open ocean are also poorly resolved spatially. Remote sensing has been a boon for oceanographers, permitting remote and logistically difficult regions of the ocean to be observed without the expense of mounting research expeditions. One such advance has been the visualization of non-linear mesoscale eddies and estimation of their potential impact on biogeochemical cycling in the upper water column (McGillicuddy et al. 1998, Chelton et al. 2007). However, there is no foreseeable way to get around the necessity of ship-based sampling in order to understand the coupling between biogeochemical and community-structure processes; thus it is likely that resolution in biological rate data will continue to be poor for some time. In a global review of the production and dissolution of $bSiO_2$ in ocean surface waters Nelson et al. (1995) used data from the NW Sargasso Sea (from Brzezinski and Nelson 1995) as representative for all mid-ocean gyres, because no other data on silica production rates were available from any mid-ocean gyre at that time. Three years later Brzezinski et al. (1998) published data on upper-water-column Si cycling in the North Pacific gyre. Their data demonstrated that $bSiO_2$ production rates were ~2–3x higher than in the Sargasso Sea; disproving the original assumptions of little variability in mid-ocean gyre Si processes. Additionally, an understanding of sub-surface spatial variability (most of which is not observable from satellites) is a pressing need for biological oceanographers, and specifically those studying Si cycling in the open ocean.

1.4 Dissertation Focus

In this dissertation, the data presented address some of the largest current knowledge gaps in Si biogeochemistry, specifically those related open-ocean areas. Data reported are from cruises to the northwestern Sargasso Sea on the *R.V. Oceanus* in February/March of 2004 and 2005 and to the equatorial Pacific on the *R.V. Roger Revelle* in December, 2004 and September, 2005.

The impact of event-scale physical forcing on Si cycling in the Sargasso Sea is explored in Chapter 2. This research specifically examines the role of late-winter storms in enhancing $bSiO_2$ production and export, and the potential contribution of diatoms to community new production during that time of year. Measurement of $bSiO_2$ production during the late winter also allows for reassessment of annual $bSiO_2$ production in this region.

Chapter 3 examines the spatial variance in $bSiO_2$ production in the equatorial Pacific, in both a meridional and zonal axis. There is also a reassessment of the potential diatom contribution to primary and new production. This is estimated by a coupling of concurrent biological rate experiments using Si, C and N tracers, unprecedented in the equatorial Pacific, along with direct measurements of *in situ* diatom elemental stoichiometry. This rich data set will allow for the most reliable estimate of diatom contribution to primary and new production in this region to date.

Using data collected at the BATS site from 1989 through 2003, Chapter 4 examines how $bSiO_2$ in the upper 1000 m changes with time in the Sargasso Sea. While the $bSiO_2$ record between 1989 through 1994 has been published previously (Nelson and Brzezinski 1997), new data from 1995 through 2003 are presented and the total 15-year record is re-analyzed. The bi-weekly to monthly temporal resolution during the 15-year time frame allows for statistical assessment of seasonal variability, and is the first open-ocean study to observe how diatom biomass changes on sub-decadal and longer (i.e. 15 years) time scales. This is by far the longest time-series record on biogenic silica yet reported from the surface waters of any ocean, and it also has relatively high temporal resolution (i.e. biweekly to monthly).

Chapter 5 is a summation of the major dissertation findings, placing them within the context of existing knowledge of Si biogeochemistry in the upper ocean.

Additionally, it will focus on future research directions, as suggested by these findings.

1.5 References

Alexandre, A., Meunier, J., Colin, F., Koud, J.M., 2002. Plant impact on the biogeochemical cycle of silicon and related weathering processes. Geochimica et Cosmochimica Acta 61, 677-682.

Allen, W.E., 1934. The primary food supply of the sea. The Quarterly Review of Biology 9, 161-180.

Allen, W.E., 1936. Occurrence of marine plankton diatoms in a ten-year series of daily catches in Southern California. American Journal of Biology 23, 60-63.

Almqvist, N., Del Amo, Y., Smith, B.L., Thomson, N.H., Bartholdson, A., Lal, R., Brzezinski, M., Hansma, P.K., 2001. Micromechanical and structural properties of a pennate diatom investigated by atomic force microscopy. Journal of Microscopy 202, 518-532.

Ammerman, J.W., Hood, R.R, Case, D.A., Cotner J.B., 2003. Phosphorus Deficiency in the Atlantic: An Emerging Paradigm in Oceanography. EOS Transactions, American Geophysical Union 84, 165-170.

Archer, D., and 16 others, 1997. A meeting place of great ocean currents: shipboard observations of a convergent front at 2 degrees N in the Pacific. Deep-Sea Research II 44, 1827-1849.

Barber, R.T., Sanderson, M.P., Lindley, S.T., Chai, F., Newton, J., Trees, C.C., Foley, D.G., Chavez, F.P., 1996. Primary productivity and its regulation in the equatorial Pacific during and following the 1991-1992 El Niño. Deep-Sea Research II 43, 933-969.

Beebe, W., 1932. Nonsuch: land of water. New York: Brewer, Warren & Putnam, 259 pgs.

Beebe, W., 1934. Half mile down. New York: Harcourt, Brace and Company, 334 pgs.

Behrenfeld, M.J., Falkowski, P.G., 1997. Photosynthetic rates derived from satellite-based chlorophyll concentration. Limnology and Oceanography 42, 1-20.

Bidigare, R.R., Ondrusek, M.E., 1996. Spatial and temporal variability of phytoplankton pigment distributions in the central equatorial Pacific Ocean. Deep-Sea Research II 43, 809-833.

Blain, S., Leynaert, A., Tréguer, Chretiennot-Dinet, M., Rodier, M., 1997. Biomass, growth rates and limitation of Equatorial Pacific diatoms. Deep-Sea Research I 44, 1255-1275.

Blain, S., Tréguer, P, Rodier, M., 1999. Stocks and fluxes of biogenic silica in the western oligotrophic equatorial Pacific. Journal of Geophysical Research 104, 3357-3367.

Boyd, P.W., Trull, T.W., 2007. Understanding the export of biogenic particles in oceanic waters: Is there consensus? Progress in Oceanography 72, 276-312.

Brzezinski, M.A., 1985. The Si:C:N ratio of marine diatoms: interspecific variability and the effect of some environmental variables. Journal of Phycology 21, 347-57.

Brzezinski, M.A., 1992. Cell-cycle effects on the kinetics of silicic acid uptake and resource competition among diatoms. Journal of Plankton Research 14, 1511-1539.

Brzezinski, M.A., Conley, D.J., 1994. Silicon deposition during the cell cycle of Thalassiosira weissflogii (Bacillariophyceae) determined using dual rhodamine 123 and propidium iodide staining. Journal of Phycology 30, 45-55.

Brzezinski, M.A., Kosman, C.A., 1996. Silica production in the Sargasso Sea during spring 1989. Marine Ecology Progress Series 142, 39-45.

Brzezinski, M.A., Nelson, D.M., 1989. Seasonal changes in the silicon cycle within a Gulf Stream warm-core ring. Deep-Sea Research I 36, 1009-1030.

Brzezinski, M.A., Nelson, D.M., 1995. The annual silica cycle in the Sargasso Sea near Bermuda. Deep-Sea Research I 42, 1215-1237.

Brzezinski, M.A., Nelson D.M., 1996. Chronic substrate limitation of silicic acid uptake rates in the western Sargasso Sea. Deep-Sea Research II 43, 437-453.

Brzezinski, M.A., Phillips, D.R., 1997. Evaluation of ^{32}Si as a tracer for measuring silica production rates in marine surface waters. Limnology and Oceanography 42: 856-865.

Brzezinski, M.A., Olson, R.J., Chisholm, S.W., 1990. Silicon availability and cell-cycle progression in marine diatoms. Marine Ecology Progress Series 67, 83-96.

Brzezinski, M.A., Phillips, D.R., Chavez, F.P., Friederich, G.E., Dugdale, R.C., 1997. Silica production in the Monterery, California, upwelling system. Limnology and Oceanography 42, 1694-1705.

Brzezinski, M.A., Villareal, T.A., Lipschultz, F., 1998. Silica production and the contribution of diatoms to new and primary production in the central North Pacific. Marine Ecology Progress Series 167, 89-104.

Brzezinski, M.A., Nelson, D.M., Franck, V.M., Sigmon, D.E., 2001. Silicon dynamics within an intense open-ocean diatom bloom in the Pacific sector of the Southern Ocean. Deep-Sea Research II 48, 3997–4018.

Brzezinski, M.A., Dumousseaud, C., Krause, J.W., Measures, C.I., Nelson, D.M., 2008. Iron and silicic acid concentrations together regulate Si uptake in the equatorial Pacific Ocean. Limnology and Oceanography 53, 875-889.

Buesseler, K. O. 1998. The decoupling of production and particulate export in the surface ocean. Global Biogeochemical Cycles 12, 297–310.

Chai, F., Dugdale, R.C., Peng, T.-H., Wilkerson, F.P., Barber, R.T., 2002. One-dimensional ecosystem model of the equatorial Pacific upwelling system. Part I: model development and silicon and nitrogen cycle. Deep-Sea Research II 49, 2713-2745.

Chai, F., Jiang, M.-S., Chao, Y., Dugdale, R.C., Chavez, F., Barber, R.T., 2007. Modeling responses of diatom productivity and biogenic silica export to iron enrichment in the equatorial Pacific Ocean. Global Biogeochemical Cycles 21, doi: 10.1029/2006GB002804

Chavez, F.P, Barber, R.T, 1987. An estimate of new production in the equatorial Pacific. Deep-Sea Research I 34, 1229-1243.

Chavez, F.P., Buck, K.R., Barber, R.T., 1990. Phytoplankton taxa in relation to primary production in the equatorial Pacific. Deep-Sea Research I 37, 1733-1752.

Chavez, F.P., Buck, K.R., Coale, K.H., Martin, J.H., DiTullo, G.R., Welschmeyer, N.A., Jacobson, A.C., Barber, R.T., 1991. Growth rates, grazing, sinking, and iron limitation of equatorial Pacific phytoplankton. Limnology and Oceanography 36, 1816-1833.

Chelton, D.B., Schlax, M.G., Samelson, R.M., de Szoeke R.A., 2007. Global observations of large oceanic eddies. Geophysical Research Letters 34, doi: 10.1029/2007/GL030812.

Coale, K.H., and 18 others, 1996. A massive phytoplankton bloom induced by an ecosystem-scale iron fertilization experiment in the equatorial Pacific Ocean. Nature 383, 495-501.

Conkright, M., Levitus, S., Boyer, T., 1994. World Ocean Atlas 1994 Volume 1: Nutrients. NOAA Atlas NESDIS 1, U.S. Department of Commerce, Washington, D.C.

Conley, D.J., 2002. Terrestrial ecosystems and the global biogeochemical silica cycle. Global Biogeochemical Cycles 16, doi: 10.1029/2002GB001884.

Conte, M.H., Ralph, N., Ross, E.H., 2001. Seasonal and interannual variability in deep ocean particle fluxes at the Oceanic Flux Program (OFP)/Bermuda Atlantic Time Series (BATS) site in the western Sargasso Sea near Bermuda. Deep-Sea Research II 48, 1471-1505.

Conte, M.H., Dickey, T.D., Weber, J.C., Johnson, R.J., Knap, A.H., 2003. Transient physical forcing of pulsed export of bioreactive material to the deep Sargasso Sea. Deep-Sea Research I 50, 1157-1187.

De La Rocha, C.L., 2003. Silicon isotope fractionation by marine sponges and the reconstruction of the silicon isotope composition of ancient deep water. Geology 31, 423-426.

Del Amo, Y., Brzezinski, M.A., 1999. The chemical form of dissolved Si taken up by marine diatoms. Journal of Phycology 35, 1162-1170.

DeMaster, D.J., Dunbar, R.B., Gordon, L.I., Leventer, A.R., Morrison, J.M., Nelson, D.M., Nittrouer, C.A., Smith, W.O., 1992. Cycling and accumulation of organic matter and biogenic silica in high-latitude environments: The Ross Sea. Oceanography 5, 146-153.

Deuser, W. G., 1986. Seasonal and interannual variations in deep-water particle fluxes in the Sargasso Sea and their relation to surface hydrography. Deep-Sea Research I 33, 225-246.

Dickey, T.D., and 13 others, 1998. Initial results from the Bermuda Testbed Mooring program. Deep-Sea Research I 45, 771-794.

Dickey, T.D., and 13 others. 2001. Physical and biogeochemical variability from hours to years at the Bermuda Testbed Mooring site: June 1994-March 1998. Deep-Sea Research II 48, 2105-2140.

Dortch, Q., 1982. Effect of growth conditions on accumulation of internal nitrate, ammonium, amino acids, and protein in three marine diatoms. Journal of Experimental Marine Biology and Ecology 61, 243-264.

Dugdale, R.C., Goering, J.J., 1967. Uptake of new and regenerated forms of nitrogen in primary productivity. Limnology and Oceanography 12, 196-206.

Dugdale, R.C., Wilkerson, F.P., 1998. Silicate regulation of new production in the equatorial Pacific upwelling. Nature 391, 270-273.

Dugdale, R.C., Wilkerson, F.P., Chai, F., Feely, R., 2007. Size-fractioned nitrogen uptake measurements in the equatorial Pacific and confirmation of the low Si-high-nitrate-low-chlorophyll condition. Global Biogeochemical Cycles 21, doi: 10.1029/2006GB002722.

Eppley, R.W., Peterson, B.J., 1979. Particulate organic matter flux and planktonic new production in the deep ocean. Nature 282, 677-680.

Falkowski, P.G., Katz, M.E., Knoll, A.H., Quigg, A., Raven, J.A., Schofield, O., Taylor, F.J.R., 2004. The evolution of modern eukaryotic phytoplankton. Science 305, 354-360.

Feely, R.A., Takahashi, T., Wanninkhof, R., McPhaden, M.J., Cosca, C.E., Sutherland, S.C., Carr, M., 2006. Decadal variability of the air-sea CO_2 fluxes in the equatorial Pacific Ocean. Journal of Geophysical Research 111, doi: 10.1029/2005JC003129.

Fields, K., Kontrovitz, M., 1980. An invisible art blazes into life under the microscope. Smithsonian 11, 108-113.

Franck, V.M., Brzezinski, M.A., Coale, K.H., Nelson, D.M., 2000. Iron and silicic acid concentrations regulate Si uptake north and south of the Polar Frontal Zone in the Pacific Sector of the Southern Ocean. Deep-Sea Research II 47, 3315-3338.

Gebeshuber, I.C., Kindt, J.H., Thompson, J.B., Del Amo, Y., Stachelberger, H., Brzezinski, M.A., Stucky, G.D., Morse, D.E., Hansma, P.K., 2003. Atomic force microscopy study of living diatoms in ambient conditions. Journal of Microscopy 212, 292-299.

Ginoux, P., Chin, M., Tegen, I., Prospero, J.M., Holben, B., Dubovik, O., Lin, S-J., 2001. Sources and distribution of dust aerosols simulated with the GOCART model. Journal of Geophysical Research 106, 20255-20273.

Ginoux, P., Prospero, J.M., Torres, O., Chin, M., 2004. Long-term simulation of global dust distribution with the GOCART model: correlation with North Atlantic Oscillation. Environmental Modelling & Software 19, 113-128.

Goericke, R., 1998. Response of phytoplankton community structure and taxon specific growth rates to seasonally varying physical forcing in the Sargasso Sea off Bermuda. Limnology and Oceanography 43, 921-935.

Goering, J.J., Nelson, D.M., Carter, J.A., 1973 Silicic acid uptake by natural populations of marine phytoplankton. Deep-Sea Research I 20, 777-789.

Goldman J. C., 1993. Potential role of large oceanic diatoms in new primary production. Deep-Sea Research 40, 159-168.

Goldman, J.C., McGillicuddy, D.J., 2003. Effect of large marine diatoms growing at low light on episodic new production. Limnology and Oceanography 48, 1176-1182

Goldman, J.C., Hansell, D.A., Dennett, M.R., 1992. Chemical characterization of three large oceanic diatoms: potential impact on water column chemistry. Marine Ecology Progress Series 88, 257-270.

Hamm, C.E., Merkel, R., Springer, O., Jurkojc, P., Maier, C., Prechtel, K., Smetacek, V., 2003. Architecture and material properties of diatom shells provide effective mechanical protection. Nature 421, 841-843.

Harrison, P.J., Conway, H.L., Holmes, R.W., Davis, C.O., 1977. Marine diatoms grown in chemostats under silicate or ammonium limitation. III. Cellular chemical composition and morphology of *Chaetoceros debilis*, *Skeletonema costatum*, and *Thalassiosira gravida*. Marine Biology 43, 19-31.

Hildebrand, M., Dahlin, K., 2000. Nitrate transporter genes from the diatom Cylindrotheca fusiformis (Bacillariophyceae): mRNA levels controlled by nitrogen source and by the cell cycle. Journal of Phycology 36, 702-713.

Hildebrand, M., York, E., Kelz, J.I., Davis, A.K., Frigeri, L.G., Allison, D.P., Doktycz, M.J., 2006. Nanoscale control of silica morphology and three-dimensional structure during cell wall formation. Journal of Material Research 21, 2689-2698.

Honjo, S., Dymond, J., Collier, R., Manganini, S.J., 1995. Export production of particles to the interior of the equatorial Pacific Ocean during the 1992 EqPac experiment. Deep-Sea Research II 42, 831-870.

Honjo, S., Manganini, S.J., Krishfield, R.A., Francois, R., 2008. Particulate organic carbon fluxes to the ocean interior and factors controlling the biological pump: A synthesis of global sediment trap programs since 1983. Progress in Oceanography 76, 217-285.

Hulburt, E.M., Ryther, J.H., Guillard, R.R.L., 1960. The phytoplankton of the Sargasso Sea off Bermuda. Journal du Conseil International d'Exploration da la Mer 25, 115-128.

Jacquet, N., Whitehead, H., Lewis, M., 1996. Coherence between 19th century sperm whale distributions and satellite-derived pigments in the tropical Pacific. Marine Ecology Progress Series 145, 1-10.

Kaczmarkska, I., Fryxell, G.A., 1995. Micro-phytoplankton of the equatorial Pacific: 140°W meridianal transect during the 1992 El Niño. Deep-Sea Research II 42, 535-558.

Kennan, S.C., Flament, P.J., 2000. Observations of a Tropical Instability Vortex. Journal of Physical Oceanography 30, 2277-2301.

Kidder DL, Irwin DH. 2001. Secular distribution of biogenic silica through the phanerozoic: comparison of silica-replaced fossils and bedded cherts at the series level. Journal of Geology 109, 509–522.

Knap, A. H., and 19 others, 1997. U.S. Joint Global Ocean Flux Study- Bermuda Atlantic Time- Series Study Methods Manual: Version 4. U.S. JGOFS Planning and Coordination Office: Woods Hole.

Kobayashi, F., Takahaski, K., 2002. Distribution of diatoms along the equatorial transect in the western and central Pacific during the 1999 La Niña conditions. Deep-Sea Research II 49, 2801-2821.

Ku, T., Luo, S., Kusakabe, M., Bishop, J.K.B., 1995. ^{228}Ra-derived nutrient budgets in the upper equatorial Pacific and the role of "new" silicate in limiting productivity. Deep-Sea Research I 42, 479-497.

Landry, M.R., and 12 others, 1997. Iron and grazing constraints on primary production in the central equatorial Pacific: an EqPac synthesis. Limnology and Oceanography 42, 405-418.

Latasa, M., Landry, M.R., Schlüter, L., Bidigare, R.R., 1997. Pigment-specific growth and grazing rates of phytoplankton in the central equatorial Pacific. Limnology and Oceanography 42, 289-298.

Leblanc, K., Hutchins, D.A., 2005. New applications of a biogenic silica deposition fluorophore in the study of oceanic diatoms. Limnology and Oceanography: Methods 3, 462-476.

Levitus, S., Burgett, R., Boyer, T., 1994. World Ocean Atlas 1994 Volume 3: Nutrients. NOAA Atlas NESDIS 3, U.S. Department of Commerce, Washington, D.C..

Leynaert, A., Nelson, D.M., Quéguiner, B., Tréguer, P., 1993. The silica cycle in the Antarctic Ocean: Is the Weddell Sea atypical? Marine Ecology Progress Series 96, 1-15.

Leynaert, A., Tréguer, P., Lancelot, C., Rodier, M., 2001. Silicon limitation of biogenic silica production in the Equatorial Pacific. Deep-Sea Research I 48, 639-600.

Lipschultz, F., 2001. A time-series assessment of the nitrogen cycle at BATS. Deep-Sea Research Part II 48, 1897-1924.

Lipschultz, F., Bates, N.R., Carlson, C.A., Hansell, D.A., 2002. New production in the Sargasso Sea: History and current status. Global Biogeochemical Cycles 16, doi: 10.1029/2000GB001319.

Lomas, M.W., Bates, N.R., 2004. Potential controls on interannual partitioning of organic carbon during the winter/spring phytoplankton bloom at the Bermuda Atlantic time-series study (BATS) site. Deep-Sea Research I 51, 1619-1636.

Lopez, P.J., Gautier, C., Livage, J., Coradin, T., 2005. Mimicking biogenic silica nanostructures formation. Current Nanoscience 1, 73-83.

Maldonado, M., Carmona, M.C., Uriz, M.J., Cruzado, A., 1999. Decline in Mesozoic reef-building sponges explained by silicon limitation. Nature 401, 785-788.

Margalef, R, 1997. Excellence in ecology, Book 10: Our biosphere. Oldendorf/Luhe: International Ecology Institute.

Martin, J.H., Gordon, R.M., Fitzwater, S.E., 1991. The case for iron. Limnology and Oceanography 36, 1793-1802.

Martin-Jézéquel, V., Hildebrand, M., Brzezinski, M.A., 2000. Silicon metabolism in diatoms: implications for growth. Journal of Phycology 36, 821-840.

McGillicuddy, D.J., Robinson, A.R., Siegel, D.A., Jannasch, H.W., Johnson, R., Dickey, T.D., McNeil, J., Michaels, A.F., Knap, A.H., 1998. Influence of mesoscale eddies on new production in the Sargasso Sea. Nature 394, 263-266.

McGillicuddy, D.J., and 17 others, 2007. Eddy/wind interactions stimulate extraordinary mid-ocean plankton blooms. Science 316, 1021-1026.

McNeil, J.D., Jannasch, H.W., Dickey, T., McGillicuddy, D.J., Brzezinski, M., Sakamoto, C.M., 1999. New chemical, bio-optical and physical observations of upper ocean response to the passage of a mesoscale eddy off Bermuda. Journal of Geophysical Research 104. 15537–15548.

Menkes, C.E., and 14 others, 2002. A whirling ecosystem in the equatorial Atlantic. Geophysical Research Letters 29, doi: 10.1029/2001GL014576.

Menzel, D.W., Ryther, J.H., 1960. The annual cycle of primary production in the Sargasso Sea off Bermuda. Deep-Sea Research I 6, 351-366.

Michaels, A.F., Knap, A.H., 1996. Overview of the U.S. JGOFS Bermuda Atlantic Time-series Study and the Hydrostation S program. Deep-Sea Research II 43, 129-156.

Michaels, A.F., Silver, M.W., 1988. Primary production, sinking fluxes and the microbial food web. Deep-Sea Research I 35, 473-490.

Minas, H.J., Minas, M., Packard, T.T., 1986. Productivity in upwelling areas deduced from hydrographic and chemical fields. Limnology and Oceanography 31, 1182-1206.

Mongin, M., Nelson, D.M., Pondaven, P., Brzezinski, M.A., Tréguer, P., 2003. Simulation of upper-ocean biogeochemistry with a flexible-composition phytoplankton model: C, N and Si cycling in the western Sargasso Sea. Deep-Sea Research I 50, 1445-1480.

Nelson, D.M., Brzezinski, M.A., 1990. Kinetics of silicic acid uptake by natural diatom assemblages in two Gulf Stream warm-core rings. Marine Ecology Progress Series 62, 283-292.

Nelson, D.M., Brzezinski, M.A., 1997. Diatom growth and productivity in an oligotrophic midocean gyre: a 3-yr record from the Sargasso Sea near Bermuda. Limnology and Oceanography 43, 473-486.

Nelson, D.M., Dortch, Q., 1996. Silicic acid depletion and silicon limitation in the plume of the Mississippi River: evidence from kinetic studies in spring and summer. Marine Ecology Progress Series 136, 163-178.

Nelson, D.M., Goering, J.J., 1977. Near-surface silica dissolution in the upwelling region off northwest Africa. Deep-Sea Research I 24, 65-73.

Nelson, D.M., Goering, J.J., 1978. Assimilation of silicic acid by phytoplankton in the Baja California and northwest Africa upwelling systems. Limnology and Oceanography 23, 508-517.

Nelson, D.M., Gordon, L.I., 1982. Production and pelagic dissolution of biogenic silica in the Southern Ocean. Geochimica Cosmochimica Acta 46, 491-501.

Nelson, D.M., Tréguer, P., 1992. Role of silicon as a limiting nutrient to Antarctic diatoms: evidence from kinetic studies in the Ross Sea ice-edge zone. Marine Ecology Progress Series 80, 255-264.

Nelson, D.M., Ducklow, H.L., Hitchcock, G.L., Brzezinski, M.A., Cowles, T.J., Fryxell, G.A., Garside, C., Gould, R.W., Joyce, T.M., McCarthy, J.J., Yentsch, C.S., 1985. Distribution and composition of biogenic particulate matter in a Gulf Stream warm-core ring. Deep-Sea Research I 32, 1347-1369.

Nelson, D.M., Ahern, J.A., Herlihy, L.J., 1991. Cycling of biogenic silica within the upper water column of the Ross Sea. Marine Chemistry 35, 461-476.

Nelson, D.M., Tréguer, P., Brzezinski, M.A., Leynaert, A., Quéguiner, B., 1995. Production and dissolution of biogenic silica in the ocean: Revised global estimates, comparison with regional data and relationship to biogenic sedimentation. Global Biogeochemical Cycles 9, 359–372.

Nelson, D.M., DeMaster, D.J., Dunbar, R.B., Smith, W.O., 1996. Cycling of organic carbon and biogenic silica in the Southern Ocean: Estimates of water-column and sedimentary fluxes over the Ross Sea continental shelf. Journal of Geophysical Research 101, 18519-18532.

Nelson, D.M., Brzezinski, M.A., Sigmon, D.E., Franck, V.M., 2001. A seasonal progression of Si limitation in the Pacific sector of the Southern Ocean. Deep-Sea Research Part II 48, 3973–3995.

Nelson, D.M., and 15 others, 2002. Vertical budgets for organic carbon and biogenic silica in the Pacific sector of the Southern Ocean, 1996-1998. Deep-Sea Research II 49, 1645-1673.

Paasche, E, 1973. Silicon and the ecology of marine planktonic diatoms. I. Thalassiosira pseudonana (Cyclotella nana) grown in a chemostat with silicate as the limiting nutrient. Marine Biology 19, 117-126.

Parker, M.S., Armbrust, E.V., 2005. Synergistic effects of light, temperature, and nitrogen source on transcription of genes for carbon and nitrogen metabolism in the centric diatom Thalassiosira pseduonana (Bacillariophyceae). Journal of Phycology 41, 1142-1153.

Patrick, R., 1940. A Suggested Starting-Point for the Nomenclature of Diatoms. Bulletin of the Torrey Botanical Club 67, 614-615.

Quéguiner, B., Tréguer, P., Nelson, D.M., 1991. The production of biogenic silica in the Weddell and Scotia Seas. Marine Chemistry 35, 449-460.

Quinn, W.H., Zopf, D.O., Short, K.S., Yang, R.T.W.K., 1978. Historical trends and statistics of the Southern Oscillation, El Niño, and Indonesian droughts. Fishery Bulletin 76, 663-678.

Quinn, W.H., Neal, V.T., Antunez de Mayolo, S.E., 1987. El Niño occurrences over the past four and a half centuries. Journal of Geophysical Research 92, 14449-14461.

Racki G, Cordey F., 2000. Radiolarian palaeoecology and radiolarites: is the present the key to the past? Earth-Science Reviews 52, 83–120.

Raven, J.A., 1983. The transport and function of silicon in plants. Biological Review 58, 179-207.

Raven, J.A., Waite, A.M., 2004. The evolution of silicification in diatoms: inescapable sinking and sinking as escape? New Phytologist 162, 45-61.

Round, F.E., Crawford, R.M., Mann, D.G., 1990. The diatoms: biology and morphology of the genera. Cambridge University Press: Cambridge. 747 pgs.

Sambrotto, R.N., Niebauer, H.J., Goering, J.J., Iverson, R.L., 1986. Relationships among vertical mixing, nitrate uptake, and phytoplankton growth during the spring bloom in the southeast Bering Sea middle shelf. Continental Shelf Research 5, 161-198.

Schiermeier, Q., 2007. Observing the Ocean from within. Nature 450, 780-781.

Schubert JK, Kidder DL, Irwin DH. 1997. Silica-replaced fossils through the Phanerozoic. Geology 25, 1031–1034.

Schütt, F. 1896. Bacillariales (Diatomeae). Engler, A. & Prantl, K.(Eds.). In Die Naturlichen Pflanzenfamilien. Verlag von Wilhelm Engelmann, Leipzig, pp. 31–153

Sedwick, P.N., Church, T. M., Bowie, A. R., Marsay, C. M., Ussher, S.J., Achilles, K.M., Lethaby. P.J., Johnson, R.J., Sarin, M.M., D. J. McGillicuddy, D.J., 2005. Iron in the Sargasso Sea (Bermuda Atlantic Time-series Study region) during summer: Eolian imprint, spatiotemporal variability, and ecological implications. Global Biogeochemical Cycles 19, doi: 10.1029/2004GB002445.

Shackleton, E., 1962. Men against the sea, p. 295. *In* Seas, Deacon, G.E.R. (Ed.). Maps, and Men. Crescent, London.

Shimizu, K., Del Amo, Y., Brzezinski, M.A., Stucky, G.D., Morse, D.E., 2001. A novel fluorescent silica tracer for biological silicification studies. Chemistry and Biology 8, 1051-1060.

Siever, R., 1991. Silica in the oceans: biological–geochemical interplay, p. 287-295. *In*: Schneider S.H., Boston P.J. (Eds.) Scientists on gaia. MIT Press: Cambridge.

Sigmon, D.E., Nelson, D.M., Brzezinski, M.A., 2002. The Si cycle in the Pacific sector of the Southern Ocean: Seasonal diatom production in the surface layer and export to the deep sea. Deep-Sea Research II 49, 1747-1763.

Simpson, T.L., Volcani, B.E. (Eds.), 1981. Silicon and siliceous structures in biological systems. New York: Springer-Verlag.

Sosik, H.M., Olson, R.J., 2007. Automated taxonomic classification of phytoplankton sampled with imagine-in-flow cytometry. Limnology and Oceanography: Methods 5, 204-216.

Steinberg, D. K., Carlson, C. A., Bates, N. R., Johnson, R. J., Michaels, A. F., Knap, A. H. 2001. Overview of the US JGOFS Bermuda Atlantic Time-series Study (BATS): a decade-scale look at ocean biology and biogeochemistry. Deep-Sea Research Part II 48, 1405-1447.

Strutton, P.G., Ryan, J.P., Chavez, F.P., 2001. Enhanced chlorophyll associated with tropical instability waves in the equatorial Pacific. Geophysical Research Letters 28, 2005-2008.

Stumm, W., Morgan, J.J., 1996. Aquatic chemistry: chemical equilibria and rates in natural waters. Wiley and Sons, New York.

Sunda, W.G., Huntsman, S.A., 1995. Iron uptake and growth limitation in oceanic and coastal phytoplankton. Marine Chemistry 50, 189-196.

Takahashi, T., and 11 others, 2002. Global sea-air CO_2 flux based on climatological surface ocean pCO_2, and seasonal biological and temperature effects. Deep-Sea Research II 49, 1601-1622.

Tréguer, P., Nelson, D.M., Gueneley, S., Zeyons, C., Morvan, J., Buma, A., 1990. The distribution of biogenic and lithogenic silica and the composition of particulate organic matter in the Scotia Sea and the Drake Passage during autumn 1987. Deep-Sea Research I 37, 833-851.

Tréguer, P., Lindner, L., van Bennekom, A.J., Leynaert, A., Panouse, M., Jacques, G., 1991. Production of biogenic silica in the Weddell-Scotia Seas measured with ^{32}Si. Limnology and Oceanography 36, 1217-1227.

Wright, S.M., Jeffrey, S.W., 1987. Fucoxanthin pigment markers of marine phytoplankton analyzed by HPLC and HPTLC. Marine Ecology Progress Series 38, 259-26.

Wyrtki, K., 1981. An estimate of equatorial upwelling in the Pacific. Journal of Physical Oceanography 11, 1205-1214.

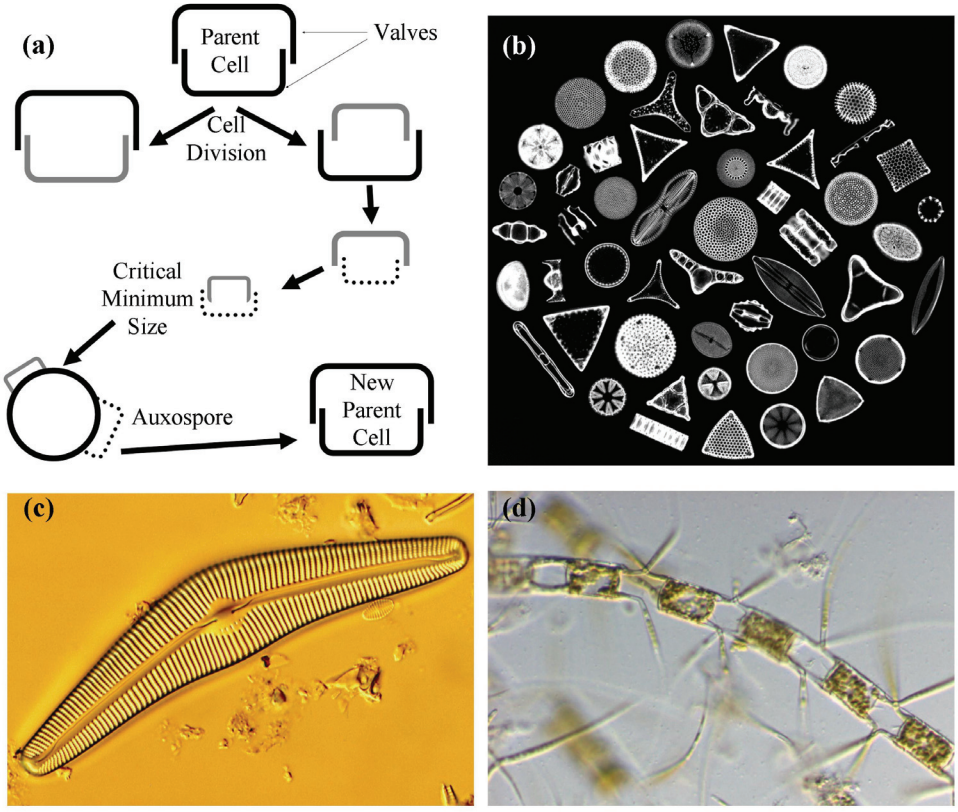

Figure 1.1 – (a) Schematic view of the diatom life cycle. Diatoms, consisting of two interconnecting valves, asexually divide and new valves are deposited to fit into the parent valve template. This results in the formation of one cell equivalent in size to the parent (from the larger valve) and one smaller than the parent (from smaller valve). Multiple asexual divisions will result in a critical minimum size where sexual reproduction will form an auxospore, resetting the size back to that of the parent cell. (b-d) The diversity of diatom sizes, shapes, and frustule intricacy. (b) Photomicrograph showing the frustules of fifty species of diatoms. Photo credit: Randolph Femmer (Public domain, from the National Biological Information Infrastructure Digital Image Library, USA). (c) *Cymbella cistula*, cell length and width ~ 60 and 20 µm, respectively. Photo credit: Mark B. Edlund (Public domain, from the National Science Foundation Multimedia Gallery, USA). (d) A chain of *Chaetoceros dichaeta*, cell length and width (single cell, not including spines) ~ 47 and 53 µm, respectively. Photo credit – Jeffrey W. Krause.

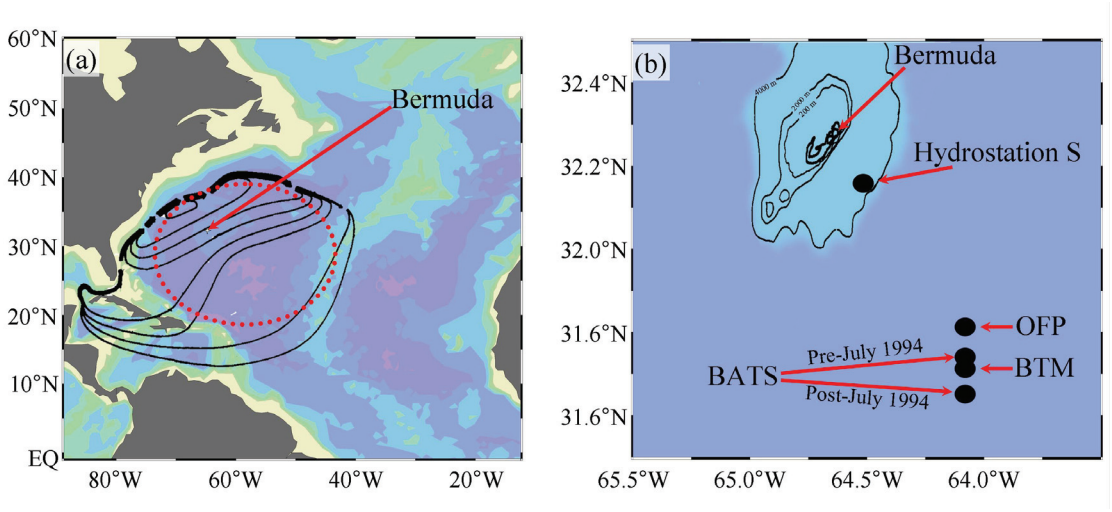

Figure 1.2 – (a) Schematic representation of the Sargasso Sea (red dotted circle). The Gulf Stream current progression and recirculation is overlaid on a bathymetric map of the North Atlantic (lighter blue/green bathymetry contours indicates shallower depth). The Gulf Stream circulation region shown here shows the approximate boundaries of the Sargasso Sea. (b) Location of oceanic time-series stations near Bermuda. Stations include Hydrostation S (32°10'N, 64°30'W), Oceanic Flux Program (OFP, 31°50'N, 64°10'W), Bermuda Atlantic Time-series Study (BATS, pre-July 1994 31°45'N, 64°10'W, post-July 1994 31°40'N, 64°10'W), and the Bermuda Testbed Mooring (BTM, 31°43'N, 64°10'W). Both figures modified from Michaels and Knap (1996)

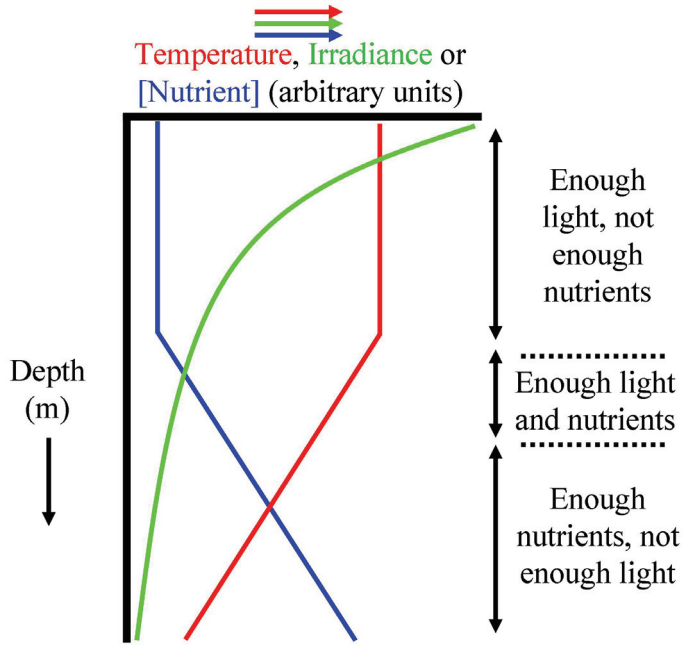

Figure 1.3 – A hypothetical vertical profile of temperature (red), irradiance (green) and a limiting nutrient (blue) in the euphotic zone of a thermally stratified open-ocean region. Within the mixed layer (i.e. layer of constant temperature) the limiting nutrient (blue) is drawn down to a uniformly low concentration. At the base of the mixed layer, the nutrient begins to increase towards a deep water maximum value, while the temperature decreases towards a deep water minimum. Light (green) is absorbed by the water (and particulate and dissolved material within the water) represented by a logarithmic decay function. This physical and chemical condition sets up three layers for primary producers: a shallow layer with ample light but not enough of the limiting nutrient, a mid-layer with there is less light than the shallow layer but more nutrients, and a deep layer with plenty of nutrients but little light. These physical and chemical distributions within the water column should determine the vertical orientation of autotrophic biomass.

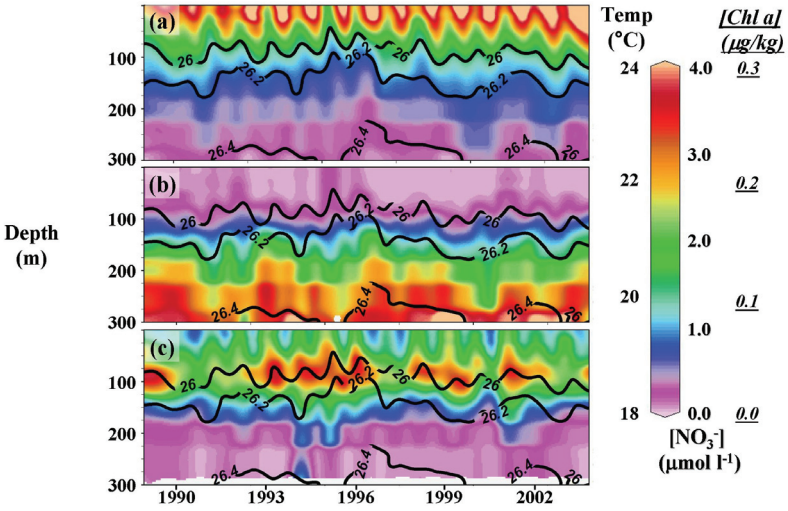

Figure 1.4 – Data from the BATS program (1989-2003, year tick is January 1st). (a) temperature in °C, (b) $[NO_3^-]$ in μmol l^{-1}, (c) [Chlorophyll a] in μg kg^{-1}. Potential density (σ_θ)contours in kg m^{-3} (black) over-lay each plot. Temperature variability (a) is highly seasonal in the upper 100 m, with winter periods of strong convective overturn followed by seasonal stratification. $[NO_3^-]$ (b) is near analytical detection limits in the upper 100 m for most of the year; however, some injections can be visualized during winter periods (e.g. winters in 1995, 1996). [Chlorophyll a] (c) is generally maximum subsurface, and absolute levels of chlorophyll are an order of magnitude smaller than those found in coastal regions. Data available at http://bats.bios.edu.

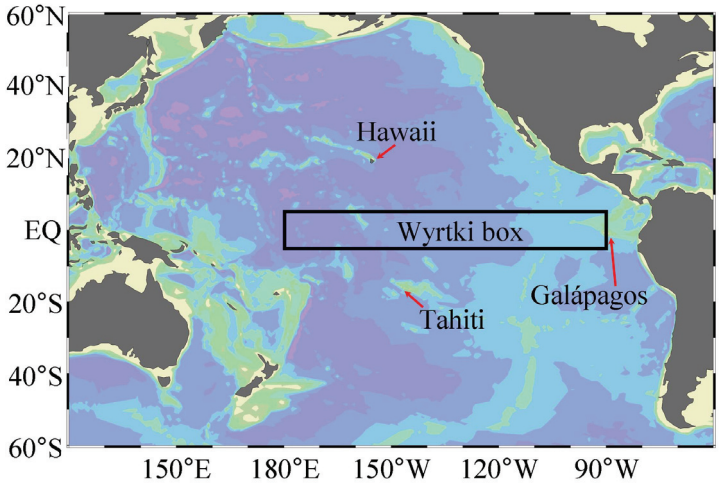

Figure 1.5 – Map of the Pacific Ocean (colored bathymetry as in Figure 1.2a) with approximate locations of Hawaii, Tahiti and the Galápagos island groups. The 'Wyrtki box' (Wyrtki 1981) is drawn to show general area of equatorial Pacific studies, and is bounded from 5°S-5°N and 180°E-90°W. Captain Cook navigated from Tahiti to Hawaii during his voyage, and crossed the equatorial Pacific; however, it was not until the HMS Challenger did this same route that the equatorial Pacific was explored with the intent to gather oceanographic data.

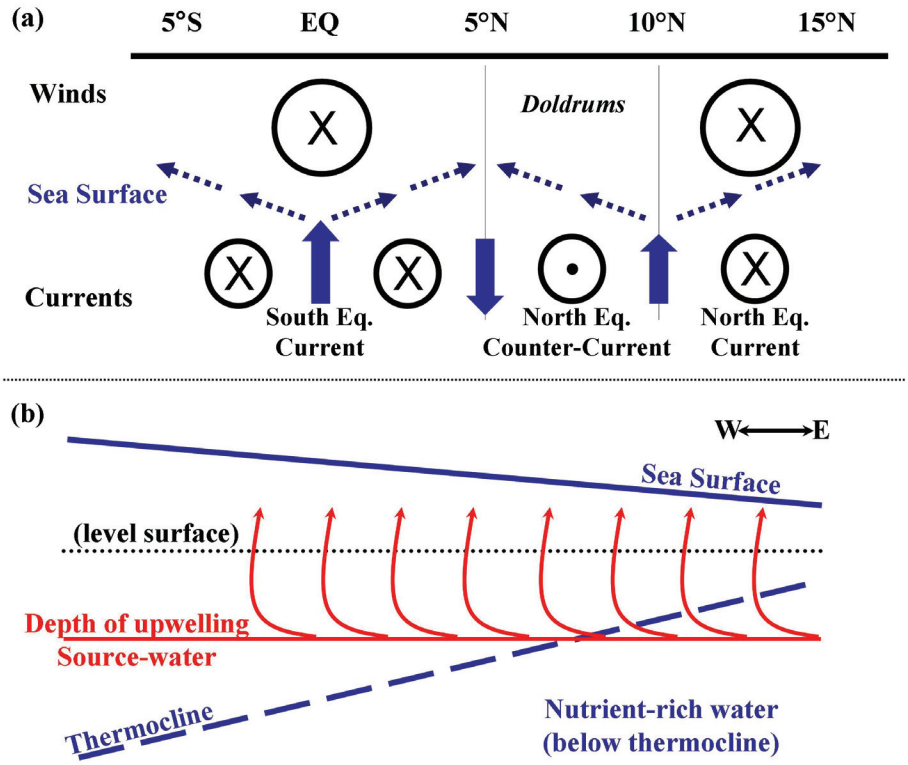

Figure 1.6 – A schematic view of the physical forcing in the equatorial Pacific Ocean. (a) Looking westward, the dominant winds are easterly and the dominant currents are westerly (note: convention dictates that wind direction is referred to by the origin of the wind, e.g., easterly wind blows from east to west; while current direction is referred to by the direction of flow, e.g., westerly currents flow from east to west). A change in the Coriolis parameter between the northern and southern hemispheres results in net deflection of the surface water to the left south of the equator, and to the right north of the equator. The resulting divergence leads to upwelling of subsurface water to the surface. A similar divergence can be seen at ~10°N, while a convergence occurs at ~5°N, causing surface water to be downwelled to deeper depths. (b) Looking northward at a depth section along the equator, the sea surface is higher in the west than in the east as a result of the easterly winds moving water west. This 'piling up' of water to the west deepens the thermocline, and shoals the thermocline in the east. The upwelling source-water depth is set by the wind field and results in a near constant depth across the basin. This leads to upwelling in the east bring nutrient-rich water, from below the thermocline, into the euphotic zone for use by the autotrophic community; whereas upwelling does not penetrate the thermocline in the west.

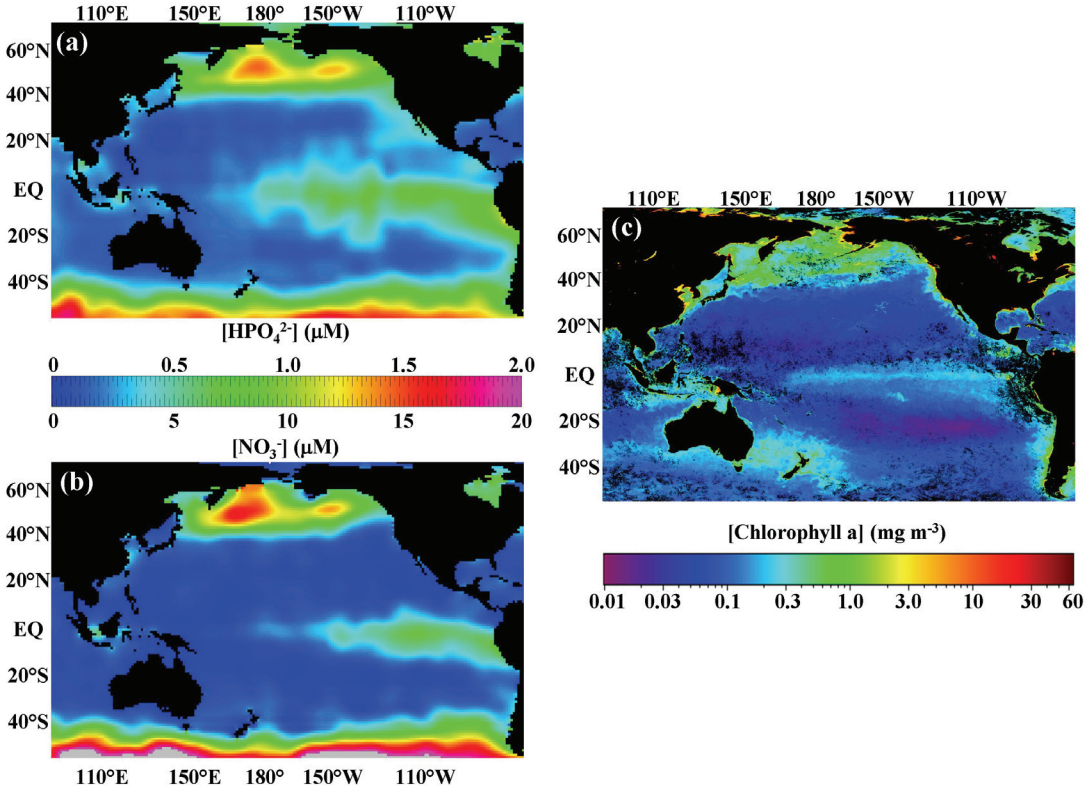

Figure 1.7 – Surface characteristics of the Pacific Ocean. (a) $[HPO_4^{2-}]$ and (b) $[NO_3^-]$ in μM. (c) satellite-derived surface chlorophyll a in mg m^{-3}. Panels (a, b) created at http://ingrid.ldeo.columbia.edu/SOURCES/.LEVITUS94/ with nutrient data from Conkright et al. (1994) and Levitus et al. (1994). Chlorophyll data is a monthly mean for September 2003, observed via satellite (Level-3 Standard Mapped Images, Aqua-MODIS, http://oceancolor.gsfc.nasa.gov/). Note the spatial coupling between nutrients and chlorophyll, specifically in the equatorial Pacific.

Table 1.1 – Studies examining surface-water Si biogeochemistry in the open ocean before 2003.

Open-ocean region	Reference
[+]NW Sargasso Sea	[*]Brzezinski and Nelson 1995, [*]Brzezinski and Nelson 1996, Brzezinski and Kosman 1996, [*]Nelson and Brzezinski 1997
Gulf Stream Warm Core Rings	Nelson et al. 1985, Brzezinski and Nelson 1989, Nelson and Brzezinski 1990
[+]North Pacific Gyre	Brzezinski et al. 1998,
[+]Equatorial Pacific	Blain et al. 1997, Blain et al. 1999, Leynaert et al. 2001
[#]Southern Ocean (all sectors)	Nelson and Gordon 1982, Tréguer et al. 1990, Nelson et al. 1991, Quéguiner et al. 1991 Nelson and Tréguer 1992, DeMaster et al. 1992, Leynaert et al. 1993, Nelson et al. 1996, Franck et al. 2000, Brzezinski et al. 2001, Nelson et al. 2001, Nelson et al. 2002, Sigmon et al. 2002

[+]***List is exhaustive***
[*]Conducted at the BATS site
[#]List is ***not*** exhaustive

2. Biogeochemical responses to late-winter storms in the Sargasso Sea. II. Increased rates of biogenic silica production and export

Jeffrey W. Krause, David M. Nelson, Michael W. Lomas

Paper II of IV in coordinated series, submitted October 2007 to Deep-Sea Research I
In revision for resubmission
DSR Editorial Office
Department of Marine Chemistry & Geochemistry
Woods Hole Oceanographic Institution, MS 25
Woods Hole, MA 02543
USA

2.1 Abstract

Previous studies measuring biogenic silica production in the Sargasso Sea, all conducted when no phytoplankton bloom was in progress, have reported a mean rate of 0.4 mmol Si m^{-2} d^{-1} and maximum rate of 0.9 mmol Si m^{-2} d^{-1}, the lowest rates yet recorded in any ocean habitat. During February/March of 2004 and 2005 we studied the effects of late-winter storms prior to seasonal stratification on the production rate, standing stock and vertical export of biogenic silica in the Sargasso Sea. In 2004, alternating storm and stratification events provided pulsed input of nutrients to the euphotic zone. In contrast, nearly constant storm conditions in 2005 caused the mixed layer to deepen to ~350 m toward the end of the cruise. Biogenic silica production rates in the upper 140 m were statistically indistinguishable between years, averaging ~1.1 mmol Si m^{-2} d^{-1}. In early March 2004, a storm event entrained nutrients into the euphotic zone and, upon stabilization, vertically integrated biogenic silica in the upper 140 m nearly doubled in two days. Within four days, 75–100% of the accumulated biogenic silica was exported, sustaining a flux to 200 m of ~0.5 mmol Si m^{-2} d^{-1} (4x greater than export measured during February and March in the mid 1990s). In 2005, destabilization without stratification increased biogenic silica flux at 200 m by ~2x above previously measured export in late winter, with little or no increase in water-column biogenic silica. Despite comprising <5% of total chlorophyll, diatoms accounted for an estimated 25–50% of the nitrate uptake in the upper 140 m and 35–97% of the particulate organic nitrogen export from the upper 200 m during both cruise periods. These previously unobserved brief episodes of diatom production and export in response to late winter storms, increase the estimated production and export of diatom-derived material in the Sargasso Sea in late winter by >150%, and increase estimated annual biogenic silica production in this region by ~9%.

2.2 Introduction

The Sargasso Sea is thermally stratified most of the year (Steinberg et al. 2001). Deep convective mixing in winter entrains nutrients and supports a spring bloom following seasonal stratification (e.g. Michaels et al. 1994, Steinberg et al. 2001). Primary production in the Sargasso Sea is believed to be limited by N throughout most of the stratified period (Lipschultz 2001) with some reports of P limitation (Ammerman et al. 2003). Since 1988 the Sargasso Sea has been sampled monthly to bi-weekly (during the spring only) by the Bermuda Atlantic Time-series Study (BATS) and the resulting data have greatly improved estimates of biological rates in the system (e.g. Steinberg et al. 2001, Lipschultz et al. 2002).

New production, defined as primary production supported by N from outside sources (Dugdale and Goering 1967), has been estimated in the Sargasso Sea by a variety of indirect methods, including seasonal changes in subsurface oxygen (Jenkins and Goldman 1985), nitrate flux as estimated via ^{3}He profiles (Jenkins 1988, Jenkins and Doney 2003) and the combination of noble gas and oxygen tracers (Spitzer and Jenkins 1989). These estimates integrate over large spatial scales and time periods of months, and are applicable only to the period after water-column stratification in spring. New production has been estimated on shorter time scales from the subsurface $[O_2]$ anomaly, euphotic-zone $[NO_3^-]$ changes, drawdown of dissolved inorganic carbon in surface waters (Michaels et al. 1994) and from measurements of ^{15}N uptake (e.g. Lipschultz 2001). Similar to the longer-term and larger-scale estimation methods, most of the shorter time scale estimates of new production apply only to the period after seasonal stratification. Lipschultz (2001) showed, by ^{15}N uptake rates, that uptake of NO_3^- is sometimes rapid in late winter (>150 nmol l^{-1} d^{-1}, March 1992), potentially supporting high rates of new production.

It has been suggested (Lipschultz et al. 2002, Lomas et al. *in revision* a) that pulses of rapid phytoplankton growth in response to short-term mixing and stratification events associated with the passage of storms in late winter may be a source of new production. This type of new production has not been caught either by geochemical estimates (because those estimates generally apply only to stratified periods) or by the BATS sampling regime (because the BATS research vessel has

been incapable of operating during storms). It has been hypothesized that the passage of a storm would entrain nutrients into the euphotic zone, then water-column stabilization would cause the mixed layer to shoal to less than the critical depth (Sverdrup 1953), allowing for pulsed new production and export, most likely on time scales of days to a week (Lomas et al. *in revision* a).

Diatoms account for an estimated 30% of global oceanic primary production (Nelson et al. 1995, Tréguer et al. 1995, Raven and Waite 2004) and a potentially higher fraction of export production (Michaels and Silver 1988, Honjo et al. 2008). In the Sargasso Sea, biogenic particulate silica ($bSiO_2$) concentrations (a proxy for diatom biomass) and $bSiO_2$ production rates (a proxy for diatom productivity) are among the lowest reported from the world ocean (Table 2.1). Microscopy and pigment analysis indicate that the diatom contribution to total autotrophic biomass in the Sargasso Sea is quite small, <5% of total chlorophyll (Goericke 1998, Steinberg et al. 2001). Despite generally low diatom biomass, large and numerically rare diatoms reside at the base of the euphotic zone and have been hypothesized to contribute substantially to new production through episodic pulses of rapid growth (Goldman 1993, Goldman et al. 1992, Goldman and McGillicuddy 2003). Previous studies indicate that diatoms contribute ~30% of annual POC export in the Sargasso Sea, and >90% during the spring bloom (Nelson and Brzezinski 1997). The diatoms' physiological capacity for nutrient storage (Lomas and Glibert 1999, and references therein) coupled with observed rapid N turnover in late winter (Lipschultz 2001), suggests that new production resulting from late-winter destabilization and stabilization could be driven largely by diatoms. The goal of the study reported here was to quantify the diatom response to late-winter storms in the Sargasso Sea, by measuring temporal changes in dissolved [$Si(OH)_4$] and [$bSiO_2$], and rates of $bSiO_2$ production and export as storms altered nutrient availability and water-column stability. Because the BATS program does not sample during storms, it is likely that physical perturbations and biological responses of the kind reported here have not been previously observed in the Sargasso Sea.

2.3 Methods

We tracked changes induced by destabilization and subsequent stabilization events in the upper water column of the Sargasso Sea during two 30-day cruises (15 February through 15/16 March 2004 and 2005). We sampled in a quasi-Lagrangian fashion by following a holey-sock drogue deployed at 10 m. To avoid eddies (which can inject nutrients into the surface water via their flow characteristics, McGillicuddy et al. 1998) sea-level anomaly (SLA) maps were used to deploy drogues in eddy-free areas (SLA ≈ 0, maps courtesy of D. McGillicuddy). Four drogue deployments were made in eddy-free areas, lasting from ~5 to 12 days; drogue trajectories and station locations are shown in Figure 2.1. Drogue deployments will be referred to as 2004-1, 2004-2, 2005-1 and 2005-2 as shown in Figure 2.1.

Hydrocasts were conducted within 0.5 km of the drogue and a suite of rate and standing stock measurements was performed on the collected water, most in accordance with BATS protocols (Knap et al. 1997). Two bottles were closed at each of eight depths (0, 20, 40, 60, 80, 100, 120 and 140 m), with some profiles extending to 220 m during the deployment 2005-2. Bottle contents were immediately drained into acid-cleaned 20-liter high-density polyethylene carboys; this allowed the sample to be mixed frequently while sub-sampling. The focus of this study was Si cycle parameters; those methods will be described below. For a description of other measurements and results see Lomas et al. (*in revision* a, b) and Maiti et al. (*in revision*).

Samples drawn for analysis of ambient [$Si(OH)_4$] were syringe-filtered through 0.45 μm pore size acetate filters. The filtrate was analyzed as described by Strickland and Parsons (1972), with a modified reagent blank (Brzezinski and Nelson 1986). Sodium hexaflurosilicate (Na_2SiF_6) standard curves were made in deionized water; empirically-derived corrections were applied to the measured [$Si(OH)_4$] to adjust for sample salinity (Nelson and Sigmon unpublished).

Two-liter samples for $bSiO_2$ analysis were filtered under gentle vacuum onto 0.6 μm pore size, 47 mm diameter polycarbonate filters, which were then folded into quarters, placed in polystyrene Petri-dishes, dried in an oven, and sealed until laboratory analysis was performed on land. Samples were analyzed by NaOH

digestion (Paasche 1973) with the 2-h modification of digestion time recommended for Sargasso Sea samples by Brzezinski and Nelson (1995). Digestions of samples from the 2004 cruise were carried out in 15-ml polypropylene tubes, which yielded acceptably low blanks. However, for an unknown reason, tubes bought for these analyses in 2005 gave high and irregular blanks. Therefore, samples from the 2005 cruise were digested in 10-ml Teflon tubes which gave low and consistent blank values. Lithogenic silica concentrations in the surface waters of the Sargasso Sea are low during winter (<5 nmol l^{-1}; Nelson and Brzezinski 1997) and <2% of that material dissolves during a 2-h NaOH digestion (Brzezinski and Nelson 1995); therefore, the measured $bSiO_2$ was essentially free of interference from lithogenic silica.

Biogenic silica production rates were measured daily, concurrent with nitrate uptake and primary productivity measurements. Day and night rate measurements were made with water collected from casts begun at ~02:00 and ~19:00 (local time) respectively. Tracer additions were made with the radioisotope ^{32}Si. For daytime incubations, bottles were placed in mesh bags and secured to a free-floating spar array, allowing the samples to be held at the depth from which they had been collected and experience *in situ* light and temperature. Spars were deployed just before dawn and retrieved just after sunset. For night incubations, bottles were placed in on-deck incubators with flow-through surface seawater; because the mixed layer depth was generally deeper than 140 m (c.f. Figure 2.2), the surface seawater properly simulated *in situ* temperatures at all depths sampled. The rough weather sometimes created conditions unsafe for CTD casts, thus some days only had one rate profile (e.g. either day or night). Hence we assessed daily integrated ρ only for those 24-h periods during which vertical profiles of both day and night rates were obtained.

We used high specific activity (HSA; >500 kBq/μmol Si) or lower specific activity (LSA; 6.25 kBq/μmol Si) $^{32}Si(OH)_4$ stocks. The target HSA and LSA activities were ~0.75 and ~2.5 kBq (~45,000 and ~150,000 DPM) respectively, in a nominal 300-ml seawater volume. No ^{32}Si incubations were replicated; this was due mainly to the exceptionally high cost of ^{32}Si (>$1000 USD per μCi of ^{32}Si), and the fact that production of the isotope has ceased (it was formerly produced at the Los Alamos National Laboratory, USA). Owing to these constraints, we are unaware of

any published field study using ^{32}Si that has replicated production-rate measurements (c.f. studies in Table 2.1 and references therein). Prior to use, the ^{32}Si isotope stock was passed through Chelex resin to removal trace metals. After ^{32}Si addition, samples were gently agitated to mix the tracer, and incubated as described above. Following incubation, the bottle contents were filtered onto a 0.6 μm pore, 25 mm diameter polycarbonate filter under gentle vacuum (<25 cm Hg). Dry filters were placed in plastic liquid scintillation vials, loosely capped until dry, and then stored in the dark until analyzed on land.

Liquid scintillation counting was performed by methods described by Nelson et al. (2001) after waiting at least 100 days for ^{32}Si to reach secular equilibrium with its daughter isotope ^{32}P. The measured uptake rate (ρ in nmol Si l^{-1} h^{-1}) was integrated to the deepest sample depth (140 m or 220 m) by trapezoidal integration.

A biomass-specific uptake rate (V in h^{-1}) was calculated as:

$$V = \rho / [bSiO_2]$$

where $[bSiO_2]$ = the biogenic silica concentration (nmol Si l^{-1}).

Chronically low $[Si(OH)_4]$ in the Sargasso Sea made it necessary to account for the $Si(OH)_4$ added in our tracer solutions. Previous studies at BATS have shown a linear increase of V with $[Si(OH)_4]$ from ambient to >5 μmol Si l^{-1} (Brzezinski and Nelson 1996). ρ was therefore scaled by:

$$\rho_{CORRECTED} = \rho_{MEASURED} \times \{[Si(OH)_4]_{In\ situ} / ([Si(OH)_4]_{In\ situ} + [Si(OH)_4]_{TRACER})\}$$

Our isotope addition never resulted in a total (*in situ* plus added) $[Si(OH)_4]$ >2.4 μmol Si l^{-1} and >97% of all samples had $[Si(OH)_4]$ <2.0 μmol Si l^{-1}.

To quantify gravitational particle flux, BATS-style surface-tethered particle interceptor traps (PITS; Knap et al. 1997) were deployed for 2–5 days at depths of 200, 300, and 400 m. Eight PITS were deployed at each depth, of which three (randomized with respect to rack position) were allocated to $bSiO_2$. Trap deployment, recovery, design and the quantification of particulate organic carbon (POC) and nitrogen (PON) fluxes are described by Knap et al. (1997). Particulate matter fluxes measured by sediment traps can be biased due to hydrodynamic effects (Gust et al. 1994), release of dissolved matter (Knauer et al. 1984) and presence of swimmers (Michaels et al. 1990). Under-collection is a well noted problem in sediment traps

deployed at depths <500 m; however, Stanley et al. (2004) showed that PITS measure a statistically higher $bSiO_2$ flux, compared to neutrally-buoyant sediment trap designs, while simultaneously under-collecting other elements. With no published quantitative corrections available (for either over or under-collection), PITS $bSiO_2$ in this study was not corrected for possible sediment trap bias.

After recovery, the contents of each PIT designated for measurement of $bSiO_2$ flux were gravity filtered through a 0.8 μm pore size, 76 mm diameter, polycarbonate filter. Immediately after filtration, each filter was folded into quarters, placed in a polystyrene Petri dish and oven dried. Swimmers were not picked off the filters that were to be analyzed for $bSiO_2$, as significant contamination of $bSiO_2$ by swimmers is unlikely (Brzezinski and Nelson 1995). Because seawater is undersaturated in $Si(OH)_4$, a significant and variable amount of $bSiO_2$ entering the trap may dissolve during the deployment. We therefore measured $[Si(OH)_4]$ in the brine solution before and after deployment, allowing for quantification of any increase in $[Si(OH)_4]$ in PITS tubes that resulted from dissolution of $bSiO_2$ from settled particles during the deployment. Initial PITS brine solution (seawater with ~85 g NaCl l^{-1} and ~0.7% formaldehyde; brine filtered prior to deployment) was used to make a seven-point $[Si(OH)_4]$ standard-addition curve with two reagent blanks for each deployment solution. Using the initial brine standard-addition curve, the filtrate from the PITS tubes was analyzed for $[Si(OH)_4]$ as described above for seawater samples,. $bSiO_2$ on PITS filters was analyzed by NaOH digestion method described for $bSiO_2$ samples; modifications were made in digestion volume because the $bSiO_2$ mass collected was much larger than that collected in standing stock samples. And after digestion, samples were centrifuged to remove optical interference from the remaining particulate matter; 0.3 ml of the supernatant fluid was diluted to 10 ml for analysis of $Si(OH)_4$ (dissolved $bSiO_2$). The total $bSiO_2$ flux was calculated as the sum of the measured particulate $bSiO_2$ flux (from NaOH digestions) and the $bSiO_2$ that dissolved in PITS tube before recovery.

2.4 Results

2.4.1 Physical conditions

During both 2004 and 2005 we experienced wind stress and relaxation events that lasted from one to several days (Figure 2.2a, d). In 2005, the storm forcing was stronger, more frequent and of longer duration than in 2004 (t-test comparisons between years for wind speed, net heat flux and mixed layer depth; $p<0.001$ for all, Figure 2.2). During both cruises the net heat flux was predominantly negative (from the ocean to the atmosphere; Figure 2.2b, e). Periods of intensified negative heat flux resulted from dramatically increased wind speeds and decreased relative humidity associated with the passage of storm fronts (e.g. year day 61, 2004; Figure 2.2a,b). For most of both cruise periods the sea-surface temperature exceeded air temperature, increasing the negative net heat flux and convective mixing. In 2005 the duration of intensified negative net heat flux events was typically ~3–4 days, ~2x longer than events in 2004. Crossover to positive heat flux in 2004 was generally associated with the mid-day maximum solar radiation; however, in 2005 the mid-day solar radiation was seldom strong enough to yield positive net heat flux. During deployment 2005-2 mixed layer (ML) depths were consistently >300 m, whereas ML depths >200 m were unusual in 2004 (Figure 2.2c, f).

2.4.2 Nitrate dynamics

Temporal variance of $[NO_3^-]$ in the upper 140 m was on the scale of days (Figures 2.3, 2.4, note: NO_3^- measurements were made more often than $Si(OH)_4$). In 2004, during drogue deployment 2004-1, the 100 nmol l^{-1} $[NO_3^-]$ isopleth shoaled to a minimum of ~50 m on day 56, then deepened rapidly to > 100 m by the end of day 57 (Figure 2.3). From days 68 through 75, during deployment 2004-2, the 500 nmol l^{-1} $[NO_3^-]$ isopleth shoaled to a minimum of ~60 m, shallower than at any time during deployment 2004-1; however, the 100 nmol l^{-1} $[NO_3^-]$ isopleth remained ~50 m for the entirety of this drogue deployment. The 100 nmol l^{-1} $[NO_3^-]$ isopleth did not penetrate the surface water during either deployment, but remained at or below ~50 m. The nitrate input-drawdown cycles were more prominent in 2004 than in 2005. $[NO_3^-]$ in

the euphotic zone was higher, with less temporal variability in 2005 than in 2004. Upper water column [NO_3^-], during deployment 2005-1, increased from ~150 to > 200 nmol l^{-1}; while during deployment 2005-2 [NO_3^-] was consistently >400 nmol l^{-1} throughout the euphotic zone (Figure 2.4).

2.4.3 Silicic acid and biogenic silica

Silicic acid had a pulse/drawdown behavior similar to that of nitrate in 2004 (Figure 2.3). The average [$Si(OH)_4$] in the upper 140 m during the 2004 cruise was 0.84 ±0.11 μmol l^{-1} (mean ±std. dev.). During deployment 2004-2 [$Si(OH)_4$] in the lower euphotic zone reached ~1.0 μmol l^{-1} with ~0.9 μmol l^{-1} penetrating to ~15 m on days 67 and 68; this was coincident with increased convective mixing (Figure 2.2a) and upward movement of nitrate (Figure 2.3b). Considering all data from the 2004 cruise, [$Si(OH)_4$] upper 140 m ranged from ~0.7 to ~1.1 μmol l^{-1}, a smaller range than for [NO_3^-] (Figure 2.3). Net increase in [$bSiO_2$] was confined to brief (~1 day) periods coincident in time with $Si(OH)_4$ and NO_3^- injections (Figure 2.3). The average [$bSiO_2$] during 2004 was 15±10 nmol l^{-1}, with a range of ~5 to ~70 nmol l^{-1}. Thus [$bSiO_2$] was consistently <10% of [$Si(OH)_4$] and the total range in [$bSiO_2$] (~65 nmol l^{-1}) was < 20% of that in [$Si(OH)_4$] (400 nmol l^{-1}). Vertically integrated $bSiO_2$ ($\int bSiO_2$; all nutrient, biomass, and rate integrations extend from the surface to 140 m unless otherwise stated) varied only by a factor 2–3 for the entirety of the 2004 cruise, with maximum $\int bSiO_2$ occurring between days 68 and 70.

There were statistically significant differences in both vertically integrated $Si(OH)_4$ and vertically integrated $bSiO_2$ between years, with $\int Si(OH)_4$ higher and $\int bSiO_2$ lower in 2004 (Table 2.2). On drogue deployment 2005-1 [$Si(OH)_4$] decreased with time between days 58 and 60, while [NO_3^-] was increasing (Figure 2.4). In contrast, a pronounced increase in [$Si(OH)_4$] occurred during deployment 2005-2; during a ~3 day period (days 69 through 71) surface-layer [$Si(OH)_4$] rose monotonically from ~0.65 to ~0.85 μmol l^{-1} (Figure 2.4). As [$Si(OH)_4$] rose, [$bSiO_2$] decreased by ~50% within a ~5 day period (days 68 through 72; Figure 2.4).

2.4.4 Biogenic silica production

Biogenic silica production rates (ρ) in 2004 were variable with time, but in most profiles ρ was nearly uniform with depth (Figure 2.3). Integrated rates for the upper 140 m (∫ρ) ranged from ~0.010 to 0.250 mmol Si m^{-2} h^{-1}, with a mean of 0.060 mmol Si m^{-2} h^{-1}. Daily ∫ρ (calculated from coupled profiles from the same 24-h period; see methods) in 2004 was 1.03 ±0.82 mmol Si m^{-2} d^{-1} (n=10). A statistically significant difference in ∫ρ between day and night was observed in 2004 (t-test, $p<0.005$). The mean ∫ρ from all night incubations was 0.098 ±0.071 mmol Si m^{-2} h^{-1}, more than four times the mean ∫ρ in daytime, 0.023 ±0.027 mmol Si m^{-2} h^{-1}. Similar day versus night trends were observed on both deployments.

In 2005, ∫ρ was not significantly different from that in 2004 (Table 2.2). The total range was nearly identical to that in 2004, with a mean of 0.058 mmol Si m^{-2} h^{-1}. The daily ∫ρ for 2005 was 1.17±1.26 mmol Si m^{-2} d^{-1} (n=12). A day versus night difference was observed on deployment 2005-1, but not on 2005-2. Considering all data from 2005, ∫ρ at night was 0.075 ±0.084 mmol Si m^{-2} h^{-1} versus 0.040 ±0.041 mmol Si m^{-2} h^{-1} during the day; these rates were not significantly different (t-test, $p = 0.209$). During deployment 2005-2, ρ measurements were extended to 220 m because of the very deep ML encountered (see Figure 2.2f); however, >85% of integrated production to 220 m was within the upper 140 m. ρ decreased abruptly in the upper water column during deployment 2005-2, between days 66 and 67; this rapid drop in ρ preceded the monotonic increase in $[Si(OH)_4]$ and decrease of $\int bSiO_2$ described above by ~2 days (Figure 2.4).

Specific rates of $bSiO_2$ production (V) in 2004 were 0.03 ±0.04 h^{-1}, corresponding to a mean $bSiO_2$ doubling time of ~23 h. During 2004 vertical variability in V was much less pronounced than variability in time, with some profiles having specific rates > 0.10 h^{-1}, while in other profiles V was < 0.01 h^{-1} at all depths (Figure 2.3). In 2005 the mean V was 0.02 ±0.03 h^{-1}, corresponding to an average doubling time of ~35 h. As in 2004, there was significant temporal variability in V. This is seen most dramatically in the comparison between deployments 2005-1 and

2005-2; during 2005-1 V was ~5–10x higher than near the end of deployment 2005-2 (Figure 2.4).

2.4.5 Biogenic silica export

During both 2004 and 2005 the gravitational $bSiO_2$ export flux decreased with depth between 200 and 400 m. In 2004 the average $bSiO_2$ fluxes were 0.36 ±0.16, 0.28 ±0.20, and 0.18 ±0.11 mmol m^{-2} d^{-1} at 200, 300, and 400 m, respectively (Figure 2.5). The ratio of silica export at 200 m to integrated silica production in the upper 140 m ($E/\int\rho$, using the daily $\int\rho$) in 2004 was 0.32, indicating that on average ~32% of the $bSiO_2$ produced in the upper 140 m was being captured in sediment traps deployed at 200m. Similarly, ~50% of the $bSiO_2$ flux reaching 200 m was remineralized by 400 m. Deployment 2004-2 had the highest $bSiO_2$ export flux measured on any drogue deployment in either year (ANOVA, $F=12.4$, $p<0.001$); this high flux was coincident in time with pulsed inputs of NO_3^- and $Si(OH)_4$ to the euphotic zone (Figure 2.3).

The mean export flux of $bSiO_2$ from the upper 200 m measured during 2005 was not significantly different from that in 2004 (t-test, $p = 0.056$); however, fluxes from both deployments in 2005 were significantly lower than those on 2004-2 (direct t-test comparisons, $p<0.01$, or see ANOVA results comparing all deployment fluxes, above). Mean $bSiO_2$ fluxes at 200, 300, and 400 m were 0.26 ±0.10, 0.18 ±0.08, and 0.12 ±0.07 mmol m^{-2} d^{-1}, respectively (Figure 2.5). The average $E/\int\rho$ ratio at 200 m in 2005 was ~0.22. The difference in $E/\int\rho$ ratios between years was driven by the higher export fluxes measured during drogue deployment 2004-2, as the mean $\int\rho$ varied little between 2004 and 2005. As in 2004, ~50% of the $bSiO_2$ flux reaching 200 m remineralized by 400 m.

2.5 Discussion

During both cruises the average vertically integrated $bSiO_2$ production rates ($\int\rho$) were ~1.1 mmol Si m^{-2} d^{-1}, ~20% higher than the single highest daily $\int\rho$ previously measured in the Sargasso Sea, and nearly three times the mean $\int\rho$ from previous observations (Brzezinski and Nelson 1995; Brzezinski and Kosman 1996, Nelson and Brzezinski 1997). Higher diatom productivity was also evident in the

higher $bSiO_2$ export fluxes at 200 m compared to similar times of year at the BATS site in the early 1990s (Nelson and Brzezinski 1997). Despite these higher rates of $bSiO_2$ production and export during both of our late-winter cruises, variability in the standing stock of biogenic silica was quite small; the $\int bSiO_2$ coefficient of variation (i.e. std. dev./mean) was 0.57 and 0.18 for 2004 and 2005, respectively. $\int bSiO_2$ during both years was similar to $\int bSiO_2$ during the seasonally stratified periods in the early 1990s and much lower than those during the spring bloom (Brzezinski and Nelson 1995). During spring bloom periods, Brzezinski and Nelson (1995) reported $\int bSiO_2$ near 10 mmol m^{-2}, ~4–5 times the values we observed in late winter (Table 2.2). This raises the question: how can such high rates of $bSiO_2$ production and export occur in late winter with little or no net accumulation of $bSiO_2$ in the surface layer?

The physical data show stark contrasts between the late winter periods of 2004 and 2005. The sustained intensity of the winds and the persistent negative net heat flux in 2005 deepened the ML from ~200 m during drogue deployment 2005-1 to >300 m during 2005-2, with none of the intermittent shoaling that was seen in 2004 (Figure 2.2). The result was a significant difference in nutrient concentrations and $bSiO_2$ standing stock (Table 2.2). These conditions are discussed below, separately for the two years.

2.5.1 Biogenic silica production and export during late winter 2004

During 2004 we observed destabilization and stabilization events similar to those hypothesized by Lomas et al. (*in revision* a). A net heat loss resulted from storms (Figure 2.2), causing a deepening of the ML which convectively entrained NO_3^- and $Si(OH)_4$ into the euphotic zone; subsequently, there was biological drawdown of both nutrients (Figure 2.3). Diatom growth and primary production in the Sargasso Sea are generally thought to be N-limited (Nelson and Brzezinski 1997), with additional limitation of Si uptake rates by low $[Si(OH)_4]$ (e.g. Brzezinski and Nelson 1996, Mongin et al. 2003). The increases in $[NO_3^-]$ and $[Si(OH)_4]$ supplied by convective entrainment, thus potentially relieved a certain degree of limitation to both diatom primary production (from NO_3^- enrichment) and silicification (from $Si(OH)_4$ enrichment).

The nutrient injection event observed during drogue deployment 2004-2 (between days 66 and 70) resulted in a >3x increase in $\int NO_3^-$, a ~20% increase in $\int Si(OH)_4$, and an initial enhancement of $\int \rho$ (Figure 2.6). The rapid increase of $\int Si(OH)_4$ in the euphotic zone from day 67 to 68 was not seen in $\int NO_3^-$ (Figure 2.6), despite the fact that the maximum vertical gradient in $[NO_3^-]$ in the Sargasso Sea is consistently shallower than that for $[Si(OH)_4]$ (Sarmiento et al. 2007, see also Lomas et al. *in revision* a). This suggests biological removal of NO_3^- on time scales shorter than the spacing of our casts (typically 6–8 h) and, indeed, rates of NO_3^- uptake (2.17 mmol N m^{-2} d^{-1}) and primary production (74.6 mmol C m^{-2} d^{-1}) on day 68 were the highest observed on deployment 2004-2 (Lomas et al., *in revision* a). An increase in $\int bSiO_2$ (over the mean value during 2004-2) occurred on day 68, following the injection of NO_3^- and $Si(OH)_4$ (between day 67 and 68; Figure 2.3, 2.6). The accumulation of $\int bSiO_2$ was supported by initially high uptake rates of $Si(OH)_4$ prior to the actual accumulation of nutrients in the upper 140 m (Figure 2.6). This nutrient pulse event was followed by a high $bSiO_2$ flux to 200 m, doubling the measured $bSiO_2$ flux during the 2004-1 deployment (Figure 2.5). By days 71 and 72 the ambient nutrient conditions were back near the cruise average (c.f. Table 2.2), and $\int bSiO_2$ had declined to < 50% of the peak value it attained on day 69 (Figure 2.6).

During drogue study 2004-2 we deployed PITS from day 66.6 to 70.4, and 70.5 to 74.3 (Figure 2.5). The increase in $bSiO_2$ flux during 2004-2 (versus 2004-1) corresponded in time with the nutrient enhancement observed on day 66 at the start of deployment 2004-2). Thus the storm-driven injection of NO_3^- and $Si(OH)_4$ between days 66 and 68 appears to have initiated a chain of events: higher $\int \rho$, followed by an increase in $\int bSiO_2$ (Figure 2.6), followed by increased $bSiO_2$ export (Figure 2.5). During this same period, Lomas et al. (*in revision* b) reported an increase in the diatom pigment marker fucoxanthin. This succession started during the first PITS deployment (days 66 through 70), but because both PITS deployments lasted approximately four days it is unknown precisely when the enhanced export started. However, all measured properties of the system indicate intensified diatom activity, for a period of about four days, following a storm-induced nutrient injection.

Following the nutrient injection on ~day 67, the decrease in $\int bSiO_2$ from day ~70 to 72 corresponded with lower, but still relatively high, ρ (Figure 2.6). The magnitude of the net $\int bSiO_2$ decrease over this 4-day period was ~2.4 mmol m^{-2} (Figure 2.6) and the length of the PITS deployment, covering that decline period, was 3.74 d. If all the net decrease in $\int bSiO_2$ in the upper 140 m were exported to 200 m, without any dissolution, then the loss of $\int bSiO_2$ would have supported a maximum export flux of 0.64 mmol Si m^{-2} d^{-1} during the 3.74 d deployment. This maximum estimate is ~25% higher than the measured $bSiO_2$ flux at 200 m during that period (Figure 2.5). Consequently we estimate that ~75% of the net $\int bSiO_2$ accumulation, which was stimulated by the nutrient injection event, was accounted for as $bSiO_2$ flux in the 200 m PITS between days 70.6 and 74.4.

It is evident from this time course that a large fraction of the $\int bSiO_2$ that accumulated in response to a pulsed nutrient event was rapidly exported (i.e. ~4 days) to depths > 200 m. The chances of sampling the nutrient injection, $bSiO_2$ accumulation and $bSiO_2$ export event (all induced by a winter storm), would be very low considering their short duration. Beyond that, previous BATS cruises would not have sampled during the weather conditions sampled in this study. Thus, it is unlikely that an event of this nature would have been sampled in the 16 years of the BATS program before these cruises, even if it were a common occurrence in late winter. Sampling events of this type should be possible in the future with the new research vessel at the BATS program (*R/V Atlantic Explorer*, operating since spring 2006).

2.5.2 Biogenic silica production and export during late winter 2005

The consistently higher $[NO_3^-]$ in 2005 is perhaps the most striking chemical difference between the two years. This increased N supply presumably led to the ~30% higher $\int bSiO_2$ measured in 2005 and to the lower $\int Si(OH)_4$ observed the same year, while the mean daily $\int \rho$ was statistically indistinguishable between years (t-test, p=0.75). The year-to-year increase in average $\int bSiO_2$ is only ~7% of the corresponding decrease in $\int Si(OH)_4$. This could imply a decrease in the source-water $[Si(OH)_4]$ between 2004 and 2005; however, $\int Si(OH)_4$ from 300–500 m was statistically indistinguishable between 2004 and 2005 (t-test, p=0.75, Lomas et al. *in*

revision a), making that explanation unlikely. Another possible explanation is that considerably more export of $bSiO_2$ happened before day 46 (February 15) in 2005 than in 2004, resulting in a lower inventory of Si (dissolved + particulate) in the upper water column at the start of our observations in 2005.

The high variance in $\int\rho$ was due to a systematic difference between rates on the two drogue deployments: during deployment 2005-1 $\int\rho$ was nearly an order of magnitude higher than $\int\rho$ during 2005-2 (Table 2.2). The deeper ML during 2005-2 was ~3x the average euphotic zone depth (c.f. Siegel et al. 2001) with little or no evidence of even temporary shoaling. Given the high nitrate availability in 2005, this combination almost undoubtedly led to increased light limitation (Sverdrup 1953, Siegel et al. 2001) of diatom productivity. The observed decrease in ρ was likely a result of diminished respiratory energy (which is used for silicification, Raven 1983). Despite temporal, and sometimes vertical, decoupling, energy derived from photosynthesis is needed to sustain Si uptake. Within a well-mixed surface layer, cells can be randomly moved between lighter and darker depths (e.g. Backhaus et al. 2003). As the ML deepened to ~350 m during deployment 2005-2, severe light limitation likely diminished diatom growth and viability; this may be part of the reason for the marked decrease in upper water column ρ and $[bSiO_2]$ (Figure 2.4), and also the decline in $bSiO_2$ export with time (compare PITS deployments from 2005-2, Figure 2.5). Interestingly, while diatom biomass was apparently declining total autotrophic biomass was increasing (Lomas et al. *in revision* a, b). This suggests that light-limitation imposed by deep convective mixing may be sufficient to overcome the diatoms' competitive edge under otherwise high-nutrient and high-turbulence conditions; this situation should be incorporated into biogeochemical models that include diatoms and Si cycling.

During deployment 2005-2 a monotonic increase in $[Si(OH)_4]$ was observed from day 69 through 71, corresponding in time with declining ρ and $[bSiO_2]$ throughout the upper water column (Figure 2.4), and declining $bSiO_2$ flux at 200, 300, and 400 m (see second PITS deployment during 2005-2, Figure 2.5). The net heat flux during most of the 2005 cruise was negative (Figure 2.2); thus the ML deepened, and more $Si(OH)_4$ was entrained into the euphotic zone. However, the monotonic

buildup of $Si(OH)_4$ in the upper water column happened only after diatom growth throughout the same vertical interval declined precipitously between day 66 and 67 (Figure 2.4); this suggests that diatom uptake of $Si(OH)_4$ before day 68 was sufficient to prevent any sizable accumulation of $Si(OH)_4$ in the euphotic zone. This would support the idea that the N-replete diatom community was able to take up any new $Si(OH)_4$ introduced from depth by physical processes. Considering that the mean $\int NO_3^-$ in February/March 2005 was >2x greater than in the corresponding period in 2004 (Table 2.2), the greater input of NO_3^- from deep water was likely fueling enhanced $bSiO_2$ production, export and depletion of $Si(OH)_4$, until the abrupt drop in diatom activity between day 66 and 67.

From day 66 through 73 $\int\rho$ was ~0.015 μmol Si m^{-2} h^{-1} (Table 2.2, note: daily rate during this period was ~0.3 mmol Si m^{-2} d^{-1}) and the export flux at 200 m during this same period was ~0.3 mmol Si m^{-2} d^{-1} (Figure 2.5). The resulting $E/\int\rho$ was near ~1.0, indicating either exceptionally high export efficiency or – much more likely – a temporal decoupling between $bSiO_2$ production and export.

The flux of $bSiO_2$ during the PITS deployment from day 73 to 75 was ~0.20 mmol Si m^{-2} d^{-1}, 33% lower than during the previous deployment (Figure 2.5). Thus it would appear that the upper water column decrease in ρ that occurred between day 66 and 67 (see Figure 2.4) affected gravitational fluxes at 200 m some time between days 73 and 75. The flux reaching the 200 m traps during both PITS deployments on 2005-2 (days 67–73) was most likely supported by higher $bSiO_2$ production, which had occurred before our observations began on day 66. If we assume an $E/\int\rho$ of 0.22 (the mean for the 2005 cruise period) and apply this ratio to the 200 m export data from the two PITS deployments during 2005-2 (and convert flux to an hourly rate for comparison with $\int\rho$ from Table 2.2), then the $\int\rho$ in surface waters that would be needed to support the measured export flux was ~0.06 and 0.04 mmol Si m^{-2} h^{-1}, respectively. These indirect $bSiO_2$ production rate estimates are ~1 standard deviation lower than the mean $\int\rho$ measured at during 2005-1 deployment, but are 2.5-4x higher than the mean $\int\rho$ measured during 2005-2 (Table 2.2). The differences between $\int\rho$ measured in 2005-1 and $\int\rho$ indirectly estimated to support the flux during 2005-2 may be representative of real spatial variability; which could have been due to the deep ML

depths likely preceding the 2005-2 drogue deployment (Figure 2.2). Thus, during deployment 2005-2 we suggest a temporal offset between this inferred higher biogenic silica production rate and the measured export rates on the order of 4–7 days.

While both late-winter periods showed enhanced export of $bSiO_2$, the pulsed mechanism in 2004 (the cycle of input, accumulation and export during deployment 2004-2) was more efficient in terms of rapid export of accumulated $\int bSiO_2$ to depth. In contrast, the high $[NO_3^-]$ conditions in 2005 allowed for high $\int \rho$ and high $bSiO_2$ export during drogue deployment 2005-1. But the deep ML during deployment 2005-2 led to a scenario where diatoms declined rapidly after day 68, thus slowing export rates for the remainder of the cruise.

2.5.3 Diatom new production during late winter in the Sargasso Sea

The impact of diatoms on new production in response to late winter storms has not been estimated previously. However, enhanced diatom new production has been hypothesized (Goldman 1993, Goldman and McGillicuddy 2003), observed in some Sargasso Sea models (e.g. Mongin et al. 2003) and inferred from instantaneous diatom abundance or biomass, $[Si(OH)_4]$ profiles and opal flux (Riley 1957, Hulburt et al. 1960, Siegel et al. 1990, McNeil et al. 1999, Steinberg et al. 2001, Conte et al. 2003).

Vertically integrated NO_3^- uptake in the upper water column ($\int \rho_{NO3}$), measured by ^{15}N incubation studies, was 2.19 ±1.34 and 2.14 ±1.79 mmol N m^{-2} d^{-1} for 2004 and 2005, respectively (Lomas et al. *in revision* a). Given our observed $\int \rho$ for $Si(OH)_4$, and making the maximizing assumption that diatoms were assimilating NO_3^- as their only N source (e.g. Dugdale and Wilkerson 1998) with a mean Si:N mole ratio of 1.0 (Brzezinski 1985), the mean estimated vertically integrated rate of nitrate uptake by diatoms would be 1.0 mmol N m^{-2} d^{-1} in 2004 and 1.2 mmol N m^{-2} d^{-1} in 2005. These estimates suggest that, if diatoms used NO_3^- as their sole N source, they would have been responsible for ~50% of the total NO_3^- uptake measured in both years. It is highly unlikely that diatoms use NO_3^- as their sole N source in the Sargasso Sea, even under the relatively high $[NO_3^-]$ conditions that prevailed in the late winters of 2004 and 2005. However, if diatoms had an f-ratio ($\int \rho_{NO3} / \int \rho \Sigma N$; Eppley and Peterson 1979) of 0.5 under late winter conditions in the Sargasso Sea, the observed mean $\int \rho$ for

$Si(OH)_4$ would imply that they are responsible for ~25% of new production in the system. Thus their contribution to new production is almost certainly several times greater then their < 5% contribution to autotrophic biomass (e.g. Goericke 1998, Steinberg et al. 2001).

During some PITS deployments of this study POC and PON export were also elevated above the long-term average (Lomas et al. *in revision* a). Assuming that alteration of diatom $bSiO_2$:PON ratios between the time of growth and arrival at 200 m is minimal, and applying a diatom Si:N of 1.0 (Brzezinski 1985, Nelson and Brzezinski 1997), we can convert 200 m $bSiO_2$ flux to an estimate of PON flux derived from organic matter produced by diatoms. By that calculation we estimate that diatoms were responsible for 88–97% and 35–82% of the observed flux in 2004 and 2005, respectively (the estimated range represents temporal variability in $bSiO_2$ flux between individual PITS deployments in 2004 and 2005, PON flux data from Lomas et al. *in revision* a). Similarly, we can estimate the diatom contribution to POC flux by using a diatom Si:C mole ratio of 0.13 (Brzezinski 1985, Nelson and Brzezinski 1997), and compare the estimated diatom POC flux with measured total POC flux (Figure 2.5). This comparison yields an estimated diatom contribution of 64–93% of the POC export in 2004, and 41–100% in 2005, with the range in estimates again representing temporal variability in $bSiO_2$ flux between individual PITS deployments in each year.

These high diatom contributions to POC and PON export are similar to values estimated by Nelson and Brzezinski (1997) for the spring bloom period in the Sargasso Sea. The above conversions assume that diatom remineralization within the upper 200 m does not alter ratios of $bSiO_2$ to diatom C or N. A bias would occur if there is preferential remineralization of diatom organic matter versus diatom $bSiO_2$, i.e., if the ratio of exported $bSiO_2$ to exported, diatom-derived POC and PON is actually > 0.13 and >1.0, respectively, then the diatom contribution to POC and PON export obtained by our fixed stoichiometry conversion would be less than we have estimated. However, the measured $E/\int\rho$ in the overlying water column during the time of our observations was only ~ 0.2–0.3, meaning that ~70–80% of diatom $bSiO_2$ produced within the upper 140 m apparently dissolved in the upper 200 m. This

argues against any large increase in the ratio of $bSiO_2$ export to diatom-derived PON and POC export in late winter, unless diatom-derived PON and POC remineralization in the upper 200 m is significantly greater than 70–80%. Additionally, there was no significant difference in the mean ratio of $bSiO_2$ flux to PON flux between 200, 300, and 400 m traps in 2004; while in 2005 there was a significant increase in that ratio between 200 and 300 m (i.e. 0.60±0.22 and 1.2±0.20, respectively, t-test, $p<0.01$), but not between 300 and 400 m.

The magnitude of the observed $bSiO_2$ flux in 2004, while pulsed, could be important in an annual Si budget in the Sargasso Sea. Using export rates obtained primarily during stratified periods in the Sargasso Sea, Nelson and Brzezinski (1997) proposed a conservative estimate of 23 mmol Si m^{-2} y^{-1} for the annual $bSiO_2$ export from the upper 150 m. The pulsed addition of nutrients to the euphotic zone during deployment 2004-2 resulted in a time-averaged export flux of 0.5 mmol Si m^{-2} d^{-1} to 200 m; an ~8-fold increase over the mean flux of 0.063 mmol Si m^{-2} d^{-1} implied by Nelson and Brzezinski's estimate (i.e. 23 mmol Si m^{-2} y^{-1}/365 d y^{-1}). The eight days of enhanced flux actually observed during deployment 2004-2 would be equivalent to ~15% of the Nelson and Brzezinski's conservative estimate of the annual $bSiO_2$ export flux.

The two storm events that increased wind speed during the 2004-2 deployment (i.e. day ~69 and ~73) were likely from storms reported to originate near the North Carolina coast (USA) and the Southeast coast (USA), respectively (Bancroft 2004). Mariner logs during this period indicate that both storms moved north along the eastern coast of the USA and terminated to the north of Newfoundland (Canada); both storm systems lasted 2–4 days (Bancroft 2004). Our data suggest that biogeochemical responses to storms occur within a few days, specifically enhancing nutrient uptake and export of $bSiO_2$ and organic matter. Thus the biogeochemical importance of late-winter storms is probably not restricted to the area that we sampled, but widespread over western the North Atlantic.

Nutrient injections resulting from storm-driven destabilization/stabilization cycles have been observed in other oceanic regions. Sambrotto et al. (1986) observed that during the transition from the spring bloom to a post-bloom water column (May)

in the Bering Sea, NO_3^- was depleted in the ML. A supply of new nutrients was needed to continue new production, but an intensified (and shallow <30 m) pycnocline restricted access to deeper nutrients. Passing storms during this post-bloom period deepened the ML and penetrated the pycnocline. The deep mixing entrained NO_3^- and also re-suspended bloom-forming diatoms; the net result was the highest NO_3^- uptake rates observed during their study (i.e. higher than those during the spring bloom). Sambrotto et al. calculated that enhancement of new production by this forcing mechanism accounted for ~37% of the total new production associated with the spring bloom, suggesting that storm events (on the time scale of days) are important quantitatively in annual new production on the Bering Sea continental shelf. The results of both Sambrotto et al. (1986) and this study show that short-term (i.e. scale of days) destabilization-stabilization mechanisms, either before or after formation of the seasonal thermocline, can enhance new production. Therefore, considering the clear physical and biogeochemical differences between the Sargasso and Bering Seas, we propose that intermittent physical forcing of this kind may enhance new production in many other oceanic regions.

2.5.4 The annual biogenic silica production budget in the Sargasso Sea

Previous estimates of annual $bSiO_2$ production in the Sargasso Sea (Nelson and Brzezinski 1997) inferred a mean $\int\rho$ of ~3.3 mmol Si m^{-2} d^{-1} during the spring bloom and applied that rate to 30 days per year. While Nelson and Brzezinski's $\int\rho$ estimate for the spring bloom period is three times higher than the mean measured $\int\rho$ during our late-winter cruises (Table 2.2), it was based on standard spring bloom periods in late March, April and May. A $bSiO_2$ production rate higher than our observed late winter rate is likely during the spring bloom period, as [$bSiO_2$] during the spring bloom at BATS is typically ~4–5 times higher than what we measured in late winters of 2004 and 2005 (Brzezinski and Nelson 1995). The mean daily $\int\rho$ in late winter of both 2004 and 2005 was ~1.1 mmol Si m^{-2} d^{-1}. Therefore if V for $Si(OH)_4$ uptake during the spring bloom is similar to that measured during late winter, the higher [$bSiO_2$] during the spring bloom would make the earlier estimate of 3.3 mmol Si m^{-2} d^{-1} reasonable. Nelson and Brzezinski applied their measured $\int\rho$ for non-

bloom periods (0.42 mmol Si m^{-2} d^{-1}) to the remaining 335 days per year. If our measured rate of 1.1 mmol Si m^{-2} d^{-1} in late winter also applies to 30 days per year (~15 February–15 March) we can recalculate the estimated annual $bSiO_2$ production in the Sargasso Sea:

Late winter:	1.1 mmol Si m^{-2} d^{-1} x 30 days y^{-1}	= 33 mmol Si m^{-2} y^{-1}
Spring bloom:	3.3 mmol Si m^{-2} d^{-1} x 30 days y^{-1}	= 99 mmol Si m^{-2} y^{-1}
Stratified period:	0.42 mmol Si m^{-2} d^{-1} x 305 days y^{-1}	= 128 mmol Si m^{-2} y^{-1}

Summing these estimates yields an annual total of 260 mmol Si m^{-2} y^{-1}; the previous estimate, which did not account for increased production in late winter, was of 239 mmol Si m^{-2} y^{-1} (Nelson and Brzezinski 1997). Thus, the addition of our late winter rate to an annual silica production budget yields only a ~9% increase over the previous estimate. While this change is small, inclusion of our data from this period better constrains an annual budget, and provides a second line of evidence supporting the (as yet unmeasured) spring bloom rate of biogenic silica production. Because the annual estimate of $bSiO_2$ production in the Sargasso Sea is low in global terms, it remains highly sensitive to any future data on $bSiO_2$ production during typical spring blooms or on the variability of $bSiO_2$ production at other times of year in response to storms and mesoscale physical features such as eddies.

Acknowledgements

We thank M. Mongin and C. Dumousseaud for shipboard and lab assistance. Appreciation also goes to the science party and crew of *R.V. Oceanus* on cruises 399-3 and 408-2, D.J. McGillicuddy (WHOI) for sea level anomaly maps, and M.A. Brzezinski (UCSB) for early 1990s BATS Si data. This work was supported by NSF Chemical Oceanography award OCE-0244612 awarded to MWL and DMN and an Oregon Space Grant Consortium Fellowship awarded to JWK.

2.6 References

Ammerman, J.W., Hood, R.R, Case, D.A., Cotner J.B., 2003. Phosphorus Deficiency in the Atlantic: An Emerging Paradigm in Oceanography. EOS Transactions, American Geophysical Union 84, 165-170.

Backhaus, J.O., Hegseth, E.N., Wehde, H., Irigoien, X., Hatten, K., Logemann, K., 2003. Convection and primary production in winter. Marine Ecology Progress Series 251, 1-14.

Banahan, S., Goering, J.J., 1986. The production of biogenic silica and its accumulation on the southeastern Bering Sea shelf. Continental Shelf Research 5, 199-213.

Bancroft, G.P., 2004. Marine Weather Review – North Atlantic Area: January to April 2004. Mariners We Weather Log 48 (2), http://www.vos.noaa.gov/mwl.shtml.

Brzezinski, M.A., 1985. The Si:C:N ratio of marine diatoms: interspecific variability and the effect of some environmental variables. Journal of Phycology 21, 347-57.

Brzezinski, M.A., Kosman, C.A., 1996. Silica production in the Sargasso Sea during spring 1989. Marine Ecology Progress Series 142, 39-45.

Brzezinski M. A., Nelson, D.M., 1986. A solvent extraction method for the calorimetric the determination of nanomolar concentrations of silicic acid in seawater. Marine Chemistry 18, 59-69.

Brzezinski, M.A., Nelson, D.M., 1989. Seasonal changes in the silicon cycle within a Gulf Stream warm-core ring. Deep-Sea Research I 36, 1009-1030.

Brzezinski, M.A., Nelson, D.M., 1995. The annual silica cycle in the Sargasso Sea near Bermuda. Deep-Sea Research I 42, 1215-1237.

Brzezinski, M.A., Nelson D.M., 1996. Chronic substrate limitation of silicic acid uptake rates in the western Sargasso Sea. Deep-Sea Research II 43, 437-453.

Brzezinski, M.A., Phillips, D.R., Chavez, F.P., Friederich, G.E., Dugdale, R.C., 1997. Silica production in the Monterrey, California, upwelling system. Limnology and Oceanography 42, 1694-1705.

Brzezinski, M.A., Nelson, D.M., Franck, V.M., Sigmon, D.E., 2001. Silicon dynamics within an intense open-ocean diatom bloom in the Pacific sector of the Southern Ocean. Deep-Sea Research II 48 3997–4018.

Conte, M.H., Dickey, T.D., Weber, J.C., Johnson, R.J., Knap, A.H., 2003. Transient physical forcing of pulsed export of bioreactive material to the deep Sargasso Sea. Deep-Sea Research I 50, 1157-1187.

DeMaster, D.J., McKee, B.A., Moore, W.S., Nelson, D.M., Showers, W.J., Smith, W.O., 1991. Geochemical processes occurring at the Amazon River/ocean boundary. Oceanography 4, 15-20.

Dugdale, R. C., Goering, J. J., 1967. Uptake of new and regenerated forms of nitrogen in primary productivity. Limnology and Oceanography 121, 196-206.

Dugdale, R.C., Wilkerson, F.P., 1998. Silicate regulation of new production in the equatorial Pacific upwelling. Nature 391, 270-273.

Eppley, R.W., Peterson, B.J., 1979. Particulate organic matter flux and planktonic new production in the deep ocean. Nature 282, 677-680.

Goericke, R., 1998. Response of phytoplankton community structure and taxon specific growth rates to seasonally varying physical forcing in the Sargasso Sea off Bermuda. Limnology and Oceanography 43, 921-935.

Goldman J. C., 1993. Potential role of large oceanic diatoms in new primary production. Deep-Sea Research I 40, 159-168.

Goldman, J.C., McGillicuddy, D.J., 2003. Effect of large marine diatoms growing at low light on episodic new production. Limnology and Oceanography 48, 1176-1182.

Goldman, J.C., Hansell, D.A., Dennett, M.R., 1992. Chemical characterization of three large oceanic diatoms: potential impact on water column chemistry. Marine Ecology Progress Series 88, 257-270.

Gust, G., Michaels, A.F., Johnson, R., Deuser, W.G., Bowles, W., 1994. Mooring line motions and sediment trap hydrodynamics: in-situ intercomparison of three common deployment designs. Deep-Sea Research I 41, 831-857.

Honjo, S., Manganini, S.J., Krishfield, R.A., Francois, R., 2008. Particulate organic carbon fluxes to the ocean interior and factors controlling the biological pump: A synthesis of global sediment trap programs since 1983. Progress in Oceanography 76, 217-285.

Hulburt, E.M., Ryther, J.H., Guillard, R.R.L., 1960. The phytoplankton of the Sargasso Sea off Bermuda. Journal du Conseil International d'Exploration da la Mer 25, 115-128.

Jenkins, W., 1988. Nitrate flux into the euphotic zone near Bermuda. Nature 331, 521-523.

Jenkins, W., Doney, S. C., 2003. The subtropical nutrient spiral. Global Biogeochemical Cycles 17: doi:10.1029/2003GB002085.

Jenkins, W., Goldman, J., 1985. Seasonal oxygen cycling and primary production in the Sargasso Sea. Journal of Marine Research 43, 465-491.

Knap, A. H., and 19 others, 1997. U.S. Joint Global Ocean Flux Study- Bermuda Atlantic Time- Series Study Methods Manual: Version 4. U.S. JGOFS Planning and Coordination Office: Woods Hole.

Knauer G. A., Karl, D. M., Martin, J. H., Hunter, C.N., 1984. In situ effects of selected preservatives on total carbon, nitrogen, and metals collected in sediment traps. Journal of Marine Research 42, 445-462.

Leynaert, A., Nelson, D.M., Quéguiner, B., Tréguer, P., 1993. The silica cycle in the Antarctic Ocean: Is the Weddell Sea atypical? Marine Ecology Progress Series 96, 1-15.

Lipschultz, F., 2001. A time-series assessment of the nitrogen cycle at BATS. Deep-Sea Research Part II 48, 1897-1924.

Lipschultz, F., Bates, N., Carlson, C., Hansell, D., 2002. New production in the Sargasso Sea: History and current status. Global Biogeochemical Cycles 16 (1), 1-17.

Lomas, M.W., Glibert, P.M., 1999. Temperature regulation of nitrate uptake: A novel hypothesis about nitrate uptake and reduction in cool-water diatoms. Limnology and Oceanography 44, 556-572.

Lomas, M.W., Lipschultz, F. , Nelson, D. M., Bates, N.R. (*in revision*)-a. Biogeochemical responses to late-winter storms in the Sargasso Sea. I. Pulses of primary and new production. *In revision*, Deep-Sea Research I.

Lomas, M.W., Roberts, N., Lipschultz, F., Krause, J.W., Nelson, D.M , Bates, N.R. (*in revision*)-b. Biogeochemical responses to late-winter storms in the Sargasso Sea. III. Rapid successions of major phytoplankton groups. *In revision*, Deep-Sea Research I.

Maiti, K., Benitez-Nelson, C.R., Lomas, M.W., Krause. J.W. (*in revision*). Biogeochemical responses to late-winter storms in the Sargasso Sea. IV. Comparison of Export Production by ^{234}Th and Sediment Traps. *In revision*, Deep-Sea Research I.

McGillicuddy, D.J., Robinson, A.R., Siegel, D.A., Jannasch, H.W., Johnson, R., Dickey, T. D., McNeil, J., Michaels, A.F., Knap, A.H., 1998. Influence of mesoscale eddies on new production in the Sargasso Sea. Nature 394, 263-266.

McNeil, J.D., Jannasch, H.W., Dickey, T., McGillicuddy, D.J., Brzezinski, M., Sakamoto, C.M., 1999. New chemical, bio-optical and physical observations of upper ocean response to the passage of a mesoscale eddy off Bermuda. Journal of Geophysical Research 104, 15537–15548.

Michaels, A.F., Silver, M.W., 1988. Primary production, sinking fluxes and the microbial food web. Deep-Sea Research I 35, 473-490.

Michaels A. F., Silver, M. W., Gowing, M., Knauer, G.A., 1990. Cryptic zooplankton "swimmers" in upper ocean sediment traps. Deep-Sea Research I 37, 1285-1296.

Michaels, A., Knap, A., Dow, R., Gundersen, K., Johnson, R., Sorensen, J., Close, A., Knauer, G., Lohrenz, S., Asper, V., Tuel, M., Bidigare, R., 1994. Seasonal patterns of ocean biogeochemistry at the U.S. JGOFS Bermuda Atlantic Time-series study site. Deep-Sea Research 41, 1013-1038.

Mongin, M., Nelson, D.M., Pondaven, P., Brzezinski, M.A., Tréguer, P., 2003. Simulation of upper-ocean biogeochemistry with a flexible-composition phytoplankton model: C, N and Si cycling in the western Sargasso Sea. Deep-Sea Research I 50, 1445-1480.

Nelson, D.M., Brzezinski, M.A., 1997. Diatom growth and productivity in an oligotrophic midocean gyre: a 3-yr record from the Sargasso Sea near Bermuda. Limnology and Oceanography 43, 473-486.

Nelson, D.M., Gordon, L.I., 1982. Production and pelagic dissolution of biogenic silica in the Southern Ocean. Geochimica Cosmochimica Acta 46, 491-501.

Nelson, D.M., Ahren, J.A., Herlihy, L.J., 1991. Cycling of biogenic silica within the upper water column of the Ross Sea. Marine Chemistry 35, 461-476.

Nelson, D.M., Tréguer, P., Brzezinski, M.A., Leynaert, A., Quéguiner, B., 1995. Production and dissolution of biogenic silica in the ocean: Revised global estimates, comparison with regional data and relationship to biogenic sedimentation. Global Biogeochemical Cycles 9, 359–372.

Nelson, D.M., DeMaster, D.J., Dunbar, R.B., Smith, W.O., 1996. Cycling of organic carbon and biogenic silica in the Southern Ocean: Estimates of water-column and sedimentary fluxes over the Ross Sea continental shelf. Journal of Geophysical Research 101, 18519-18532.

Nelson, D.M., Brzezinski, M.A., Sigmon, D.E., Franck, V.M., 2001. A seasonal progression of Si limitation in the Pacific sector of the Southern Ocean. Deep-Sea Research Part II 48, 3973–3995.

Paasche, E., 1973. Silicon and the ecology of marine planktonic diatoms. I. *Thalassiosira pseudonana (Cyclotella nana*) grown in chemostats with silicate as the limiting nutrient. Marine Biology 19, 117-126.

Pondaven, P., Ragueneau, O., Tréguer, P., Hauvespre, A., Dezileau, L., Reyss, J.L., 2000. Resolving the 'opal paradox' in the Southern Ocean. Nature 405, 168-172.

Raven, J.A., 1983. The transport and function of silicon in plants. Biological Review 58, 179-207.

Raven, J.A., Waite, A.M., 2004. The evolution of silicification in diatoms: inescapable sinking and sinking as escape? New Phytologist 162, 45-61.

Riley, G.A., 1957. Phytoplankton of the North Central Sargasso Sea, 1950-1952. Limnology and Oceanography 2, 252-269.

Sambrotto, R.N., Niebauer, H.J., Goering, J.J., Iverson, R.L., 1986. Relationships among vertical mixing, nitrate uptake, and phytoplankton growth during the spring bloom in the southeast Bering Sea middle shelf. Continental Shelf Research 5, 161-198.

Sarmiento, J.L., Simeon, J., Gnanadesikan, A., Gruber, N., Key, R.M., Schlitzer, R., 2007. Deep ocean biogeochemistry of silicic acid and nitrate. Global Biogeochemical Cycles 21, doi:10.1029/2006GB002720.

Schlitzer, R., Ocean Data View, http://odv.awi-bremerhaven.de, 2006.

Siegel, D.A., Itturiaga, R., Bidigare, R.R., Smith, R.C., Pak, H., Dickey, T.D., Marra, J., Baker, K.S., 1990. Meridional variations of the spring-time phytoplankton community in the Sargasso Sea. Journal of Marine Research 48, 379 - 412.

Siegel, D.A., and 13 others, 2001. Bio-optical modeling of primary production on regional scales: the Bermuda Bio-Optics project. Deep-Sea Research Part II 48, 1865-1896.

Spitzer, W., Jenkins, W., 1989. Rates of vertical mixing, gas exchange and new production: estimates from seasonal gas cycles in the upper ocean near Bermuda. Journal of Marine Research 47, 169-196.

Stanley, R.H.R., Buesseler, K.O., Manganini, S.J., Steinberg, D.K., Valdes, J.R., 2004. A comparison of major and minor elemental fluxes collected in neutrally buoyant and surface-tethered sediment traps. Deep-Sea Research I 51, 1387–1395

Steinberg, D. K., Carlson, C. A., Bates, N. R., Johnson, R. J., Michaels, A. F., Knap, A. H. 2001. Overview of the US JGOFS Bermuda Atlantic Time-series Study (BATS): a decade-scale look at ocean biology and biogeochemistry. Deep-Sea Research Part II 48, 1405-1447.

Strickland J. D. H., Parsons, T.R., 1972. A practical handbook of seawater analysis. 2nd Ed., Vol. 167, Bulletin of the Fisheries Research Board of Canada, Ottawa, 310 pp.

Sverdrup, H. 1953. On conditions for the vernal blooming of phytoplankton. Journal du Conseil International d'Exploration da la Mer 18: 287-295.

Tréguer, P., Lindner, L., van Bennekom, A.J., Leynaert, A., Panouse, M., Jacques, G., 1991. Production of biogenic silica in the Weddell-Scotia Seas measured with ^{32}Si. Limnology and Oceanography 36, 1217-1227.

Tréguer, P., Nelson, D.M., van Bennekom, A.J., DeMaster, D.J., Leynaert, A., Quéguiner, B., 1995. The silica balance in the world ocean: A re-estimate. Science 268, 375-379.

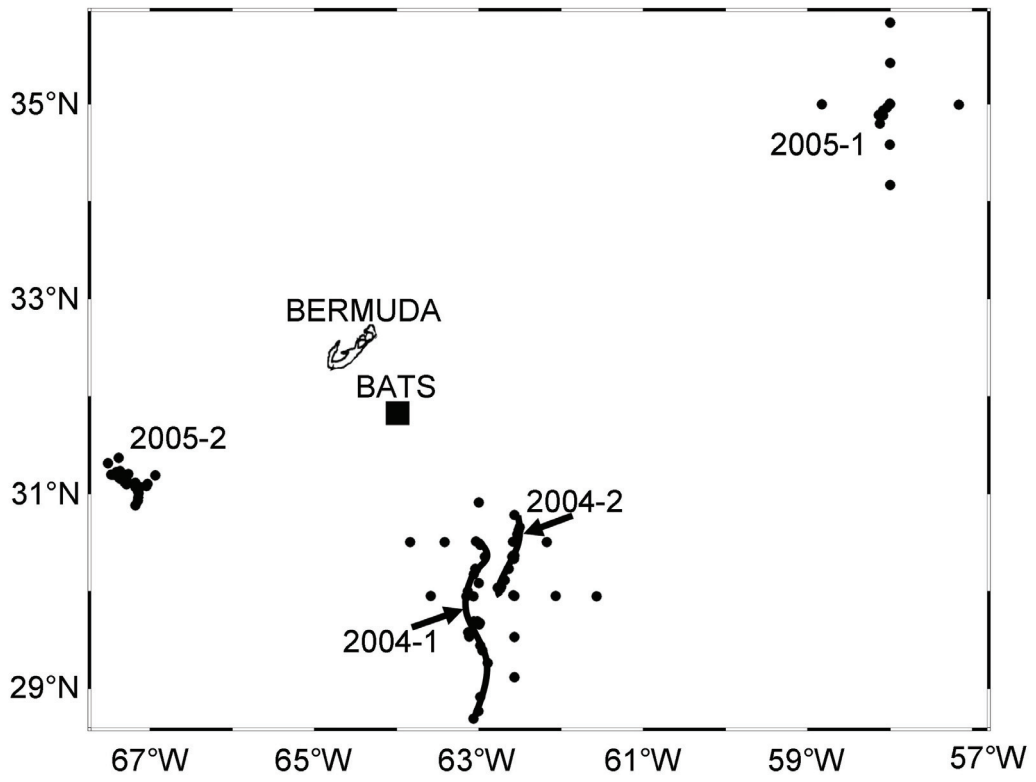

Figure 2.1 - Map of all CTD stations during the two cruises. The approximate locations of Bermuda (not to scale) and the BATS site (black square) are indicated for reference. The four primary drogue deployments will be referred to by order of occupation during each cruise (e.g. 2004-1, 2004-2, 2005-1, and 2005-2).

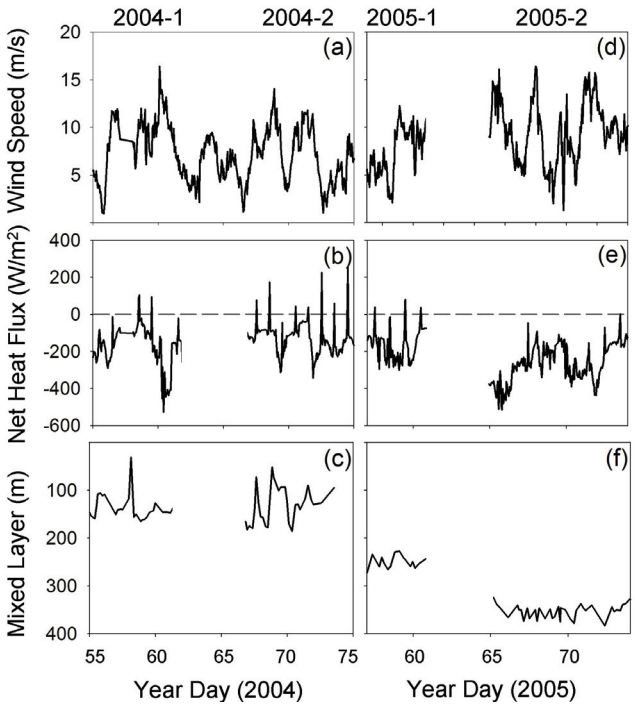

Figure 2.2 - Physical data for 2004 (year day 55-75) and 2005 (year day 57-74). (a, d) Wind speed in m s^{-1}, (b, e) net heat flux in W m^{-2} (data from Lomas et al. *in revision* a), and (c, f) mixed layer depth in m. For reference, dashed line (b, e) is where net heat flux equals zero. Mixed layer depth is based upon a density change of 0.125 kg m^{-3} from surface. Deployment is listed above panels a, d. Temporal break in wind data (d) indicates period when no data available (vessel had to go into port), other breaks (b, c, e, f) indicate periods between deployments.

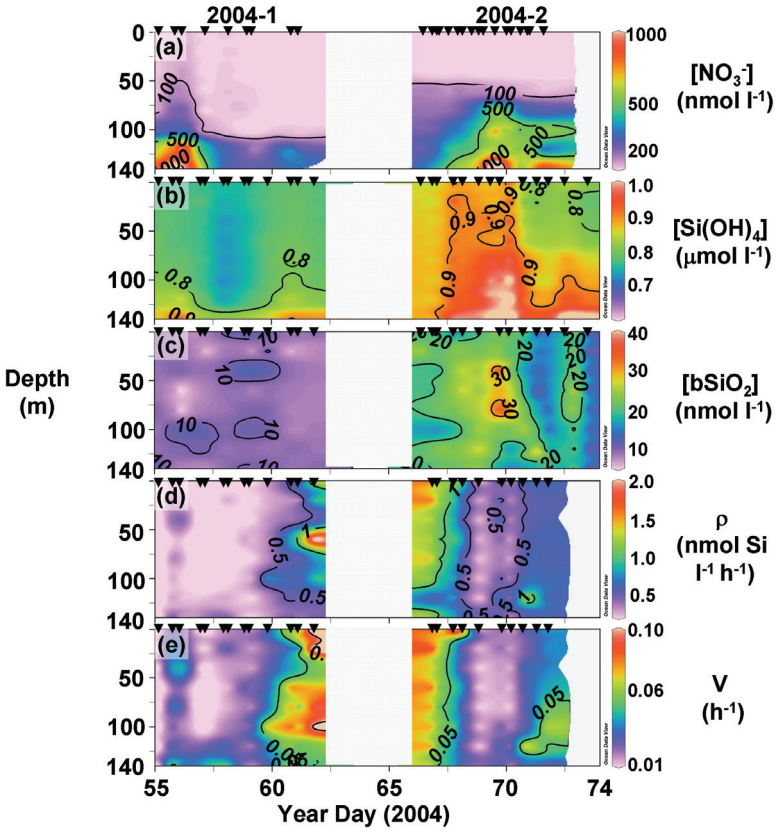

Figure 2.3 - Time course profiles of nutrient and biogenic silica concentrations, and biogenic silica production rates during 2004. (a) $[NO_3^-]$ in nmol l^{-1}, (b) $[Si(OH)_4]$ in μmol l^{-1}, (c) $[bSiO_2]$ in nmol l^{-1}, (d) ρ in nmol Si l^{-1} h^{-1}, (e) V in h^{-1}. X-axis is day of year (2004), and y-axis is depth (surface – 140 m). Vertical blocked sections represent temporal separation of 2004-1 and 2004-2 drogue deployments. All contour plots were generated with Ocean Data View (Schlitzer 2006), smoothing was done by the software's built-in variable resolution gridding algorithm using a consistent number of interations for all panels. Sampling periods denoted with ▼ on each panel.

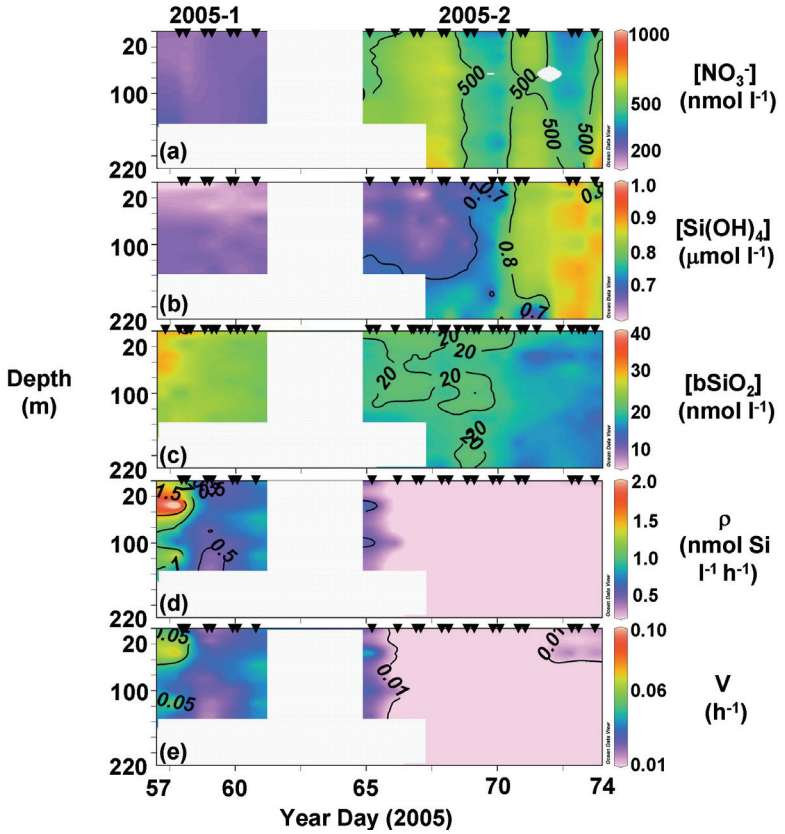

Figure 2.4 - Time course profiles of nutrient and biogenic silica concentrations, and biogenic silica production rates during 2005. (a) $[NO_3^-]$ in nmol l^{-1}, (b) $[Si(OH)_4]$ in μmol l^{-1}, (c) $[bSiO_2]$ in nmol l^{-1}, (d) ρ in nmol Si l^{-1} h^{-1}, (e) V in h^{-1}. X-axis is day of year (2005), and y-axis is depth (surface – 220 m). Vertical blocked sections represent temporal separation of 2005-1 and 2005-2 drogue deployments. Note: 220 m profiles started during deployment 2005-2 because of the deep mixed layer (c.f. Figure 2.2). Sampling periods denoted with ▼ on each panel.

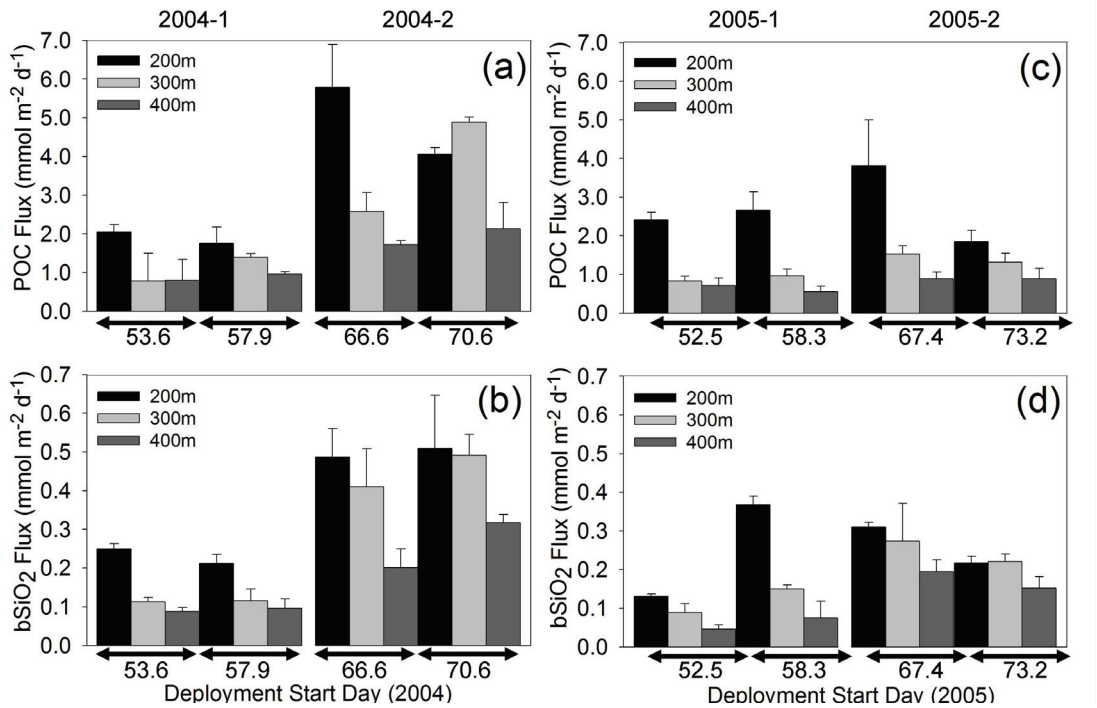

Figure 2.5 - PITS flux during 2004 (a, b) and 2005 (c, d). (a, c) POC flux in mmol C m^{-2} d^{-1}, from Lomas et al., *in revision* a, (b, d) $bSiO_2$ flux in mmol Si m^{-2} d^{-1}. Fill color: black =200 m, light gray =300 m, dark gray =400 m. Time-axis indicates deployment start (day of year, 2004 or 2005). Deployments lengths were 3.9±0.1 and 3.9±1.7 days in 2004 and 2005 respectively. Error bars ±1 standard deviation for PITS tubes at same depth (n=3). Measurements of POC and $bSiO_2$ were not made on same material, i.e., three distinct tubes for POC and three others for $bSiO_2$. Two PITS deployments were done per study area with the gap between 2004-1/2004-2, 2005-1/2005-2 indicating the temporal gap between study areas. For comparison, average 150 m $bSiO_2$ flux during the stratified period at BATS ~0.06 mmol m^{-2} d^{-1} whereas average flux during February & March (1992-1994) was ~0.13 and ~0.12 mmol m^{-2} d^{-1} for 200 and 300 m respectively (Nelson & Brzezinski 1997).

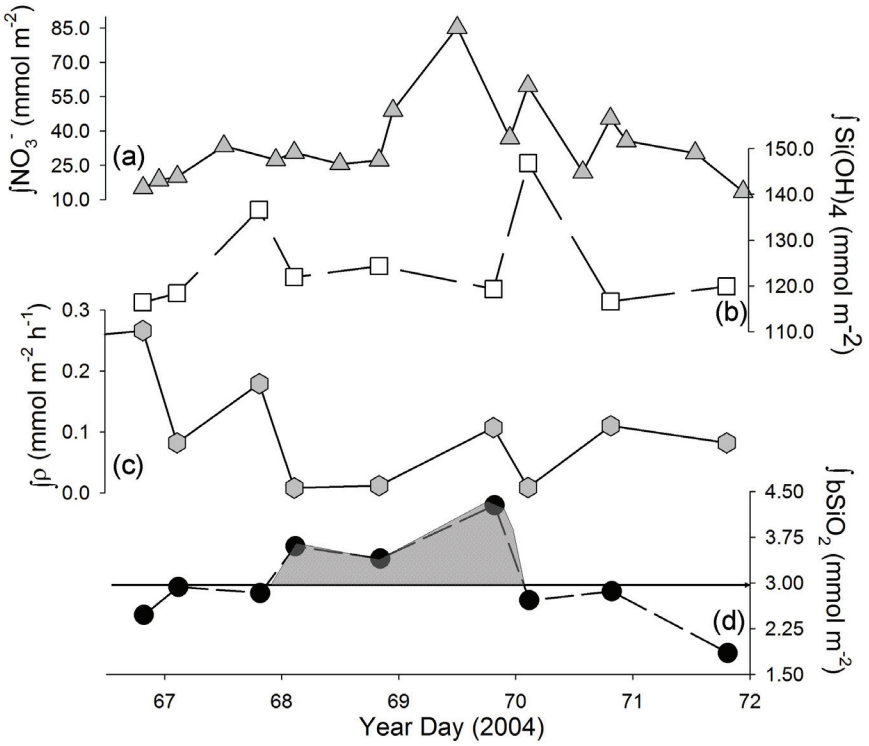

Figure 2.6 - Change in vertically integrated stocks and $bSiO_2$ production rate ($\int\rho$) during the 2004-2 deployment. (a) $\int NO_3^-$ in mmol m^{-2} (shaded triangles), (b) $\int Si(OH)_4$ in mmol m^{-2} (open squares), (c) $\int\rho$ in mmol Si l^{-1} h^{-1} (shaded hexagons), and (d) $\int bSiO_2$ in mmol m^{-2} (filled circles). Shaded areas (d) represents $bSiO_2$ accumulation above the mean for 2004-2 deployment (black arrow, see also Table 2.2). Integrations were done from the surface to 140 m. No smoothing was done and apparent temporal differences in integrated stocks (or rates), compared Figure 2.3 is an artifact of the ODV contouring algorithm.

Table 2.1 - Inter-system comparison of $bSiO_2$ production rates. For areas with multiple references, a single estimate for each study was used and all single values were averaged; no weighting was done for studies having more data profiles than another. Values in table are meant to illustrate $bSiO_2$ production range in the ocean. *Denotes ~90% ice cover during Weddell Sea study (see Leynaert et al., 1993).

Location	**Time of Year**	**$bSiO_2$ production (mmol Si m^{-2} d^{-1})**	**Reference**
Sargasso Sea	Stratified	0.4	Nelson and Brzezinski 1997
Equatorial Pacific (125-140°W)	September	1.5	<Krause and Nelson unpublished 2005>
Weddell Sea	Early Spring* (Austral)	2.0	Leynaert et al. 1993
Gulf Stream Warm Core Ring	Spring & Summer	6.4	Brzezinski and Nelson 1989
Southern Ocean	Spring & Summer (Austral)	11.0	Nelson and Gordon 1982, Nelson et al. 1991, Tréguer et al. 1991, Nelson et al. 1996, Pondaven et al. 2000, Brzezinski et al. 2001
Bering Sea	Summer	17.7	Banahan and Goering 1986
Amazon River Plume	May, August	36.7	DeMaster et al. 1991
Monterey, USA	Upwelling Season	200	Brzezinski et al. 1997

Table 2.2 – Integrated $bSiO_2$ production rates ($\int\rho$), suspended $bSiO_2$ ($\int bSiO_2$), silicic acid ($\int Si(OH)_4$), and nitrate ($\int NO_3^-$) in the upper 140 m during the drogue deployments performed in this study. Note: not all $\int\rho$ profiles were used to calculate daily $\int\rho$ (see methods). Comparisons were made by t-test (two-tail, unequal variance) between drogue deployments in each year (e.g. 2004-1 vs. 2004-2), and between years (2004 and 2005); significant p-values are reported. All values reported as mean (bold) ± 1 standard deviation (number of profiles).

	$\int\rho$ (mmol m^{-2} h^{-1})	$\int bSiO_2$ (mmol m^{-2})	$\int Si(OH)_4$ (mmol m^{-2})	$\int NO_3^-$ (mmol m^{-2})
2004-1	**0.043** ±0.043 (17)	**1.24** ±0.23 (18)	**107.3** ±7.37 (16)	**22.5** ±14.5 (17)
2004-2	**0.095** ±0.086 (9)	**2.99** ±0.70 (9)	**124.5** ±10.4 (9)	**30.4** ±18.4 (6)
2004-1 vs. 2004-2	NS	$p < 0.01$	$p < 0.01$	$p < 0.01$
2005-1	**0.123** ±0.064 (10)	**2.79** ±0.64 (11)	**107.3** ±21.0 (10)	**62.6** ±63.2 (10)
2005-2	**0.015** ±0.018 (15)	**2.54** ±0.29 (15)	**102.8** ±11.9 (15)	**78.2** ±11.1 (14)
2005-1 vs. 2005-2	$p < 0.01$	NS	NS	NS
2004 (all data)	**0.061** ±0.065 (26)	**1.96** ±1.11 (27)	**113.9** ±11.2 (27)	**24.4** ±14.7 (23)
2005 (all data)	**0.058** ±0.068 (25)	**2.65** ±0.47 (26)	**104.6** ±15.9 (25)	**71.7** ±41.2 (24)
2004 vs. 2005	NS	$p < 0.01$	$p < 0.05$	$p < 0.01$

3. Biogenic silica production and the estimated contribution of diatoms to primary and new production in the equatorial Pacific

Jeffrey W. Krause, David M. Nelson, Mark. A. Brzezinski

For submission to Deep-Sea Research II: Topical Studies in Oceanography
DSR II Editorial Office
Virginia Institute of Marine Science, School of Marine Science
The College of William and Mary
PO BOX 1346
Gloucester Point, VA 23062-1346
USA

3.1 Abstract

We measured zonal and meridional variability in euphotic zone silicification rates on two cruises in the eastern equatorial Pacific. Transects were conducted on 110°W (4°N - 3°S) and the equator (116.7°W - 140°W) in December 2004, and 140°W (4°N - 2.5°S) and 0.5°N (132°5 - 125°W) in September 2005. Silicification was generally highest in the upper 50 m, decreasing with depth to analytical zero at 150 m. Day period silicification rates were consistently higher than night rates. Along 110°W, the maximum euphotic zone integrated daily silicification rate ($\int\rho_{24H}$) was highest at the equator; however, on 140°W the maximum was at 2.5°S. $\int\rho_{24H}$ at 110°W was statistically higher than at 140°W, likely driven by significantly higher euphotic zone [$Si(OH)_4$] at 110°W. The $\int\rho_{24H}$ for both cruises was 1.4 mmol m^{-2} d^{-1}; with no statistical difference between years. The average specific rate of $bSiO_2$ production in the euphotic zone (V_{AVE}) during both years was 0.15 d^{-1}. Unlike $\int\rho_{24H}$, there was no statistically significant differences in V_{AVE} between 110°W and 140°W or between years; indicating little spatial variability within a ~$2.6x10^6$ km^2 area (i.e. 30° longitude x 7° latitude). Converting $\int\rho_{24H}$ to C and N uptake rates indicates that diatoms were responsible for ~20% and ~50% of primary and new production, respectively. Our results confirm that diatoms, despite their minor contribution to the autotrophic community biomass, have a disproportional impact on important biogeochemical processes in the eastern equatorial Pacific.

3.2 Introduction

The equatorial Pacific upwelling zone plays a large role in the global carbon cycle. It is the largest oceanic source of CO_2 to the atmosphere (Takahashi et al. 2002), and has been estimated to support >10% of global new production (Chavez and Barber 1987). Surface waters in this region have high macronutrient content (compared to the Pacific subtropical gyres) despite relatively high rates of new and export production (Murray et al. 1995). Thus, the equatorial Pacific has been characterized as one of the world's three main high-nutrient low-chlorophyll (HNLC) systems (Minas et al. 1986).

There has been no clear consensus regarding the mechanisms that sustain HNLC conditions in the equatorial Pacific. Proposed causes include Fe limitation (Coale et al. 1996), tight coupling between primary production and grazing (Landry et al. 1997) and a low supply of $Si(OH)_4$ relative to NO_3^- (Ku et al. 1995, Dugdale and Wilkerson 1998). The $Si(OH)_4$ supply hypothesis asserts that diatom new and export production are limited in this region by a low ratio of $[Si(OH)_4]$ to $[NO_3^-]$ in the upwelling source waters. Diatoms have been shown to have an average Si:N ratio of ~1:1 under nutrient-replete culture conditions (Brzezinski 1985), and the $[Si(OH)_4]$:$[NO_3^-]$ ratio of water upwelling in the equatorial Pacific is ~0.5 (Ku et al., 1995). Thus these waters are deficient in Si, relative to N, in comparison with diatom requirements, making Si potentially limiting to diatoms.

Dugdale and Wilkerson (1998) noted that nutrient conditions within the equatorial Pacific upwelling zone are remarkably invariant in space and time, and hypothesized that new production in the system is controlled by processes analogous to those occurring in a Si-limited chemostat. Si can play a significant role in limiting new production only if diatoms are the main agents of new production in the system under consideration. Their estimated quantitative importance in the equatorial Pacific depends on the nature of the comparison. Diatoms occur in relatively low numerical abundances and comprise <5% of the community chlorophyll a standing stock in the system (see Landry et al. 1997 and references therein). However, measured rates of biogenic silica production in the equatorial Pacific imply that diatoms may be

responsible for a significant proportion of the new production (Leynaert et al. 2001), consistent with Dugdale and Wilkerson's (1998) model.

Previous studies in the equatorial Pacific have shown that diatoms can occasionally occur in massive blooms, especially at convergence zones (Yoder et al. 1994, Archer et al. 1997). Even when no major bloom is in progress, estimated diatom growth rates in the system are relatively high (>1 d^{-1}, Latasa et al. 1997). Moreover, diatom abundance has been shown to be higher under normal upwelling conditions versus El Niño conditions (ibid.). While many studies in the equatorial Pacific have measured diatom pigments and/or estimated their numerical abundances (e.g. Kaczmarkska and Fryxell 1995, Bidigare and Ondrusek 1996, Kobayashi and Takahashi 2002), there is a limited understanding of how diatom silicification varies in space and time in this system. In the mid 1990s studies near 180°W (dateline) provided the first information on the vertical structure, general range, and meridional variability of biogenic silica production rates (Blain et al. 1997, Leynaert et al. 2001). Those studies also observed that rates of Si uptake by diatoms in this system are kinetically limited by the ambient [$Si(OH)_4$]. These reports of kinetic Si limitation, taken in conjunction with the large increases in diatom abundance and biomass that are observed during iron addition experiments (Coale et al. 1996) have created debate on whether Fe or Si plays the greater role in limiting rates of diatom growth, silicification and organic-matter export in this system.

In a recent study Brzezinski et al. (2008) observed a combined effect of [Fe] and [$Si(OH)_4$] on Si uptake by ambient diatom assemblages in the equatorial Pacific. Those results showed kinetic limitation of Si uptake rates similar to that observed previously (Leynaert et al. 2001); however, they also demonstrated a separate and nearly equal limitation of diatom Si uptake by Fe availability. When both Fe and $Si(OH)_4$ were added at high concentrations, the resulting enhancement of Si uptake observed 48 h later was nearly double that resulting from addition of Fe or $Si(OH)_4$ alone. These results suggest that diatoms are co-limited by Fe and Si the equatorial Pacific, with low [$Si(OH)_4$] limiting the rate of silicification and low [Fe] limiting the rate of cell division (Brzezinski et al., 2008).

This paper reports rates of biogenic silica production measured by ^{32}Si tracer incubations in the surface waters of the equatorial Pacific between 110°W and 140°W in December, 2004 and September, 2005, well to the east of previous studies (Blain et al. 1997, Leynaert et al. 2001) and generally within the equatorial cold tongue. We found remarkably little change in biogenic silica production rates over an east-west distance of >3,300 km, and negligible differences between rates observed during the two sampling periods. This study comprises part of a larger project examining control of plankton dynamics and carbon cycling by Fe, Si and grazing, and we use the measured silica production rates in conjunction with data on C and N uptake to revisit the estimated contribution of diatoms to total primary production and new production in the system. The availability of Si, C, and N rate measurements from the same stations and depths, with all measurements made over an extensive spatial range, makes this data set the first of its type obtained in the equatorial Pacific.

3.3 Methods

Sampling was conducted along one meridional and one zonal transect on each cruise (Figure 3.1). At a total of 30 stations, rates of biogenic silica ($bSiO_2$) production were measured in vertical profiles from the surface to ~150 m. Seventeen profiles were obtained between 9 and 29 December 2004 on a north-south transect from 4°N to 3°S on 110°W and an east-west transect from 116.7° to 140°W on the equator (Figure 3.1). Thirteen profiles were obtained between 8 and 24 September 2005, on a north-south transect from 4°N to 2.5°S on 140°W and a west-east transect from 132°5 to 125°W on 0.5°N (Figure 3.1). The zonal transect in 2005 was offset 0.5° to the north of the equator in order to sample through the greatest possible range in sea-surface temperature (SST) associated with westward-propagating tropical instability waves (TIWs). Rates of primary production and nitrate and ammonium uptake were also measured at the same stations and depths by ^{14}C and ^{15}N tracer incubations; for methodological descriptions see Balch et al. (*in preparation*) and Dugdale et al. (*in preparation*).

Seawater was collected from a trace-metal clean CTD rosette system in 2004, as described in Brzezinski et al. (2008). In 2005 profiles were collected with a

standard CTD rosette. During both years, sampling was done at depths to which 100, 31, 13, 8, 5, 0.8, and 0.1% of the photosynthetically available radiation at the sea surface (I_0) penetrated. An additional sample was collected at 150 m and incubated in the dark. All profiles in 2004 and six in 2005 had one sample per depth, while seven profiles in 2005 had triplicate samples per depth. Seawater was directly subsampled into acid-cleaned ~300 ml polycarbonate bottles from the CTD rosette using acid-washed silicone tubing, or drained into an acid-cleaned polypropylene container when using the trace-metal clean rosette (2004) or when performing sample replication (2005). When there was sample replication, the container was mixed as subsamples were drawn, to keep the particle assemblage homogenized.

At each station and depth where the rate of biogenic silica production was measured we also measured the ambient silicic acid concentration, $[Si(OH)_4]$, and the standing stock of biogenic particulate silica, $[bSiO_2]$. These measurements are less laborious, and do not require any tracer additions; therefore, to improve spatial resolution we also measured both at stations where no biogenic silica production was measured. For measurement of $[Si(OH)_4]$, 50-ml subsamples were drawn and analyzed as described by Brzezinski and Nelson (1995). A 1.0-liter subsample was filtered using a 47 mm, 0.6 μm pore, polycarbonate filter for measurement of $[bSiO_2]$ via NaOH digestion, which was performed as described by Nelson et al. (2001).

The rate of $bSiO_2$ production (ρ, in nmol Si l^{-1} h^{-1}) was measured in incubation experiments using high specific activity (>500 kBq/μmol Si) ^{32}Si. Prior to use, trace metals were removed from all ^{32}Si stocks by passage through Chelex resin. The added ^{32}Si activity ranged from ~330 to ~830 Bq (~20,000 – 50,000 DPM)/sample, depending on the ambient $[Si(OH)_4]$. After the tracer was added all bottles were incubated on deck in acrylic incubators that maintained sea-surface temperature by continuous flow of surface seawater. Seven separate incubators were used, each screened with neutral density filters to simulate *in situ* irradiance at one of the sampling depths. Samples from 150 m were incubated in bottles darkened with black electrical tape. Samples were incubated for ~8 – 24 h (see below for details regarding incubation times).

After incubation, samples were filtered under gentle vacuum (<25 cm Hg) onto 25 mm diameter, 0.6 μm pore, polycarbonate membrane filters, and rinsed with 0.6-μm filtered seawater to remove excess tracer not incorporated into the $bSiO_2$ matrix. Filters were then placed in 20 ml plastic scintillation vials, loosely capped and allowed to dry. After drying, all vials were kept tightly capped until analyzed for ^{32}Si activity on shore.

The ^{32}Si activity collected from the incubated samples was measured by liquid scintillation counting, which was done at least 100 days after filtration. This aging allowed for secular equilibrium between ^{32}Si and its daughter isotope ^{32}P to be reached. After aging, samples were prepared by adding 2.0 ml of 2.5 M HF to each vial, capping, and waiting 2 h to dissolve the $bSiO_2$ before adding 10 ml of scintillation cocktail (HP Ultima Gold XR). ρ calculated from the combined activities of ^{32}Si and ^{32}P in each sample (as the ^{32}P present after 100 days is > 99% derived from post-filtration decay of ^{32}Si) as described by Nelson et al. (2001).

On the 110°W transect ρ was measured separately in daylight hours and at night (ρ_{DAY} and ρ_{NIGHT}, respectively) on two profiles at each station; one from a cast begun at ~04:00 and the other from a cast begun at ~18:00 (local time). Samples from the ~04:00 cast were incubated for ~8 h in daylight and those from the ~18:00 cast for ~8 h at night. On the equatorial transect (2004), and at all stations in 2005, ρ_{DAY} and ρ_{NIGHT} were measured by taking two samples at the each of eight depths, incubating one for ~8 h in daylight and the other for 24 h. Both samples from a given depth received the same ^{32}Si activity; the ~8-h daylight incubation was used to measure ρ_{DAY} and the difference in ^{32}Si activity between the samples filtered after 8 h and 24 h of incubation was used to calculate ρ_{NIGHT}. In 2005, ρ_{DAY} was measured at 04:00 for comparison with ^{14}C (Balch et al. *in preparation*) and ^{15}N (Dugdale et al. *in preparation*) rate measurements. Due to water availability we did not measure ρ_{NIGHT} on the ~04:00 cast, and measured both ρ_{DAY} and ρ_{NIGHT} by incubating samples from casts that began at ~07:00. Thus in 2005 we have two measurements of ρ_{DAY} and one measurement of ρ_{NIGHT} at each station.

Vertically integrated rates of ρ ($\int\rho$, in mmol Si m^{-2} h^{-1}) were calculated by integrating ρ from the surface to 0.1% I_0 At stations on the transect at 110°W, where ρ_{DAY} and ρ_{NIGHT} were measured separately, these rates were converted to vertically integrated daily rates ($\int\rho_{24\text{-}H}$, in mmol Si m^{-2} d^{-1}) by:

$$\int\rho_{24\text{-}H} = [12 \times \int\rho_{DAY}\,(\mu\text{mol Si m}^{-2}\text{ h}^{-1}) + 12 \times \int\rho_{NIGHT}\,(\mu\text{mol Si m}^{-2}\text{ h}^{-1})] /1000 \quad (1)$$

At all other stations, where incubations of ~24 h were performed, $\int\rho_{24\text{-}H}$ was calculated directly from the ρ values measured:

$$\int\rho_{24\text{-}H} = [24 \times \int\rho_{24\text{-}H}\,(\mu\text{mol Si m}^{-2}\text{ h}^{-1})] / 1000 \quad (2)$$

This calculation allows for the fact that the nominally 24-h incubations very seldom lasted exactly 24.0 h.

The biomass-specific uptake rate (V, in h^{-1}) at each sampling depth was calculated as:

$$V = \rho / [bSiO_2] \quad (3)$$

where the units of ρ and the ambient $bSiO_2$ are nmol l^{-1} h^{-1} and nmol l^{-1}, respectively; V is thus expressed in h^{-1}. Vertically averaged specific uptake rates (from the surface to 0.1% I_0) during daylight hours (V_{DAY}) and at night (V_{NIGHT}) were calculated, respectively, as:

$$V_{DAY}\,(h^{-1}) = \int\rho_{DAY}\,(\mu\text{mol Si m}^{-2}\text{ h}^{-1}) / [\int bSiO_2\,(\text{mmol Si m}^{-2})] \times 1000] \quad (4)$$

$$V_{NIGHT}\,(h^{-1}) = \int\rho_{NIGHT}\,(\mu\text{mol Si m}^{-2}\text{ h}^{-1}) / [\int bSiO_2\,(\text{mmol Si m}^{-2})] \times 1000] \quad (5)$$

The mean V for the euphotic zone, averaged both vertically and over the day/night cycle (V_{AVE} in d^{-1}) was calculated as:

$$V_{AVE}\,(h^{-1}) = \int\rho_{24\text{-}H}\,(\text{mmol Si m}^{-2}\text{ d}^{-1}) / \int[bSiO_2]\,(\text{mmol Si m}^{-2}) \quad (6)$$

3.4 Results

3.4.1 Nutrient and biogenic silica distributions

The observed distributions of macronutrients ($[NO_3^- + NO_2^-]$ and $[Si(OH)_4]$) in the upper 300 m were typically 6 – 30 and 3 – 25 μM, respectively, over the zonal

range; in line with previous data from this region (Archer et al. 1996, Wilkerson and Dugdale 1996 and references therein). Differences were observed between meridional transects at 110°W and 140°W, likely stemming either from persistent east-west differences or from the different times of year and years (2004 vs. 2005) which they were sampled (Figure 3.2, 3.3). The 20 μM [NO_3^-+NO_2^-] isopleth was located at ~100 ± 20 m on the 110°W line in December 2004 (Figure 3.2), and ~130 ± 20 m on the 140°W line in September, 2005 (Figure 3.3). Zonal sections of [NO_3^-+ NO_2^-] showed an eastward shoaling of all isopleths between 110 – 140°W (Figure 3.2). In 2005, the zonal transect on 0.5°N extended only ~1/3 of the distance covered by the transect on the equator in 2004; shoaling of [NO_3^-+NO_2^-] isopleths over this shorter spatial scale is more pronounced at higher nutrient concentrations (e.g. 30 μM). [$Si(OH)_4$] showed a spatial distribution similar to that of [NO_3^-+NO_2^-], with isopleths shoaling west to east and latitudinal variability on meridional transects (Figures 3.2, 3.3). The 20 μM [$Si(OH)_4$] isopleth was deeper than the corresponding [NO_3^-+NO_2^-] isopleth on all transects. On the 110°W transect this [$Si(OH)_4$] isopleth was ~150-200 m, deepening to 200-300 m on the 140°W transect, and 200-250 m for the equator and 0.5°N transects (Figures 3.2, 3.3). Our data is consistent with previous observations that [$Si(OH)_4$] is consistently < [NO_3^-] in the upper water column of the equatorial Pacific (Ku et al. 1995, Dugdale and Wilkerson 1998).

In the upper 150 m [$bSiO_2$] was higher at 110°W than at 140°W (Figures 3.2, 3.3). However [$bSiO_2$] was generally ~75 – 150 nmol Si l^{-1} along both zonal transects, similar to levels measured in the equatorial Pacific near 180° (Leynaert et al. 2001). These concentrations are < 10% of those found in many coastal systems (e.g. Brzezinski et al. 2003, Leblanc and Hutchins 2005) and only ~2 – 3x higher than [$bSiO_2$] reported in the North Pacific central gyre (Brzezinski et al. 1998). Most profiles on the equator showed a minimum in [$bSiO_2$] between ~100 and ~200 m, with higher values both above and below. This [$bSiO_2$] minimum is associated with the layer in which the eastward-flowing Eastern Equatorial Undercurrent (EEU) is strongest (Kessler 2006). The EEU signature is seen in better detail during the equatorial transect in 2004 (Figure 3.2c) where the minimum [$bSiO_2$] layer deepens and becomes lower in [$bSiO_2$] to the west. As in the meridional transects, the zonal

transect in 2004 showed an increase in [$bSiO_2$] below the EEU layer. The 2005 transect on 0.5°N covered less distance and traversed the cold cusp of a TIW (as seen from daily SST data, provided daily from P. Strutton (OSU), data archived at ftp://ftp.ssmi.com/sst/daily/tmi_amsre), which may account for the less consistent vertical structure in [$bSiO_2$] compared to that observed along the 2004 equatorial transect.

Despite temporal and spatial differences, the mean [$bSiO_2$] and general range in [$bSiO_2$] were similar on the two cruises. The average [$bSiO_2$] between the surface and 150 m was 93 nmol l^{-1} (range 18 – 224) in 2004, and 99 nmol l^{-1} (range 24 – 268) in 2005. When all data from each cruise was pooled, euphotic zone $\int bSiO_2$ was not significantly different between years (t-test, $p=0.73$). Spatial differences were observed as $\int bSiO_2$ on the 110°W transect in 2004 was significantly higher than on the 140°W transect in 2005 (t-test, $p<0.05$, Table 3.1); similarly, $\int bSiO_2$ during the 0.5°N transect in 2005 was higher than on the equatorial transect in 2004 (t-test, $p<0.01$, Table 3.1).

3.4.2 Biogenic silica production

Biogenic silica production rates (ρ in nmol Si l^{-1} h^{-1}) were consistently higher during daylight hours than at night during both years (Figure 3.4). Euphotic-zone integrated rates during the day ($\int \rho_{DAY}$) were significantly higher than night ($\int \rho_{NIGHT}$, t-test, $p<0.01$, Table 3.1). Leynaert et al. (2001) observed a similar day–night difference in ρ. The higher rates measured during daylight hours imply that biogenic silica production in the equatorial Pacific is more tightly coupled to light availability than it is in other parts of the ocean, where reported day and night rates of biogenic silica production are statistically indistinguishable (e.g. Gulf stream warm-core rings, Brzezinski and Nelson 1989, Sargasso Sea, Nelson and Brzezinski 1997). $\int \rho_{DAY}$ was 2.3x higher than $\int \rho_{NIGHT}$ (mean for both cruises). The southernmost stations, on both meridianal transects, both showed $\int \rho_{NIGHT}$ higher than $\int \rho_{DAY}$, a trend driven by dramatic enhancement of $\int \rho_{NIGHT}$ and little change in $\int \rho_{DAY}$ (Table 3.1). The vertical structure in ρ was similar at all locations. Generally, the maximum ρ was found somewhere in the upper 50 m, with ρ then decreasing with depth to values near

analytical zero at 150 m (Figure 3.4). Despite statistically significant differences in $\int bSiO_2$ between transects, there were no significant differences in either $\int \rho_{DAY}$ or $\int \rho_{NIGHT}$ between those transects (Table 3.1). Pooled data from both years indicate that $\int \rho_{DAY}$ and $\int \rho_{NIGHT}$ were 87.3 ±44.1 and 46.3 ±25.4 μmol m^{-2} h^{-1} respectively, where the (±) term represents one standard deviation.

Average specific uptake rates in the euphotic zone (V_{AVE}, Figure 3.5) showed no statistically significant difference between 110°W in 2004 and 140°W in 2005 when all stations were considered (t-test, p=0.18). However, there was a statistically significant increase in $\int \rho_{24\text{-}H}$ at 110°W versus 140°W (t-test, $p<0.05$).

Pooled data from all stations along the two zonal transects showed no statistically significant difference in $\int \rho_{24\text{-}H}$ or V_{AVE} between years (t-test, p = 0.79 and p = 0.16 for $\int \rho_{24\text{-}H}$ and $V_{AVE,}$ respectively). Both cruises were carried out during periods of enhanced TIW activity (Gorgues et al. 2005). In 2004, variability in euphotic zone $\int \rho_{24\text{-}H}$ and V_{AVE} with longitudinal distance was less than during 2005 (Figure 3.5, note data undulation in both years, with 2005 data more compressed). This difference in variability was likely a result of the east to west sampling scheme in 2004 (same direction as TIW propagation, Strutton et al. 2001 and references therein) whereas in 2005 the 0.5°N zonal transect was sampled from west to east (opposite to TIW).

In 2005 we also sampled a station at 1.75°N, 125°W, located within the coldest area of the TIW as judged by daily satellite SST, likely a divergent zone in the trailing edge of the TIW. This station had a $\int \rho_{24\text{-}H}$ and $\int bSiO_2$ nearly equal to those at the TIW convergent boundary station (i.e., 0.5°N, 129.9°W; Table 3.1, Figure 3.5). Thus, our data are consistent with the mooring observations of Strutton et al. (2001) in showing elevated biological activity, in this case diatom $bSiO_2$ and silica production rates, associated with both the convergent and divergent fronts of a TIW.

In 2005 ρ was measured with replication (triplicate samples taken at each depth) on seven selected profiles (Figure 3.6). Within the euphotic zone the coefficient of variation in ρ_{24-H} ranged from 0.02 to 0.39 with a mean of 0.16 (n=49 individual sample depths with ρ measured in triplicate). At 150 m the coefficient of

variation was much higher (mean of 0.82, n = 7 individual sample depths with replication). The ^{32}Si activity recovered from this depth was uniformly low, and often difficult to distinguish from background activity. The coefficient of variation in $\int\rho_{24\text{-}H}$ averaged 0.12 with a range 0.05–0.18 (Figure 3.6, n = 7 profiles with replication). Due largely to the high cost of ^{32}Si, and the larger water requirements and more laborious sample-preparation procedures for stable Si isotopes mass spectrometry procedures (e.g. Nelson et al. 1996; Nelson and Brzezinski 1997), we are confident this is the first field study that has reported replicate measurements of biogenic silica production rates. Our data from 2005 demonstrate that variability among replicate samples is measurable, but generally quite small in the euphotic zone. In terms of uncertainty in integrated production estimates, our data indicate a coefficient of variation of ~10% (n=7 profiles). These data provide an estimate of the experimental uncertainty in $\int\rho_{24\text{-}H}$ when interpreting spatial differences in this area of the ocean.

3.5 Discussion

3.5.1 Comparing biogenic silica production in the equatorial Pacific with other systems

The mean $\int\rho_{24\text{-}H}$ was ~1.5 mmol Si m^{-2} d^{-1} in 2004 and ~1.3 mmol Si m^{-2} d^{-1} in 2005 (Table 3.1). Compared to other open-ocean regions, these rates are somewhat higher than mean rates measured in both the central North Pacific (1.2 mmol Si m^{-2} d^{-1} from Brzezinski et al. 1998), and at least three times those measured in the North Atlantic subtropical gyre during thermally stratified periods (0.4 mmol Si m^{-2} d^{-1} from Nelson and Brzezinski 1997). In a review of global silicification and dissolution, Nelson et al. (1995) reported a mean $\int\rho_{24\text{-}H}$ of 20 mmol Si m^{-2} d^{-1} in the Southern Ocean (another open-ocean region); that mean was compiled from seven different Southern Ocean studies, all conducted during the productive summer season (see Nelson et al. 1995 and references therein). Thus mean rates of biogenic silica production in the eastern equatorial Pacific are only ~6 – 8% of those in the Southern Ocean in summer. Similarly, $\int\rho_{24\text{-}H}$ in the equatorial Pacific is quite low compared to coastal systems. Brzezinski et al. (2003) presented data from Monterey Bay (USA), which is a site of seasonal upwelling. Their mean $\int\rho_{24\text{-}H}$, measured during periods of

active upwelling, was 43 mmol Si m^{-2} d^{-1}. This inter-system comparison indicates that $\int\rho_{24\text{-}H}$ in the equatorial Pacific is ~20-300% higher than the subtropical gyres (note: range is reflective of difference between North Atlantic and North Pacific gyres), but less than <10% of that in the Southern Ocean in summer or in areas of coastal upwelling.

In general, these differences in silicification mirror those in primary productivity, but they are larger in a proportional sense. Primary production in the equatorial Pacific averages ~75 mmol C m^{-2} d^{-1} (Chavez et al. 1996), almost twice that reported from the mid-ocean gyre of the North Pacific, where it averages ~39 mmol C m^{-2} d^{-1} (Karl et al. 1995). But, when compared to coastal systems, primary productivity in the equatorial Pacific is only ~50% of the annual mean productivity reported in coastal waters off Washington and Oregon, USA, (~150 mmol C m^{-2} d^{-1} (Perry et al. 1989) calculated by dividing the annual productivity over the continental shelf by 365 days). Low-productivity surface waters tend also to have a lower proportion of diatoms than do the Southern Ocean and many coastal systems, where diatoms often dominate. Thus it is not surprising that rates of biogenic silica production differ more between oligotrophic and eutrophic systems than do overall rates of primary production.

3.5.2 Spatial uniformity in silicification rates and the equatorial Pacific chemostat analogy

ρ_{DAY} was measured consistently on the ~04:00 cast at each station during both cruises. Measurements of ρ_{NIGHT} were measured in nocturnal incubations with water collected at ~18:00 on the 110°W transect (2004), or calculated from the difference in ^{32}Si activity in samples from 8-h daylight and 24-h incubations with water collected at ~04:00 on the equatorial transect (2004) and ~07:00 during all of 2005. Table 3.1 presents data from all casts, averaging ρ_{DAY} from casts at ~04:00 and ~07:00 in 2005. There was no statistically significant difference between the ~04:00 and ~07:00 casts with respect to either $\int\rho_{DAY}$ or V_{DAY} (t-test, $p = 0.51$ and 0.74 for $\int\rho_{DAY}$ and V_{DAY}, respectively). However, for the strictest comparison of spatial variability within the

equatorial Pacific, we will first compare $\int\rho_{DAY}$ and V_{DAY} measured on ~04:00 casts at each station.

During each cruise a very large area was covered (Figure 3.1); meridional transects were on 110°W and 140°W covering a 7° maximum latitude span (4°N–3°S). If we were to consider this as a box, this would be ~$2.6x10^6$ km^2 (i.e. 30° longitude x 7° latitude) or a region >10% larger than the Bering Sea (~$2.3x10^6$ km^2, from Libes 1992 and references therein). The mean $\int\rho_{DAY}$ and V_{DAY} measured on the ~04:00 casts were 91±47 μmol m^{-2} h^{-1}, and 0.0087±0.0028 h^{-1}, respectively (note: these means are different from Table 3.1, since they do not include $\int\rho_{DAY}$ or V_{DAY} from the –07:00 casts). The average $\int\rho_{DAY}$ and V_{DAY} measured at ~04:00 on the 110°W and 140°W transects were indistinguishable (t-test, p = 0.10 and 0.50 for $\int\rho_{DAY}$ and V_{DAY}, respectively). Likewise, mean $\int\rho_{DAY}$ and V_{DAY} measured at ~04:00 on the equator and 0.5°N transects were also indistinguishable (t-test, p = 0.33 and 0.45 for $\int\rho_{DAY}$ and V_{DAY}, respectively). Finally, when comparing all data from 2004 versus 2005, no significant differences in average $\int\rho_{DAY}$ and V_{DAY} measured at ~04:00 were observed (t-test, p = 0.80 and 0.61 for $\int\rho_{DAY}$ and V_{DAY}, respectively).

Expanding our analysis by examining $\int\rho_{24\text{-}H}$ and V_{AVE} (i.e. using all data, including those from nocturnal and 24-h incubations) we observed some spatial differences (Table 3.1). Variations with latitude were observed on each meridional transect across the equatorial upwelling zone (Figure 3.5, Table 3.1). Both southern stations on the merdianal transects were anomalous as the only two stations where $\int\rho_{NIGHT} > \int\rho_{DAY}$. Comparing mean $\int\rho_{24\text{-}H}$ between the two meridional transects indicates significantly higher rates at 110°W than at 140°W (t-test, $p<0.05$) and the difference in V_{AVE} was not statistically significant, with (t-test, p=0.18) and without (t-test, p=0.07) southernmost stations. Additionally, we found no statistically significant difference between 2004 and 2005 with respect to $\int\rho_{24\text{-}H}$ (t-test, p=0.18) or V_{AVE} (t-test, p=0.07).

The spatial gradient in $\int\rho_{24\text{-}H}$ from east (higher) to west (lower) is likely a direct result from differences in nutrient supply. Satellite SST data from December 2004 and September 2005 observed the SST at 110°W was at least 1 – 2°C cooler

(depending on latitude) than at 140°W on both cruises (SST data available at ftp://ftp.ssmi.com/sst/daily/tmi_amsre). This SST variability results from the west-east shoaling of the thermocline along the equator (e.g. sloping isotherms and isopycnals in Figure 3.2, see also Pennington et al. 2006 and references therein). The net result of the equatorial flow field and physical forcing on the subsurface nutrient fields is the upward slope of nutrient isopleths from west to east along the equator (Figure 3.2a, b). When comparing the euphotic-zone integrated $Si(OH)_4$ ($\int Si(OH)_4$) between stations at 110°W and 140°W, $\int Si(OH)_4$ was higher at 110°W (t-test, $p<0.01$).

Dugdale and Wilkerson (1998) hypothesized that new production in the equatorial Pacific system is controlled by processes similar to those operating in a Si-limited chemostat. During our cruises there was remarkably little spatial variability in either $\int \rho_{DAY}$ or V_{DAY}, with the data from the 04:00 casts (i.e. the data set that was common to all stations on both cruises) indicating lack of significant spatial variability (t-test, $p<0.05$). In addition, there were no differences between pooled $\int \rho$ or V data between cruises. Our measured rates of biogenic silica production representing something reasonably close to steady-state values; the general absence of statistically significant spatial variability in silicification rates over a vast area (2.6×10^6 km^2), notwithstanding the higher $\int \rho_{24\text{-}H}$ measured at 110°W in 2004 that at 140°W in 2005, tends to support the aspect of Dugdale and Wilkerson's hypothesis that suggests the equatorial Pacific operates in a manner analogous to a chemostat.

3.5.3 Biogenic silica in living diatoms and detrital particles

The measurement of diatom growth rates (μ) by dilution experiments indicates that diatoms in the equatorial Pacific sustain growth rates >1 d^{-1} in the upper euphotic zone (Latasa et al. 1997). Latasa et al. reported a mean rate between 10-20 m of >1.5 d^{-1}, while between 40-50 m the rate decreased to ~1.0 d^{-1}; to calculate the diatom μ in the upper 50 m (denoted as $\mu_{AVE\text{-}50m}$), we will use the mean of the 10-20 m and 40-50 m rates, 1.25 d^{-1}. During our cruises the mean V_{AVE} in the upper 50 m (denoted as $V_{AVE\text{-}50m}$) was 0.21 d^{-1}, ~6.0x lower than diatom $\mu_{AVE\text{-}50m}$.

The rate that is directly determined in a ^{32}Si uptake experiment is ρ, which is then normalized to total $bSiO_2$ for calculation of V (see eqs. 3 – 5). The $bSiO_2$

analysis does not distinguish between silica associated with living diatom cells and that present as siliceous detritus (empty frustules, fragments etc.). Thus the measured V always underestimates the V for living cells, and in any given sample the magnitude of the underestimate is proportional to the (unmeasured) ratio of detrital $bSiO_2$ to total $bSiO_2$ (Nelson and Goering 1977). If growth (i.e. cell division) and silicification are tightly coupled over a 24-h incubation experiment, then the offset between $V_{AVE\text{-}50m}$ and $\mu_{AVE\text{-}50m}$ provides an estimate of the proportion of detrital silica in the total silica pool. We can approximate the fraction of $bSiO_2$ associated with living diatoms (F) by:

$$F = V_{AVE\text{-}50m} \times (\mu_{AVE\text{-}50m})^{-1} = 0.21\ d^{-1} \times (1.25\ d^{-1})^{-1} \approx 0.17$$

By this estimate, $bSiO_2$ detritus dominates the total $bSiO_2$ pool, i.e. $bSiO_{2\text{-}Detritus} >> bSiO_{2\text{-}Live}$. Brzezinski et al. (2008), using the same approach, estimated a live fraction of 0.32; however, their analysis considered data from only the 52% light depth (~10-15 m) while our estimate is an average through the upper 50 m. Given the evidence that the total $bSiO_2$ assemblage in the upper 50 m layer may be dominated by detritus, we will address the potential impact this would have on Si recycling in surface waters via $bSiO_2$ dissolution.

Living diatoms minimize the rate of $bSiO_2$ dissolution by an organic matrix which coats the frustule (e.g. Bidle et al. 2003). Once a diatom dies it can be rapidly colonized by bacteria, which can then break down that organic coating. Thus, temperature control of bacterial metabolism has been shown to regulate silica preservation (ibid.). Despite upwelling, the annual mean SST in the eastern equatorial Pacific (1°S-1°N, 110°W-140°W) is >24°C (Pennington et al. 2006), much warmer than in other areas with high diatom biomass, e.g. Bay of Brest, France ~14°C (Beucher et al. 2004), the Ross Sea <2°C (Nelson et al. 1991). Hence biogenic silica detritus within the surface waters of this region would be expected to dissolve rapidly.

Our calculation of a low F value, is strengthened by empirical evidence of intense zooplankton grazing on diatoms in this system (Latasa et al. 1997), and low $bSiO_2$ export efficiency (<10% at 125 m, measured by Blain et al. 1999). Grazing on diatoms by microzooplankton would not result in the formation of dense and rapidly sinking fecal pellets, commonly associated with mesozooplankton grazers (e.g. large copepods, krill, etc. see Small et al. 1979 and references therein). It is likely that

detrital $bSiO_2$ residence time in the euphotic zone, at least to the extent that it is controlled by sinking, would increase under heavy microzooplankton grazing, or sloppy feeding by mesozooplankton (resulting in small $bSiO_2$ fragments which are not rapidly exported like $bSiO_2$ associated with dense fecal pellets). In the euphotic zone, either microzooplankton grazing or sloppy feeding by mesozooplankton may increase the residence time of $bSiO_2$ detritus. Coupling this possibility with the warm equatorial Pacific surface waters (compared to other diatom dominated systems) there is a high probability of rapid $bSiO_2$ dissolution by either direct temperature effect (Kamatani 1982) and/or bacterial mediation (Bidle et al. 2003). This indirect argument suggests it is likely that the main fate of detrital $bSiO_2$ in the surface waters of the equatorial Pacific is dissolution rather than sinking, and that the true residence time of $bSiO_2$ in the surface waters of the eastern equatorial Pacific is controlled by dissolution.

3.5.4 The estimated contribution of diatoms to primary production and new production

Dugdale and Wilkerson's (1998) model assumes that diatoms in the equatorial Pacific use NO_3^- as their sole nitrogen source, and thus all diatom production is new production. It further assumes that diatoms are responsible for essentially all new production in the system, thus $Si(OH)_4$ availability limits new production in this region by limiting diatom growth. In the equatorial Pacific region, diatoms accounted for <5% of the total community chlorophyll, and are vastly outnumbered by prokaryotes and picoeukaryotes (Landry et al. 1997 and references therein). Therefore, is it reasonable to conclude that they are the main agents of new production in the system?

Other studies have also inferred that diatoms support most of the new production in the equatorial Pacific (e.g. Dunne et al. 1999, Leynaert et al. 2001). A problem in those studies has been that Si tracer experiments were either not done or not done concurrently with C or N tracer studies in a way that permits direct comparison of measured rates. Thus current estimates of the diatoms' contribution to C and N uptake hinge on conversion of $\int\rho_{24\text{-}H}$ to previously published rates of primary

production or new production in the same general vicinity during some other time period (e.g. Leynaert et al. 2001). Most conversions use Si:C and Si:N ratios from diatoms growing under nutrient-replete culture conditions (e.g. Brzezinski 1985). However, some studies have used ratios from diatom cultures grown in low iron conditions (e.g. Hutchins and Bruland 1998, Takeda 1998), which are thought to be more representative of the *in situ* diatom ratios in the equatorial Pacific.

Dugdale et al. (2007), using data from the 2004 cruise, reported the first size-fractioned rates of new and regenerated production in the equatorial Pacific upwelling zone. They reported the near surface f-ratio ($\rho_{NO3}/(\rho_{NO3} + \rho_{NH4})$) for the >5 μm size-fraction in daylight hours along the 110°W transect ranging from ~0.4 to ~0.6 at all but one station (4°N, which had very low surface [NO_3^-]), while f-ratio for the <5 μm size-fraction ranged from ~0.1 to ~0.3. Near-surface f-ratios on the equator (from 116.7°W-140°W) ranged from ~0.5 to 0.8 for the > 5 μm size-fraction, and ~0.1 to 0.4 for the <5 μm fraction. These results demonstrate that > 5 μm cells proportionally use more NO_3^- for production than do < 5 μm cells. However, they cannot be compared directly with uptake rates of other elements, such as C or Si, due to differences in the vertical distribution and day/night timing of C, N and Si uptake. Direct comparison of that kind requires vertically integrated, daily uptake rates (i.e. $\int\rho_{24\text{-}H}$) for all elements. The data collected during our cruises in 2004 and 2005 enable us to make that comparison.

The reported $bSiO_2$ production rates in this study were measured in ^{32}Si incubations that were run concurrently with ^{14}C (Balch et al. *in preparation*) and ^{15}N (Dugdale et al. *in preparation*) uptake experiments. In addition, the elemental composition of individual diatom cells was measured using a synchrotron-based x-ray fluorescence (SXRF) microprobe (Twining et al. 2004, Twining et al. *in preparation*); enabling us to make a novel estimate of diatoms' contribution to new and primary production.

The SXRF-based estimates of Si:C and Si:N mole ratios (Twining et al. *in preparation*) are based on measured Si:S ratios in the most abundant pennate diatoms during 2004 (data not yet available for 2005). The SXRF method is not yet capable of measuring cellular C or N directly due to their low atomic mass and relatively weak

fluorescence signal. Cellular P can be measured and cellular C and N estimated by the using the Redfield ratio of 106 C: 16 N: 1P (Redfield et al. 1963). However in diatoms the cellular P fluorescence peak shows up as a shoulder on the very strong cellular Si peak; thus S-based estimates of diatom cellular C and N appear to be more reliable (S. Baines personal communication). The measured Si:S ratios were converted to estimates of Si:C and Si:N ratios using a culture-based S:C ratio of 0.010 (C:S ratio of 100) and a Redfield C:N ratio of 6.6 (106:16).

Previous studies in the equatorial Pacific have demonstrated that the ambient diatom community is dominated by small pennate genera (Blain et al. 1997, Kobayashi and Takahashi 2002). The S-based, 2004 cruise average Si:C and Si:N mole ratios for the dominant pennate diatoms were 0.13 and 0.85, respectively (Twining et al., *in preparation*). These *in situ* diatom Si:C and Si:N ratios are similar to, but slightly lower than, the mean Si:C and Si:N ratios reported for nutrient replete diatoms in culture (Si:C ≈0.15, Si:N ≈1, Brzezinski 1985).

In 2005, $\int\rho_{24\text{-}H}$ was measured on casts beginning at ~07:00, whereas $\int\rho_{DAY}$, ^{14}C and ^{15}N rates were measured on casts beginning ~04:00. Comparing $\int\rho_{DAY}$ from ~04:00 casts versus ~07:00 casts indicates no significant differences (t-test, p= 0.51); therefore, we will use $\int\rho_{24\text{-}H}$ from ~07:00 casts to compare with daily (i.e. 24 h) ^{14}C and ^{15}N rates. Balch et al. (*in preparation*) calculated daily rates from primary production measured during dawn to dusk incubations. Dugdale et al. (*in preparation*) derived daily ^{15}N-based rates by multiplying day-time hourly rates for $\int\rho NO_3^-$ and $\int\rho NH_4^+$ by 12 and 18, respectively (Dugdale et al. *in preparation*, see also McCarthy et al. 1996).

Our results suggest that diatoms accounted for ~20% of the mean total primary production and ~70-80% of the >3 μm (size-fractioned) primary production in both years (Table 3.2). Diatoms' estimated contribution to total nitrogen (i.e. $\int\rho NO_3^- + \int\rho NH_4^+$) uptake was similar to total primary production in 2004 (mean ~17%, Table 3.2) and lower than primary production in 2005 (mean ~8%, Table 3.2). If we assume the diatoms' sole source of N is NO_3^- (e.g. Dugdale and Wilkerson 1998), we can estimate their maximum contribution to total NO_3^- uptake. By that maximizing assumption diatoms were potentially responsible for 40-60% of the NO_3^- uptake (i.e.

new production) in both years (Table 3.2). During 2005, size-fractioned NO_3^- uptake samples were taken throughout the entire euphotic zone (Dugdale et al. *in preparation*). Again, assuming diatoms' sole source of N is NO_3^- indicates they potentially carried out >60% of the >5 μm size-fractioned $\int \rho NO_3^-$ in the euphotic zone on the 2005 cruise (Table 3.2).

Goldman et al. (1992), referring to numerically rare diatoms in the Sargasso Sea, emphasized that a large diatom is equivalent in biomass to thousands of smaller cells. Considering diatom biomass is <5% of the total community chlorophyll and they are numerically rare cells (compared to the picoplankton majority, see Landry et al. 1997 and references therein), their role in primary and new production is disproportionately large (c.f. Table 3.2). Our estimates would indicate that diatoms were carrying out ~20% of the community primary production and most (>70%) of the primary production for cells >3 μm. In terms of new production, diatoms were potentially responsible for ~50% of the total new production during both cruise periods, increasing to >60% of the new production for cells >5 μm during 2005.

These results indicate that the diatoms' contribution to primary and new production in the equatorial Pacific is many times higher than their contribution to autotrophic biomass (<5%; Landry et al. 1997 and references therein). This situation is similar to that estimated by Nelson and Brzezinski (1997) in the Sargasso Sea. Diatoms in the Sargasso Sea are similarly a very minor component of the autotrophic community in terms of biomass (typically <5%, see Goericke 1998, Steinberg et al. 2001). But the diatom contribution to annual organic matter production, estimated by methods similar to those used here, but without SXRF data to estimate the Si:C or Si:N ratios of diatoms in the system, is ~20% on an annual basis (Nelson and Brzezinski, 1997). Their contribution to organic matter export, based on POC, PON and $bSiO_2$ collection over periods of 2 – 4 days by sediment traps at 150, 200 and 300 m, was estimated to be ~30% on an annual basis, increasing to >90% during the spring bloom period. Our data, coupled with those of Nelson and Brzezinski (1997), indicate that diatoms have a disproportional impact on biogeochemical processes, particularly new production, in these open-ocean systems.

Acknowledgements

We thank S. Baines, W. Balch, R. Dugdale, and B. Twining for permission to use their data. J. Arrington, C. Beucher, M. Demarest, C. Dumousseaud, and J. Jones provided valuable shipboard and laboratory assistance. Thanks to the science party and crew on each cruise aboard the *R.V. Roger Revelle* for outstanding technical and logistical support. This work was funded by the National Science Foundation Biocomplexity Grant OCE 03-22074 awarded to DMN, additional support awarded to JWK was provided by the Oregon Space Grant and Leynore Bayley Fellowships at Oregon State University.

3.6 References

Archer, D.E., Takahashi, T., Sutherland, S., Goddard, J., Chipman, D., Rodgers, K., Ogura, H., 1996. Daily, seasonal and interannual variability of sea-surface carbon and nutrient concentration in the equatorial Pacific Ocean. Deep-Sea Research II 43, 779-808.

Archer, D., and 16 others, 1997. A meeting place of great ocean currents: shipboard observations of a convergent front at 2 degrees N in the Pacific. Deep-Sea Research II 44, 1827-1849.

Balch, W., Drapeau D., Poulton A., Bowler, B., Windecker, L., Booth, E, *in preparation*. Calcification and photosynthesis rates in the Equatorial Pacific Ocean between 110°W and 140°W. For submission to Deep-Sea Research II.

Beucher, C., Tréguer, P., Corvaisier, R., Hapette, A.M., Elskens., M., 2004. Production and dissolution of biosilica, and changing microphytoplankton dominance in the Bay of Brest (France). Marine Ecology Progress Series 267 57–69.

Bidigare, R.R., Ondrusek, M.E., 1996. Spatial and temporal variability of phytoplankton pigment distributions in the central equatorial Pacific Ocean. Deep-Sea Research II 43, 809-833.

Bidle, K.D., Brzezinski, M.A., Long, R.A., Jones, J.L., Azam, F., 2003. Diminished efficiency in the oceanic silica pump caused by bacteria-mediated silica dissolution. Limnology and Oceanography 48, 1855-1868.

Blain, S., Leynaert, A., Treguer, P., ChretiennotDinet, M.J., Rodier, M., 1997. Biomass, growth rates and limitation of Equatorial Pacific diatoms. Deep-Sea Research I 44, 1255-1275.

Blain, S., Treguer, P., Rodier, M., 1999. Stocks and fluxes of biogenic silica in the western oligotrophic equatorial Pacific. Journal of Geophysical Research-Oceans 104, 3357-3367.

Brzezinski, M.A., 1985. The Si:C:N ratio of marine diatoms: Interspecific variability and the effect of some environmental variables. Journal of Phycology 21, 347-357.

Brzezinski, M.A., Nelson, D.M., 1989. Seasonal changes in the silicon cycle within a Gulf Stream warm-core ring. Deep-Sea Research 36, 1009-1030.

Brzezinski, M.A., Nelson, D.M., 1995. The annual silica cycle in the Sargasso Sea near Bermuda. Deep-Sea Research I 42, 1215-1237.

Brzezinski, M.A., Villareal, T.A., Lipschultz, F., 1998. Silica production and the contribution of diatoms to new and primary production in the central North Pacific. Marine Ecology-Progress Series 167, 89-104.

Brzezinski, M.A., Jones, J.L., Bidle, K.D., Azam, F., 2003. The balance between silica production and silica dissolution in the sea: Insights from Monterey Bay, California, applied to the global data set. Limnology and Oceanography 48, 1846-1854.

Brzezinski, M.A., Cynthia Dumousseaud, C., Krause, J.W., Measures, C.I., Nelson, D.M., 2008. Iron and silicic acid concentrations together regulate Si uptake in the equatorial Pacific Ocean. Limnology and Oceanography 53, 875-889.

Chavez, F.P, Barber, R.T, 1987. An estimate of new production in the equatorial Pacific. Deep-Sea Research 34, 1229-1243.

Chavez, F.P., Buck, K.R., Service, S.K., Newton, J., Barber, R.T., 1996. Phytoplankton variability in the central and eastern tropical Pacific. Deep-Sea Research II 43, 835-870.

Coale, K.H., and 18 others, 1996. A massive phytoplankton bloom induced by an ecosystem-scale iron fertilization experiment in the Equatorial Pacific Ocean. Nature 383, 495-501.

Dugdale, R.C., Wilkerson, F.P., 1998. Silicate regulation of new production in the equatorial Pacific upwelling. Nature 391, 270-273.

Dugdale, R.C., Wilkerson, F.P., Chai, F., Feely, R., 2007. Size-fractionated nitrogen uptake measurements in the equatorial Pacific and confirmation of the low Si-high-nitrate low-chlorophyll condition. Global Biogeochemical Cycles 21, GB2005, doi:10.1029/2006GB002722.

Dugdale, R.C., and colleagues *in preparation*. N-uptake and size-fractioned estimates of new production in the eastern equatorial Pacific. For submission to Deep-Sea Research II.

Dunne, J.P, Murray, J.W., Aufdenkampe, A.K., Blain, S., Rodier, M., 1999. Silicon-nitrogen coupling in the equatorial Pacific upwelling zone. Global Biogeochemical Cycles 13, 715-726.

Goericke, R., 1998. Response of phytoplankton community structure and taxon specific growth rates to seasonally varying physical forcing in the Sargasso Sea off Bermuda. Limnology and Oceanography 43, 921-935.

Goldman, J.C., Hansell, D.A., Dennet, M.R., 1992. Chemical characterization of three large oceanic diatoms: potential impact on water column chemistry. Marine Ecology Progress Series 88, 257-270.

Gorgues, T., Menkes, C., Aumont, O., Vialard, J., Dandonneau, Y., Bopp, L., 2005. Biogeochemical impact of tropical instability waves in the equatorial Pacific. Geophysical Research Letters 32, L24615, doi:10.1029/2005GL024110.

Hutchins, D.A., Bruland, K.W., 1998. Iron-limited diatom growth and Si:N uptake ratios in a coastal upwelling regime. Nature 393, 561-564.

Kaczmarkska, I., Fryxell, G.A., 1995. Micro-phytoplankton of the equatorial Pacific: 140°W meridianal transect during the 1992 El Niño. Deep-Sea Research II 42, 535-558.

Kamatani, A., 1982. Dissolution rates of silica from diatoms decomposing at various temperatures. Marine Biology 68, 91-96.

Karl, D.M., Christian, J.R., Dore, J.E., Hebel, D.V., Letelier, R.M., Tupas, L.M., Winn, C.D., 1995. Seasonal and interannual variability in primary production and particle flux at Station ALOHA. Deep-Sea Research II 43, 539-568.

Kessler, W.S., 2006. The circulation of the eastern tropical Pacific: A review. Progress in Oceanography 69, 181-217.

Kobayashi, F., Takahashi, K., 2002. Distribution of diatoms along the equatorial transect in the western and central Pacific during the 1999 La Nina conditions. Deep-Sea Research II 49, 2801-2821.

Ku, T.-L., Luo, S., Kusakabe, M., Bishop, J.K.B., 1995. ^{228}Ra-derived nutrient budgets in the upper Equatorial Pacific and the role of "new" silicate in limiting productivity. Deep-Sea Research II 42, 479-497.

Landry, M.R., Barber, R.T., Bidigare, R.R., Chai, F., Coale, K.H., Dam, H.G., Lewis, M.R., Lindley, S.T., McCarthy, J.J., Roman, M.R., Stoecker, D.K., Verity, P.G., White, J.R., 1997. Iron and grazing constraints on primary production in the central equatorial Pacific: An EqPac synthesis. Limnology and Oceanography 42, 405-418.

Latasa, M., Landry, M.R., Schluter, L., Bidigare, R.R., 1997. Pigment-specific growth and grazing rates of phytoplankton in the central equatorial Pacific. Limnology and Oceanography 42, 289-298.

Leblanc, K., Hutchins, D.A., 2005. New applications of a biogenic silica deposition fluorophore in the study of oceanic diatoms. Limnology and Oceanography: Methods 3, 462-476.

Leynaert, A., Treguer, P., Lancelot, C., Rodier, M., 2001. Silicon limitation of biogenic silica production in the Equatorial Pacific. Deep-Sea Research I 48, 639-660.

Libes, S.M., 1992. An introduction to marine biogeochemistry. Wiley & Sons: New York. 734 pgs.

McCarthy, J.J., Garside, C., Nevins, J.L., Barber, R.T., 1996. New production along 140°W in the equatorial Pacific during and following the 1992 El Niño event. Deep-Sea Research II 43, 1065-1093.

Minas, H.J., M. Minas, M., Packard, T.T., 1986. Productivity in upwelling areas deduced from hydrographic and chemical fields. Limnology and Oceanography 31, 1182-1206.

Murray, J.W., Johnson, E., Garside, C., 1995. A U.S. JGOFS Process Study in the equatorial Pacific (EqPac): Introduction. Deep-Sea Research II 42, 275-293.

Nelson, D.M., Brzezinski, M.A., 1997. Diatom growth and productivity in an oligotrophic midocean gyre: A 3-yr record from the Sargasso Sea near Bermuda. Limnology and Oceanography 42, 473-486.

Nelson, D.M., Goering, J.J., 1977. Near-surface silica dissolution in the upwelling region off northwest Africa. Deep-Sea Research 24: 65-73.

Nelson, D.M., Ahern, J.A., Herlihy, L.J., 1991. Cycling of biogenic silica within the upper water column of the Ross Sea. Marine Chemistry 35: 461-476.

Nelson, D.M., Tréguer, P., Brzezinski, M.A., Leynaert, A., and B. Queguiner. 1995. Production and dissolution of biogenic silica in the ocean: Revised global estimates, comparison with regional data and relationship to biogenic sedimentation. Global Biogeochemical Cycles 9: 359–372.

Nelson, D.M., De Master, D.J., Dunbar, R.J., Smith, W.O., Jr., 1996. Cycling of organic carbon and biogenic silica in the Southern Ocean: Estimates of water-column and sedimentary fluxes over the Ross Sea continental shelf. Journal of Geophysical Research 101, 18519-18532

Nelson, D.M., Brzezinski, M.A., Sigmon, D.E., Franck, V.M., 2001. A seasonal progression of Si limitation in the Pacific sector of the Southern Ocean. Deep-Sea Research II 48, 3973-3995.

Pennington, J.T., Mahoney, K.L., Kuwahara, V.S., Kolber, D.D., Calienes, R., Chavez, F.P., 2006. Primary production in the eastern tropical Pacific: A review. Progress in Oceanography 69, 285-317.

Perry, M.J., Bolger, J.P., English, D.C., 1989. Primary production in Washington coastal waters, p. 117-138. *In* M.R. Landry and B.M. Hickey (Eds) Coastal Oceanography of Washington and Oregon. Elsevier: Amsterdam.

Redfield, A.C.,Ketchum, B.H., Richards, F.A., 1963. The influence of organisms on the composition of sea water, p. 26-77. *In* M.N. Hill (ed.) The Sea v. 2. Wiley: New York.

Schlitzer, R. 2006. Ocean Data View, http://odv.awi-bremerhaven.de.

Small, L.F., Fowler, S.W., Ünlü, M.Y., 1979. Sinking rates of natural copepod fecal pellets. Marine Biology 51, 233-241.

Steinberg, D. K., Carlson, C. A., Bates, N. R., Johnson, R. J., Michaels, A. F., Knap, A. H. 2001. Overview of the US JGOFS Bermuda Atlantic Time-series Study (BATS): a decade-scale look at ocean biology and biogeochemistry. Deep-Sea Research Part II 48, 1405-1447.

Strutton, P.G., Ryan, J.P., Chavez, F.P., 2001. Enhanced chlorophyll associated with tropical instability waves in the equatorial Pacific. Geophysical Research Letters 28, 2005-2008.

Takahashi, T., Sutherland, S.C., Sweeney, C., Poisson, A., Metzl, N., Tilbrook, B., Bates, N., Wanninkhof, R., Feely, R.A., Sabine, C., Olafsson, J., Nojiri, Y., 2002. Global sea-air CO_2 flux based on climatological surface ocean pCO_2, and seasonal biological and temperature effects. Deep-Sea Research II 49, 1601-1622.

Takeda, S., 1998. Influence of iron availability on nutrient consumption ratio of diatoms in oceanic waters. Nature 393, 774-777.

Twining, B.S., and colleagues *in preparation*. Elemental stoichiometries of individual plankton cells in the equatorial Pacific. For submission to Deep-Sea Research II.

Twining, B.S., Baines, S.B., Fisher, N.S., 2004. Element stoichiometries of individual plankton cells collected during the Southern Ocean Iron Experiment (SOFeX). Limnology and Oceanography 49, 2115-2128.

Wilkerson, F.P., Dugdale, R.C., 1996. Silicate versus nitrate limitation in the equatorial Pacific estimated from satellite-derived sea-surface temperatures. Advances in Space Research 18, 81-89.

Yoder, J.A., Ackleson, S.G., Barber, R.T., Flament, P., Balch, W.M., 1994. A line in the sea. Nature 371, 689-692.

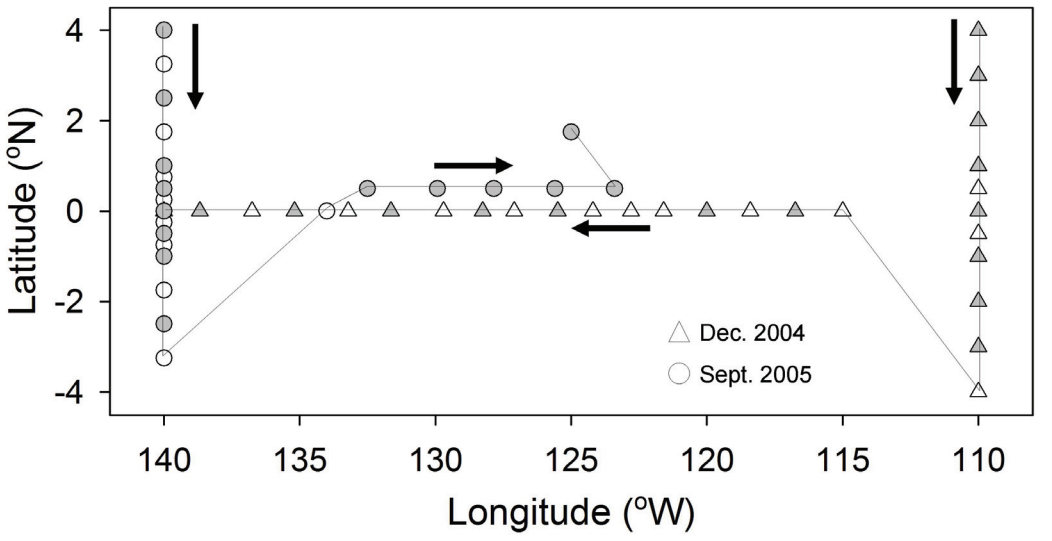

Figure 3.1 – Station locations for cruises during December 2004 (triangles) and September 2005 (circles). Meridional track was from north to south in both years while zonal track was in opposite directions in each year (westward 2004, eastward 2005). Shaded symbols indicate stations where silicification rates were measured.

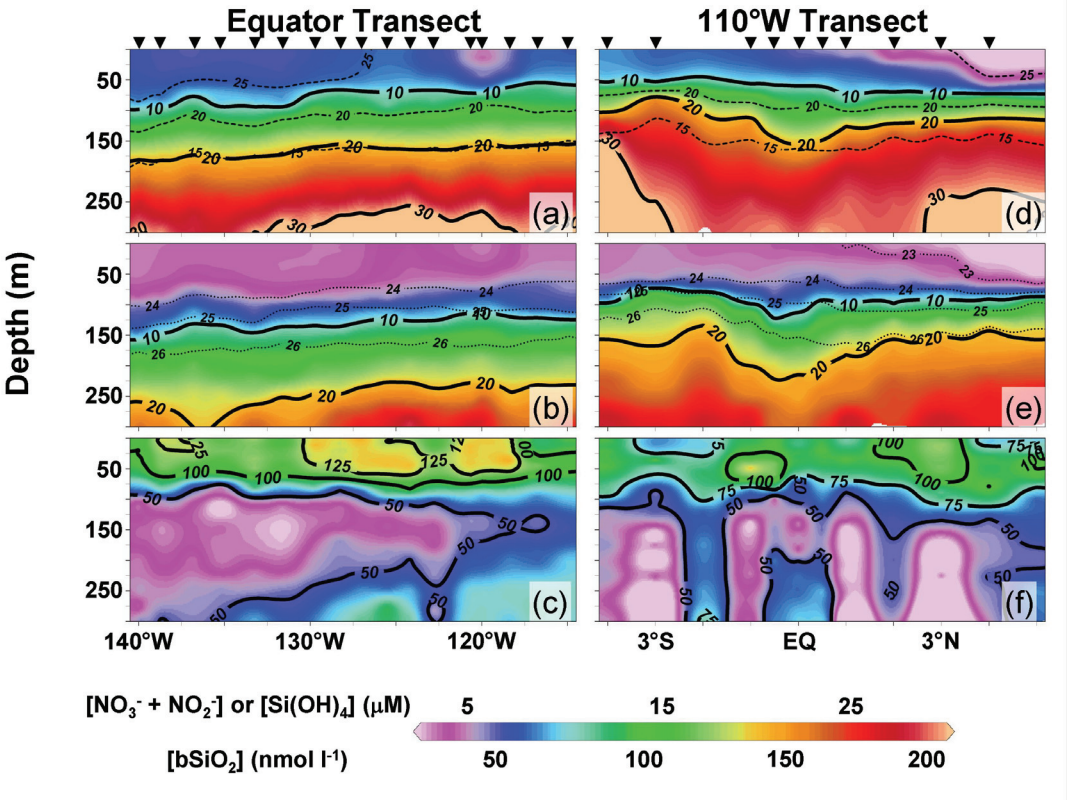

Figure 3.2 – Dissolved nutrients (in μM) and biogenic silica (nmol l^{-1}) on the equator (a, b, c) and 110°W (d, e, f) in 2004. (a, d) [NO_3^-+NO_2^-], (b, e) [$Si(OH)_4$] and (c, f) [$bSiO_2$]. Solid contour lines (all panels) are the measured property. Dashed contour lines (a, d) are the 15, 20, and 25 °C isotherms, while dotted contour lines (b, e) are the 23, 24, 25, and 26 σ_θ kg m^{-3} isopycnals. ▼ above panels a and d denote station locations. Contouring was done with a built-in algorithm in the Ocean Data View software package (Schlitzer 2006). Nutrient data courtesy of R. Dugdale.

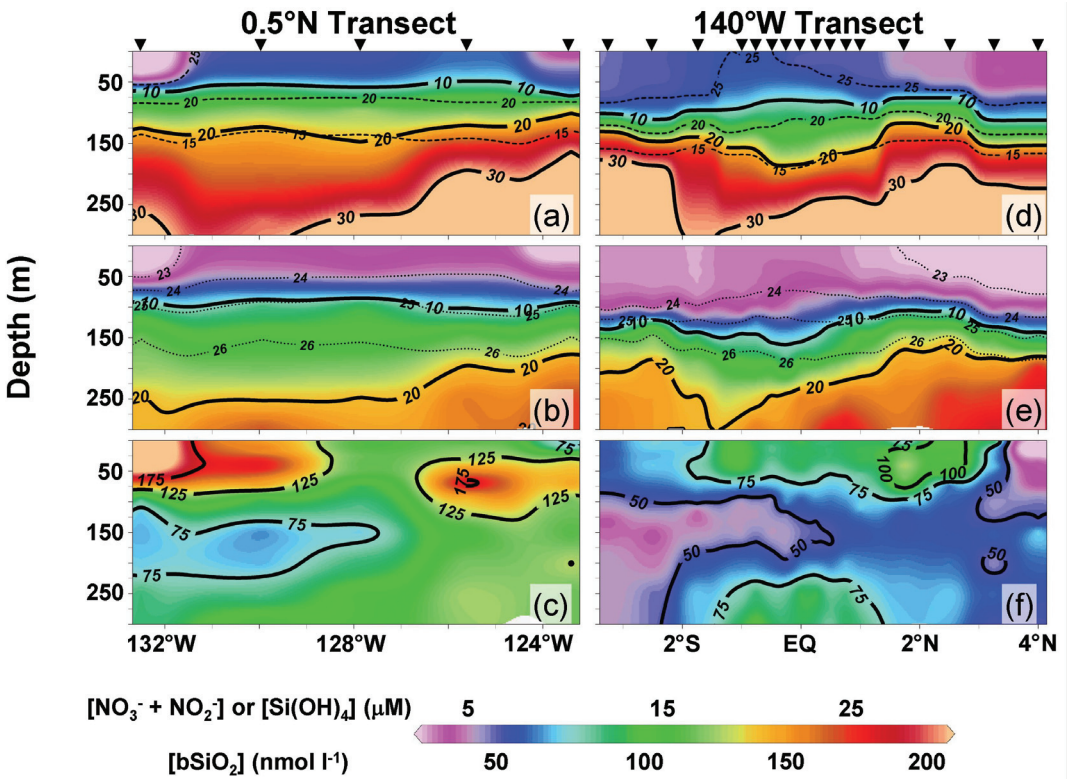

Figure 3.3 – Dissolved nutrients (in μM) and biogenic silica (nmol l^{-1}) on 0.5°N (a, b, c) and 140°W (d, e, f) in 2005. (a, d) [NO_3^-+NO_2^-], (b, e) [$Si(OH)_4$] and (c, f) [$bSiO_2$]. Solid contour lines (all panels) are the measured property. Dashed contour lines (a, d) are the 15, 20, and 25 °C isotherms, while dotted contour lines (b, e) are the 23, 24, 25, and 26 σ_θ kg m^{-3} isopycnals. ▼ above panels a and d denote station locations. Contouring and data source information, same as in Figure 3.2.

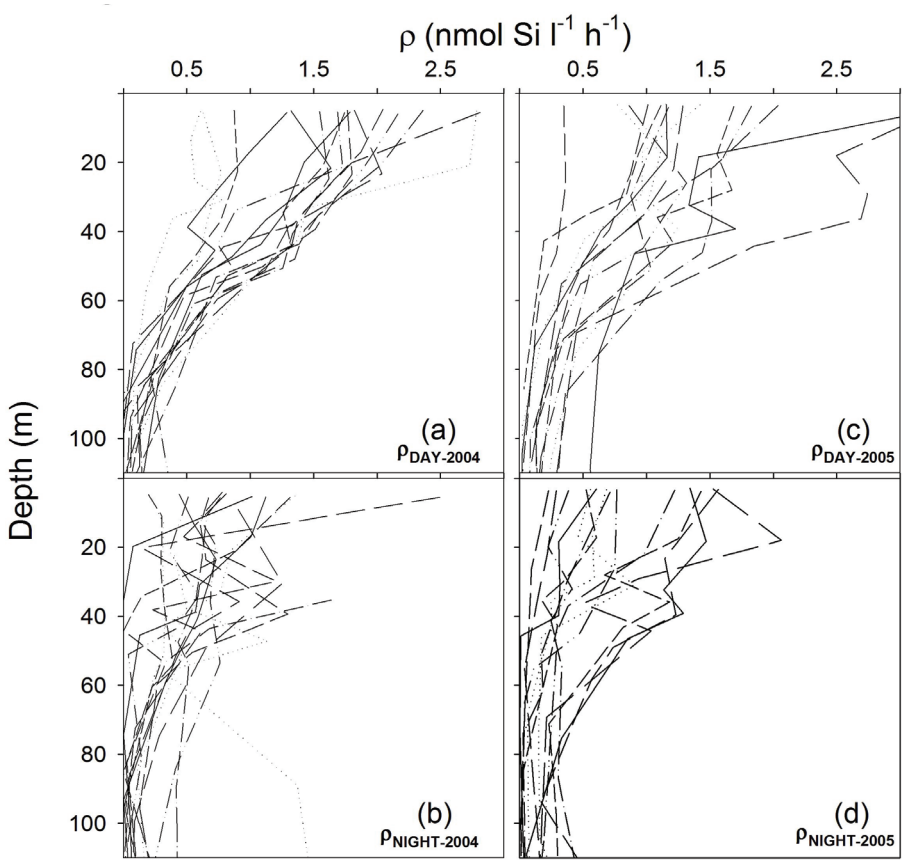

Figure 3.4 – Vertical profiles of $bSiO_2$ production (ρ) in 2004 (a, b) and 2005 (c, d) during the day (a, c) and night (b, d). Day rates (ρ_{DAY}) were consistently higher than night rates (ρ_{NIGHT}) regardless of space and time.

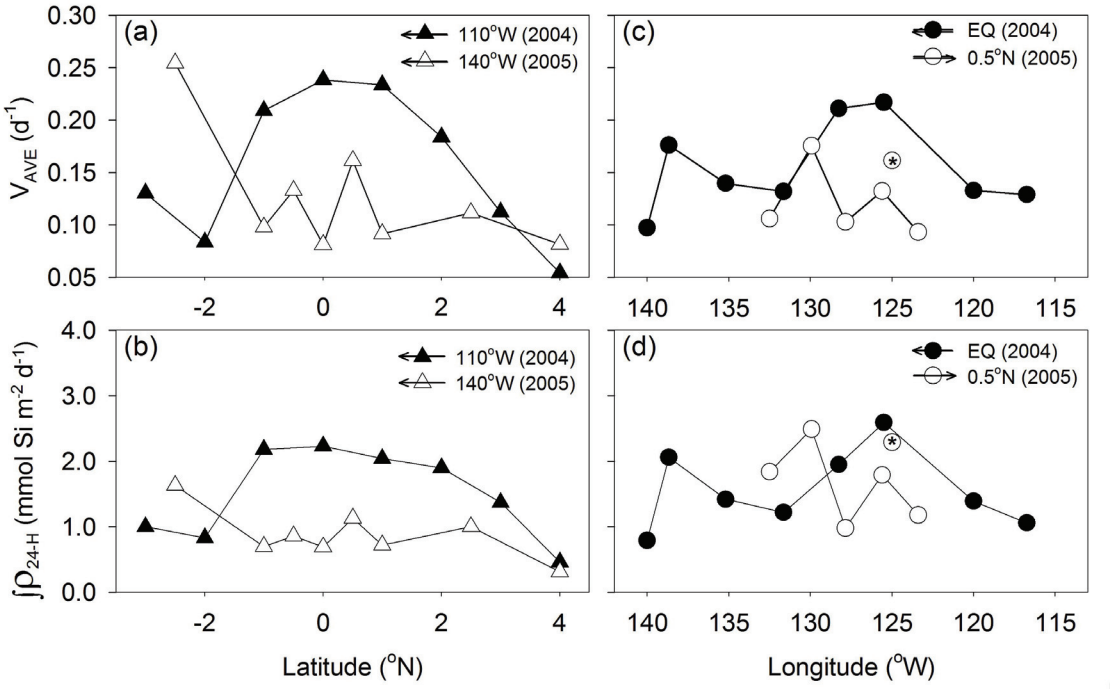

Figure 3.5 – Spatial variation in euphotic zone integrated $bSiO_2$ production ($\int\rho_{24\text{-}H}$) and average specific $bSiO_2$ production (V_{AVE}) for 2004 (solid shapes) and 2005 (open shapes). (a, c) V_{AVE} on meridional (a) and zonal (c) transects. (b, d) $\int\rho_{24\text{-}H}$ on meridional (b) and zonal (d) transects. * in (b) and (d) indicates TIW station at 1.75°N and 125°W in 2005. Arrows on legend indicates the direction traveled on each transect.

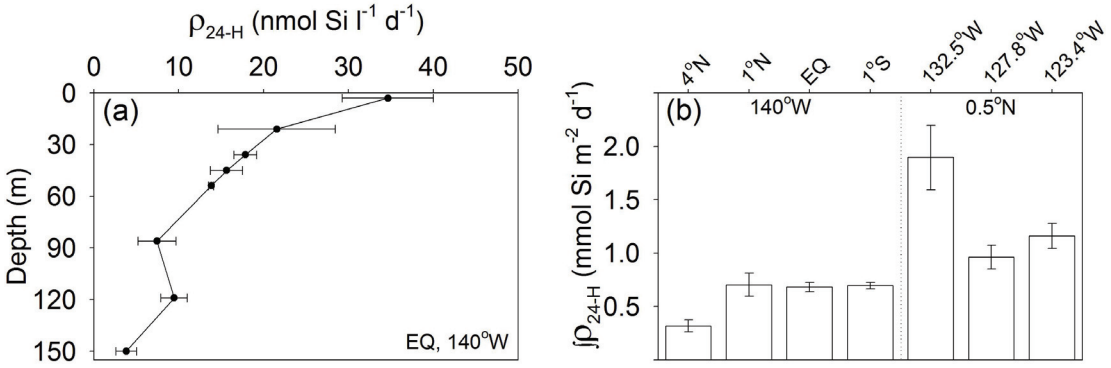

Figure 3.6 – Variability in ρ measurements at seven stations in 2005. (a) $\rho_{24\text{-H}}$ with triplicate replication at each depth; station location at 0° (EQ) x 140°W. (b) $\int\rho_{24\text{-H}}$ for each profile (n = 7) with triplicate replication at each depth. Dotted line separates profiles on 140°W and 0.5°N transects. Error bars in (a, b) are ±1 standard deviation.

Table 3.1 – Euphotic zone $\int bSiO_2$, $bSiO_2$ production ($\int \rho$), and average euphotic zone specific production (V). ρ and V are broken down into day, night and daily rates. *Indicates average of two day profiles taken at the same station (e.g. 04:00 and 07:00 local time). #Indicates stations where triplicate $\int \rho_{24-H}$ samples were taken (2005 only). Grand average for $\int bSiO_2$ includes all profiles where $bSiO_2$ samples were taken (n = 84), ρ samples were not taken as often (n=44 day, 30 night, 30 24-h). +Indicates the single TIW station. For clarity individual cruise and grand average values are **bold**, "std." is the standard deviation.

Transect	Station	$\int bSiO_2$ (mmol m^{-2})	$\int \rho_{DAY}$ (μmol m^{-2} h^{-1})	$\int \rho_{NIGHT}$ (μmol m^{-2} h^{-1})	$\int \rho_{24-H}$ (mmol m^{-2} d^{-1})	V_{DAY} (h^{-1})	V_{NIGHT} (h^{-1})	V_{AVE} (d^{-1})
110.0W	4.0-N	8.51	30.1	21.8	0.46	0.0042	0.0022	0.054
	3.0-N	12.22	76.6	40.1	1.37	0.0062	0.0033	0.112
	2.0-N	10.32	99.3	58.1	1.90	0.0096	0.0056	0.183
	1.0-N	8.74	102.1	62.7	2.04	0.0110	0.0076	0.234
	0-EQ	9.35	109.0	67.1	2.23	0.0105	0.0081	0.239
	1.0-S	10.42	109.3	66.8	2.18	0.0100	0.0067	0.209
	2.0-S	9.93	54.8	22.5	0.83	0.0064	0.0020	0.084
	3.0-S	7.70	42.2	102.9	1.00	0.0051	0.0145	0.130
EQ	116.7-W	8.25	53.6	39.0	1.06	0.0065	0.0047	0.129
	120.0-W	10.47	87.2	42.2	1.39	0.0083	0.0040	0.133
	125.5-W	11.93	119.5	81.3	2.59	0.0100	0.0068	0.217
	128.3-W	9.23	117.7	59.5	1.95	0.0128	0.0064	0.211
	131.6-W	9.22	92.5	27.4	1.22	0.0100	0.0030	0.132
	135.2-W	10.20	95.4	40.0	1.42	0.0093	0.0039	0.140
	138.7-W	11.73	134.1	55.9	2.06	0.0114	0.0048	0.176
	140.0-W	8.11	90.5	13.9	0.79	0.0112	0.0017	0.097
	2004 Ave	**10.31**	**88.4**	**50.1**	**1.53**	**0.0089**	**0.0053**	**0.162**
	Std.	1.66	29.6	23.7	0.62	0.0025	0.0032	0.052
140.0W	4.0-N	3.76	*20.3	8.3	#0.31	0.0054	0.0022	0.081
	2.5-N	8.99	*63.1	26.5	1.00	0.0071	0.0030	0.111
	1.0-N	9.49	*68.4	12.6	#0.72	0.0074	0.0016	0.091
	0.5-N	7.34	*64.5	37.1	1.13	0.0088	0.0051	0.161
	0-EQ	8.10	*60.9	23.3	#0.69	0.0076	0.0027	0.081
	0.5-S	6.69	*55.2	28.2	0.86	0.0083	0.0043	0.133
	1.0-S	8.31	*56.0	17.1	#0.70	0.0069	0.0024	0.098
	2.5-S	6.50	*55.8	81.4	1.63	0.0086	0.0125	0.254
0.5N	132.5-W	18.07	*143.8	63.4	#1.84	0.0080	0.0035	0.106
	129.9-W	15.20	*186.7	78.2	2.49	0.0122	0.0055	0.175
	127.9-W	9.41	*86.9	22.0	#0.98	0.0092	0.0024	0.103
	125.6-W	14.48	*93.8	70.1	1.79	0.0065	0.0052	0.132
	123.4-W	12.85	*79.4	35.4	#1.18	0.0062	0.0028	0.093
+1.75	125.0-W	14.16	*179.3	83.4	2.29	0.0127	0.0058	0.161
	2005 Ave	**10.06**	**86.7**	**41.9**	**1.26**	**0.0082**	**0.0042**	**0.127**
	Std.	4.06	51.1	27.3	0.65	0.0025	0.0028	0.048
	Grand Ave	**10.20**	**87.3**	**46.3**	**1.40**	**0.0085**	**0.0048**	**0.146**
	Std.	2.95	44.1	25.4	0.64	0.0025	0.0030	0.053

Table 3.2 – Estimated diatom contribution (% of total) to euphotic zone integrated primary production and nitrogen uptake. Total and >3 μm size-fractioned primary productivity mean (±std.) from each cruise are from Balch et al. (*in preparation*). Total N uptake (i.e. $\int\rho NH_4^+ + \int\rho NO_3^-$), total $\int\rho NO_3^-$ and >5 μm size-fractioned $\int\rho NO_3^-$ (no integrated data from 2004) means (±std.) from each cruise are from Dugdale et al. (*in preparation*). $\int\rho_{24\text{-}H}$ was converted to C and N by Si:C = 0.13, and Si:N = 0.85 (from Twining et al. *in preparation*). Calculated contribution to $\int\rho NO_3^-$ assumes that diatoms use NO_3^- as their only N source. Error term in diatom contribution % is the coefficient of variation (std./mean) from $\int\rho_{24\text{-}H}$ applied to each estimate.

Euphotic Zone Integrated Rates	2004	Estimated Diatom Contribution	2005	Estimated Diatom Contribution
$\int\rho_{24\text{-}H}$ (mmol m^{-2} d^{-1})	1.5 ±0.6	-	1.3 ±0.6	-
∫1° Prod (mmol C m^{-2} d^{-1})	57.9 ±16.7	20.3% ±8.2%	48.7 ±15.3	19.9% ±10.3%
∫1° Prod, >3μm (mmol C m^{-2} d^{-1})	16.0 ±15.4	73.4% ±29.6%	12.0 ±3.4	80.9% ±41.8%
∫ρN, Total (mmol N m^{-2} d^{-1})	10.4 ±5.5	17.3% ±7.0%	19.8 ±5.4	7.5% ±3.9%
$\int\rho NO_3^-$ (mmol N m^{-2} d^{-1})	3.0 ±1.5	60.7% ±24.5%	3.4 ±1.8	43.0% ±22.2%
$\int\rho NO_3^-$, >5 μm (mmol N m^{-2} d^{-1})	-	-	2.4 ±1.4	61.8% ±31.9%

4. Biogenic silica at the Bermuda Atlantic Time-series Study site in the Sargasso Sea: Temporal changes and their inferred controls based on a 15-year record

Jeffrey W. Krause, Michael W. Lomas, David M. Nelson

Submitted April 2008 to Global Biogeochemical Cycles
GBC Editorial Office
Max-Planck Institute for Chemistry
P.O. Box 3060
D-55020 Mainz
Germany

4.1 Abstract

Biogenic silica ($bSiO_2$) in the upper water column at the Bermuda Atlantic Time-series Study (BATS) site in the western Sargasso Sea, measured biweekly to monthly from 1989 through 2003, shows changes on four distinct time scales. Mesoscale physical features, such as eddies, occasionally increase vertically integrated $bSiO_2$ in the upper 120 m ($\int bSiO_2$) by an order of magnitude or more (only 5 of 217 total profiles). There is a strong seasonal cycle in $\int bSiO_2$, with a maximum in spring followed by a ~50% decline to a fall minimum. $\int bSiO_2$ also varies on time scales of 3–6 years, parallel with phase shifts in the North Atlantic Oscillation; those changes appear to reflect diatom responses to the combined effects of changes in 18°C subtropical mode water volume and in the meteorological forcing that entrains nutrients into the lower euphotic zone. Removal of the seasonal cycle reveals a secular, ~40% decline in $\int bSiO_2$ over the 15 years of the BATS record, concurrent in time with increases in vertically integrated abundances of dinoflagellates and prasinophytes in the upper 120 m. At the same time there has been a linear increase in density stratification in the upper 200 m, and a linear decline in winter silicic acid supply in the upper 120 m. The apparent 15-year shift in autotrophic community composition, with decreasing $\int bSiO_2$ and increasing flagellates, may impact future biogeochemical processes in the Sargasso Sea by reducing the role of diatoms in this system.

4.2 Introduction

Diatoms are responsible for an estimated 30% of the global oceanic primary production (Nelson et al. 1995, Tréguer et al. 1995, Raven and Waite 2004). In addition, diatoms have been shown, or hypothesized, to be the autotrophic source of most of the organic matter exported to the ocean interior in a wide variety of habitats (e.g. Sargasso Sea, Goldman 1993; equatorial Pacific, Dugdale and Wilkerson 1998; Southern Ocean, Nelson et al. 2002).

Numerous methods for estimating diatom abundance and biomass have been used through the years. Early studies in the Sargasso Sea quantified diatom cell abundance by microscopic enumeration (Riley 1957, Hulburt et al. 1960), while more recent studies have used the diagnostic diatom pigment fucoxanthin to estimate diatom biomass (Malone et al. 1993, Goericke 1998). Diatoms have an absolute Si requirement for growth; this, coupled with their ubiquitous distribution and sometimes very high abundances, causes them to dominate the oceanic cycling of Si (see Martin-Jézéquel et al. 2000). Thus, biogenic particulate silica ($bSiO_2$) provides another estimate of diatom biomass (e.g. Brzezinski and Nelson 1995).

In the late 1980s the US Joint Global Ocean Flux Study established time-series sites in the central gyres of the North Atlantic and North Pacific. In the North Atlantic, the Bermuda Atlantic Time-series Study (BATS) site was positioned in the Sargasso Sea 85 km southeast of Bermuda. The BATS site is located near other time-series stations including Hydrostation S (HS), and the Oceanic Flux Program (OFP) and Bermuda Testbed Mooring (BTM) sites. Since October 1988, the BATS program has sampled with bi-weekly (during spring only) to monthly resolution for a suite of biogeochemical measurements. BATS sampling has included $bSiO_2$ as a routine core measurement since January 1989. The method for $bSiO_2$ analysis (Brzezinski and Nelson 1995) has remained the same since the beginning of the time-series, resulting in a methodologically consistent 15-year data record with bi-weekly to monthly temporal resolution. This represents the first multi-year time-series record of biogenic silica reported from anywhere in the ocean.

In the Sargasso Sea, $bSiO_2$ concentrations and production rates are among the lowest in the world ocean (Brzezinski and Nelson 1995, Nelson and Brzezinski 1997).

Early studies observed the highly seasonal nature of diatom abundance in the Sargasso Sea (Riley 1957, Hulburt et al. 1960), with a maximum during the spring bloom period. BATS-era studies of Si cycling reinforced pre-BATS observations of diatom seasonality in the Sargasso Sea (Brzezinski and Nelson 1995) while also demonstrating that low ambient [$Si(OH)_4$] chronically limits the rate of Si uptake by diatoms (Brzezinski and Nelson 1996). Microscopy and pigment analysis (by high performance liquid chromatography, HPLC) suggest that the contribution of diatoms to total chlorophyll biomass is generally <5% both at the BATS site and elsewhere in the Sargasso Sea (Goericke 1998, Steinberg et al. 2001). Conversion of annual $bSiO_2$ production rates, estimated from ^{30}Si incubation studies, to primary production rates indicates that diatoms contribute a maximum of ~13% to annual primary productivity at the BATS site (Nelson and Brzezinski 1997). However, their estimated contribution to the annual POC export is ~30%, increasing to >90% during the late-winter and spring bloom period (Nelson and Brzezinski 1997, Krause et al. *in revision*).

The 1989–1994 portion of the BATS $bSiO_2$ time-series has been reported previously (Nelson and Brzezinski 1997). While those data show the general range of $bSiO_2$ concentrations ([$bSiO_2$]) in the upper water column and a noticeable seasonal cycle, they do not cover enough time to calculate statistically robust seasonal means or reveal modes of temporal variability beyond the annual cycle. Moreover, recent data have shown that [$bSiO_2$] and $bSiO_2$ production rates in the Sargasso Sea can vary on time scales less than a week, responding rapidly to nutrient injections driven by late winter storms (Krause et al. *in revision*, Lomas et al. *in revision*) and over spatial scales < 100 km in response to eddies and other mesoscale physical features (McNeil et al. 1999, Conte et al. 2003, McGillicuddy et al. 2007). With 15 years of BATS $bSiO_2$ data, complemented by the full suite of BATS core measurements, we have analyzed short-term, seasonal and interannual trends in the $bSiO_2$ record, along with trends in other properties measured over the same 15-year period at the BATS site, to explore the controls on diatom abundance and the potentially changing role of diatoms in export production in this part of the North Atlantic.

4.3 Methods

4.3.1 Sampling and data availability

Reported data were collected on BATS cruises from January, 1989 through December, 2003, and comprise a total of 217 vertical [$bSiO_2$] profiles from the surface to at least 120 m. Sampling of suspended $bSiO_2$ has remained consistent, according to methods established at the outset of BATS (Brzezinski and Nelson 1995, Nelson and Brzezinski 1997). Two-liter samples were filtered on 0.6 μm pore, 47mm diameter polycarbonate filters; each filter was then placed in a polystyrene Petri-dish, dried in an oven at ~60^{o}C, sealed and stored at room temperature. BATS core cruises, conducted monthly throughout the year, sample $bSiO_2$ at 12 depths in the upper 250 m and, on a separate cast, 8 depths between 300 and 1000 m. BATS bloom cruises, conducted to increase sampling frequency during the time of the spring phytoplankton bloom (March–May), do not collect samples at depths > 250 m. From January 1989 through March 1991 sampling on core cruises extended only to 500 m; the current 20 depth, surface to 1000 m sampling resolution started in April 1991. For information on BATS core methodology see Knap et al. (1997) and Steinberg et al. (2001). The biogeochemical and hydrographic data from the BATS program were used to help interpret the observed temporal changes in $bSiO_2$. All treatments of the other BATS core data, such as analysis of temporal trends (see below), were done by the same method as used for the $bSiO_2$ data. The BATS data set is accessible through the Bermuda Institute for Ocean Sciences website, http://bats.bios.edu.

4.3.2 Biogenic silica analysis

Samples were analyzed according to Brzezinski and Nelson (1995) using a modification of the NaOH digestion method of Paasche (1973). Modifications included a 2-h digestion time (a specific modification for Sargasso Sea samples) to ensure that all biogenic silica has dissolved and a reverse addition reagent blank to achieve a lower limit of detection (Brzezinski and Nelson 1995). NaOH digestions for samples collected from 1989 through 1994 were run in polymethylpentene tubes, and data have been published elsewhere (Nelson and Brzezinski 1997). Digestions for

samples collected from 1995 through 2003 (new data) were run in polypropylene tubes due to the unavailability of polymethylpentene tubes; the polypropylene tubes yielded similarly low blank values. All $bSiO_2$ digestions were conducted in the same laboratory, by the same methods and by only two individuals: (J. Arrington for 1989–1994 samples and J. Krause for 1995–2003).

4.3.3 Analysis of temporal trends

Data were integrated vertically to 120 m, from 121 to 300 m, and from 301 to 1000 m (see results for reasons why these depth intervals were chosen). For $bSiO_2$ profiles where no sample was collected at the target depth for integration, a linearly interpolated value was calculated using data from the nearest bracketing depths. For profiles not extending to the target depth, no extrapolation was done, e.g. BATS bloom cruises sample only to 250 m; therefore those profiles were left out of both the 121-300 m and 301-1000 m integrations. When any concentration was undetectable, a value of one-half the detection limit was assigned for the sake of integration. See Brzezinski and Nelson (1995) for $bSiO_2$ detection limits and Knap et al. (1997) for all others.

We assessed long-term trends in vertically integrated $bSiO_2$ ($\int bSiO_2$) by a least squares linear regression to the full time series from 1989 through 2003, after seasonal de-trending of the time-series. The seasonal cycle was removed by log transforming the $\int bSiO_2$ and subtracting the corresponding log transformed 15-year monthly mean from each time point. Seasons were defined as periods between equinox and solstice (e.g. winter = winter solstice to the vernal equinox; spring = vernal equinox to the summer solstice, etc.). Due to anomalously high [$bSiO_2$] in mesoscale physical features (e.g. eddies), those profiles (n = 5) were not used to calculate the seasonal means (see results and discussion for justification).

Residual de-trended data (from which both seasonality and the linear 15-year trend had been removed) were compared to the monthly North Atlantic Oscillation (NAO) index (data available at http://www.cgd.ucar.edu/cas/jhurrell/indices.html). The NAO index is a monthly composite (i.e. a mean of data collected over 30 days) while $bSiO_2$ measurements have a temporal resolution of 1 or 2 profiles per month.

$\int bSiO_2$ values were interpolated linearly to the mid-point day of each month (to match the monthly average NAO); then the NAO and residual, de-trended $\int bSiO_2$ values were compared by a correlation analysis (2-tailed analysis, df = n-2, significance if $p<0.05$). The five outlier profiles associated with identified mesoscale physical features were omitted from this NAO correlation analysis.

4.4 Results

4.4.1 Nutrient trends

The 15-year time series of $[HPO_4^{2-}]$, $[NO_3^-]$, and $[Si(OH)_4]$ in the upper 500 m are shown in Figure 4.1. All show strong depletion in the upper 100 m through most of the year. Nutrients are injected into the euphotic zone in winter, when convective mixing entrains deeper water with higher nutrient content. Upon water-column stabilization in spring, a phytoplankton bloom develops and the available nutrients are used (Michaels and Knap 1996). Over the spring, and into the summer and fall, the drawdown of nutrients leads to surface depletion of $[NO_3^-]$ and $[HPO_4^{2-}]$ to levels at or below detection limits of the colorimetric methods used for the BATS core measurements (Lipschultz 2001, Steinberg et al. 2001); $[Si(OH)_4]$ also reaches an annual minimum in summer and fall but generally remains above colorimetric detection limits at ~0.6–0.8 μmol L^{-1} (Brzezinski and Nelson 1995). For studies of C, N, or P cycling at the BATS station see Michaels and Knap (1996), Cotner et al. (1997), Lipschultz (2001), and Lomas and Lipschultz (2006).

$Si(OH)_4$, unlike NO_3^- and HPO_4^{2-}, is used in surface waters almost exclusively by diatoms. The $[Si(OH)_4]$ in the upper 100 m at BATS during the stratified period progressively decreased year to year, from 1995 through 2000 (to a minimum of ~0.4 μmol L^{-1}, Figure 4.1). In 2001, stratified period $[Si(OH)_4]$ was higher than the previous years (i.e. 1995 through 2000), then in 2002, $[Si(OH)_4]$ remained lower than either 2001 or 2003. $[Si(OH)_4]$ during the pre-1995, 2001, and 2003 stratified periods was ~0.6–0.8 μmol L^{-1}. When considering depths below 100 m, stratified periods during 1999, 2000, 2002 showed the deepest and most chronic depletion of $[Si(OH)_4]$ during the first 15 years of the BATS record (Figure 4.1).

4.4.2 Vertical structure in biogenic silica

Biogenic silica concentrations in the Sargasso Sea have previously been reported to be among the lowest, if not the lowest, in the surface waters of the world ocean (Nelson and Brzezinski 1997). The global range of reported [$bSiO_2$] in marine surface waters spans almost four orders of magnitude, with the Sargasso Sea being the lowest (Table 4.1).

Using all data, we compared [$bSiO_2$] in specific depth intervals with the adjacent interval immediately below (data from Table 4.2); significant differences were found in only two comparisons within the upper 1000 m (t-test between adjacent depth intervals, $p<0.05$ for significance). The breaks delineated three vertical layers as follows: surface to 120 m (referred to as surface) where [$bSiO_2$] was highest, 121 to 300m (referred to as middle) where it was intermediate, and 301 to 1000 m (referred to as deep) where it was lowest. Data from these layers were pooled and statistical differences between them were confirmed (ANOVA, $F=63.5$, $p<0.001$). The mean [$bSiO_2$] in the surface, middle and deep layers was 24.4±1.1, 16.3±0.5, and 10.8±0.4 nmol L^{-1}, respectively (±standard error for vertical structure data). Thus there was, on average, a ~33% attenuation of [$bSiO_2$] from each of these layers to the next. The three-layer character of the [$bSiO_2$] distribution in the upper 1000 m at the BATS site is robust, being statistically significant despite the lack of correction for seasonality or removal of profiles with anomalously high [$bSiO_2$].

4.4.3 Temporal changes in biogenic silica

The seasonal cycle in the $bSiO_2$ record at BATS drives most of the variability (Table 4.3). Generally, [$bSiO_2$] is highest in spring, and declines during the stratified period to a minimum in fall and winter. This seasonal trend is seen in the time-series record of [$bSiO_2$] with depth, and integrated $bSiO_2$ time-series within the surface and middle vertical intervals (Figure 4.2, Table 4.3). For brevity, vertically integrated $bSiO_2$ in the surface, middle and deep layers will be referred to as $\int bSiO_{2\text{-}S}$, $\int bSiO_{2\text{-}M}$, and $\int bSiO_{2\text{-}D}$, respectively.

There were occasional vertical profiles in which [$bSiO_2$] was 10–30x higher than the interval mean (Figure 4.2). These profiles were all associated with

independently identified mesoscale physical features, such as eddies. During the BATS record five of these anomalously high [$bSiO_2$] events occurred (April 1990, May 1993, July 1995, April 1996 and December 1996), with each exerting a high influence on the calculation of seasonal and monthly means for the entire time series. Considering these anomalous profiles represent <3% of the total data set and that all were associated with known mesoscale features, we omitted them from calculation of seasonal and monthly means. The adjusted $\int bSiO_{2\text{-}S}$, $\int bSiO_{2\text{-}M}$, and $\int bSiO_{2\text{-}D}$ seasonal means are shown in Table 4.3. Comparison of seasonal means shows significant seasonal differences in the surface and middle depth intervals (ANOVA, $p<0.001$), but not in the deep interval.

Vertically integrated [$bSiO_2$] in the surface and middle intervals ($\int bSiO_{2\text{-}S}$, $\int bSiO_{2\text{-}M}$) frequently shows a maximum in spring (Figure 4.2, Table 4.3), the season when diatom blooms in the Sargasso Sea have been well documented (Riley 1957, Hulburt et al. 1960, Brzezinski and Nelson 1995). After the onset of seasonal thermal stratification, $bSiO_2$ declines in the summer and reaches a minimum in the fall, when the mean $\int bSiO_{2\text{-}S}$ and $\int bSiO_{2\text{-}M}$ are both ~50% of the corresponding spring maximum (Table 4.3).

Both $\int bSiO_{2\text{-}S}$ and $\int bSiO_{2\text{-}M}$ showed statistically significant ($p<0.001$) seasonality, and after removing the annual cycle (i.e. subtracting the 15-year monthly mean, from Table 4.3) both time-series showed approximately linear, 15-year trends (Figure 4.3). Using linear regression, the slope of each 15-year detrended time-series was negative and different from zero (linear regression, $p<0.001$); the slope for the detrended regressions of $\int bSiO_{2\text{-}S}$ and $\int bSiO_{2\text{-}M}$ was -0.015 y^{-1} and -0.019 y^{-1}, respectively. These slopes show that $\int bSiO_2$, within each of these two layers, decreased by ~35–45% between 1989 and 2003.

When comparing the residual de-trended $\int bSiO_{2\text{-}S}$ and $\int bSiO_{2\text{-}M}$ (Figure 4.4) with the NAO index, no significant correlation was found. However time-lagging the de-trended $\int bSiO_2$ data to the NAO index (to assess delayed biological response to atmospheric forcing) revealed significant negative correlations ($p < 0.05$) in both depth intervals on time lags of 8 and 24 months, and a significant negative correlation ($p < 0.05$, surface-layer only) with a 39 month lag.

4.5 Discussion

4.5.1 High biogenic silica concentrations associated with mesoscale physical features

Some of the highest reported diatom biomass events in the Sargasso Sea (based upon HPLC fucoxanthin data) have been associated with mesoscale physical features (McNeil et al. 1999, Conte et al. 2003); this is confirmed by our $bSiO_2$ data (Figure 4.2). Five such profiles were observed during the BATS record, with high influences on the calculated seasonal means. The disproportional impact of these profiles can be observed in terms of the magnitude of $bSiO_2$ measured at individual depths over the entire time series. Considering the entire data set (surface to 1000 m), 27 of the top 38 highest measured [$bSiO_2$] (Note: 38 data points ≈ 1 % of all data) were found in four of these five mesoscale features (April 1990, May 1993, July 1995, April 1996). The fifth profile (December 1996) had lower [$bSiO_2$] at each individual depth (~80-115 nmol L^{-1}) but, unlike the other four, had consistently high [$bSiO_2$] from the surface to 160 m. The $\int bSiO_{2\text{-}S}$ within these five profiles ranged from 11.7 to 50.8 mmol m^{-2} (mean = 25.7). The highest, of the five mesoscale $\int bSiO_{2\text{-}S}$ events was in April 1990, $\int bSiO_{2\text{-}S}$ was 14.7x higher than the spring mean in this interval; while the lowest of the five events, in December 1996, was 6.9x higher than the fall mean (Table 4.3). Indeed, these events may be rare, but they have high influence on the calculation of seasonal or monthly $\int bSiO_2$ means (e.g. Table 4.3).

Four of the mesoscale features in which we measured high [$bSiO_2$] have been discussed in the literature. The event in July 1995 was described as a mode-water eddy which passed the BATS station and within which a diatom bloom was observed (McNeil et al. 1999, Steinberg et al. 2001). Vertical structure of [$bSiO_2$] within that eddy showed that the surface [$bSiO_2$] was only 15 nmol L^{-1}, a below-average value for that depth (Figure 4.2, Table 4.2), but at 100 m [$bSiO_2$] was 630 nmol L^{-1}, the highest single [$bSiO_2$] observed in the BATS record from 1989 through 2003. The highest fucoxanthin concentration in the BATS record was also measured on that sampling date and at that depth (Steinberg et al. 2001). The other anomalous event took place in December 1996 where [$bSiO_2$] was nearly uniform at 80–115 nmol L^{-1} through the

upper 160 m. That event was associated with a perturbation from a mesoscale feature characterized by a thick, warm, and low-salinity isothermal layer (Conte et al. 2003). Sweeney et al. (2003) identified the May 1993 event as a mode-water eddy and Mouriño-Carballido and McGillicuddy (2006) observed a depressed sea level anomaly in March and April 1996 indicating the passage of a cyclonic eddy during the April 1996 event.

The event in April 1990 has not been previously discussed in the literature. However, we have identified it as a mode-water eddy based on the perturbation in the vertical potential density (σ_θ) structure. Comparing the σ_θ during April 1990 with known mode-water eddy profiles in 1995 (as identified by Sweeney et al. 2003, Mouriño-Carballido and McGillicuddy 2006), shows a downward displacement of the 26.4 kg m^{-3} σ_θ surface, similar to that in the July 1995 mode-water eddy.

McGillicuddy et al. (2007) proposed a physical mechanism for supporting diatom blooms based on the interaction between the mesoscale circulation and the wind field. Currently, little information is available on the temporal development of diatom blooms within mesoscale eddies as they propagate through the ocean. However, if the physical mechanisms that support blooms in an eddy are persistent, the blooms could potentially last for several weeks.

4.5.2 Seasonal variability in water column biogenic silica

The seasonal means in the $\int bSiO_{2\text{-}S}$ and $\int bSiO_{2\text{-}M}$ records show clear statistical differences, whereas $\int bSiO_{2\text{-}D}$ appears to have no significant seasonality (Table 4.3). The annual maximum in both $\int bSiO_{2\text{-}S}$ and $\int bSiO_{2\text{-}M}$ coincides with the timing of the spring phytoplankton bloom, a response to the onset of stratification in a water column following enhanced nutrient supply from winter convective entrainment (Michaels and Knap 1996).

The lowest mean $\int bSiO_{2\text{-}S}$ is observed in summer and fall (Table 4.3, see also Figure 4.2). Generally these seasons are characterized by increasing vertical stratification, which reaches a maximum in late fall. There are also extended periods of low surface nutrient concentrations between the summer and winter solstices, with solar irradiance decreasing throughout that period. These factors likely drive

decreases in $\int bSiO_{2\text{-}S}$ as summer and fall progress. The lowest mean $\int bSiO_{2\text{-}M}$ is also in fall; however, unlike in the surface interval, $\int bSiO_{2\text{-}M}$ in fall is similar to that in summer and winter, showing little seasonal variance outside of spring (Table 4.3). Thus our data suggest that the temporal onset for increasing $bSiO_2$ in the surface layer precedes that in the middle layer; $\int bSiO_{2\text{-}S}$ begins to build in the winter, whereas $\int bSiO_{2\text{-}M}$ increases abruptly by 73% from winter to spring.

The mean winter $\int bSiO_{2\text{-}S}$ is 29–32% higher than means in summer and fall. In contrast to the thermally stratified conditions that prevail in fall, the progressive cooling in winter causes the mixed layer to deepen, and possibly penetrate nutriclines. However, the residual effects of stratification (i.e. low nutrient availability) in early winter, combined with the annual minimum in solar irradiance would limit the growth of diatoms (and the rest of the phytoplankton community). But in late winter the light regime improves, and water-column stratification is at an annual minimum. Consequently, nutrients can be entrained into the surface layer relatively easily by storm events, and the light regime in the upper water column may be favorable for phytoplankton growth. We have recently reported brief (2–3 d) episodes of rapid diatom growth and $\int bSiO_2$ increase in the upper 140 m under those late winter conditions (Krause et al. *in revision*). During late winter 2004, the passage of a storm and subsequent stratification event led to a near-doubling of $\int bSiO_2$ in the upper 140 m within 3 days (i.e. from ~2.2 to ~4.1 mmol m^{-2}, Krause et al. *in revision*). The increase in seasonal mean $\int bSiO_{2\text{-}S}$ from a summer/fall low to higher values in winter may result largely from late-winter blooms supported in this way.

4.5.3 Sub-decadal changes in biogenic silica

Removal of the seasonal cycle in $\int bSiO_2$ reveals a clear, 15-year trend of decreasing $\int bSiO_2$ in the upper water column at the BATS site (Figure 4.3b). That long-term trend will be discussed in detail below. However, when both the seasonal cycle and the long-term decrease are removed from the record there are clear and interpretable multi-year oscillations in $\int bSiO_2$. Higher $\int bSiO_{2\text{-}S}$ and $\int bSiO_{2\text{-}M}$ were observed starting in 1996 and reached a peak in 1998 (Figures 4.2, 4.4), coinciding in time with the uplift of the 26.4 kg m^{-3} σ_θ isopycnal with higher $[NO_3^-]$ (Figure 4.5)

and a concurrent drawdown of [$Si(OH)_4$] in the euphotic zone (Figure 4.1). A perturbation of the subtropical mode water (STMW) at the BATS site, as indicated by the vertical density structure and a stronger potential vorticity minimum (Figure 4.5), also coincided in time with these events and was a likely driver of the observed diatom response. The physical and climatic mechanism generating these multi-year trends appears to have been as follows:

4.5.3.1 Subtropical Mode Water in the late 1990s

The 18° STMW at the BATS site is located "above the permanent pycnocline and is characterized by a vertically homogenous layer that outcrops in the late winter and is capped over during spring" (Joyce et al. 2000, and Figure 4.1d). Talley (1996) described the STMW core near Bermuda as having a mean depth of 287±96 m (± standard deviation), mean potential temperature and salinity of 17.88±0.63 °C and 36.50±0.09 psu, respectively, and a mean potential density of 1026.45±0.12 kg m^{-3}. For this discussion we focus on the 26.4 and 26.5 kg m^{-3} σ_θ isopycnals (hereafter referred to without units), and the STMW potential vorticity minimum to characterize changes in the STMW at the BATS site. Variations on these potential density surfaces have been examined previously using the HS record (Jenkins and Goldman 1985) and are associated with the minimum in potential vorticity (Figure 4.5a), a tracer of the STMW core (Talley 1996). During the typical annual cycle at BATS, the 26.4 σ_θ isopycnal is uplifted in winter and then descends to > 300 m as seasonal stratification sets in. In the winter of 1996 the 26.4 σ_θ isopycnal shoaled more than in previous years (to just below 200 m, Figure 4.5) and, instead of deepening in summer to 300–350 m as observed in the early 1990s, it remained elevated, not descending to > 300 m until the stratified period in 1999 (Figure 4.5a). During 1996 and 1997 the vertical distance between the 26.4 and 26.5 σ_θ isopycnals was, on average, >180 m (see smoothed line, Figure 4.5b), as compared to an average of ~100–150 m before 1996 and ~90 – 140 m from 1998 through 2003.

The STMW is formed in an east-west band near the northern edge of the North Atlantic subtropical gyre, to the south of the Gulf Stream (Joyce et al. 2000, Palter et al. 2005). Talley (1996) pointed out that during negative phases of the NAO, STMW

formation is increased. The increased vertical distance between the 26.4 and 26.5 σ_θ isopycnals, and the lower potential vorticity between them (Figure 4.5a), indicates an increased volume of STMW reaching the BATS site in 1996 through 1998. The increase in STMW volume observed at the BATS site coincided in time with the shift in the winter NAO index from positive (pre-1996, post 1998) to negative (1996, 1997, 1998, Figure 4.5). But STMW near BATS is generally 3-4 years old (see Bates and Hansell 2004 and references therein), thus it would seem unlikely that increased STMW at BATS would be observed immediately after the onset of a negative NAO period. However, in a modeling study Hazeleger and Drijfhout (1999) found that the largest STMW thickness anomalies were induced by stochastic heat flux forcing. Deep-mixed layers were observed in 1995 and 1996 (c.f. Michaels and Knap 1996, Steinberg et al. 2001) and the STMW shoaled (see potential vorticity, Figure 4.5). Thus, local stochastic events may explain the enhanced STMW volume at BATS during 1995 and 1996, with non-local and local-residual effects maintaining the increased STMW in the winters of 1997 and 1998.

4.5.3.2 Changes in the chemical and biological stocks at the BATS site in the late 1990s

Primary production in the Sargasso Sea is generally thought to be N-limited (Lipschultz 2001). Thus the upward movement of NO_3^- on a shoaling isopycnal to depths where it could be injected into the euphotic zone, given the necessary physical forcing, should stimulate new production. $[NO_3^-]$ on the 26.4 σ_θ isopycnal at BATS was ~4 μmol L^{-1} in the early 1990's, declined to a minimum of ~ 2.5 μmol L^{-1} in 1996-97 and returned to ~4 μmol L^{-1} by 2000 (Figure 4.5c). $[Si(OH)_4]$ on the 26.4 σ_θ isopycnal remained relatively constant throughout the 1990s at ~1.5 μmol L^{-1} (Figure 4.5c).

The main vertical gradient in $[Si(OH)_4]$ is deeper than that of $[NO_3^-]$ throughout the North Atlantic (Sarmiento et al. 2007). At the BATS site $[NO_3^-]$ is consistently lower than $[Si(OH)_4]$ in surface layer and higher on the 26.4 σ_θ isopycnal (Figure 4.1). Thus any uplift in the 26.4 σ_θ isopycnal would bring more NO_3^- than $Si(OH)_4$ toward the surface, making more NO_3^- than $Si(OH)_4$ available to be injected

into the euphotic zone by local meteorological forcing. This would be true over the full range of $[NO_3^-]$ observed on the 26.4 σ_θ isopycnal (2.5–4.0 μmol L^{-1}, Figure 4.5c). Winter storms at and near the BATS site are more frequent during negative NAO years (Gruber et al. 2002, Bates and Hansell 2004) but even mixed layer depths observed in the early 1990s (see Michaels and Knap 1996, Steinberg et al. 2001) would have provided the necessary forcing to penetrate STMW potential vorticity minimum (and associated σ_θ surfaces). The significant negative correlations (e.g. ~2, ~3 year time lags, see section 4.4.3) imply that $bSiO_2$ anomalies, in general, are likely driven by a combination of non-local (e.g. STMW formation) and local physical forcing (e.g. stochastic heat flux forcing, Hazeleger and Drijfhout 1999). From mid 1996 through mid 1999 the residual $\int bSiO_2$ in the surface and middle intervals were higher than in earlier or later years, and $\int bSiO_{2\text{-}D}$ was also highest during that period (Figure 4.4).

Each winter the $[Si(OH)_4]$ was ~0.8–1.0 μmol L^{-1}; the seasonal drawdown of $Si(OH)_4$ at the BATS site during 1996–1998 caused the average $[Si(OH)_4]$ in the upper 100 m to be depleted to ~0.4 μmol L^{-1} each summer, as opposed to ~0.6–0.8 μmol L^{-1} in earlier years (Figure 4.1). A first-order approximation of the increased seasonal removal of $Si(OH)_4$ from the upper 100 m would thus be ~20–40 mmol m^{-2} , i.e., 0.6–0.8 mmol m^{-3} (normal) – 0.4 mmol m^{-3} (late 1990s) ~ 0.2–0.4 mmol m^{-3}, x 100 m. During 1996 $\int bSiO_{2\text{-}D}$ began to increase, and by 1998 the average $\int bSiO_{2\text{-}D}$ had doubled, from ~5 mmol m^{-2} before and after the peak to ~10 mmol m^{-2} during the peak, but with stronger year-to-year fluctuations (Figure 4.4c). Comparing the observed increase in $\int bSiO_{2\text{-}D}$ (5 mmol m^{-2}) with the estimated increased loss of $Si(OH)_4$ from the upper 100 m during the same time period (20–40 mmol m^{-2}), indicates that ~13–25% of the increased removal $Si(OH)_4$ from surface waters can be accounted for as increased $bSiO_2$ within the 300–1000 m depth interval. This estimate does not fully constrain a Si mass balance for this period, but it demonstrates that the increased removal of $Si(OH)_4$ from the upper 100 m could be due, at least in part, to enhanced biological utilization and increased export to the 300–1000 m layer.

Given that $bSiO_2$ produced in the upper 100 m could also be exported deeper than 1000 m, we do not expect to account for all loss of $Si(OH)_4$ from the upper 100 m

with accumulation of $bSiO_2$ between 300 and 1000 m. If 13–25% of the enhanced $Si(OH)_4$ removed from the upper 100 m during the 1996 through 1998 period was found as increased $bSiO_2$ at 300–1000 m, the fate of the remaining 75–87% must be some combination of dissolution between 100 and 1000 m and export to > 1000 m. We have no way to distinguish between those two processes based on present data. However, data from sediment traps deployed at 150 m at the BATS site during 1992–1994 (Nelson and Brzezinski 1997) indicate an annual $bSiO_2$ export of ~26–53 mmol m^{-2} y^{-1} over that period. Thus even the calculated ~20 mmol m^{-2} y^{-1} increase in $Si(OH)_4$ removal from the upper 100 m from 1996 through 1998 (at the low end of our range of estimates) would represent a ~40–80% increase over 150 m $bSiO_2$ export fluxes measured in 1992–1994.

4.5.3.3 Coupling of the STMW and the NAO with changes in integrated biogenic silica

Diatoms in the Sargasso Sea are generally thought to be severely limited by N and Si for growth and silicification, respectively (Nelson and Brzezinski 1997, Lipschultz 2001, Mongin et al. 2003). One of the most intense spring diatom blooms recorded in the Sargasso Sea (Hulburt et al. 1960) occurred after a winter when water with >1 μmol L^{-1} [NO_3^-] reached the surface at HS (Menzel and Ryther 1960), a phenomenon that was not observed at the BATS site over the 1988–2003 period (see Figure 4.1. Note: Menzel and Ryther (1960) reported the sum of [NO_3^-] + [NO_2^-]; however, the BATS data record has shown that this term is dominated by [NO_3^-], especially in winter, c.f. Lomas and Lipschultz 2006).

We suggest that an increased winter supply of NO_3^- stimulated diatom growth and silicification in spring and summer throughout the 1996–1998 period, when the 26.4 σ_θ isopycnal was anomalously shallow (increased STMW at BATS) and winter the NAO negative (indicating higher winter storm activity), leading to the observed stronger depletion of [$Si(OH)_4$] in the upper 100 m and the observed increase in [$bSiO_2$] throughout the upper 1000 m. Biogenic silica at the BATS site thus provides one of a growing number of examples in which multi-year NAO shifts impact biological processes (e.g. Ottersen et al. 2001 and references therein, Lomas and Bates 2004).

Using the HS data record, we examined whether or not a multi-year perturbation in nutrient availability of the type observed at the BATS site in 1996–1999 has been seen at other times in the last 50 years. Using the criterion of multiyear change in NAO (from positive to negative), and an increase in STMW volume (as estimated by the vertical distance between 26.4 and 26.5 σ_θ isopycnals, and vertical extent of the potential vorticity minimum), we did not find any other such events between 1955 and 2003. While similar multiyear changes in the NAO happened in both the late 1970s and mid 1980s (data not shown), the vertical structure in σ_θ and potential vorticity during those periods did not show increased STMW volume. The multiyear event in the late 1990s is thus the first of its kind observed in the Sargasso Sea. However, a caveat is the difference between the vertical resolution of physical data in the pre-1988 HS and BATS records. In the BATS record, the vertical resolution of CTD profiles is ~2 m (by use of electronic sensor), whereas older HS data (e.g. 1950s, 1960s, 1970s) are less vertically resolved (typically 12 depths in the upper 500 m) due to manual CTD profiles. This diminished vertical resolution hinders assessment of the isopycnal and potential vorticity structure. Therefore, while the HS data give no evidence of an earlier perturbation of the type observed at the BATS site in 1996–1998, we cannot entirely rule out the possibility that such a perturbation might have occurred during the late 1970s or mid 1980s.

4.5.4 Longer-term (15-year) trends

The 15-year trend indicates significant decreases in $\int bSiO_2$ both the surface (0–120 m) and middle (121–300 m) layers from 1989 through 2003 (linear regression, $p < 0.001$ for both; Figure 4.3). Diatom cell abundance estimates at the BATS site during our study period are surprisingly sparse, hindering confirmation of the long-term decline in diatoms implied by the observed decrease in $\int bSiO_2$. Samples for cell enumeration by flow-cytometry are collected as part of the BATS core sampling regime, but diatoms are not distinguished directly. We know of no systematic effort to obtain diatom cell counts in the Sargasso Sea by microscopy during the BATS era.

During the 15-year $\int bSiO_2$ decline in the surface and middle layers there was a shift in the autotrophic community structure in the surface layer; both dinoflagellate

and prasinophyte pigment biomass increased over the 15-year record (Figure 4.6. Note: BATS HPLC samples go only to 250 m, thus we have no assessment for the 121-300 m layer). Vertically integrated particulate organic carbon in the surface layer also increased in a linear manner (data not shown, slope = 3.33 mmol m^{-2} y^{-1}, $p<0.005$); however, there was no significant 15-year increase in vertically integrated particulate organic nitrogen. Margalef (1997) proposed a theoretical framework of succession in terms of phytoplankton group dominance under different combinations of environmental factors. At one end of the spectrum is a high-turbulence, high-nutrient regime where diatoms are expected to be dominant, at the other end low-turbulence and low-nutrients, where dinoflagellates (and autotrophic groups that fill a similar niche) are expected to dominate. Therefore, this community shift may be from changes in nutrient supply and/or turbulence.

The mean surface layer $\int Si(OH)_4$ was examined during the winter season. Throughout most of the year, $\int Si(OH)_4$ in the surface layer is indicative of the balance between physical supply and biological drawdown; however, during the winter period, deep mixed layers lead to light limitation of primary production. In addition, winter is the season when water column stratification breaks down, and nutrients are convectively entrained into the euphotic zone. Thus, we interpret the mean $\int Si(OH)_4$ during the winter as being a proxy for nutrient supply. From 1989 through 2003, average winter $\int Si(OH)_4$ in the surface layer decreased linearly (data not shown, slope -2.2 mmol m^{-2} y^{-1}, $p<0.05$). Putting this number in context, the magnitude of the loss per year (i.e. the slope), is greater than the mean $\int bSiO_{2\text{-}S}$ during the summer or fall and nearly equal to the winter mean (Table 4.2). To explore whether a physical change in the upper ocean environment occurred during the $\int bSiO_2$ decline and community shift, we examined water column stratification.

Stratification was calculated by seasonally de-trending σ_θ differences between the surface and 200 m. While there are both scatter and apparent oscillations in the data, a positive and statistically significant (p <0.01) linear trend emerges with time (Figure 4.7a), indicating an increase of ~0.1 kg m^{-3} in the mean density stratification between the surface and 200 m over the 1989–2003 period. Comparing the σ_θ difference between the surface and greater depths (e.g. 300, 400, and 500 m) yields a

more positive slope, with increased confidence that it is statistically different from zero (p <0.01 in all cases, data not shown). This increased stratification could be a 15-year shoaling of particular isopycnal surface, but when examining the 15-year linear trend in the σ_θ 26.4 kg m^{-3} depth there was no significant linear increase (see also 26.5 σ_θ time series in Figures 4.1, 4.5a).

We extended our temporal analysis of stratification in the upper 200 m, using the 1955–2003 HS record to determine whether the increased stratification observed at the BATS site from 1989 through 2003 is part of a longer-term trend. At HS, the same 15-year increase in stratification observed at the BATS site occurred between 1989 through 2003 (Figure 4.7b). The HS linear slope was nearly identical to that at the BATS site (0.0084 vs. 0.0087 kg m^{-3} y^{-1} at Figures 4.7a & b). However, the HS record shows no statistically significant increase in stratification in the upper 200 m over the full record (e.g. 1955–2003, p = 0.63; Figure 4.7c). The 15-year decrease in $\int bSiO_2$ is a statistically stronger mode of temporal variability than the surface and middle layer oscillations in $\int bSiO_2$ that are correlated with the NAO (data in Figure 4.4a, b); thus it is unlikely that changes in NAO drove the 15-year trend in $\int bSiO_2$.

The significance of the stratification regression is dependent on the final years of data; when 2002 and 2003 are omitted from the analysis the stratification increase between the surface and 200, 300 and 400 m becomes insignificant ($p \approx 0.50$). Likewise, the significance of the linear decrease in $\int bSiO_2$ becomes insignificant if the final four years (2000–2003) of the record are omitted (p = 0.42). To a certain extent this simply shows that a long-term data record is needed to show long-term trends with statistical confidence. However it also means that we must view hypotheses related to the observed changes with caution.

We do not fully understand the cause of the observed 15-year decline surface and middle layer $\int bSiO_2$. However we hypothesize that it is associated with changes in the upper water column related to increased stratification, such as reduced nutrient supply. The uncertainty regarding the causes of the observed decline in $\int bSiO_2$ in the upper 300 m underscores the importance in understanding temporal modes of variance beyond our present knowledge, an understanding for which multi-decadal time-series information is essential. The continuation of the BATS $bSiO_2$ sampling, especially if

coupled with diatom cell abundance measurements, will provide an opportunity to test the hypothesis that diatom abundance and biomass are declining in response to increased stratification at the BATS site and to determine whether, and how long, those temporal trends continue. Given the importance of diatoms in organic-matter export in the Sargasso Sea (Nelson and Brzezinski 1997) and in the ocean as a whole (Boyd and Trull 2007, Honjo et al. 2008 and references therein), understanding the changes in $\int bSiO_2$ over the next decade may be vital to ascertaining the validity of the trends observed during the first 15 years of the BATS record and the potential future implications for open-ocean biogeochemistry.

Acknowledgements

We thank the BATS personnel who have done the great service of keeping this time series, J. Arrington for pre-1995 $bSiO_2$ data assistance, and M. Brzezinski for providing both pre-1995 data and valuable insights. Funding was provided by the Oregon Space Grant Consortium and the Lenore Bayley Fellowships (Oregon State University) awarded to JWK, in addition to continued funding of the BATS program by the NSF JGOFS Program, and Chemical and Biological Oceanography Programs through awards OCE-8801089, -9301950, -9617795, and -0326885.

4.6 References

Bates, N.R., Hansell, D.A., 2004. Temporal variability of excess nitrate in the subtropical mode water of the North Atlantic Ocean. Marine Chemistry 84, 225–241.

Beucher, C., Tréguer, P., Corvaisier, R., Hapette, A.M., Elskens, M., 2004. Production and dissolution of biosilica, and changing microphytoplankton dominance in the Bay of Brest (France). Marine Ecology Progress Series 267, 57–69.

Boyd, P.W., Trull, T.W., 2007. Understanding the export of biogenic particles in oceanic waters: Is there consensus? Progress in Oceanography 72, 276-312.

Brzezinski, M.A., Nelson, D.M., 1989. Seasonal changes in the silicon cycle within a Gulf Stream warm-core ring. Deep-Sea Research I 36, 1009-1030.

Brzezinski, M.A., Nelson, D.M., 1995. The annual silica cycle in the Sargasso Sea near Bermuda. Deep-Sea Research I 42, 1215-1237.

Brzezinski, M.A., Nelson, D.M., 1996. Chronic substrate limitation of silicic acid uptake rates in the western Sargasso Sea. Deep-Sea Research II 43, 437-453.

Brzezinski, M.A., Phillips, D.R., Chavez, F.P., Friederich, G.E., Dugdale, R.C., 1997. Silica Production in the Monterey, California, Upwelling System. Limnology and Oceanography 42, 1694-1705.

Brzezinski, M.A., Villareal, T.A., Lipschultz, F., 1998. Silica production and the contribution of diatoms to new and primary production in the central North Pacific. Marine Ecology Progress Series 167, 89-104.

Brzezinski, M.A., Nelson, D.M., Franck, V.M., Sigmon, D.E., 2001. Silicon dynamics within an intense open-ocean diatom bloom in the Pacific sector of the Southern Ocean. Deep-Sea Research II 48, 3997–4018.

Conte, M.H., Dickey, T.D., Weber, J.C., Johnson, R.J., Knap, A.H., 2003. Transient physical forcing of pulsed export of bioreactive material to the deep Sargasso Sea. Deep-Sea Research I 50, 1157-1187.

Cotner, J.B., Ammerman, J.W., Peele, E.R., Bentzen, E., 1997. Phosphorus-limited bacterioplankton growth in the Sargasso Sea. Aquatic Microbial Ecology 13, 141-149.

Dugdale, R.C., Wilkerson, F.P., 1998. Silicate regulation of new production in the equatorial Pacific upwelling. Nature 391, 270-273.

Franck V.M., Bruland, K.W., Hutchins, D.A., Brzezinski, M.A., 2003. Iron and zinc effects on silicic acid and nitrate uptake kinetics in three high-nutrient, low-chlorophyll (HNLC) regions. Marine Ecology Progress Series 252, 15-33.

Goericke, R, 1998. Response of phytoplankton community structure and taxon specific growth rates to seasonally varying physical forcing in the Sargasso Sea off Bermuda. Limnology and Oceanography 43, 921-935.

Goldman J. C., 1993. Potential role of large oceanic diatoms in new primary production. Deep-Sea Research 40, 159-168.

Gruber, N., Keeling, C.D., Bates, N.R., 2002. Interannual variability in the North Atlantic Ocean carbon sink. Science 298, 2374-2378.

Hazeleger, W., Drijfhout, S.S., 1999. Stochastically forced mode water variability. Journal of Physical Oceanography 29, 1772-1786.

Honjo, S., Manganini, S.J., Krishfield, R.A., Francois, R., 2008. Particulate organic carbon fluxes to the ocean interior and factors controlling the biological pump: A

synthesis of global sediment trap programs since 1983. Progress in Oceanography 76, 217-285.

Hulburt, E.M., Ryther, J.H., Guillard, R.R.L., 1960. The phytoplankton of the Sargasso Sea off Bermuda. Journal du Conseil International d'Exploration da la Mer 25, 115-128.

Jenkins, W., Goldman, J., 1985. Seasonal oxygen cycling and primary production in the Sargasso Sea. Journal of Marine Research 43, 465-491

Joyce, T.M., Deser, C., Spall, M.A., 2000. The relation between decadal variability of Subtropical Mode Water and the North Atlantic Oscillation. Journal of Climate 13, 2550-2569.

Knap, A. H., and 19 others, 1997. U.S. Joint Global Ocean Flux Study- Bermuda Atlantic Time- Series Study Methods Manual: Version 4. U.S. JGOFS Planning and Coordination Office: Woods Hole.

Krause, J.W., Nelson, D.M., Lomas, M.W., (*in revision*). Biogeochemical responses to late-winter storms in the Sargasso Sea. II. Increased rates of biogenic silica production and export. *In revision*, Deep Sea Research I.

Leblanc, K., Hutchins, D.A., 2005. New applications of a biogenic silica deposition fluorophore in the study of oceanic diatoms. Limnology and Oceanography: Methods 3, 462-476.

Leynaert, A., Tréguer, P., Lancelot, C., Rodier, M., 2001. Silicon limitation of biogenic silica production in the Equatorial Pacific. Deep-Sea Research I 48, 639-600.

Lipschultz, F., 2001. A time-series assessment of the nitrogen cycle at BATS. Deep-Sea Research Part II 48, 1897-1924.

Lomas, M.W., Bates, N.R., 2004. Potential controls on interannual partitioning of organic carbon during the winter/spring phytoplankton bloom at the Bermuda Atlantic time-series study (BATS) site. Deep-Sea Research I 51, 1619-1636.

Lomas, M.W., Lipschultz, F., 2006. Forming the primary nitrite maximum: Nitrifiers or phytoplankton? Limnology and Oceanography 51, 2453-2467.

Lomas, M.W., Roberts, N., Lipschultz, F., Krause, J.W., Nelson, D.M , Bates, N.R. (*in revision*). Biogeochemical responses to late-winter storms in the Sargasso Sea. III. Rapid successions of major phytoplankton groups. *In revision*, Deep-Sea Research I.

Malone, T.C., Pike, S.E., Conley, D.J., 1993. Transient variations in phytoplankton productivity at the JGOFS Bermuda time series station. Deep-Sea Research I 40, 903-924.

Margalef, R, 1997. Excellence in ecology, Book 10: Our biosphere. Oldendorf/Luhe: International Ecology Institute.

Martin-Jézéquel, V., Hildebrand, M., Brzezinski, M.A., 2000. Silicon metabolism in diatoms: implications for growth. Journal of Phycology 36, 821-840.

McGillicuddy, D.J., and 17 others, 2007. Eddy/wind interactions stimulate extraordinary mid-ocean plankton blooms. Science 316, 1021-1026.

McNeil, J.D., Jannasch, H.W., Dickey, T., McGillicuddy, D.J., Brzezinski, M., Sakamoto, C.M., 1999. New chemical, bio-optical and physical observations of upper ocean response to the passage of a mesoscale eddy off Bermuda. Journal of Geophysical Research 104. 15537–15548.

Menzel, D.W., Ryther, J.H., 1960. The annual cycle of primary production in the Sargasso Sea off Bermuda. Deep-Sea Research 6, 351-366.

Michaels, A.F., Knap, A.H., 1996. Overview of the U.S. JGOFS Bermuda Atlantic Time-series Study and the Hydrostation S program. Deep-Sea Research II 43, 129-156.

Mongin, M., Nelson, D.M., Pondaven, P., Brzezinski, M.A., Tréguer, P., 2003. Simulation of upper-ocean biogeochemistry with a flexible-composition phytoplankton model: C, N and Si cycling in the western Sargasso Sea. Deep-Sea Research I 50, 1445-1480.

Mouriño-Carballido, B., McGillicuddy, D.J., 2006. Mesoscale variability in the metabolic balance of the Sargasso Sea. Limnology and Oceanography 51, 2675-2689.

Nelson, D.M., Brzezinski, M.A., 1997. Diatom growth and productivity in an oligotrophic midocean gyre: a 3-yr record from the Sargasso Sea near Bermuda. Limnology and Oceanography 43, 473-486.

Nelson, D.M., Ahern, J.A., Herlihy, L.J., 1991. Cycling of biogenic silica within the upper water column of the Ross Sea. Marine Chemistry 35, 461-476.

Nelson, D.M., Tréguer, P., Brzezinski, M.A., Leynaert, A., Quéguiner, B., 1995. Production and dissolution of biogenic silica in the ocean: Revised global estimates, comparison with regional data and relationship to biogenic sedimentation. Global Biogeochemical Cycles 9, 359–372.

Nelson, D.M., and 15 others, 2002. Vertical budgets for organic carbon and biogenic silica in the Pacific sector of the Southern Ocean, 1996-1998. Deep-Sea Research II 49, 1645-1673.

Ottersen, G., Planque, B., Belgrano, A., Post, E., Reid, P.C., Stenseth, N.C., 2001. Ecological effects of the North Atlantic Oscillation. Oecologia 128, 1-14.

Paasche, E, 1973. Silicon and the ecology of marine planktonic diatoms. I. Thalassiosira pseudonana (Cyclotella nana) grown in a chemostat with silicate as the limiting nutrient. Marine Biology 19, 117-126.

Palter, J.B., Lozier, M.S., Barber, R.T., 2005. The effect of advection on the nutrient reservoir in the North Atlantic subtropical gyre. Nature 437, 687-692.

Raven, J.A., Waite, A.M., 2004. The evolution of silicification in diatoms: inescapable sinking and sinking as escape? New Phytologist 162, 45-61.

Riley, G.A., 1957. Phytoplankton of the North Central Sargasso Sea, 1950-1952. Limnology and Oceanography 2, 252-269.

Sarmiento, J.L., Simeon, J., Gnanadesikan, A., Gruber, N., Key, R.M., Schlitzer, R., 2007. Deep ocean biogeochemistry of silicic acid and nitrate. Global Biogeochemical Cycles 21, doi:10.1029/2006GB002720.

Schlitzer, R., 2006. Ocean Data View, http://odv.awi-bremerhaven.de.

Steinberg, D. K., Carlson, C. A., Bates, N. R., Johnson, R. J., Michaels, A. F., Knap, A.H., 2001. Overview of the US JGOFS Bermuda Atlantic Time-series Study (BATS): a decade-scale look at ocean biology and biogeochemistry. Deep-Sea Research Part II 48, 1405-1447.

Sweeney, E.N., McGillicuddy, D.J., Buesseler, K.O., 2003. Biogeochemical impacts due to mesoscale eddy activity in the Sargasso Sea as measured at the Bermuda Atlantic Time-series Study (BATS). Deep-Sea Research Part II 50, 3017-3039.

Talley, L.D., 1996. North Atlantic circulation and variability, reviewed for the CNLS conference. Physica D 98, 625-646.

Tréguer, P., Nelson, D.M., van Bennekom, A.J., DeMaster, D.J., Leynaert, A., Quéguiner, B., 1995. The silica balance in the world ocean: A re-estimate. Science 268, 375-379.

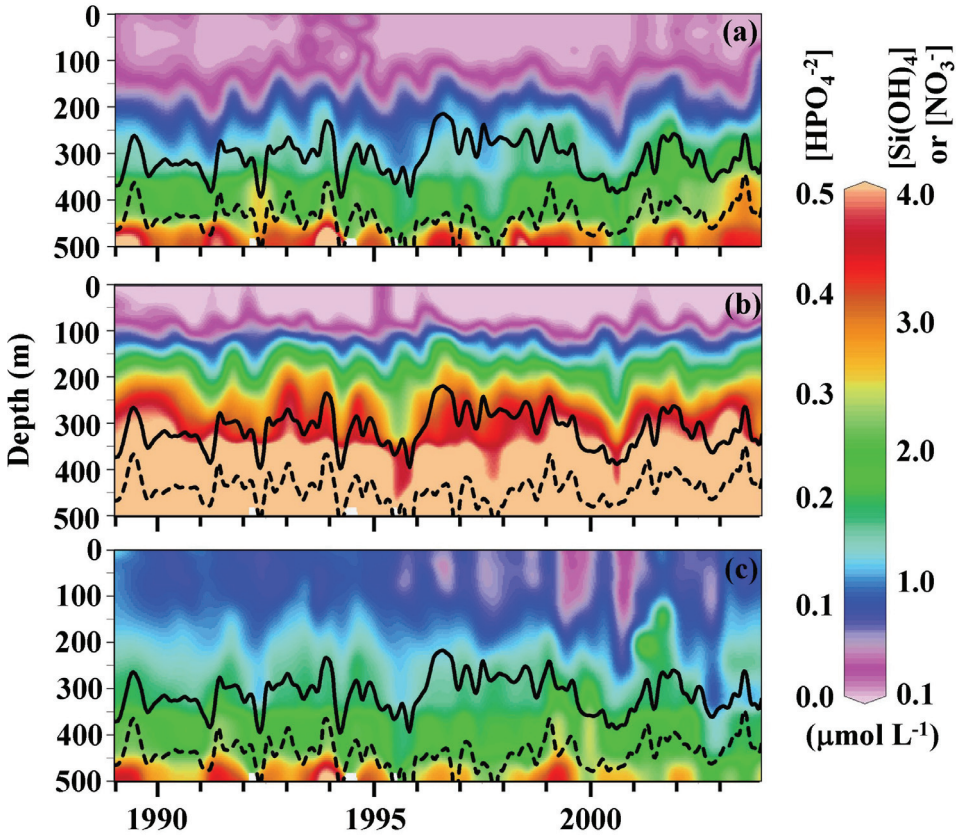

Figure 4.1 – Time series of $[HPO_4^{2-}]$ (a), $[NO_3^-]$ (b) and $[Si(OH)_4]$ (c) in the upper 500 m at the BATS site from 1989-2003, all units in μmol L^{-1}. Black lines in each contour represent σ_θ surfaces of 26.4 (solid) and 26.5 (dotted) kg m^{-3}. All contour plots (i.e. this and other figures) were generated with Ocean Data View (ODV, Schlitzer 2006). Smoothing, to show predominant seasonal trends, was done using ODV's built-in variable resolution gridding algorithm.

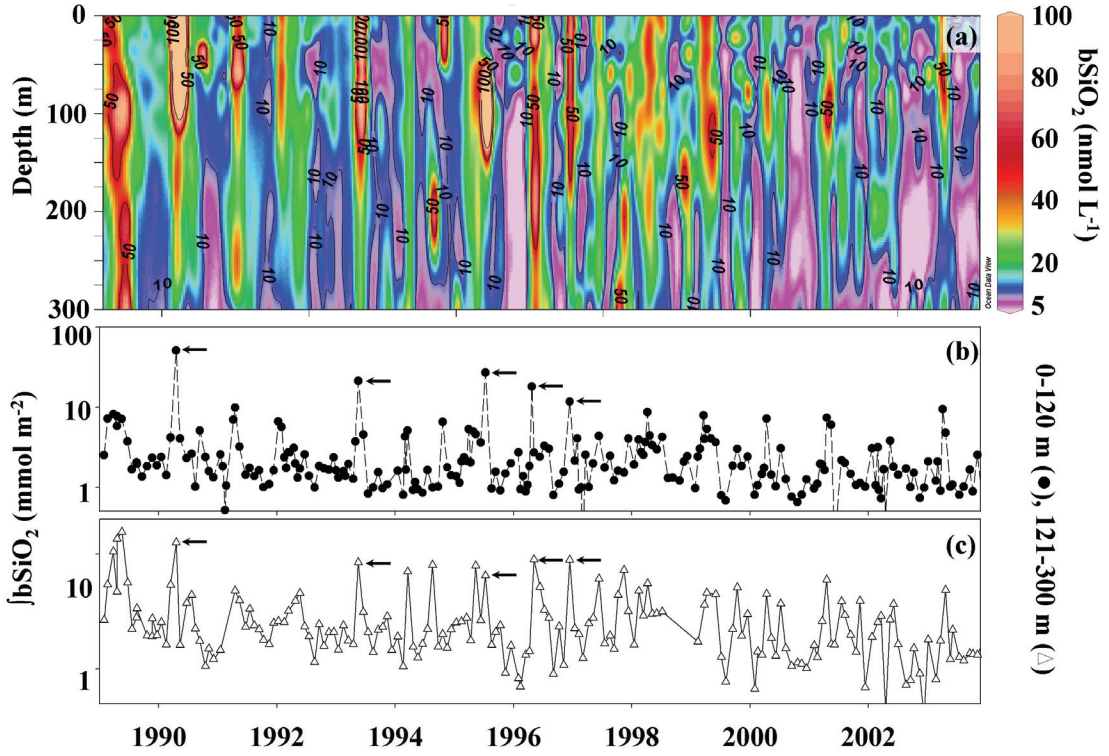

Figure 4.2 – (a) BATS era [$bSiO_2$] in the upper 300 m. [$bSiO_2$] units are in nmol L^{-1}, contours are 10, 50, and 100 nmol L^{-1}. All values >100 are colored the same (e.g. in July 1995 at 100 m the value was >600 nmol L^{-1}). (b) 0 – 120 m $\int bSiO_2$ at BATS (logarithmic scale, 0.5-100 mmol m^{-2}) (c). 121 – 300 m $\int bSiO_2$ at BATS on a logarithmic scale (logarithmic scale, 0.5-20 mmol m^{-2}). The five profiles taken within identified mesoscale features are indicated with arrows in panel (b, c).

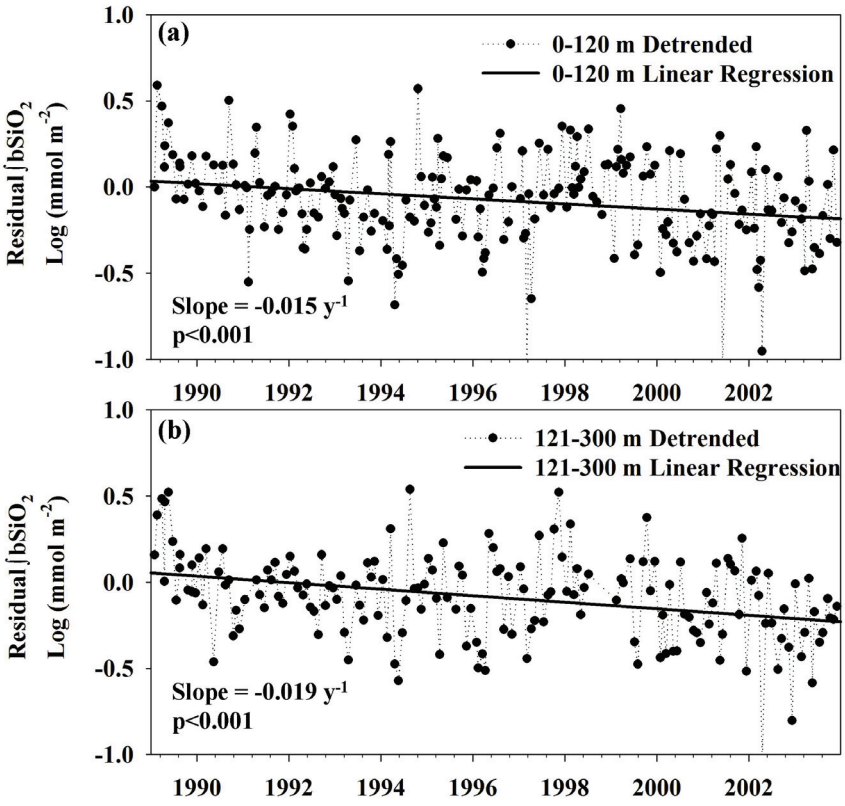

Figure 4.3 – Long-term changes in $\int bSiO_2$ from 1989 through 2003. Log transformed, seasonally de-trended residual $\int bSiO_2$ in the 0-120 m (a) and 121-300 m (b) vertical intervals. The least squares linear regression slope is shown in the bottom left; p <0.001 that the slope of the regression is equal to zero. Anomalously high $\int bSiO_2$ from mesoscale physical features (n=5) were omitted in both panels.

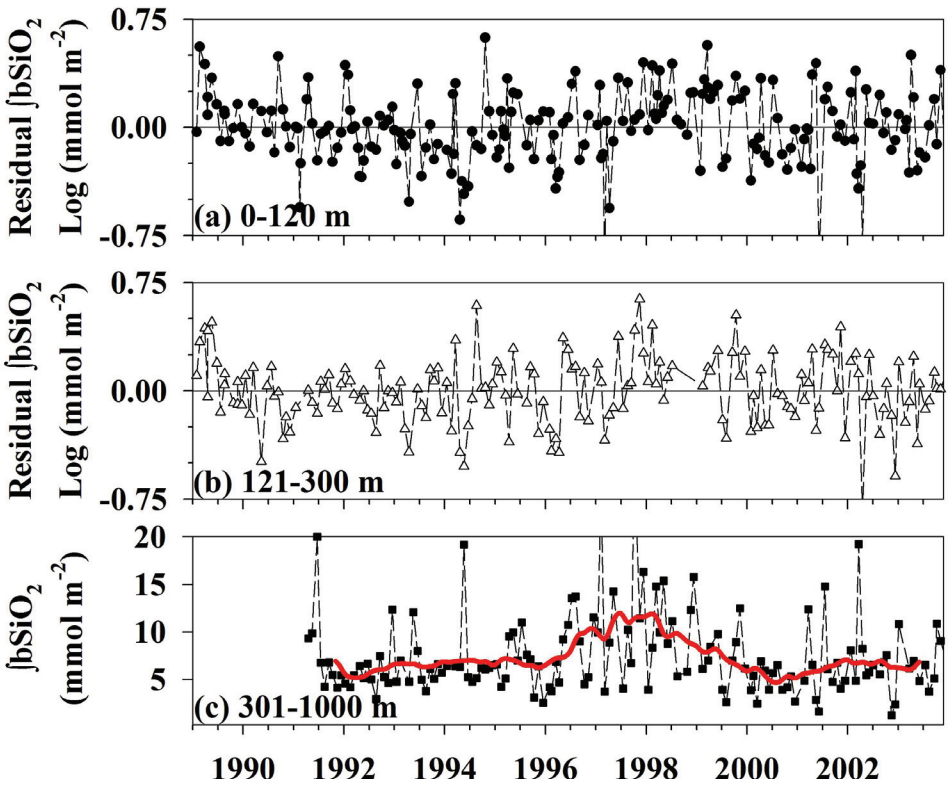

Figure 4.4 – Log transformed $\int bSiO_2$ residuals, with seasonality and the long-term decline removed, in the 0-120 m (a) and 121-300 m (b) intervals. $\int bSiO_2$ values from known mesoscale physical features (n=5) were omitted. (c) 300-1000 m $\int bSiO_2$ in mmol m^{-2}. Note: sampling to 1000 m was not initiated until April 1991. Red line (c) was generated by a 13-month smoothing function described by: $[\{(t_{-6})/2\} + (t_{-5}) + (t_{-4}) + \ldots + (t) + \ldots + (t_{-4}) + (t_{+5}) + \{(t_{+6})/2\}] / 12$, where t_{-x} and t_{+x} represent the means calculated x months before and after time t, respectively. This allowed visualization of temporal variability beyond seasonality.

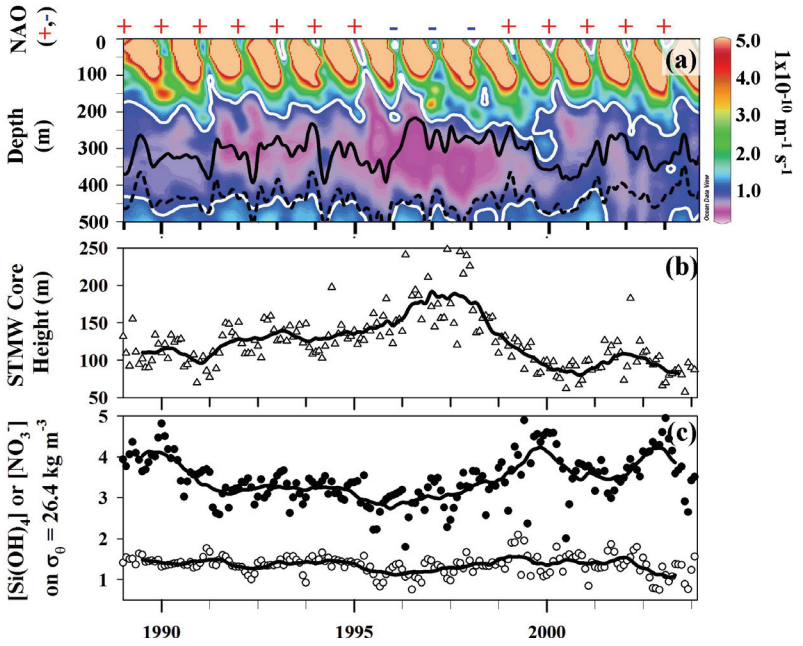

Figure 4.5 – Temporal changes in STMW characteristics and the NAO. Winter values of the NAO phase are denoted as either + (red, positive) or a – (blue, negative). (a) Upper 500 m potential vorticity at the BATS site, in units of $1x10^{-10}$ m^{-1} s^{-1}; white contour is = $1.0x10^{-10}$ m^{-1} s^{-1} (subtropical mode water core <$1.0x10^{-10}$ m^{-1} s^{-1}, Palter et al. 2005). Potential vorticity was calculated by fN^2/g, where f is the Coriolis parameter, N the Brunt–Vaisala frequency, and g is gravitational acceleration. Black σ_θ contour lines (a) are same as in Figure 4.1. (b) Vertical height of the STMW core, calculated by the vertical distance between the 26.4 and 26.5 σ_θ isopycnals (triangles = profile data points). (c) $[NO_3^-]$ (solid circles) and $[Si(OH)_4]$ (open circles) on the 26.4 σ_θ isopycnal, units in μmol L^{-1}. Lines in (b) and (c) are 13 month smoothing as in Figure 4.4c.

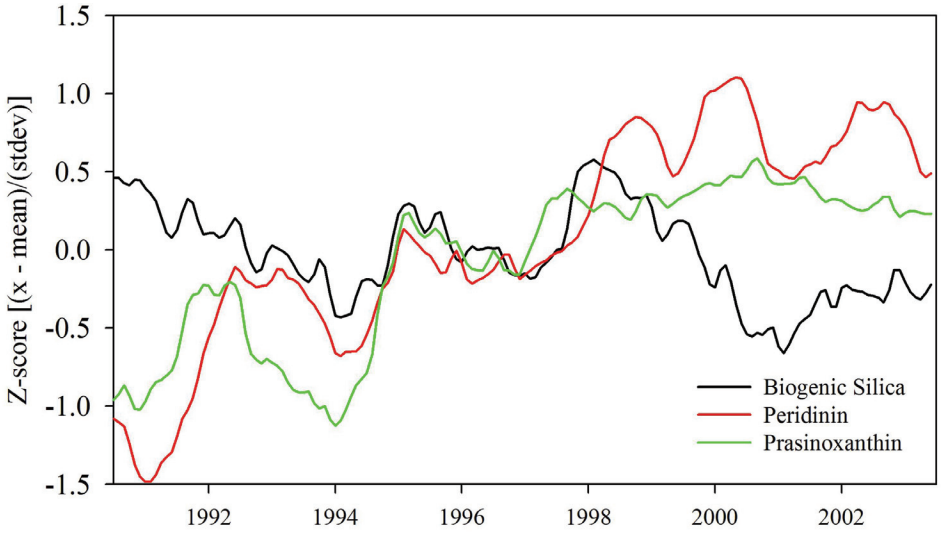

Figure 4.6 – Z-score transformations for log residuals of 0–120 m integrated dinoflagellate (peridinin, red) and prasinophyte (prasinoxanthin, green) pigment abundances (by HPLC methods) and $\int bSiO_2$ (black). All data were log transformed, linearly interpolated to common time interval and lines were smoothed by 13 month function as in Figure 4.4c. Z-score transform is depicted on y-axis with "mean and "stdev" being the time-series mean and standard deviation.

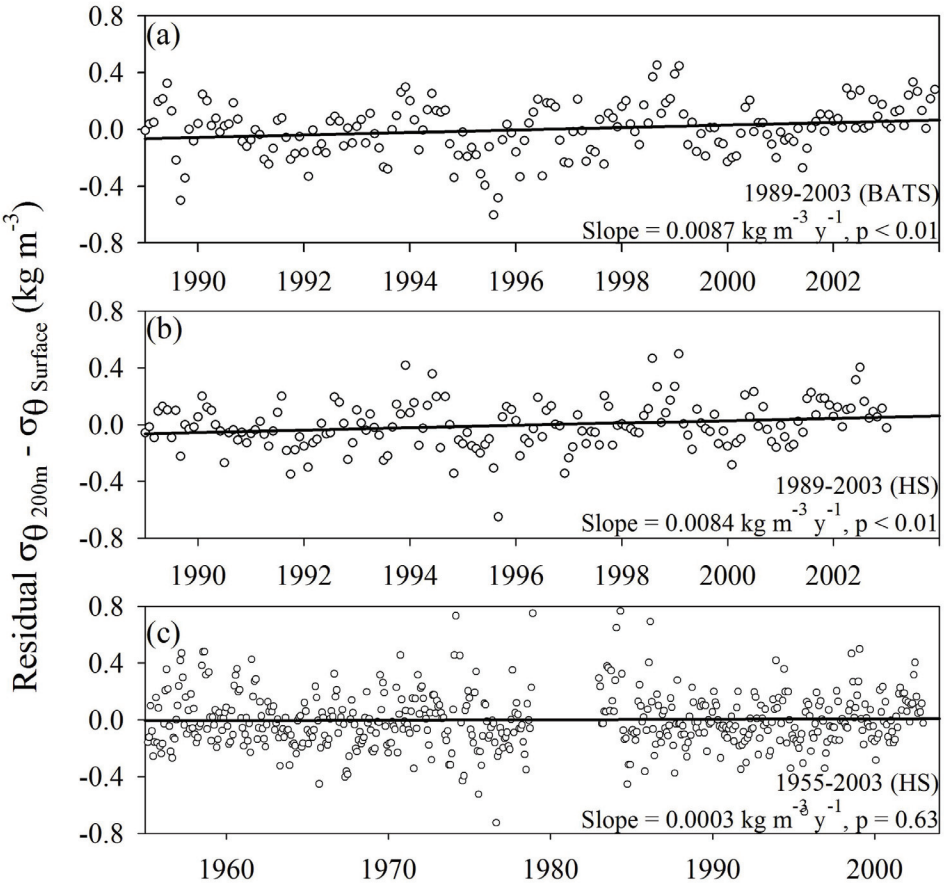

Figure 4.7 – Potential density (σ_θ, kg m^{-3}) difference between 200 m and the surface during the BATS (a) and HS (b, c) eras. BATS data (a) were averaged vertically between 190 to 210 m to obtain the mean σ_θ at 200 m, and in the upper 20 m for the mean surface σ_θ. The resulting density difference (200 m σ_θ – Surface σ_θ) was then detrended by subtracting the annual cycle (e.g. the March 1996 value was calculated by subtracting the 15-year March average (200 m σ_θ – Surface σ_θ) from the March 1996 data point). The slope of the least squares regression was 0.0087±0.0030 (±standard error) kg m^{-3} y^{-1}, with p <0.01 that the slope equals zero (degrees of freedom = 178). For HS era data (b, c), vertical resolution in individual profiles was coarse compared to BATS profiles. Thus σ_θ at 200 m and 20 m (surface) were linearly interpolated for each profile (841 profiles), the annual cycle removed (as done for the BATS data). The slope of the least squares regression for the HS data during the BATS era (1989–2003) was 0.0084 ±0.0030 (±standard error) kg m^{-3} y^{-1} (p < 0.01). However the slope for the entire HS record (1955–2003) was 0.0003 ±0.0006 (±standard error) kg m^{-3} y^{-1} and not significantly different from zero (p = 0.63).

Table 4.1 - Global range of [$bSiO_2$] (nmol L^{-1}) in the ocean. All values are rounded to show approximate levels.

Location	**Time of Year**	**[$bSiO_2$]**	**Reference**
Sargasso Sea	Stratified period	5-25	Nelson and Brzezinski 1997
Equatorial Pacific (180°W)	October/November	50	Leynaert et al. 2001
North Pacific (23-31°N)	July/August	50	Brzezinski et al. 1998
Gulf Stream Warm Core Ring	April	100	Brzezinski and Nelson 1989
Eastern Tropical Pacific	August/September	400	Franck et al. 2003
Bay of Brest, France	Annual Mean	900	Beucher et al. 2004
Gulf Stream Warm Core Ring	June	1000	Brzezinski and Nelson 1989
Monterey Bay, USA	April/May	5500	Brzezinski et al. 1997
Delaware Bay, USA	March	6000	Leblanc and Hutchins 2005
Southern Ocean (65°S)	January (Bloom)	16000	Brzezinski et al. 2001
Ross Sea, Antarctica	February (Bloom)	25000	Nelson et al. 1991

Table 4.2- Mean vertical structure of [$bSiO_2$] at the BATS site (± standard error and number of samples), all data included. Note changes in [$bSiO_2$] between the 101–120 and 121–140m layers, and between the 251–300 and 300–400m layers are the only statistically significant ($p < 0.05$) differences between adjacent layers in this record. A single factor ANOVA test was run for data grouped into surface (0-120 m), middle (121-300 m) and deep (301-1000 m) layers confirming statistically significant differences among these three layers ($F=63.5$, $p<0.001$).

Depth Interval (m)	[$bSiO_2$] (nmol L^{-1})
0-20	23.9±1.7 (612)
21-40	22.1±2.7 (220)
41-60	23.9±2.9 (221)
61-80	26.8±4.1 (221)
81-100	27.3±3.2 (235)
101-120	22.9±2.1 (236)
121-140	17.4±1.0 (205)
141-160	18.5±1.5 (209)
161-200	16.4±1.3 (222)
201-250	13.9±1.1 (216)
251-300	14.6±1.8 (171)
301-400	10.4±0.6 (167)
401-500	9.6±0.6 (179)
501-600	11.0±1.5 (151)
601-700	10.4±1.1 (149)
701-800	11.0±1.3 (148)
801-900	11.4±1.0 (149)
901-1000	10.6±0.7 (145)

Table 4.3 - Seasonal (top) and monthly (bottom) cycle of $\int bSiO_2$ in mmol m^{-2} (mesoscale physical feature profiles not included, n = 5). Single factor ANOVA test run to determine differences. Reported mean ± standard error and sample size in parentheses (n). Letter subscripts in $\int bSiO_2$ denote vertical layers: S = surface (0-120 m), M = middle (121-300 m), and D = deep (301-1000 m).

Season	$\int bSiO_{2\text{-}S}$	$\int bSiO_{2\text{-}M}$	$\int bSiO_{2\text{-}D}$
Spring	3.45±0.31 (61)	3.92±0.47 (45)	8.21±0.64 (38)
Summer	1.73±0.14 (47)	2.32±0.21 (44)	6.55±0.47 (37)
Fall	1.70±0.15 (43)	2.04±0.19 (42)	7.33±0.79 (38)
Winter	2.24±0.20 (61)	2.27±0.22 (38)	7.19±0.95 (28)
ANOVA F value	13.0	8.4	1.0
p value	<0.001	<0.001	0.390
Month	$\int bSiO_{2\text{-}S}$	$\int bSiO_{2\text{-}M}$	$\int bSiO_{2\text{-}D}$
January	2.51±0.39 (17)	1.84±0.17 (14)	6.32±0.80 (10)
February	1.84±0.29 (24)	2.20±0.37 (14)	7.42±2.04 (10)
March	2.77±0.37 (28)	3.45±0.69 (14)	8.14±1.54 (11)
April	4.44±0.62 (23)	4.11±0.81 (15)	7.46±0.48 (13)
May	3.02±0.46 (16)	4.38±1.15 (13)	9.71±1.64 (10)
June	2.43±0.35 (15)	3.26±0.39 (15)	7.70±1.34 (12)
July	1.96±0.27 (14)	2.57±0.27 (14)	7.31±1.07 (12)
August	1.48±0.16 (16)	2.32±0.46 (15)	5.96±0.86 (13)
September	1.60±0.26 (15)	1.70±0.15 (13)	6.42±0.39 (12)
October	1.76±0.38 (15)	2.17±0.32 (14)	7.79±1.75 (13)
November	1.54±0.13 (15)	2.18±0.42 (15)	6.86±0.96 (13)
December	1.80±0.22 (14)	1.76±0.23 (13)	7.36±1.40 (12)
ANOVA F value	5.4	2.9	0.8
p value	<0.001	<0.005	0.849

5. Conclusions, future questions, and new methodology

> "Nothing has such power to broaden the mind as the ability to investigate systematically and truly, all that comes under your observation in life."
>
> Marcus Aurelius (b.121 - d.180, Roman Emperor)

5.1 Major dissertation findings

The three research chapters in this dissertation reveal several new insights into open-ocean Si biogeochemistry. The general conclusions are as follows:

First, late-winter storm events (~2–5 days in duration) entrain limiting nutrients into the euphotic zone, and those nutrients stimulate rapid responses from the siliceous community. In early March, 2004 (during deployment 2004-2 reported in Chapter 2), diatom silicification rates (ρ) increased in response to a storm-driven nitrate and silicic acid injection event, resulting in a doubling of vertically integrated biogenic silica in the upper 140 m ($\int bSiO_2$) in 2–3 days. After doubling, $\int bSiO_2$ returned to its pre-storm level within four days, and 75–100% of the enhanced $\int bSiO_2$ in the upper 140 m (i.e. maximum $\int bSiO_2$ – minus the $\int bSiO_2$ after the decline) was accounted for as $bSiO_2$ flux to sediment traps at 200 m. These results, and others from this study (as presented in detail in Chapter 2) expand current knowledge by demonstrating that biogeochemical processes involving diatoms and Si can vary on the order of days, and that such changes are quantitatively important during the month before the spring bloom period in the Sargasso Sea.

Second, diatom silicification rates show remarkably little spatial variability in the eastern equatorial Pacific. This is significant because Dugdale and Wilkerson (1998) suggested that new production in the equatorial Pacific is controlled by processes similar to those within a Si-limited chemostat. In a chemostat, under Si limitation, the specific rate of diatom growth (μ, = (dX/dT)/X where X = the number of diatom cells per unit volume) is equal to the specific rate of $Si(OH)_4$ input; and if $[Si(OH)_4]$ in the inflowing medium is held constant, must equal the volumetric dilution rate of the chemostat (D, = I/V_C where I = the inflow rate of new medium and V_C the volume of medium in the experimental container). μ and D thus have dimensions of ($time^{-1}$) and in a chemostat at steady state they must be equal. Data from Chapter 3 indicate that within a spatial area of ~2.6×10^6 km^2 (an area larger than

the Bering Sea) specific rates of diatom silicification (V) showed no statistically significant spatial differences during two different one-month periods and that rates during those two periods were statistically indistinguishable from one another. Vertically integrated ρ in the euphotic zone (∫ρ) was higher at 110°W in December, 2004 than that at 140°W in September, 2005; this was the only significant spatial difference observed. This difference likely resulted from higher euphotic-zone $\int Si(OH)_4$ at 110°W, which is in turn a result of nutrient isopleths that slope upward to the east under the flow regime of the equatorial Pacific (see Figure 3.2). However the difference in ∫ρ between these transects was not reflected by a statistically significant difference in vertically averaged V; this implies that the main reason for the higher ∫ρ at 110°W was higher diatom $bSiO_2$ and not higher rates of diatom growth. These results are thus the first of their type to support one key element of Dugdale and Wilkerson's (1998) 'silicate pump' hypothesis for the equatorial Pacific, that conditions controlling diatom growth in the system are in something approaching steady state.

Third, diatoms have a disproportionately large impact on primary and new production in the equatorial Pacific. During cruises in 2004 and 2005, the estimated diatom contribution to primary production was ~20%, increasing to >70% when considering only cells > 3 μm in size (Table 3.2). Assuming diatoms utilize NO_3^- as their only N source, gives a maximum contribution to total NO_3^- uptake of ~50% in both years, increasing to >60% for cells >5 μm in size during 2005 (Table 3.2). Nelson and Brzezinski (1997) reported that the estimated diatom contribution to new production in the Sargasso Sea was ~30% annually, despite diatoms being <5% of the autotrophic biomass (see Steinberg et al. 2001 and references therein). Similarly, diatoms biogeochemical impact in the equatorial Pacific (i.e. contribution to primary and new production) is many times their proportion to the total autotrophic community biomass.

Fourth, $bSiO_2$ standing stocks in the Sargasso Sea vary on sub-decadal time scales. Data from Chapter 4 show that $\int bSiO_2$, within the upper 120 m and between 121 and 300 m at the Bermuda Atlantic Time-series Study (BATS) site in the northwestern Sargasso Sea began increasing anomalously in 1996, reaching a

maximum in 1998, and declining to normal levels by the end of 1999. This multi-year enhancement coincided in time enhanced volume of the North Atlantic subtropical mode-water (STMW, c.f. Hazeleger and Drijfhout 1999, Joyce et al. 2000) and a more southerly winter storm track in the North Atlantic (negative North Atlantic Oscillation), bringing stronger storms near the BATS site (Gruber et al. 2002, Bates and Hansell 2004). The inferred control on the $bSiO_2$ enhancement was that increased STMW volume at the BATS site resulted in shoaling of isopycnal surfaces with elevated $[NO_3^-]$ to depths where the increased storm activity (from negative winter NAO) could enhance its entrainment into the upper water column. Thus diatoms were able to utilize the additional nitrate, causing the observed increase in $\int bSiO_2$. The increased $\int bSiO_2$ coincided in time with drawdown of euphotic-zone $[Si(OH)_4]$ in summer to levels ~50% of those observed at the BATS site prior to the NAO shift (see Figure 4.1). These novel findings infer that diatoms responded to a multi-year physical-climatic forcing mechanism, enhancing upper water column $\int bSiO_2$ and presumably export of $bSiO_2$ (and associated organic matter) to the ocean interior.

Fifth, there was a linear decline $\int bSiO_2$, both in the upper 120 m and between 121 and 300 m at the BATS site, from 1989 through 2003. During that same period integrated stocks of dinoflagellate and prasinophyte biomass, particulate organic carbon and integrated primary production in the upper 120 m all increased. There was also linear increase in vertical stratification as measured by the potential density difference between 200 m and the surface, observed at both the BATS and Hydrostation S sites, and a linear decline in upper 120 m $\int Si(OH)_4$ in winter (the period of enhanced convective entrainment of nutrients into the euphotic zone) at the BATS site over those 15 years. This study is the first to observe changes in diatom biomass on such a time-scale in the open ocean. The specific mechanism forcing the $\int bSiO_2$ decline is not completely understood at this time; however, the ancillary 15-year data sets suggest that increased upper ocean stratification and decreased winter nutrient supply may have led to a shift in the composition of the autotrophic community at the BATS site, in which diatoms decreased while several nonsiliceous forms were increasing.

5.2 Results and conclusions yield more questions

> "Science, in the very act of solving problems, creates more of them."
> Abraham Flexner (b.1866- d.1959, American Educator), Universities, 1930

> "The most exciting phrase to hear in science, the one that heralds new discoveries, is not 'Eureka!' (I found it!) but 'That's funny ...' "
> Isaac Asimov (b.1920- d.1992, American Novelist & Scholar)

The work described in this dissertation sought to address knowledge gaps in open-ocean Si biogeochemistry. In the process of answering the original queries, new questions and new aspects to old questions arose. In this section three new, or at least not yet answered, questions pertaining to open-ocean Si biogeochemistry will be discussed.

5.2.1 Are diatoms the new production 'missing-link' in the Sargasso Sea?

A current estimate of annual nitrate flux into the upper ocean of the Sargasso Sea near Bermuda is 0.84± 0.26 mol N m^{-2} y^{-1} (Jenkins and Doney 2003), which is higher than previous estimates obtained by similar geochemical methods (e.g. 0.5-0.6 mol m^{-2} y^{-1}, Jenkins and Goldman 1985, Jenkins 1988, Spitzer and Jenkins 1989). Under steady-state conditions, the rate of nitrate supply to the upper ocean should be in balance with the export rate of organic nitrogen, i.e. new production (Dugdale and Goering 1967). Steinberg et al. (2001), in a review of the BATS program from 1989 through 1997, reported a mean particulate organic carbon (POC) export flux of 9.4±1.4 g C m^{-2} y^{-1} (≈ 0.8±0.12 mol C m^{-2} y^{-1}) from the upper 150 m, with an observed export ratio (i.e. ratio of export to total production) of 0.06. Converting Steinberg et al.'s POC export flux to molar units of N (i.e. C:N = 6.6) yields an estimate particulate organic nitrogen (PON) export of 0.12 mol N m^{-2} y^{-1}, <15% of Jenkins and Doney's (2003) geochemical estimate. Using ^{15}N uptake measurements made concurrently with the measurements reported in Chapter 2, Lomas et al. (*in revision* a) estimated new production during the one-month period when the water column is most impacted by late-winter storms to be ~0.12–0.18 mol N m^{-2}, 100–150% of the annual PON export indicated by the sediment trap data. This difference underscores the likelihood (Jenkins 1988, Spitzer and Jenkins, 1999) that free-floating sediment traps in the upper

100–400 m systematically underestimate organic matter export in the Sargasso Sea. Inclusion of data taken during late-winter storms, a period which had been systematically missed by the BATS sampling regime (see Chapter 2; see also Lomas et al. *in revision* a) narrows, but does not close, the gap between estimated nitrate delivery to the surface ocean and direct measurements of organic-matter export (Jenkins and Doney 2003).

Goldman and others have proposed that large and numerically rare diatoms may be a significant source of new production in the Sargasso Sea which is unaccounted for in practically all annual estimates (see Goldman 1988, 1993, Goldman et al. 1992, Goldman and McGillicuddy 2003). Goldman et al. (1992) emphasized that a large diatom is equivalent of thousands of smaller cells in terms of C biomass; e.g., the average cell volume of the large Sargasso Sea diatoms in the Goldman et al. study was ~40,000x that of the numerically abundant cyanobacteria *Prochlorococcus* and *Synechococcus*. Goldman (1993) argued that "…a very small seed population of large cells growing in response to an episodic injection of nutrients across the base of the euphotic zone could contribute sizably to annual new production." Experiments reported in Chapter 2 may have recorded events of this kind, and may thus provide a first-order estimate of their quantitative importance.

During both Sargasso Sea cruises reported in Chapter 2, ρ was measured by incubation experiments using ^{32}Si in 300-ml bottles (see Chapter 2 methods). The presence of diatom chains, other aggregates, or very large and rare individual cells in a single sample collected from a low [$bSiO_2$] system like the Sargasso Sea would result in anomalously high ρ if those chains, large cells etc. were actively growing and taking up Si. For brevity these aggregates, chains and large individual cells will be collectively referred to as large siliceous particles (LSPs). Sample volumes for incubations measuring ρ were much smaller than those for $bSiO_2$ measurements (300 ml vs. 2.0 liters). The presence of an LSP in a sample incubated with ^{32}Si would yield an anomalously high ρ; however, its effect on a 2-liter $bSiO_2$ sample would be substantially less because the measurement integrates over a larger volume. As a consequence, the calculated V (which is calculated as the ρ measured in the 300-ml sample divided by the [$bSiO_2$] measured in the two-liter sample; see Chapter 2) would

also be anomalously high. The single highest V actually measured during the cruises reported in Chapter 2 was 0.7 h^{-1}, a rate that is virtually impossible physiologically, and very likely a consequence of an LSP in the incubated sample. Biological characterization of LSPs encountered in the experiments (chains vs. aggregates vs. large and rare individual cells) is not possible because the contents of the ^{32}Si-incubated samples were not examined microscopically. (Elaborate safety precautions would have been required to examine a radioactive sample under a microscope).

The apparent LSP effect (an anomalously high single-point maximum in a vertical profile of V) was observed 11 times in 2004 (out of 247 ^{32}Si uptake samples), and 5 times in 2005 (out of 223 ^{32}Si uptake samples). The 300-ml ^{32}Si incubation volume allows for a coarse estimate of the concentration of LSP during each year. In 2004, the concentration of LSP was approximately one in every 6.7 liters of seawater sampled, ~150 LSP m^{-3}; in 2005, the estimated LSP concentration was lower, about one in every 13.4 liters or ~75 LSP m^{-3}.

Shipe et al. (1999) reported *Rhizosolenia sp*. mat abundances of ~2 m^{-3} in the North Pacific during the summer months of 1995 and 1996; the estimated late-winter LSP abundance from the chapter two Sargasso Sea data set (above) is one to two orders of magnitude higher. The difference is likely due to the combined effects of temporal and geographic differences in [$bSiO_2$] and the fact that an LSP, in Sargasso Sea samples, can be much smaller and more abundant than a *Rhizosolenia* mat. Shipe et al. calculated that the average $bSiO_2$ content of a mat was ~1.8 μmol Si for samples in 1995 and ~4.6 μmol Si in 1996. An LSP with a Si content ~10% of the average *Rhizosolenia* mat encountered by Shipe et al. in 1995 would have increased $bSiO_2$ in one of the Sargasso Sea ^{32}Si samples by ~30x, to ~600 nmol l^{-1} (compare with [$bSiO_2$] from Figure 2.3 and Figure 2.4). If that LSP were physiologically active and taking up $Si(OH)_4$ it would have an enormous effect on the measured ρ, and hence on V. It is likely that aggregates, diatom chains, and very large individual cells caused the anomalously high Vs measured in the Sargasso Sea, but that the Si content of those LSPs was << 10% those of the *Rhizosolenia* mats Shipe et al (1999) encountered in the North Pacific.

Goldman (1993) suggested that sampling this type of new production by large diatoms would be nearly 'impossible' because, if an LSP were sampled by sheer chance, it would appear to be an outlier. Observations reported in Chapter 2 appear to confirm that prediction. The LSP effect is a probable explanation of why a small fraction (~2–5%) of our ^{32}Si uptake samples could have such grossly high V (up to 0.7 h^{-1}, or almost 17 d^{-1}) and this observed effect may have been the result of the mechanism proposed by Goldman and his colleagues. The scope of the data set reported in Chapter 2 does not allow for quantification of a LSP contribution to new production; a likely LSP effect was observed, but the hypothesis that they contribute significantly to new production in the system can neither be confirmed nor refuted. The inherent difficulty in testing Goldman's large diatom hypothesis has led to no field data explicitly quantifying new production by LSPs and indicating whether or not this closes the gap between geochemical estimates and direct measurements of new production in the Sargasso Sea. Future field studies of $bSiO_2$ production in the Sargasso Sea may have to devise new experimental approaches, specifically designed to address Goldman's hypothesis in a quantitative way.

5.2.2 What is the role of mesoscale physics in open-ocean Si biogeochemistry?

One of the earliest recorded observations of the possible interaction between diatoms and mesoscale eddies in the Sargasso Sea was by Riley (1957). Riley noted:

> … species [diatoms] that comprised the localized patches found in the seasonal thermocline in summer … four of the five are regarded as being temperate water diatoms, either oceanic or neritic. Their occurrence in large concentrations, often at a single depth on a particular sampling date, suggests that they may have been transferred into the region from the north in small-scale lateral eddies.

In the Sargasso Sea diatom silicification and growth are generally limited by Si and N availability, respectively (Nelson and Brzezinski 1997). But in five profiles from eddies and other mesoscale physical features (Chapter 4) surface $\int bSiO_2$ was at least 6x higher than the seasonal mean for that respective period. Thus, by some mechanism, these physical features promote enhancement of diatom biomass.

In work related to the Sargasso Sea study reported in Chapter 2, but not performed during the two cruises that comprised that study, I measured [$Si(OH)_4$], [$bSiO_2$], ρ, Si uptake kinetics and diatom cell abundances, obtaining all of these data sets together for the first-time in a mode-water eddy in the Sargasso Sea (April 2007, Figure 5.1). Two profiles were taken in the same eddy, separated in time by six days. There was little temporal variability in [$Si(OH)_4$] profiles outside of the eddy, and it is likely that the processes of Si uptake in the upper 90 m and $bSiO_2$ remineralization from 90 through 150 m within the eddy were responsible for vertically redistributing [$Si(OH)_4$] (Figure 5.1). The average V in the upper 100 m during the first eddy profile was similar to V measured at the BATS station earlier (Figure 5.1); however, the average V in the upper 60 m during the second eddy profile was nearly double that in the other profiles in this depth interval (Figure 5.1d). In a ^{32}Si uptake kinetic experiment with 20 m water, diatoms at this depth were found to be operating at 11% of their maximum uptake capacity (i.e. $V_{AMBIENT\ [Si(OH)4]}/V_{MAX} = 0.11$; see Figure 5.2, see also section 1.1), indicating strong kinetic limitation of Si uptake. Within the upper 60 m chain forming diatoms, e.g. *Chaetoceros sp*., and smaller genera, e.g. *Cylindrotheca sp. or Nitzchia sp.*, had abundances ~1000 cells l^{-1} (data not shown). The abundance of these three genera were each approximately an order of magnitude higher than <u>total</u> diatom abundances in other studies near Bermuda during the late-winter or spring periods (Hulburt 1990, Lomas et al. *in revision* b).

The data collected within this mode-water eddy in 2007 indicate that V within the upper 100 m was ~0.06 d^{-1} (average for both profiles). Using the average [$bSiO_2$] in the upper 100 m at the BATS site on April 2 as a starting point, and assuming this average V was constant through time, it would take ~30 days for the ambient [$bSiO_2$] to reach that observed in the upper 100 m of the mode-water eddy. McGillicuddy et al. (2007) proposed a physical mechanism for supporting such blooms based on the interaction between the mesoscale circulation and the wind field. If the physical mechanism that supports upwelling in an eddy is persistent, then it may be possible for high $bSiO_2$ to accumulate without exceptionally high V; therefore the high observed $bSiO_2$ within these features may be the result of several weeks' worth of accumulation. Alternatively, if increased vertical supply of $Si(OH)_4$ resulting from the

eddy circulation allowed V to increase from its measured value of 0.11 V_{MAX} to ~0.5 V_{MAX}, then [$bSiO_2$] could have increased by enough to produce the high concentrations observed within the eddy over a period of just 7–10 days.

Mesoscale eddies are numerous within the North Atlantic subtropical gyre (McGillicuddy et al. 1998). A growing list of observations shows that diatom abundance and [$bSiO_2$] in these features is anomalously high for the open ocean, but how the high diatom biomass influences organic carbon flux to the ocean interior is just one of many lingering questions. While the data set from Benitez-Nelson et al. (2007) indicates a strong Si pump in associated with mesoscale eddies the North Pacific near Hawaii, whether or not this is the general condition in most Sargasso Sea eddies is unknown. Future studies will need to examine the temporal development of the diatom community in these mesoscale physical features in order to test McGillicuddy et al.'s (2007) proposed mechanistic control and determine whether or not diatoms can increase upper-ocean [$bSiO_2$] under conditions of strong Si uptake limitation and low V (Figures 5.1, 5.2). In addition, a better understanding of the coupling between diatom biomass and C, N and Si export during the temporal development of high-[$bSiO_2$] conditions within an eddy will allow for extrapolation to the potential importance of diatoms in these features to regional new production.

5.2.3 How is Si biogeochemistry in the eastern equatorial Pacific affected by tropical instability waves?

Tropical instability waves (TIWs) were first observed in satellite images of sea-surface temperature (SST) as cold cusps (Legeckis 1977, 1986). TIWs have since been characterized by drifter studies as westward propagating vortices (Flament et al. 1996, Kennan and Flament 2000). These physical features are present in equatorial sectors of both the Atlantic and Pacific oceans, and are most numerous in both systems from June through December (Strutton et al. 2001, Menkes et al. 2002). Interannual variability in TIW formation in the Pacific is most noticeable in response to El Niño and La Niña conditions (Strutton et al. 2001). The weakening of the easterly trade winds during an El Niño event weakens the SST gradient and current shear, which are thought to be responsible for TIW formation (c.f. Philander 1978, Yu et al. 1995).

Under La Niña conditions, the higher than normal easterly trade winds contribute to enhanced zonal flow, current shear and TIW formation.

During August of 1992, a convergent front associated with a TIW near 2°N, 140°W was observed to have anomalously high phytoplankton biomass (Yoder et al. 1994, Archer et al. 1997). At that front, chlorophyll was extremely high (ranging from 5 to 29 mg m^{-3}, compared to the 'normal' ~0.3 mg m^{-3}), and the community was mainly composed of the diatom *Rhizosolenia castracanei* (Yoder et al. 1994, Archer et al. 1997). Similarly, the passage of a TIW at 140°W in October 1992 increased upwelling south of 2°N by Barber et al. (1996), who suggested that the upwelling of Fe-rich Equatorial Undercurrent water provided temporary release of the autotrophic community from Fe limitation. They further interpreted that this Fe input increased maximum photosynthetic rates, allowing algal groups to increase biomass by decoupling growth from grazing losses. During that same event Iriarte and Fryxell (1995) and Bidigare and Ondrusek (1996) reported enhancement of diatom biomass in the high-chlorophyll portion of the TIW based on microscopic enumeration and HPLC pigment analysis, respectively. Strutton et al. (2001) also observed high chlorophyll peaks associated with both the convergent and divergent fronts of TIWs as they passed by moorings at 2°N, 110°W, and 2°N, 140°W in 1998. Thus multiple observations indicate that TIW perturbations increase phytoplankton biomass, and likely alter the autotrophic community composition by increasing diatom biomass.

During the 2005 cruise in the eastern equatorial Pacific a TIW was sampled multiple times while the *R.V. Roger Revelle* occupied an eastbound transect at 0.5°N, with an additional station at 1.75°N – the location of the coolest SST (and hence most recently upwelled surface water) as determined from satellite data (see Chapter 3). $\int\rho$ and $\int bSiO_2$ within the euphotic zone at the 1.75°N station were nearly equal to those sampled at a TIW convergent boundary station (i.e., 0.5°N x 129.9°W; Table 3.1, Figure 3.5). These data are consistent with the mooring observations of Strutton et al. (2001) in showing relatively high diatom biomass in both the convergent and divergent phases of a TIW; however, the question of how TIWs alter Si biogeochemistry and diatom new production are still very much open to debate (Murray et al. 1994, Barber et al. 1996, Gorgues et al. 2005).

Honjo et al. (1995) reported $bSiO_2$ fluxes to ≥2000 m between 5°S and 5°N (on 140°W) from 10 September through 21 December 1992. The temporally averaged $bSiO_2$ flux varied with latitude, having indistinguishable (t-test, p=0.63) maxima at 2°S and on the equator (Figure 5.3). During this period the average flux was ~0.4 mmol Si m^{-2} d^{-1}, with 10 out of 53 flux measurements were >0.5 mmol Si m^{-2} d^{-1}, and a maximum of ~0.9 mmol Si m^{-2} d^{-1}. Each individual flux measurement was from a 17-day collection period, indicating either consistently high flux over the entire collection period or the presence of pulses during which bSO_2 flux was much higher than the 17-day mean, and exert high influence on the time-averaged flux measurement. In the eastern equatorial Pacific during the 2004 and 2005 cruises, $\int\rho$ ranged from 0.3 to 2.6 mmol Si m^{-2} d^{-1}, with a mean rate of 1.4 mmol Si m^{-2} d^{-1} (Table 3.1), only four times the mean $bSiO_2$ flux measured at 2000 m in 1992 (Honjo et al., 1995). Export of $bSiO_2$ from the upper 150–200 m must be at least as great as that reaching 2000 m, and could be much greater. Comparing the measured $\int\rho$ during these cruises with the flux data from Honjo et al. (1995), and ignoring possible interannual differences, indicates that periods of high flux to ≥2000 m are sustained by either (1) continuous silicification with highly efficient export (i.e. 150 m Export/$\int\rho$ >> 0.25) or (2) relatively constant background silicification rates and export efficiency, with occasional pulsed events of high silicification with high $bSiO_2$ export.

It has been suggested that export efficiency for biogenic silica in the equatorial Pacific is lower than in most other oceanic regions (c.f. Brzezinski et al. 2003). In the western equatorial waters at 165°E (i.e. under oligotrophic conditions), Blain et al. (1999) estimated an export efficiency of 6.3% for $bSiO_2$, based on export fluxes measured at 125 m (therefore estimating that >90% of $bSiO_2$ produced in the upper 125 m dissolves there). Leynaert et al. (2001), using Si uptake data from 180°W, indirectly estimated export efficiency at 150 m to be substantially higher, ~65% and ~25% for the equatorial band (1°S–1°N) and poleward (>1°N-8°S, >1°N-7°N), respectively. These studies suggest that a large fraction of detrital $bSiO_2$ in the upper 150 m is dissolved in the upper ocean rather than exported. With the supposition of high $bSiO_2$ dissolution in the upper 150–200 m, and the near certainty that some $bSiO_2$ dissolution occurs between depths of 150–200 m and 2000 m, it would therefore

appear that the mean $\int\rho$ measured in 2004 and 2005 was insufficient to support the high fluxes of $bSiO_2$ to 2000 m which Honjo et al. (1995) measured ~20% of the time.

I hypothesize that in order to sustain the high $bSiO_2$ fluxes observed in moored sediment traps, periodic pulses of high $bSiO_2$ export to the ocean interior are required. The data presented by Honjo et al. (1995, see Figure 5.3) were from a period of increased TIW activity. Therefore, perturbations to the upper water column by TIWs, resulting in enhancement of $\int\rho$ and $\int bSiO_2$ (Chapter 3; see also Yoder et al. 1994, Archer et al. 1997) may potentially promote high $bSiO_2$ flux events. The measurements reported in Chapter 3 were also made during periods of relatively high TIW activity (c.f. Strutton et al. 2001). However the great majority of our stations on both cruises were occupied within ±0.5° latitude from the equator, and the observed enhancements in chlorophyll or diatom biomass related to TIW activity have been observed at a latitude of ~2°N (e.g. Yoder et al. 1994, Archer et al. 1997, Strutton et al. 2001). Thus the observations on each zonal transect might have missed the main enhancement of diatom growth associated with TIWs.

Barber et al. (1996) concluded that Fe limits of primary productivity in the euphotic zone, and Dugdale and Wilkerson's (1998) hypothesized that Si limits diatom new production in this region; thus TIW enhancement of ρ, the standing stock $bSiO_2$, and $bSiO_2$ export may result from enhanced supply of both nutrients, as suggested by the results of Brzezinski et al. (2008). Similarly, a TIW perturbation could lead to enhanced diatom aggregation, with only a modest enhancement of ρ; recent studies (see Moriceau et al. 2007a, b) have suggested this may be an important factor influencing $bSiO_2$ export efficiency. The specific enhancement mechanism is open to debate. However, the fact that TIWs both perturb the upper water column and are numerous in the eastern equatorial Pacific during periods when the trade winds are active, makes them a potential candidate for exploring the apparent discrepancy between relatively low and constant $\int\rho$ in the euphotic zone (Chapter 3) with high and temporally variable $bSiO_2$ export to ~2000 m (Honjo et al., 1995).

5.3 Open-ocean Si biogeochemistry in the future: a methods 'wish list'

> "Insanity: doing the same thing over and over again and expecting different results."
>
> *attributed to* Albert Einstein (b.1878- d.1955, American Physicist)

Through the process of conducting this research and analyzing the results obtained, more questions arose. A few of those questions have been discussed above. However, this research experience has also produced a hindsight wish that other properties had been quantified. The difficulty with such desires is that methods for measuring those 'other properties' were not (and still are not) available. Therefore, in this section I focus on two areas where I believe that methodological improvements will be needed before we can achieve a significantly improved understanding of Si biogeochemistry in the open ocean.

5.3.1 Biogenic silica dissolution

The biological cycling of Si in the upper ocean is predominantly a function of the uptake of $Si(OH)_4$, production of $bSiO_2$, recycling of $bSiO_2$ by dissolution, and the loss of $bSiO_2$ by export. The contribution of diatoms to global export production is significant (c.f. Boyd and Trull 2007, Honjo et al. 2008) and the loss of $bSiO_2$ in the upper ocean by dissolution influences the potential amount of $bSiO_2$ (and associated organic matter) exported to the ocean interior. Despite indirect methods for estimating of $bSiO_2$ dissolution in the upper water column (e.g. Nelson and Brzezinski 1997), the lack of measurements in the majority of the ocean has hindered understanding of $bSiO_2$ recycling on time scales similar to those for $bSiO_2$ production (i.e. hourly to daily); this represents a major unknown in present knowledge of Si cycling in the open ocean.

A better understanding of Si cycling in the open ocean will require sensitive methods for measuring $bSiO_2$ dissolution in the euphotic zone on hourly to daily time scales. A method for measuring the rate of $bSiO_2$ production in marine waters was developed over 30 years ago (Goering et al. 1973). Similar to ^{15}N studies (Dugdale and Goering 1967) this method utilized rare Si stable isotopes (^{29}Si, ^{30}Si) as tracers. Later, Nelson and Goering (1977) described a method using stable-isotope Si tracers

for the measurement of $bSiO_2$ production and $bSiO_2$ dissolution in the same sample, using a stable-isotope dilution method for the latter.

Stable-isotope dilution is the most common method for direct measurement of euphotic zone $bSiO_2$ dissolution (Nelson and Goering 1977, Nelson et al. 1981, Nelson and Gordon 1982, Brzezinski and Nelson 1989, DeMaster et al. 1991, Brzezinski et al. 2003, Beucher et al. 2004a, 2004b, Corvaisier et al. 2005). More sensitive mass spectrometers and new ways to amplify the dissolution signal have improved the measurement of $bSiO_2$ dissolution by the isotope dilution method; however, these have merely built upon the existing method, opposed to utilizing a more sensitive tracer (e.g. ^{32}Si for $bSiO_2$ production, Brzezinski and Phillips 1997). The great majority of the coupled $bSiO_2$ production/dissolution profiles obtained to date in the ocean have been carried out in areas of high diatom biomass (e.g. coastal upwelling systems, river plumes, Southern Ocean, etc.). Before 1995, the total number of coupled $bSiO_2$ dissolution and production profiles available from the world's oceans was only 45 (see Nelson et al. 1995, Table 5.1). Since 1995 that total has more than doubled (Table 5.1), but new data have not been obtained in oceanic regions where $[bSiO_2]$ is chronically low such as the subtropical gyres. Attempts to measure $bSiO_2$ dissolution rates by stable-isotope dilution in the Sargasso Sea in the early 1990s, using the best methods and most sensitive mass spectrometers then available, failed consistently (Nelson and Brzezinski 1997).

Methodological sensitivity is the primary reason that stable-isotope dilution methods have not been successful in most open-ocean regions. Many areas of the ocean lacking data on $bSiO_2$ dissolution rates in the upper water column have high ratios of dissolved Si to particulate Si, i.e., high $[Si(OH)_4]$:$[bSiO_2]$. For instance, in gyre regions such as Sargasso Sea, the surface $[Si(OH)_4]$:$[bSiO_2]$ ratio may reach 80 (Brzezinski and Nelson 1995), whereas in coastal systems it is often ≤ 1 (Brzezinski et al. 2003). The stable-isotope method for $bSiO_2$ dissolution measures the dilution of the $Si(OH)_4$, enriched in one of the heavy rare isotopes (^{29}Si or ^{30}Si), with isotopically natural Si from the ambient $bSiO_2$, which is 92.18 atom % ^{28}Si. In areas of high $[Si(OH)_4]$:$[bSiO_2]$ in surface waters there is great difficulty in trying to resolve a small dissolution signal (coming from the relatively small $bSiO_2$ pool) in the much larger

pool of isotope-enriched $Si(OH)_4$; a problem which is further exacerbated by even minute contamination. Nelson and Brzezinski (1997) commented that contamination with one nanomole of isotopically natural Si would yield an error of ±0.07 d^{-1} in the specific dissolution rate of $bSiO_2$ in the Sargasso Sea. This type of analytical difficulty is not confined to the Sargasso Sea but any location where [$bSiO_2$] is << [$Si(OH)_4$], including areas of the equatorial Pacific, and the North Pacific near Hawaii.

A new approach to measuring $bSiO_2$ dissolution utilizes a mass balance method, coupling existing methodology and circumventing the notorious effect of high [$Si(OH)_4$]:[$bSiO_2$] ratios in the surface waters. In a closed system the change in $bSiO_2$ with time is parameterized by the mass balance equation:

$$\rho_{NET} = \rho_{PROD} - \rho_{DISS}$$

where the net rate of $bSiO_2$ production (ρ_{NET}) is the difference between gross $bSiO_2$ production (ρ_{PROD}) and gross $bSiO_2$ dissolution (ρ_{DISS}). Using the mass balance equation, we can solve for dissolution:

$$\rho_{DISS} = \rho_{PROD} - \rho_{NET}$$

Theoretically, if both ρ_{PROD} and ρ_{NET} are measured in the same closed system the difference of the two rates will estimate ρ_{DISS}. There is a strong logistical constraint in measuring both ρ_{PROD} and ρ_{NET} in the same sample (i.e. trying to digest $bSiO_2$ with radioactivity); however, this may be overcome by using separate bottles for each measurement, assuming similar processes occur in each bottle, and replicating samples to understand variance. ρ_{PROD} can be measured with high precision by using ^{32}Si (e.g. methods chapters 2, 3, see also Figure 3.6), and ρ_{NET} can be measured by the change in $bSiO_2$ during an incubation period concurrent with the ρ_{PROD} incubation period. ρ_{NET} methodology has been used previously for deeper samples (e.g. 100–400 m, see Brzezinski and Nelson 1989); however, has never been coupled with a high-precision measurement of ρ_{PROD} to estimate ρ_{DISS} in the euphotic zone.

Applying this mass balance approach in an area such as the equatorial Pacific should theoretically be successful (Table 5.2). For instance, if the average $bSiO_2$ in the upper 100 m in this region were 100 nmol l^{-1} (see Chapter 3), and V were 0.69 d^{-1} (corresponding to one doubling of $bSiO_2$ per day in the absence of any losses) then

even at very low specific $bSiO_2$ dissolution rates (V_{DISS}), measuring ρ_{NET} is both easier to do (methodologically) and more sensitive than detection of the isotopic shift from a mass spectrometer (Table 5.2). This mass balance approach requires ρ_{NET} to be highly constrained; therefore logistical considerations (e.g. incubation volume and replication) and possible bottle artifacts (e.g. $bSiO_2$ adhering to the container walls and systematically missed during filtration) would have to be addressed before field use.

Application of a more sensitive dissolution methodology to areas with high $[Si(OH)_4]$:$[bSiO_2]$ will greatly assist in resolving short temporal scale imbalances between $bSiO_2$ production and dissolution. Among other uses, quantification of $bSiO_2$ dissolution on hourly to daily time-scales will also help determine effectiveness of linking short-term (<1 week), shallow sediment trap $bSiO_2$ fluxes (e.g. 150, 200, 300 m) to the Si biogeochemical processes in the overlying water column.

5.3.2 Living versus detrital biogenic silica

The current understanding of the biogenic particle assemblage, in any ocean system, lacks information on the proportion of $bSiO_2$ associated with live diatoms versus $bSiO_2$ associated with detritus (empty frustules, siliceous fragments etc.). Analytical methods currently in use cannot distinguish between living and detrital $bSiO_2$, as they are based on a NaOH digestion, which dissolves all amorphous silica, i.e. $bSiO_2$ from living diatoms and from detritus (see methods sections of Chapter 2, 3 and 4). This analytical problem has important consequences for measuring rates of biogenic silica production using either stable-isotope (^{29}Si or ^{30}Si) or radioisotope (^{32}Si) tracers. While distinguishing between living and detrital $[bSiO_2]$ is inconsequential in the measurement ρ, the inclusion of detrital $bSiO_2$ will always result in an underestimate of the true V for living diatoms (e.g. Goering et al. 1973). The proportional difference is equivalent to the ratio of detrital $bSiO_2$ to total $bSiO_2$ (i.e. living plus detrital) in the sample (Goering et al. 1973); thus, a higher proportion of detrital $bSiO_2$ yields a larger discrepancy between calculated V and the true V for living diatoms. If independent estimates of diatom growth rates (μ) are available, an estimate of detrital $bSiO_2$ can be made indirectly by comparing of diatom growth μ with V (Brzezinski et al. 2008, see also Chapter 3 discussion); while this method is

potentially powerful, it requires a reliable and independent estimate of diatom growth rates (μ). In field studies, μ for diatoms is most commonly estimated from dilution methodology (see Latasa et al. 1997 and references therein). Indirect estimates of live and detrital $bSiO_2$, based on independent estimates of V and μ, imply that ~67% of the $bSiO_2$ in the equatorial Pacific euphotic zone during the 2004 and 2005 cruises was detrital (Brzezinski et al., 2008).

New methodology to distinguish analytically between living and detrital $bSiO_2$ would open many new doors. Current methods have provided a foundation; however, there are logistical drawbacks keeping them from regular field usage. Shipe and Brzezinski (1999) used ^{32}Si autoradiography to quantify individual cell silicification of *Rhizosolenia* mats. While this method allowed for quantification of cell specific silicification rates, and can theoretically be used to distinguish metabolically active diatoms from detrital siliceous particles, it requires use of ^{32}Si, which is presently not being produced and was expensive (>$1000 USD per 1 μCi) when it was produced. Current methods also require exposure times for samples of >4 months. Similarly, Leblanc and Hutchins (2005) used the compound 2-(4-pyridyl)-5-((4-(2-dimethylaminoethylaminocarbamoyl)methoxy)-phenyl)oxazole (referred to as PDMPO) to get the same type of information as Shipe and Brzezinski's method. Unlike, Shipe and Brzezinski's method, PDMPO is not an Si isotope, and thus behaves differently. PDMPO has the unique floristic characteristic in the presence of >3 mmol l^{-1} $[Si(OH)_4]$ (Shimizu et al. 2001). When $Si(OH)_4$ is polymerized by a diatom, PDMPO is thought to be incorporated within the $bSiO_2$ polymer matrix; this results in a yellow-green fluorescence of new $bSiO_2$ which can easily be detected optically (Shimizu et al. 2001, Leblanc and Hutchins 2005). While this method holds great promise to derive cell-specific rates of silicification, a lack of understanding about the ratio of PDMPO incorporated per unit $bSiO_2$ and the logistical challenge of being able to physically separate actively silicifying cells (e.g. those with PDMPO) from those that are dormant are detrital, has hindered addressing of the proportion of live and detrital $bSiO_2$ directly in field studies. The future development and incorporation of these new methods, especially in the open ocean, will further the mechanistic understanding of diatoms' role in upper ocean biogeochemical processes.

5.4 References

Archer, D., and 16 others, 1997. A meeting place of great ocean currents: shipboard observations of a convergent front at 2 degrees N in the Pacific. Deep-Sea Research II 44, 1827-1849.

Barber, R.T., Sanderson, M.P., Lindley, S.T., Chai, F., Newton, J., Trees, C.C., Foley, D.G., Chavez, F.P., 1996. Primary productivity and its regulation in the equatorial Pacific during and following the 1991-1992 El Niño. Deep-Sea Research II 43, 933-969.

Bates, N.R., Hansell., D.A., 2004. Temporal variability of excess nitrate in the subtropical mode water of the North Atlantic Ocean. Marine Chemistry 84, 225–241.

Benitez-Nelson, C.R., and 22 others, 2007. Mesoscale eddies drive increased silica export in the Subtropical Pacific Ocean. Science 316, 1017-1021.

Beucher, C., Tréguer, P., Corvaisier, R., Hapette, A.M., Elskens, M., 2004a. Production and dissolution of biosilica, and changing microphytoplankton dominance in the Bay of Brest (France). Marine Ecology Progress Series 267, 57–69.

Beucher, C., Tréguer, P., Hapette, A., Corvaisier, R., 2004b. Intense summer Si-recycling in the surface Southern Ocean. Geophysical Research Letters 31, L09305, doi: 10.1029/2003GL018998.

Bidigare, R.R., Ondrusek, M.E., 1996. Spatial and temporal variability of phytoplankton pigment distributions in the central equatorial Pacific Ocean. Deep-Sea Research II 43, 809-833.

Blain, S., Tréguer, P, Rodier, M., 1999. Stocks and fluxes of biogenic silica in the western oligotrophic equatorial Pacific. Journal of Geophysical Research 104, 3357-3367.

Boyd, P.W., Trull, T.W., 2007. Understanding the export of biogenic particles in oceanic waters: Is there consensus? Progress in Oceanography 72, 276-312.

Brzezinski, M.A., Nelson, D.M., 1989. Seasonal changes in the silicon cycle within a Gulf Stream warm-core ring. Deep-Sea Research I 36, 1009-1030.

Brzezinski, M.A., Nelson, D.M., 1995. The annual silica cycle in the Sargasso Sea near Bermuda. Deep-Sea Research I 42, 1215-1237.

Brzezinski, M.A., Phillips, D.R., 1997. Evaluation of ^{32}Si as a tracer for measuring silica production rates in marine surface waters. Limnology and Oceanography 42: 856-865.

Brzezinski, M.A., Nelson, D.M., Franck, V.M., Sigmon, D.E., 2001. Silicon dynamics within an intense open-ocean diatom bloom in the Pacific sector of the Southern Ocean. Deep-Sea Research II 48 3997–4018.

Brzezinski, M.A., Jones, J.L., Bidle, K.D., Azam, F., 2003. The balance between silica production and silica dissolution in the sea: Insights from Monterey Bay, California, applied to the global data set. Limnology and Oceanography 48, 1846-1854.

Brzezinski, M.A., Dumousseaud, C., Krause, J.W., Measures, C.I., Nelson, D.M., 2008. Iron and silicic acid concentrations together regulate Si uptake in the equatorial Pacific Ocean. Limnology and Oceanography 53, 875-889.

Corvaisier, R., Tréguer, P., Beucher, C., Elskens, M., 2005. Determination of the rate of production and dissolution of biosilica in marine waters by thermal ionisation mass spectrometry. Analytica Chimica Acta 534, 149–155.

DeMaster, D.J., McKee, B.A., Moore, W.S., Nelson, D.M., Showers, W.J., Smith, W.O., 1991. Geochemical processes occurring at the Amazon River/ocean boundary. Oceanography 4, 15-20.

Dugdale, R.C., Goering, J.J., 1967. Uptake of new and regenerated forms of nitrogen in primary productivity. Limnology and Oceanography 12, 196-206.

Dugdale, R.C., Wilkerson, F.P., 1998. Silicate regulation of new production in the equatorial Pacific upwelling. Nature 391, 270-273.

Flament, P.J., Kennan, S.C., Knox, R.A., Niiler, P.P., Bernstein, R.L., 1996. The three-dimensional structure of an upper ocean vortex in the tropical Pacific Ocean. Nature 383, 610-613.

Goering, J. J., Nelson, D.M., and J.A. Carter. 1973. Silicic acid uptake by natural populations of marine phytoplankton. Deep-Sea Research 20: 777-789.

Goldman, J.C., 1988. Spatial and temporal discontinuities of biological processes in pelagic surface waters, p. 273-296. *In* Rothschild, B.J. (Ed.), Toward a theory on biological-physical interactions in the world ocean. Kluwer Academic, Dordrecht.

Goldman J. C., 1993. Potential role of large oceanic diatoms in new primary production. Deep-Sea Research 40, 159-168.

Goldman, J.C., McGillicuddy, D.J., 2003. Effect of large marine diatoms growing at low light on episodic new production. Limnology and Oceanography 48, 1176-1182

Goldman, J.C., Hansell, D.A., Dennett, M.R., 1992. Chemical characterization of three large oceanic diatoms: potential impact on water column chemistry. Marine Ecology Progress Series 88, 257-270.

Gorgues, T., Menkes, C., Aumont, O., Vialard, J., Dandonneau, Y., Bopp, L., 2005. Biogeochemical impact of tropical instability waves in the equatorial Pacific. Geophysical Research Letters 32, L24615, doi:10.1029/2005GL024110.

Gruber, N., Keeling, C.D., Bates, N.R., 2002. Interannual variability in the North Atlantic Ocean carbon sink. Science 298, 2374-2378.

Hazeleger, W., Drijfhout, S.S., 1999. Stochastically forced mode water variability. Journal of Physical Oceanography 29, 1772-1786.

Honjo, S., Dymond, J., Collier, R., Manganini, S.J., 1995. Export production of particles to the interior of the equatorial Pacific Ocean during the 1992 EqPac experiment. Deep-Sea Research II 42, 831-870.

Honjo, S., Manganini, S.J., Krishfield, R.A., Francois, R., 2008. Particulate organic carbon fluxes to the ocean interior and factors controlling the biological pump: A synthesis of global sediment trap programs since 1983. Progress in Oceanography 76: 217-285.

Hulburt E. M., 1990. Description of phytoplankton and nutrient in spring in the western North Atlantic Ocean. Journal of Plankton Research 12, l-28.

Iriarte, J.L., Fryxell, G.A., 1995. Micro-phytoplankton at the equatorial Pacific (140°W) during the JGOFS EqPac Time Series studies: March to April and October 1992. Deep-Sea Research II 42, 559-583.

Jenkins, W., 1988. Nitrate flux into the euphotic zone near Bermuda. Nature 331, 521-523.

Jenkins, W., Doney, S. C., 2003. The subtropical nutrient spiral. Global Biogeochemical Cycles 17: doi: 10.1029/2003GB002085.

Jenkins, W., Goldman, J., 1985. Seasonal oxygen cycling and primary production in the Sargasso Sea. Journal of Marine Research 43, 465-491.

Joyce, T.M., Deser, C., Spall, M.A., 2000. The relation between decadal variability of Subtropical Mode Water and the North Atlantic Oscillation. Journal of Climate 13, 2550-2569.

Kennan, S.C., Flament, P.J., 2000. Observations of a tropical instability vortex. Journal of Physical Oceanography 30, 2277-2301.

Latasa, M., Landry, M.R., Schlüter, L., Bidigare, R.R., 1997. Pigment-specific growth and grazing rates of phytoplankton in the central equatorial Pacific. Limnology and Oceanography 42, 289-298.

Leblanc, K., Hutchins, D.A., 2005. New applications of a biogenic silica deposition fluorophore in the study of oceanic diatoms. Limnology and Oceanography: Methods 3, 462-476.

Legeckis, R., 1977. Long waves in the eastern equatorial Pacific ocean: a view from a geostationary satellite. Science 197, 1179-1181.

Legeckis, R., 1986. A satellite time series of sea surface temperatures in the eastern equatorial Pacific Ocean 1982-1986. Journal of Geophysical Research 91, 12879-12886.

Leynaert, A., Tréguer, P., Lancelot, C., Rodier, M., 2001. Silicon limitation of biogenic silica production in the Equatorial Pacific. Deep-Sea Research I 48, 639-600.

Lomas, M.W., Lipschultz, F. , Nelson, D. M., Bates, N.R. (*in revision*)-a. Biogeochemical responses to late-winter storms in the Sargasso Sea. I. Pulses of primary and new production. *In revision*, Deep-Sea Research I.

Lomas, M.W., Roberts, N., Lipschultz, F., Krause, J.W., Nelson, D.M , Bates, N.R. (*in revision*)-b. Biogeochemical responses to late-winter storms in the Sargasso Sea. III. Rapid successions of major phytoplankton groups. *In revision*, Deep-Sea Research I.

McGillicuddy, D.J., Robinson, A.R., Siegel, D.A., Jannasch, H.W., Johnson, R., Dickey, T.D., McNeil, J., Michaels, A.F., Knap, A.H., 1998. Influence of mesoscale eddies on new production in the Sargasso Sea. Nature 394, 263-266.

McGillicuddy, D.J., and 17 others, 2007. Eddy/wind interactions stimulate extraordinary mid-ocean plankton blooms. Science 316, 1021-1026.

Menkes, C.E., and 14 others, 2002. A whirling ecosystem in the equatorial Atlantic. Geophysical Research Letters 29 (11), doi: 10.1029/2001GL014576.

Moriceau, B., Garvey, M., Ragueneau, O., Passow, U., 2007a. Evidence for reduced biogenic silica dissolution rates in diatom aggregates. Marine Ecology Progress Series 333, 129-142.

Moriceau, B., Gallinari, M., Soetaert, K., Ragueneau, O., 2007b. Importance of particle formation to reconstructed water column biogenic silica fluxes. Global Biogeochemical Cycles 21, GB3012, doi: 10.1029/2006GB002814.

Murray, J.W., Barber, R.T., Roman, M.R., Bacon, M.P., Feely, R.A., 1994. Physical and biological controls on carbon cycling in the equatorial Pacific. Science 266, 58-65.

Nelson, D.M., Brzezinski, M.A., 1997. Diatom growth and productivity in an oligotrophic midocean gyre: a 3-yr record from the Sargasso Sea near Bermuda. Limnology and Oceanography 43, 473-486.

Nelson, D.M., Goering, J.J., 1977. Near-surface silica dissolution in the upwelling region off northwest Africa. Deep-Sea Research 24, 65-73.

Nelson, D.M., Gordon, L.I., 1982. Production and pelagic dissolution of biogenic silica in the Southern Ocean. Geochimica Cosmochimica Acta 46, 491-501.

Nelson, D.M., Goering, J.J., Boisseau, D.W., 1981. Consumption and regeneration of silicic acid in three coastal upwelling systems, p. 242-256. *In* F.A. Richards (ed.), Coastal Upwelling. American Geophysical Union.

Nelson, D.M., Ahern, J.A., Herlihy, L.J., 1991. Cycling of biogenic silica within the upper water column of the Ross Sea. Marine Chemistry 35, 461-476.

Nelson, D.M., Tréguer, P., Brzezinski, M.A., Leynaert, A., Quéguiner, B., 1995. Production and dissolution of biogenic silica in the ocean: Revised global estimates, comparison with regional data and relationship to biogenic sedimentation. Global Biogeochemical Cycles 9, 359–372.

Philander, S.G.H., 1978. Instabilities of zonal equatorial currents, 2. Journal of Geophysical Research 83, 3679-3682.

Riley, G.A., 1957. Phytoplankton of the North Central Sargasso Sea, 1950-1952. Limnology and Oceanography 2, 252-269.

Shimizu, K., Del Amo, Y., Brzezinski, M.A., Stucky, G.D., Morse, D.E., 2001. A novel fluorescent silica tracer for biological silicification studies. Chemistry and Biology 8, 1051-1060.

Shipe, R.F., Brzezinski, M.A., 1999. A study of Si deposition synchrony in *Rhizosolenia* (Bacillariophyceae) mats using a novel ^{32}Si autoradiographic method. Journal of Phycology 35, 995-1004.

Shipe, R.F., Brzezinski, M.A., Pilskaln, C. Villareal, T.A., 1999. Rhizosolenia mats: An overlooked source of silica production in the open sea. Limnology and Oceanography 44, 1282-1292.

Spitzer, W., Jenkins, W., 1989. Rates of vertical mixing, gas exchange and new production: estimates from seasonal gas cycles in the upper ocean near Bermuda. Journal of Marine Research 47, 169-196.

Steinberg, D. K., Carlson, C. A., Bates, N. R., Johnson, R. J., Michaels, A. F., Knap, A. H. 2001. Overview of the US JGOFS Bermuda Atlantic Time-series Study (BATS): a decade-scale look at ocean biology and biogeochemistry. Deep-Sea Research Part II 48, 1405-1447.

Strutton, P.G., Ryan, J.P., Chavez, F.P., 2001. Enhanced chlorophyll associated with tropical instability waves in the equatorial Pacific. Geophysical Research Letters 28, 2005-2008.

Yoder, J.A., Ackleson, S.G., Barber, R.T., Flament, P., Balch, W.M., 1994. A line in the sea. Nature 371, 689-692.

Yu, Z., McCreary, J.P., Proehl, J.A., 1995. Meridional asymmetry and energetics of tropical instability waves. Journal of Physical Oceanography 25, 2997-3007.

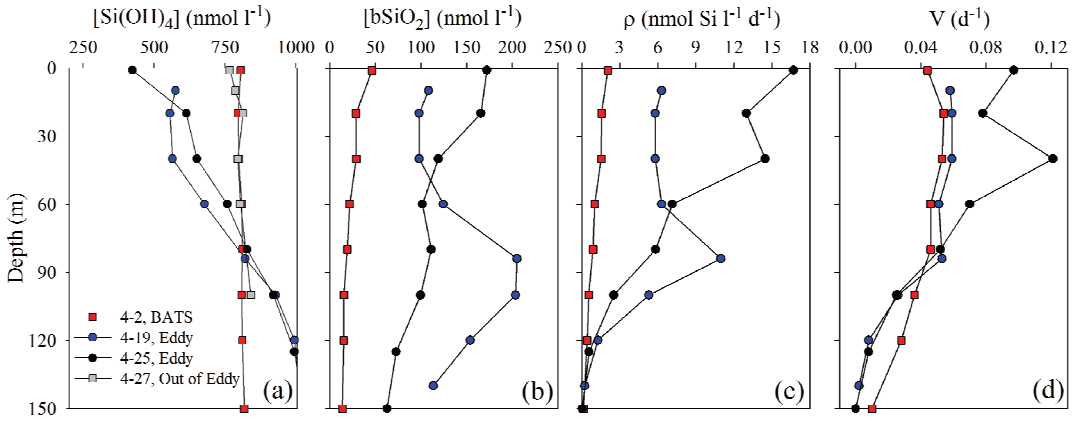

Figure 5.1 - Upper water column Si stocks and silicification rates within (circles) and out (squares) of a Sargasso Sea mode-water eddy. (a) $[Si(OH)_4]$ and (b) $[bSiO_2]$ in nmol l^{-1}. (c) ρ in nmol Si l^{-1} d^{-1} and (d) V in d^{-1}. Profiles were done on ships of opportunity in spring 2007 (stations referred to by month-day, e.g. 2 April is 4-2). The first and second occupations of the same mode-water eddy were done less than one week apart; with strong storm activity during the first occupation (4-19, blue circles), and sunny and calm conditions during the second (4-25, black circles).

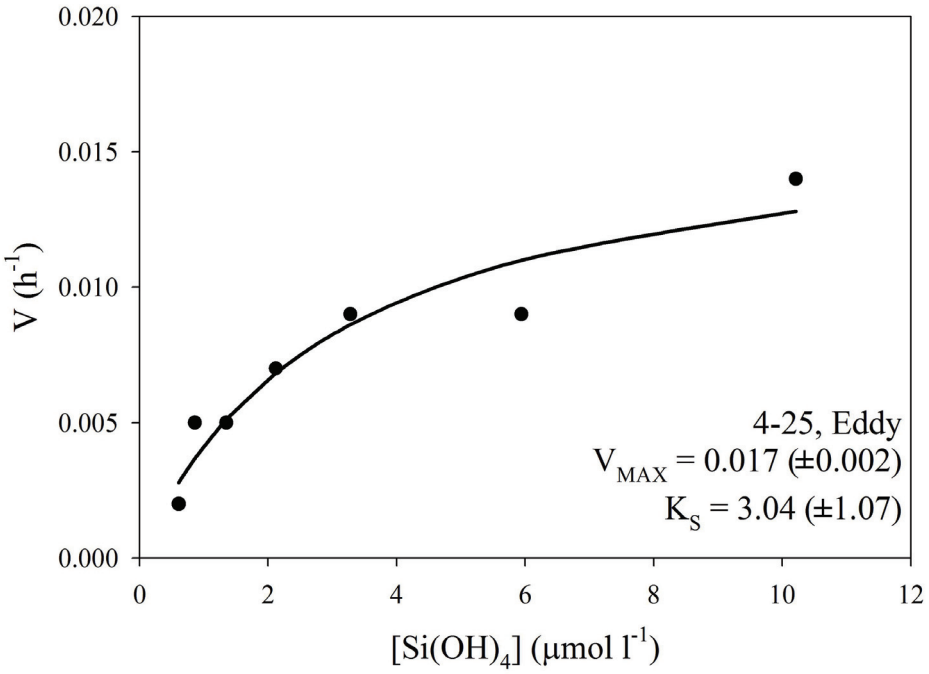

Figure 5.2 - Kinetic uptake experiment taken during second occupation of mode-water eddy in spring 2007. Water was sampled on 4-25-07 from 20 m, from the same niskin bottle as 4-25, 20 m data shown in Figure 5.1. Data was fit to the Michaelis-Menten function $V = V_{MAX} \times [Si(OH)_4] \times \{K_S+[Si(OH)_4]\}^{-1}$ using an iterative non-linear curve-fitting algorithm in S-PLUS © statistical software, while solving for V_{MAX} (i.e. theoretical asymptotic maximum for uptake), and K_S (i.e. $[Si(OH)_4]$ were $V = ½ V_{MAX}$), ± the standard error. Incubation time was ~12 h.

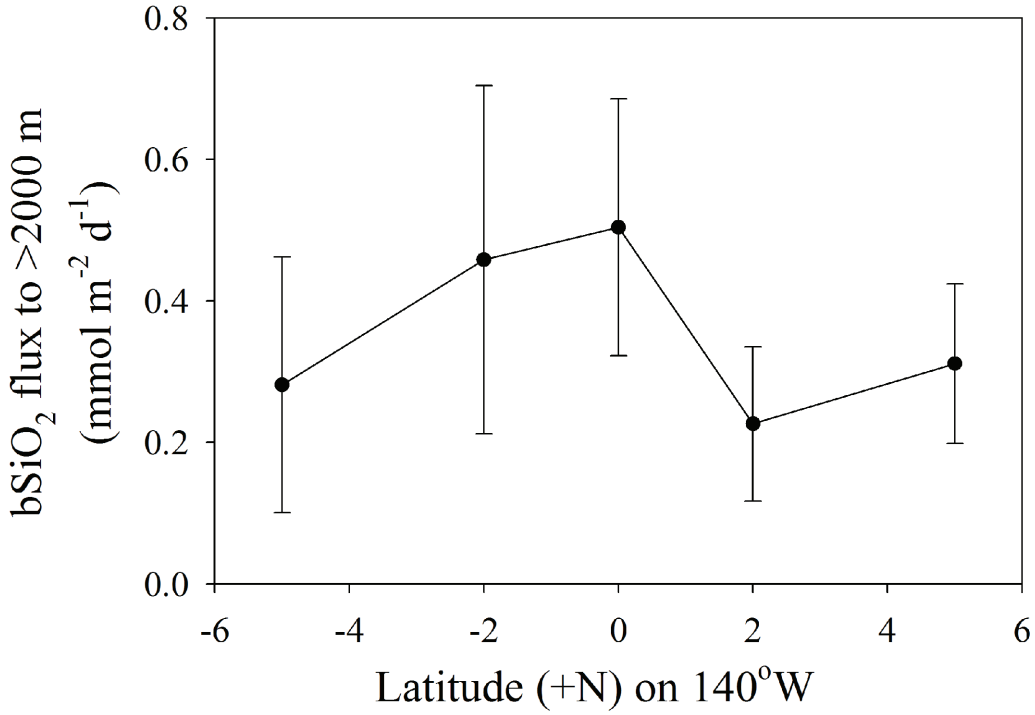

Figure 5.3 - $bSiO_2$ flux to >2000 m (in mmol m^{-2} d^{-1}) from late summer and fall on 140°W. Trap depths range from ~2000 to ~3800 m (different depths at different locations). Error bars are the temporal standard deviation of all the 17-day trap deployments from 10 September through 21 December 1992. Data from Honjo et al. (1995)

Table 5.1 – $\int bSiO_2$ dissolution: $\int bSiO_2$ production profiles in surface waters from which vertically integrated data are available.

Location	Time, Year	n =	Low	Mean	High	Reference
NW Africa coast	Apr.-May, 1974	7	0.45	1.00	5.80	Nelson and Goering, 1977
Peru coast	Mar., 1976	1		0.10		Nelson et al. 1981
California coast, USA	Apr., 1992	2	0.05	0.10	0.16	Brzezinski unpublished data
Antarctic Circumpolar Current	Oct./Nov., 1978	6	0.18	0.34	0.58	Nelson and Gordon 1982
Gulf Stream Warm Core Ring	Apr./June, 1982	9	0.00†	0.47	0.79	Brzezinski and Nelson 1989
Amazon River Plume	Aug., 1989, May, 1990	11	0.22	0.65	2.40	DeMaster et al. 1991 & unpublished data
Ross Sea	Jan.-Feb., 1990	9	0.41	0.61	1.10	Nelson et al. 1991 & unpublished data
Southern Ocean	Pre/Post Stratification 1997, 1998	16		0.64		Brzezinski et al. 2001
Monterrey Bay, USA	Apr., 2000	7	0.02	0.15	0.61	Brzezinski et al. 2003
Bay of Brest, FRANCE	Apr. 2001-Apr. 2002	48	0.00†	0.45	3.80	Beucher et al. 2004a
Southern Ocean (East Indian)	Jan./Feb., 2003	6	0.00†	1.40	3.20	Beucher et al. 2004b

† Values below analytical detection limits

Table 5.2 – Measuring $bSiO_2$ dissolution using a stable-isotope dilution method at different specific dissolution rates (i.e. V_{DISS} d^{-1}) versus detection of ρ_{NET} (mass balance method). In this example the ambient $[Si(OH)_4]$ is 2.5 μmol l^{-1}, and 2.5 μmol l^{-1} $[Si(OH)_4]$ is added by the Si tracer (total = 5 μmol l^{-1}). The tracer addition changes the ^{28}Si% (of total Si isotopes) from 92.18 % (ambient) to 48.5% (ambient + tracer). The initial $[bSiO_2]$ is 100 nmol l^{-1}; with a specific Si uptake rate of 0.693 d^{-1}, table data is after a ~24-hour incubation period. Colorimetric ΔSi (μmol l^{-1}) is the change in measured $[Si(OH)_4]$ (by spectrophotometer) after NaOH digestion dissolves $bSiO_2$. For example, to calculate the $[Si(OH)_4]$ from the final $bSiO_2$ (dissolved in a 5.0 ml NaOH digestion) when V_{DISS} is 0.01 d^{-1} then: 198 nmol l^{-1} ($[bSiO_2]_{initial}$ + {ρ_{NET} x 1 d}) x 0.300 ml (sample volume filtered) x 5.0 ml^{-1} (NaOH digestion volume) = 11.88 μmol l^{-1} $[Si(OH)_4]$; therefore, $\Delta Si = [Si(OH)_4]_{final\text{-}bSiO2} - [Si(OH)_4]_{initial\text{-}bSiO2}$.

	V_{DISS} (d^{-1})					
	0.01	0.05	0.10	0.15	0.25	0.50
Isotope Shift (atom %)	0.0087	0.0437	0.0874	0.1310	0.2184	0.4368
ρ_{NET} (nmol Si l^{-1} d^{-1})	98.0	90.2	81.0	72.1	55.8	21.3
Spectrophotometric ΔSi (μmol l^{-1})	5.88	5.41	4.86	4.33	3.35	1.28

6. Bibliography

Alexandre, A., Meunier, J., Colin, F., Koud, J.M., 2002. Plant impact on the biogeochemical cycle of silicon and related weathering processes. Geochimica et Cosmochimica Acta 61, 677-682.

Allen, W.E., 1934. The primary food supply of the sea. The Quarterly Review of Biology 9, 161-180.

Allen, W.E., 1936. Occurrence of marine plankton diatoms in a ten-year series of daily catches in Southern California. American Journal of Biology 23, 60-63.

Almqvist, N., Del Amo, Y., Smith, B.L., Thomson, N.H., Bartholdson, A., Lal, R., Brzezinski, M., Hansma, P.K., 2001. Micromechanical and structural properties of a pennate diatom investigated by atomic force microscopy. Journal of Microscopy 202, 518-532.

Ammerman, J.W., Hood, R.R, Case, D.A., Cotner J.B., 2003. Phosphorus Deficiency in the Atlantic: An Emerging Paradigm in Oceanography. EOS Transactions, American Geophysical Union 84, 165-170.

Archer, D.E., Takahashi, T., Sutherland, S., Goddard, J., Chipman, D., Rodgers, K., Ogura, H., 1996. Daily, seasonal and interannual variability of sea-surface carbon and nutrient concentration in the equatorial Pacific Ocean. Deep-Sea Research II 43, 779-808.

Archer, D., and 16 others, 1997. A meeting place of great ocean currents: shipboard observations of a convergent front at 2 degrees N in the Pacific. Deep-Sea Research II 44, 1827-1849.

Backhaus, J.O., Hegseth, E.N., Wehde, H., Irigoien, X., Hatten, K., Logemann, K., 2003. Convection and primary production in winter. Marine Ecology Progress Series 251, 1-14.

Balch, W., Drapeau D., Poulton A., Bowler, B., Windecker, L., Booth, E *in preparation*. Calcification and photosynthesis rates in the Equatorial Pacific Ocean between 110°W and 140°W. For submission to Deep-Sea Research II.

Banahan, S., Goering, J.J., 1986. The production of biogenic silica and its accumulation on the southeastern Bering Sea shelf. Continental Shelf Research 5, 199-213.

Bancroft, G.P., 2004. Marine Weather Review – North Atlantic Area: January to April 2004. Mariners We Weather Log 48 (2), http://www.vos.noaa.gov/mwl.shtml.

Barber, R.T., Sanderson, M.P., Lindley, S.T., Chai, F., Newton, J., Trees, C.C., Foley, D.G., Chavez, F.P., 1996. Primary productivity and its regulation in the equatorial Pacific during and following the 1991-1992 El Niño. Deep-Sea Research II 43, 933-969.

Bates, N.R., Hansell, D.A., 2004. Temporal variability of excess nitrate in the subtropical mode water of the North Atlantic Ocean. Marine Chemistry 84, 225–241.

Beebe, W., 1932. Nonsuch: land of water. New York: Brewer, Warren & Putnam, 259 pgs.

Beebe, W., 1934. Half mile down. New York: Harcourt, Brace and Company, 334 pgs.

Behrenfeld, M.J., Falkowski, P.G., 1997. Photosynthetic rates derived from satellite-based chlorophyll concentration. Limnology and Oceanography 42, 1-20.

Benitez-Nelson, C.R., and 22 others, 2007. Mesoscale eddies drive increased silica export in the Subtropical Pacific Ocean. Science 316, 1017-1021.

Beucher, C., Tréguer, P., Corvaisier, R., Hapette, A.M., Elskens, M., 2004a. Production and dissolution of biosilica, and changing microphytoplankton dominance in the Bay of Brest (France). Marine Ecology Progress Series 267, 57–69.

Beucher, C., Tréguer, P., Hapette, A., Corvaisier, R., 2004b. Intense summer Si-recycling in the surface Southern Ocean. Geophysical Research Letters 31, L09305, doi: 10.1029/2003GL018998.

Bidigare, R.R., Ondrusek, M.E., 1996. Spatial and temporal variability of phytoplankton pigment distributions in the central equatorial Pacific Ocean. Deep-Sea Research II 43, 809-833.

Bidle, K.D., Brzezinski, M.A., Long, R.A., Jones, J.L., Azam, F., 2003. Diminished efficiency in the oceanic silica pump caused by bacteria-mediated silica dissolution. Limnology and Oceanography 48, 1855-1868.

Blain, S., Leynaert, A., Tréguer, Chretiennot-Dinet, M., Rodier, M., 1997. Biomass, growth rates and limitation of Equatorial Pacific diatoms. Deep-Sea Research I 44, 1255-1275.

Blain, S., Treguer, P., Rodier, M., 1999. Stocks and fluxes of biogenic silica in the western oligotrophic equatorial Pacific. Journal of Geophysical Research-Oceans 104, 3357-3367.

Boyd, P.W., Trull, T.W., 2007. Understanding the export of biogenic particles in oceanic waters: Is there consensus? Progress in Oceanography 72, 276-312.

Brzezinski, M.A., 1985. The Si:C:N ratio of marine diatoms: interspecific variability and the effect of some environmental variables. Journal of Phycology 21, 347-57.

Brzezinski, M.A., 1992. Cell-cycle effects on the kinetics of silicic acid uptake and resource competition among diatoms. Journal of Plankton Research 14, 1511-1539.

Brzezinski, M.A., Conley, D.J., 1994. Silicon deposition during the cell cycle of Thalassiosira weissflogii (Bacillariophyceae) determined using dual rhodamine 123 and propidium iodide staining. Journal of Phycology 30, 45-55.

Brzezinski, M.A., Kosman, C.A., 1996. Silica production in the Sargasso Sea during spring 1989. Marine Ecology Progress Series 142, 39-45.

Brzezinski, M. A., Nelson, D.M., 1986. A solvent extraction method for the calorimetric the determination of nanomolar concentrations of silicic acid in seawater. Marine Chemistry 18, 59-69.

Brzezinski, M.A., Nelson, D.M., 1989. Seasonal changes in the silicon cycle within a Gulf Stream warm-core ring. Deep-Sea Research 36, 1009-1030.

Brzezinski, M.A., Nelson D.M., 1996. Chronic substrate limitation of silicic acid uptake rates in the western Sargasso Sea. Deep-Sea Research II 43, 437-453.

Brzezinski, M.A., Nelson, D.M., 1995. The annual silica cycle in the Sargasso Sea near Bermuda. Deep-Sea Research I 42, 1215-1237.

Brzezinski, M.A., Nelson, D.M., 1996. Chronic substrate limitation of silicic acid uptake rates in the western Sargasso Sea. Deep-Sea Research II 43, 437-453.

Brzezinski, M.A., Phillips, D.R., 1997. Evaluation of ^{32}Si as a tracer for measuring silica production rates in marine surface waters. Limnology and Oceanography 42: 856-865.

Brzezinski, M.A., Olson, R.J., Chisholm, S.W., 1990. Silicon availability and cell-cycle progression in marine diatoms. Marine Ecology Progress Series 67, 83-96.

Brzezinski, M.A., Phillips, D.R., Chavez, F.P., Friederich, G.E., Dugdale, R.C., 1997. Silica Production in the Monterey, California, Upwelling System. Limnology and Oceanography 42, 1694-1705.

Brzezinski, M.A., Villareal, T.A., Lipschultz, F., 1998. Silica production and the contribution of diatoms to new and primary production in the central North Pacific. Marine Ecology Progress Series 167, 89-104.

Brzezinski, M.A., Nelson, D.M., Franck, V.M., Sigmon, D.E., 2001. Silicon dynamics within an intense open-ocean diatom bloom in the Pacific sector of the Southern Ocean. Deep-Sea Research II 48, 3997–4018.

Brzezinski, M.A., Jones, J.L., Bidle, K.D., Azam, F., 2003. The balance between silica production and silica dissolution in the sea: Insights from Monterey Bay, California, applied to the global data set. Limnology and Oceanography 48, 1846-1854.

Brzezinski, M.A., Dumousseaud, C., Krause, J.W., Measures, C.I., Nelson, D.M., 2008. Iron and silicic acid concentrations together regulate Si uptake in the equatorial Pacific Ocean. Limnology and Oceanography 53, 875-889.

Buesseler, K. O. 1998. The decoupling of production and particulate export in the surface ocean. Global Biogeochemical Cycles 12, 297–310.

Chai, F., Dugdale, R.C., Peng, T.-H., Wilkerson, F.P., Barber, R.T., 2002. One-dimensional ecosystem model of the equatorial Pacific upwelling system. Part I: model development and silicon and nitrogen cycle. Deep-Sea Research II 49, 2713-2745.

Chai, F., Jiang, M.-S., Chao, Y., Dugdale, R.C., Chavez, F., Barber, R.T., 2007. Modeling responses of diatom productivity and biogenic silica export to iron enrichment in the equatorial Pacific Ocean. Global Biogeochemical Cycles 21, doi: 10.1029/2006GB002804

Chavez, F.P, Barber, R.T, 1987. An estimate of new production in the equatorial Pacific. Deep-Sea Research I 34, 1229-1243.

Chavez, F.P., Buck, K.R., Barber, R.T., 1990. Phytoplankton taxa in relation to primary production in the equatorial Pacific. Deep-Sea Research I 37, 1733-1752.

Chavez, F.P., Buck, K.R., Coale, K.H., Martin, J.H., DiTullo, G.R., Welschmeyer, N.A., Jacobson, A.C., Barber, R.T., 1991. Growth rates, grazing, sinking, and iron limitation of equatorial Pacific phytoplankton. Limnology and Oceanography 36, 1816-1833.

Chavez, F.P., Buck, K.R., Service, S.K., Newton, J., Barber, R.T., 1996. Phytoplankton variability in the central and eastern tropical Pacific. Deep-Sea Research II 43, 835-870.

Chelton, D.B., Schlax, M.G., Samelson, R.M., de Szoeke R.A., 2007. Global observations of large oceanic eddies. Geophysical Research Letters 34, doi: 10.1029/2007/GL030812.

Coale, K.H., and 18 others, 1996. A massive phytoplankton bloom induced by an ecosystem-scale iron fertilization experiment in the equatorial Pacific Ocean. Nature 383, 495-501.

Conkright, M., Levitus, S., Boyer, T., 1994. World Ocean Atlas 1994 Volume 1: Nutrients. NOAA Atlas NESDIS 1, U.S. Department of Commerce, Washington, D.C.

Conley, D.J., 2002. Terrestrial ecosystems and the global biogeochemical silica cycle. Global Biogeochemical Cycles 16, doi: 10.1029/2002GB001884.

Conte, M.H., Ralph, N., Ross, E.H., 2001. Seasonal and interannual variability in deep ocean particle fluxes at the Oceanic Flux Program (OFP)/Bermuda Atlantic Time Series (BATS) site in the western Sargasso Sea near Bermuda. Deep-Sea Research II 48, 1471-1505.

Conte, M.H., Dickey, T.D., Weber, J.C., Johnson, R.J., Knap, A.H., 2003. Transient physical forcing of pulsed export of bioreactive material to the deep Sargasso Sea. Deep-Sea Research I 50, 1157-1187.

Corvaisier, R., Tréguer, P., Beucher, C., Elskens, M., 2005. Determination of the rate of production and dissolution of biosilica in marine waters by thermal ionisation mass spectrometry. Analytica Chimica Acta 534, 149–155.

Cotner, J.B., Ammerman, J.W., Peele, E.R., Bentzen, E., 1997. Phosphorus-limited bacterioplankton growth in the Sargasso Sea. Aquatic Microbial Ecology 13, 141-149.

De La Rocha, C.L., 2003. Silicon isotope fractionation by marine sponges and the reconstruction of the silicon isotope composition of ancient deep water. Geology 31, 423-426.

Del Amo, Y., Brzezinski, M.A., 1999. The chemical form of dissolved Si taken up by marine diatoms. Journal of Phycology 35, 1162-1170.

DeMaster, D.J., McKee, B.A., Moore, W.S., Nelson, D.M., Showers, W.J., Smith, W.O., 1991. Geochemical processes occurring at the Amazon River/ocean boundary. Oceanography 4, 15-20.

DeMaster, D.J., Dunbar, R.B., Gordon, L.I., Leventer, A.R., Morrison, J.M., Nelson, D.M., Nittrouer, C.A., Smith, W.O., 1992. Cycling and accumulation of organic

matter and biogenic silica in high-latitude environments: The Ross Sea. Oceanography 5, 146-153.

Deuser, W. G., 1986. Seasonal and interannual variations in deep-water particle fluxes in the Sargasso Sea and their relation to surface hydrography. Deep-Sea Research I 33, 225-246.

Dickey, T.D., and 13 others, 1998. Initial results from the Bermuda Testbed Mooring program. Deep-Sea Research I 45, 771-794.

Dickey, T.D., and 13 others. 2001. Physical and biogeochemical variability from hours to years at the Bermuda Testbed Mooring site: June 1994-March 1998. Deep-Sea Research II 48, 2105-2140.

Dortch, Q., 1982. Effect of growth conditions on accumulation of internal nitrate, ammonium, amino acids, and protein in three marine diatoms. Journal of Experimental Marine Biology and Ecology 61, 243-264.

Dugdale, R.C., Goering, J.J., 1967. Uptake of new and regenerated forms of nitrogen in primary productivity. Limnology and Oceanography 12, 196-206.

Dugdale, R.C., Wilkerson, F.P., 1998. Silicate regulation of new production in the equatorial Pacific upwelling. Nature 391, 270-273.

Dugdale, R.C., Wilkerson, F.P., Chai, F., Feely, R., 2007. Size-fractioned nitrogen uptake measurements in the equatorial Pacific and confirmation of the low Si-high-nitrate-low-chlorophyll condition. Global Biogeochemical Cycles 21, doi: 10.1029/2006GB002722.

Dugdale, R.C., and colleagues *in preparation*. N-uptake and size-fractioned estimates of new production in the equatorial Pacific. For submission to Deep-Sea Research II.

Dunne, J.P, Murray, J.W., Aufdenkampe, A.K., Blain, S., Rodier, M., 1999. Silicon-nitrogen coupling in the equatorial Pacific upwelling zone. Global Biogeochemical Cycles 13, 715-726.

Eppley, R.W., Peterson, B.J., 1979. Particulate organic matter flux and planktonic new production in the deep ocean. Nature 282, 677-680.

Falkowski, P.G., Katz, M.E., Knoll, A.H., Quigg, A., Raven, J.A., Schofield, O., Taylor, F.J.R., 2004. The evolution of modern eukaryotic phytoplankton. Science 305, 354-360.

Feely, R.A., Takahashi, T., Wanninkhof, R., McPhaden, M.J., Cosca, C.E., Sutherland, S.C., Carr, M., 2006. Decadal variability of the air-sea CO_2 fluxes in

the equatorial Pacific Ocean. Journal of Geophysical Research 111, doi: 10.1029/2005JC003129.

Fields, K., Kontrovitz, M., 1980. An invisible art blazes into life under the microscope. Smithsonian 11, 108-113.

Flament, P.J., Kennan, S.C., Knox, R.A., Niiler, P.P., Bernstein, R.L., 1996. The three-dimensional structure of an upper ocean vortex in the tropical Pacific Ocean. Nature 383, 610-613.

Franck, V.M., Brzezinski, M.A., Coale, K.H., Nelson, D.M., 2000. Iron and silicic acid concentrations regulate Si uptake north and south of the Polar Frontal Zone in the Pacific Sector of the Southern Ocean. Deep-Sea Research II 47, 3315-3338.

Franck V.M., Bruland, K.W., Hutchins, D.A., Brzezinski, M.A., 2003. Iron and zinc effects on silicic acid and nitrate uptake kinetics in three high-nutrient, low-chlorophyll (HNLC) regions. Marine Ecology Progress Series 252, 15-33.

Gebeshuber, I.C., Kindt, J.H., Thompson, J.B., Del Amo, Y., Stachelberger, H., Brzezinski, M.A., Stucky, G.D., Morse, D.E., Hansma, P.K., 2003. Atomic force microscopy study of living diatoms in ambient conditions. Journal of Microscopy 212, 292-299.

Ginoux, P., Chin, M., Tegen, I., Prospero, J.M., Holben, B., Dubovik, O., Lin, S-J., 2001. Sources and distribution of dust aerosols simulated with the GOCART model. Journal of Geophysical Research 106, 20255-20273.

Ginoux, P., Prospero, J.M., Torres, O., Chin, M., 2004. Long-term simulation of global dust distribution with the GOCART model: correlation with North Atlantic Oscillation. Environmental Modelling & Software 19, 113-128.

Goericke, R., 1998. Response of phytoplankton community structure and taxon specific growth rates to seasonally varying physical forcing in the Sargasso Sea off Bermuda. Limnology and Oceanography 43, 921-935.

Goering, J.J., Nelson, D.M., Carter, J.A., 1973 Silicic acid uptake by natural populations of marine phytoplankton. Deep-Sea Research I 20, 777-789.

Goldman, J.C., 1988. Spatial and temporal discontinuities of biological processes in pelagic surface waters, p. 273-296. *In* Rothschild, B.J. (Ed.), Toward a theory on biological-physical interactions in the world ocean. Kluwer Academic, Dordrecht.

Goldman J. C., 1993. Potential role of large oceanic diatoms in new primary production. Deep-Sea Research 40, 159-168.

Goldman, J.C., McGillicuddy, D.J., 2003. Effect of large marine diatoms growing at low light on episodic new production. Limnology and Oceanography 48, 1176-1182

Goldman, J.C., Hansell, D.A., Dennett, M.R., 1992. Chemical characterization of three large oceanic diatoms: potential impact on water column chemistry. Marine Ecology Progress Series 88, 257-270.

Gorgues, T., Menkes, C., Aumont, O., Vialard, J., Dandonneau, Y., Bopp, L., 2005. Biogeochemical impact of tropical instability waves in the equatorial Pacific. Geophysical Research Letters 32, L24615, doi:10.1029/2005GL024110.

Gruber, N., Keeling, C.D., Bates, N.R., 2002. Interannual variability in the North Atlantic Ocean carbon sink. Science 298, 2374-2378.

Gust, G., Michaels, A.F., Johnson, R., Deuser, W.G., Bowles, W., 1994. Mooring line motions and sediment trap hydrodynamics: in-situ intercomparison of three common deployment designs. Deep-Sea Research I 41, 831-857.

Hamm, C.E., Merkel, R., Springer, O., Jurkojc, P., Maier, C., Prechtel, K., Smetacek, V., 2003. Architecture and material properties of diatom shells provide effective mechanical protection. Nature 421, 841-843.

Harrison, P.J., Conway, H.L., Holmes, R.W., Davis, C.O., 1977. Marine diatoms grown in chemostats under silicate or ammonium limitation. III. Cellular chemical composition and morphology of *Chaetoceros debilis*, *Skeletonema costatum*, and *Thalassiosira gravida*. Marine Biology 43, 19-31.

Hazeleger, W., Drijfhout, S.S., 1999. Stochastically forced mode water variability. Journal of Physical Oceanography 29, 1772-1786.

Hildebrand, M., Dahlin, K., 2000. Nitrate transporter genes from the diatom Cylindrotheca fusiformis (Bacillariophyceae): mRNA levels controlled by nitrogen source and by the cell cycle. Journal of Phycology 36, 702-713.

Hildebrand, M., York, E., Kelz, J.I., Davis, A.K., Frigeri, L.G., Allison, D.P., Doktycz, M.J., 2006. Nanoscale control of silica morphology and three-dimensional structure during cell wall formation. Journal of Material Research 21, 2689-2698.

Honjo, S., Dymond, J., Collier, R., Manganini, S.J., 1995. Export production of particles to the interior of the equatorial Pacific Ocean during the 1992 EqPac experiment. Deep-Sea Research II 42, 831-870.

Honjo, S., Manganini, S.J., Krishfield, R.A., Francois, R., 2008. Particulate organic carbon fluxes to the ocean interior and factors controlling the biological pump: A

synthesis of global sediment trap programs since 1983. Progress in Oceanography 76, 217-285.

Hulburt E. M., 1990. Description of phytoplankton and nutrient in spring in the western North Atlantic Ocean. Journal of Plankton Research 12, l-28.

Hulburt, E.M., Ryther, J.H., Guillard, R.R.L., 1960. The phytoplankton of the Sargasso Sea off Bermuda. Journal du Conseil International d'Exploration da la Mer 25, 115-128.

Hutchins, D.A., Bruland, K.W., 1998. Iron-limited diatom growth and Si:N uptake ratios in a coastal upwelling regime. Nature 393, 561-564.

Iriarte, J.L., Fryxell, G.A., 1995. Micro-phytoplankton at the equatorial Pacific (140°W) during the JGOFS EqPac Time Series studies: March to April and October 1992. Deep-Sea Research II 42, 559-583.

Jacquet, N., Whitehead, H., Lewis, M., 1996. Coherence between 19th century sperm whale distributions and satellite-derived pigments in the tropical Pacific. Marine Ecology Progress Series 145, 1-10.

Jenkins, W., 1988. Nitrate flux into the euphotic zone near Bermuda. Nature 331, 521-523.

Jenkins, W., Doney, S. C., 2003. The subtropical nutrient spiral. Global Biogeochemical Cycles 17: doi: 10.1029/2003GB002085.

Jenkins, W., Goldman, J., 1985. Seasonal oxygen cycling and primary production in the Sargasso Sea. Journal of Marine Research 43, 465-491.

Joyce, T.M., Deser, C., Spall, M.A., 2000. The relation between decadal variability of Subtropical Mode Water and the North Atlantic Oscillation. Journal of Climate 13, 2550-2569.

Kaczmarkska, I., Fryxell, G.A., 1995. Micro-phytoplankton of the equatorial Pacific: 140°W meridianal transect during the 1992 El Niño. Deep-Sea Research II 42, 535-558.

Kamatani, A., 1982. Dissolution rates of silica from diatoms decomposing at various temperatures. Marine Biology 68, 91-96.

Karl, D.M., Christian, J.R., Dore, J.E., Hebel, D.V., Letelier, R.M., Tupas, L.M., Winn, C.D., 1995. Seasonal and interannual variability in primary production and particle flux at Station ALOHA. Deep-Sea Research II 43, 539-568.

Kennan, S.C., Flament, P.J., 2000. Observations of a Tropical Instability Vortex. Journal of Physical Oceanography 30, 2277-2301.

Kessler, W.S., 2006. The circulation of the eastern tropical Pacific: A review. Progress in Oceanography 69, 181-217.

Kidder DL, Irwin DH. 2001. Secular distribution of biogenic silica through the phanerozoic: comparison of silica-replaced fossils and bedded cherts at the series level. Journal of Geology 109, 509–522.

Knap, A. H., and 19 others, 1997. U.S. Joint Global Ocean Flux Study- Bermuda Atlantic Time- Series Study Methods Manual: Version 4. U.S. JGOFS Planning and Coordination Office: Woods Hole.

Knauer G. A., Karl, D. M., Martin, J. H., Hunter, C.N., 1984. In situ effects of selected preservatives on total carbon, nitrogen, and metals collected in sediment traps. Journal of Marine Research 42, 445-462.

Kobayashi, F., Takahashi, K., 2002. Distribution of diatoms along the equatorial transect in the western and central Pacific during the 1999 La Nina conditions. Deep-Sea Research II 49, 2801-2821.

Krause, J.W., Nelson, D.M., Lomas, M.W., (*in revision*). Biogeochemical responses to late-winter storms in the Sargasso Sea. II. Increased rates of biogenic silica production and export. *In revision*, Deep Sea Research I.

Ku, T., Luo, S., Kusakabe, M., Bishop, J.K.B., 1995. ^{228}Ra-derived nutrient budgets in the upper equatorial Pacific and the role of "new" silicate in limiting productivity. Deep-Sea Research I 42, 479-497.

Landry, M.R., and 12 others, 1997. Iron and grazing constraints on primary production in the central equatorial Pacific: an EqPac synthesis. Limnology and Oceanography 42, 405-418.

Latasa, M., Landry, M.R., Schlüter, L., Bidigare, R.R., 1997. Pigment-specific growth and grazing rates of phytoplankton in the central equatorial Pacific. Limnology and Oceanography 42, 289-298.

Leblanc, K., Hutchins, D.A., 2005. New applications of a biogenic silica deposition fluorophore in the study of oceanic diatoms. Limnology and Oceanography: Methods 3, 462-476.

Legeckis, R., 1977. Long waves in the eastern equatorial Pacific ocean: a view from a geostationary satellite. Science 197, 1179-1181.

Legeckis, R., 1986. A satellite time series of sea surface temperatures in the eastern equatorial Pacific Ocean 1982-1986. Journal of Geophysical Research 91, 12879-12886.

Levitus, S., Burgett, R., Boyer, T., 1994. World Ocean Atlas 1994 Volume 3: Nutrients. NOAA Atlas NESDIS 3, U.S. Department of Commerce, Washington, D.C..

Leynaert, A., Nelson, D.M., Quéguiner, B., Tréguer, P., 1993. The silica cycle in the Antarctic Ocean: Is the Weddell Sea atypical? Marine Ecology Progress Series 96, 1-15.

Leynaert, A., Treguer, P., Lancelot, C., Rodier, M., 2001. Silicon limitation of biogenic silica production in the Equatorial Pacific. Deep-Sea Research I 48, 639-660.

Libes, S.M., 1992. An introduction to marine biogeochemistry. Wiley & Sons: New York. 734 pgs.

Lipschultz, F., 2001. A time-series assessment of the nitrogen cycle at BATS. Deep-Sea Research Part II 48, 1897-1924.

Lipschultz, F., Bates, N.R., Carlson, C.A., Hansell, D.A., 2002. New production in the Sargasso Sea: History and current status. Global Biogeochemical Cycles 16, doi: 10.1029/2000GB001319.

Lomas, M.W., Bates, N.R., 2004. Potential controls on interannual partitioning of organic carbon during the winter/spring phytoplankton bloom at the Bermuda Atlantic time-series study (BATS) site. Deep-Sea Research I 51, 1619-1636.

Lomas, M.W., Glibert, P.M., 1999. Temperature regulation of nitrate uptake: A novel hypothesis about nitrate uptake and reduction in cool-water diatoms. Limnology and Oceanography 44, 556-572.

Lomas, M.W., Lipschultz, F., 2006. Forming the primary nitrite maximum: Nitrifiers or phytoplankton? Limnology and Oceanography 51, 2453-2467.

Lomas, M.W., Lipschultz, F. , Nelson, D. M., Bates, N.R. (*in revision*)-a. Biogeochemical responses to late-winter storms in the Sargasso Sea. I. Pulses of primary and new production. *In revision*, Deep-Sea Research I.

Lomas, M.W., Roberts, N., Lipschultz, F., Krause, J.W., Nelson, D.M , Bates, N.R. (*in revision*)-b. Biogeochemical responses to late-winter storms in the Sargasso Sea. III. Rapid successions of major phytoplankton groups. *In revision*, Deep-Sea Research I.

Lopez, P.J., Gautier, C., Livage, J., Coradin, T., 2005. Mimicking biogenic silica nanostructures formation. Current Nanoscience 1, 73-83.

Maiti, K., Benitez-Nelson, C.R., Lomas, M.W., Krause. J.W. (*in revision*). Biogeochemical responses to late-winter storms in the Sargasso Sea. IV. Comparison of Export Production by ^{234}Th and Sediment Traps. *In revision*, Deep-Sea Research I.

Maldonado, M., Carmona, M.C., Uriz, M.J., Cruzado, A., 1999. Decline in Mesozoic reef-building sponges explained by silicon limitation. Nature 401, 785-788.

Malone, T.C., Pike, S.E., Conley, D.J., 1993. Transient variations in phytoplankton productivity at the JGOFS Bermuda time series station. Deep-Sea Research I 40, 903-924.

Margalef, R, 1997. Excellence in ecology, Book 10: Our biosphere. Oldendorf/Luhe: International Ecology Institute.

Martin, J.H., Gordon, R.M., Fitzwater, S.E., 1991. The case for iron. Limnology and Oceanography 36, 1793-1802.

Martin-Jézéquel, V., Hildebrand, M., Brzezinski, M.A., 2000. Silicon metabolism in diatoms: implications for growth. Journal of Phycology 36, 821-840.

McCarthy, J.J., Garside, C., Nevins, J.L., Barber, R.T., 1996. New production along 140°W in the equatorial Pacific during and following the 1992 El Niño event. Deep-Sea Research II 43, 1065-1093.

McGillicuddy, D.J., Robinson, A.R., Siegel, D.A., Jannasch, H.W., Johnson, R., Dickey, T.D., McNeil, J., Michaels, A.F., Knap, A.H., 1998. Influence of mesoscale eddies on new production in the Sargasso Sea. Nature 394, 263-266.

McGillicuddy, D.J., and 17 others, 2007. Eddy/wind interactions stimulate extraordinary mid-ocean plankton blooms. Science 316, 1021-1026.

McNeil, J.D., Jannasch, H.W., Dickey, T., McGillicuddy, D.J., Brzezinski, M., Sakamoto, C.M., 1999. New chemical, bio-optical and physical observations of upper ocean response to the passage of a mesoscale eddy off Bermuda. Journal of Geophysical Research 104. 15537–15548.

Menkes, C.E., and 14 others, 2002. A whirling ecosystem in the equatorial Atlantic. Geophysical Research Letters 29, doi: 10.1029/2001GL014576.

Menzel, D.W., Ryther, J.H., 1960. The annual cycle of primary production in the Sargasso Sea off Bermuda. Deep-Sea Research 6, 351-366.

Michaels, A.F., Knap, A.H., 1996. Overview of the U.S. JGOFS Bermuda Atlantic Time-series Study and the Hydrostation S program. Deep-Sea Research II 43, 129-156.

Michaels, A.F., Silver, M.W., 1988. Primary production, sinking fluxes and the microbial food web. Deep-Sea Research I 35, 473-490.

Michaels A. F., Silver, M. W., Gowing, M., Knauer, G.A., 1990. Cryptic zooplankton "swimmers" in upper ocean sediment traps. Deep-Sea Research I 37, 1285-1296.

Michaels, A., Knap, A., Dow, R., Gundersen, K., Johnson, R., Sorensen, J., Close, A., Knauer, G., Lohrenz, S., Asper, V., Tuel, M., Bidigare, R., 1994. Seasonal patterns of ocean biogeochemistry at the U.S. JGOFS Bermuda Atlantic Time-series study site. Deep-Sea Research 41, 1013-1038.

Minas, H.J., M. Minas, M., Packard, T.T., 1986. Productivity in upwelling areas deduced from hydrographic and chemical fields. Limnology and Oceanography 31, 1182-1206.

Mongin, M., Nelson, D.M., Pondaven, P., Brzezinski, M.A., Tréguer, P., 2003. Simulation of upper-ocean biogeochemistry with a flexible-composition phytoplankton model: C, N and Si cycling in the western Sargasso Sea. Deep-Sea Research I 50, 1445-1480.

Moriceau, B., Garvey, M., Ragueneau, O., Passow, U., 2007a. Evidence for reduced biogenic silica dissolution rates in diatom aggregates. Marine Ecology Progress Series 333, 129-142.

Moriceau, B., Gallinari, M., Soetaert, K., Ragueneau, O., 2007b. Importance of particle formation to reconstructed water column biogenic silica fluxes. Global Biogeochemical Cycles 21, GB3012, doi: 10.1029/2006GB002814.

Mouriño-Carballido, B., McGillicuddy, D.J., 2006. Mesoscale variability in the metabolic balance of the Sargasso Sea. Limnology and Oceanography 51, 2675-2689.

Murray, J.W., Barber, R.T., Roman, M.R., Bacon, M.P., Feely, R.A., 1994. Physical and biological controls on carbon cycling in the equatorial Pacific. Science 266, 58-65.

Murray, J.W., Johnson, E., Garside, C., 1995. A U.S. JGOFS Process Study in the equatorial Pacific (EqPac): Introduction. Deep-Sea Research II 42, 275-293.

Nelson, D.M., Brzezinski, M.A., 1990. Kinetics of silicic acid uptake by natural diatom assemblages in two Gulf Stream warm-core rings. Marine Ecology Progress Series 62, 283-292.

Nelson, D.M., Brzezinski, M.A., 1997. Diatom growth and productivity in an oligotrophic midocean gyre: a 3-yr record from the Sargasso Sea near Bermuda. Limnology and Oceanography 43, 473-486.

Nelson, D.M., Dortch, Q., 1996. Silicic acid depletion and silicon limitation in the plume of the Mississippi River: evidence from kinetic studies in spring and summer. Marine Ecology Progress Series 136, 163-178.

Nelson, D.M., Goering, J.J., 1977. Near-surface silica dissolution in the upwelling region off northwest Africa. Deep-Sea Research 24, 65-73.

Nelson, D.M., Goering, J.J., 1978. Assimilation of silicic acid by phytoplankton in the Baja California and northwest Africa upwelling systems. Limnology and Oceanography 23, 508-517.

Nelson, D.M., Gordon, L.I., 1982. Production and pelagic dissolution of biogenic silica in the Southern Ocean. Geochimica Cosmochimica Acta 46, 491-501.

Nelson, D.M., Tréguer, P., 1992. Role of silicon as a limiting nutrient to Antarctic diatoms: evidence from kinetic studies in the Ross Sea ice-edge zone. Marine Ecology Progress Series 80, 255-264.

Nelson, D.M., Goering, J.J., Boisseau, D.W., 1981. Consumption and regeneration of silicic acid in three coastal upwelling systems, p. 242-256. *In* F.A. Richards (ed.), Coastal Upwelling. American Geophysical Union.

Nelson, D.M., Ducklow, H.L., Hitchcock, G.L., Brzezinski, M.A., Cowles, T.J., Fryxell, G.A., Garside, C., Gould, R.W., Joyce, T.M., McCarthy, J.J., Yentsch, C.S., 1985. Distribution and composition of biogenic particulate matter in a Gulf Stream warm-core ring. Deep-Sea Research I 32, 1347-1369.

Nelson, D.M., Ahern, J.A., Herlihy, L.J., 1991. Cycling of biogenic silica within the upper water column of the Ross Sea. Marine Chemistry 35, 461-476.

Nelson, D.M., Tréguer, P., Brzezinski, M.A., Leynaert, A., Quéguiner, B., 1995. Production and dissolution of biogenic silica in the ocean: Revised global estimates, comparison with regional data and relationship to biogenic sedimentation. Global Biogeochemical Cycles 9, 359–372.

Nelson, D.M., DeMaster, D.J., Dunbar, R.B., Smith, W.O., 1996. Cycling of organic carbon and biogenic silica in the Southern Ocean: Estimates of water-column and sedimentary fluxes over the Ross Sea continental shelf. Journal of Geophysical Research 101, 18519-18532.

Nelson, D.M., Brzezinski, M.A., Sigmon, D.E., Franck, V.M., 2001. A seasonal progression of Si limitation in the Pacific sector of the Southern Ocean. Deep-Sea Research Part II 48, 3973–3995.

Nelson, D.M., and 15 others, 2002. Vertical budgets for organic carbon and biogenic silica in the Pacific sector of the Southern Ocean, 1996-1998. Deep-Sea Research II 49, 1645-1673.

Ottersen, G., Planque, B., Belgrano, A., Post, E., Reid, P.C., Stenseth, N.C., 2001. Ecological effects of the North Atlantic Oscillation. Oecologia 128, 1-14.

Paasche, E, 1973. Silicon and the ecology of marine planktonic diatoms. I. Thalassiosira pseudonana (Cyclotella nana) grown in a chemostat with silicate as the limiting nutrient. Marine Biology 19, 117-126.

Palter, J.B., Lozier, M.S., Barber, R.T., 2005. The effect of advection on the nutrient reservoir in the North Atlantic subtropical gyre. Nature 437, 687-692.

Parker, M.S., Armbrust, E.V., 2005. Synergistic effects of light, temperature, and nitrogen source on transcription of genes for carbon and nitrogen metabolism in the centric diatom Thalassiosira pseduonana (Bacillariophyceae). Journal of Phycology 41, 1142-1153.

Patrick, R., 1940. A Suggested Starting-Point for the Nomenclature of Diatoms. Bulletin of the Torrey Botanical Club 67, 614-615.

Pennington, J.T., Mahoney, K.L., Kuwahara, V.S., Kolber, D.D., Calienes, R., Chavez, F.P., 2006. Primary production in the eastern tropical Pacific: A review. Progress in Oceanography 69, 285-317.

Perry, M.J., Bolger, J.P., English, D.C., 1989. Primary production in Washington coastal waters, p. 117-138. *In* M.R. Landry and B.M. Hickey (Eds) Coastal Oceanography of Washington and Oregon. Elsevier: Amsterdam.

Philander, S.G.H., 1978. Instabilities of zonal equatorial currents, 2. Journal of Geophysical Research 83, 3679-3682.

Pondaven, P., Ragueneau, O., Tréguer, P., Hauvespre, A., Dezileau, L., Reyss, J.L., 2000. Resolving the 'opal paradox' in the Southern Ocean. Nature 405, 168-172.

Quéguiner, B., Tréguer, P., Nelson, D.M., 1991. The production of biogenic silica in the Weddell and Scotia Seas. Marine Chemistry 35, 449-460.

Quinn, W.H., Neal, V.T., Antunez de Mayolo, S.E., 1987. El Niño occurrences over the past four and a half centuries. Journal of Geophysical Research 92, 14449-14461.

Quinn, W.H., Zopf, D.O., Short, K.S., Yang, R.T.W.K., 1978. Historical trends and statistics of the Southern Oscillation, El Niño, and Indonesian droughts. Fishery Bulletin 76, 663-678.

Racki G, Cordey F., 2000. Radiolarian palaeoecology and radiolarites: is the present the key to the past? Earth-Science Reviews 52, 83–120.

Raven, J.A., 1983. The transport and function of silicon in plants. Biological Review 58, 179-207.

Raven, J.A., Waite, A.M., 2004. The evolution of silicification in diatoms: inescapable sinking and sinking as escape? New Phytologist 162, 45-61.

Redfield, A.C.,Ketchum, B.H., Richards, F.A., 1963. The influence of organisms on the composition of sea water, p. 26-77. *In* M.N. Hill (ed.) The Sea v. 2. Wiley: New York.

Riley, G.A., 1957. Phytoplankton of the North Central Sargasso Sea, 1950-1952. Limnology and Oceanography 2, 252-269.

Round, F.E., Crawford, R.M., Mann, D.G., 1990. The diatoms: biology and morphology of the genera. Cambridge University Press: Cambridge. 747 pgs.

Sambrotto, R.N., Niebauer, H.J., Goering, J.J., Iverson, R.L., 1986. Relationships among vertical mixing, nitrate uptake, and phytoplankton growth during the spring bloom in the southeast Bering Sea middle shelf. Continental Shelf Research 5, 161-198.

Sarmiento, J.L., Simeon, J., Gnanadesikan, A., Gruber, N., Key, R.M., Schlitzer, R., 2007. Deep ocean biogeochemistry of silicic acid and nitrate. Global Biogeochemical Cycles 21, doi:10.1029/2006GB002720.

Schiermeier, Q., 2007. Observing the Ocean from within. Nature 450, 780-781.

Schlitzer, R. 2006. Ocean Data View, http://odv.awi-bremerhaven.de.

Schubert JK, Kidder DL, Irwin DH. 1997. Silica-replaced fossils through the Phanerozoic. Geology 25, 1031–1034.

Schütt, F. 1896. Bacillariales (Diatomeae). Engler, A. & Prantl, K.(Eds.). In Die Naturlichen Pflanzenfamilien. Verlag von Wilhelm Engelmann, Leipzig, pp. 31–153

Sedwick, P.N., Church, T. M., Bowie, A. R., Marsay, C. M., Ussher, S.J., Achilles, K.M., Lethaby. P.J., Johnson, R.J., Sarin, M.M., D. J. McGillicuddy, D.J., 2005.

Iron in the Sargasso Sea (Bermuda Atlantic Time-series Study region) during summer: Eolian imprint, spatiotemporal variability, and ecological implications. Global Biogeochemical Cycles 19, doi: 10.1029/2004GB002445.

Shackleton, E., 1962. Men against the sea, p. 295. *In* Seas, Deacon, G.E.R. (Ed.). Maps, and Men. Crescent, London.

Shimizu, K., Del Amo, Y., Brzezinski, M.A., Stucky, G.D., Morse, D.E., 2001. A novel fluorescent silica tracer for biological silicification studies. Chemistry and Biology 8, 1051-1060.

Shipe, R.F., Brzezinski, M.A., 1999. A study of Si deposition synchrony in *Rhizosolenia* (Bacillariophyceae) mats using a novel ^{32}Si autoradiographic method. Journal of Phycology 35, 995-1004.

Shipe, R.F., Brzezinski, M.A., Pilskaln, C. Villareal, T.A., 1999. Rhizosolenia mats: An overlooked source of silica production in the open sea. Limnology and Oceanography 44, 1282-1292.

Siegel, D.A., Itturiaga, R., Bidigare, R.R., Smith, R.C., Pak, H., Dickey, T.D., Marra, J., Baker, K.S., 1990. Meridional variations of the spring-time phytoplankton community in the Sargasso Sea. Journal of Marine Research 48, 379 - 412.

Siegel, D.A., and 13 others, 2001. Bio-optical modeling of primary production on regional scales: the Bermuda Bio-Optics project. Deep-Sea Research Part II 48, 1865-1896.

Siever, R., 1991. Silica in the oceans: biological–geochemical interplay, p. 287-295. *In*: Schneider S.H., Boston P.J. (Eds.) Scientists on gaia. MIT Press: Cambridge.

Sigmon, D.E., Nelson, D.M., Brzezinski, M.A., 2002. The Si cycle in the Pacific sector of the Southern Ocean: Seasonal diatom production in the surface layer and export to the deep sea. Deep-Sea Research II 49, 1747-1763.

Simpson, T.L., Volcani, B.E. (Eds.), 1981. Silicon and siliceous structures in biological systems. New York: Springer-Verlag.

Small, L.F., Fowler, S.W., Ünlü, M.Y., 1979. Sinking rates of natural copepod fecal pellets. Marine Biology 51, 233-241.

Sosik, H.M., Olson, R.J., 2007. Automated taxonomic classification of phytoplankton sampled with imagine-in-flow cytometry. Limnology and Oceanography: Methods 5, 204-216.

Spitzer, W., Jenkins, W., 1989. Rates of vertical mixing, gas exchange and new production: estimates from seasonal gas cycles in the upper ocean near Bermuda. Journal of Marine Research 47, 169-196.

Stanley, R.H.R., Buesseler, K.O., Manganini, S.J., Steinberg, D.K., Valdes, J.R., 2004. A comparison of major and minor elemental fluxes collected in neutrally buoyant and surface-tethered sediment traps. Deep-Sea Research I 51, 1387–1395

Steinberg, D. K., Carlson, C. A., Bates, N. R., Johnson, R. J., Michaels, A. F., Knap, A. H. 2001. Overview of the US JGOFS Bermuda Atlantic Time-series Study (BATS): a decade-scale look at ocean biology and biogeochemistry. Deep-Sea Research Part II 48, 1405-1447.

Strickland J. D. H., Parsons, T.R., 1972. A practical handbook of seawater analysis. 2nd Ed., Vol. 167, Bulletin of the Fisheries Research Board of Canada, Ottawa, 310 pp.

Strutton, P.G., Ryan, J.P., Chavez, F.P., 2001. Enhanced chlorophyll associated with tropical instability waves in the equatorial Pacific. Geophysical Research Letters 28, 2005-2008.

Stumm, W., Morgan, J.J., 1996. Aquatic chemistry: chemical equilibria and rates in natural waters. Wiley and Sons, New York.

Sunda, W.G., Huntsman, S.A., 1995. Iron uptake and growth limitation in oceanic and coastal phytoplankton. Marine Chemistry 50, 189-196.

Sverdrup, H. 1953. On conditions for the vernal blooming of phytoplankton. Journal du Conseil International d'Exploration da la Mer 18: 287-295.

Sweeney, E.N., McGillicuddy, D.J., Buesseler, K.O., 2003. Biogeochemical impacts due to mesoscale eddy activity in the Sargasso Sea as measured at the Bermuda Atlantic Time-series Study (BATS). Deep-Sea Research Part II 50, 3017-3039.

Takahashi, T., and 11 others, 2002. Global sea-air CO_2 flux based on climatological surface ocean pCO_2, and seasonal biological and temperature effects. Deep-Sea Research II 49, 1601-1622.

Takeda, S., 1998. Influence of iron availability on nutrient consumption ratio of diatoms in oceanic waters. Nature 393, 774-777.

Talley, L.D., 1996. North Atlantic circulation and variability, reviewed for the CNLS conference. Physica D 98, 625-646.

Tréguer, P., Nelson, D.M., Gueneley, S., Zeyons, C., Morvan, J., Buma, A., 1990. The distribution of biogenic and lithogenic silica and the composition of

particulate organic matter in the Scotia Sea and the Drake Passage during autumn 1987. Deep-Sea Research I 37, 833-851.

Tréguer, P., Lindner, L., van Bennekom, A.J., Leynaert, A., Panouse, M., Jacques, G., 1991. Production of biogenic silica in the Weddell-Scotia Seas measured with ^{32}Si. Limnology and Oceanography 36, 1217-1227.

Tréguer, P., Nelson, D.M., van Bennekom, A.J., DeMaster, D.J., Leynaert, A., Quéguiner, B., 1995. The silica balance in the world ocean: A re-estimate. Science 268, 375-379.

Twining, B.S., Baines, S.B., Fisher, N.S., 2004. Element stoichiometries of individual plankton cells collected during the Southern Ocean Iron Experiment (SOFeX). Limnology and Oceanography 49, 2115-2128.

Twining, B.S., and colleagues *in preparation*. Elemental stoichiometries of individual plankton cells in the equatorial Pacific. For submission to Deep-Sea Research II.

Wilkerson, F.P., Dugdale, R.C., 1996. Silicate versus nitrate limitation in the equatorial Pacific estimated from satellite-derived sea-surface temperatures. Advances in Space Research 18, 81-89.

Wright, S.M., Jeffrey, S.W., 1987. Fucoxanthin pigment markers of marine phytoplankton analyzed by HPLC and HPTLC. Marine Ecology Progress Series 38, 259-26.

Wyrtki, K., 1981. An estimate of equatorial upwelling in the Pacific. Journal of Physical Oceanography 11, 1205-1214.

Yoder, J.A., Ackleson, S.G., Barber, R.T., Flament, P., Balch, W.M., 1994. A line in the sea. Nature 371, 689-692.

Yu, Z., McCreary, J.P., Proehl, J.A., 1995. Meridional asymmetry and energetics of tropical instability waves. Journal of Physical Oceanography 25, 2997-3007.

7. Appendix

7. Appendix

Data from the Chapters 2 and 4 are available as ASCII (tab delimited) files in the accompanying compact disc (for bound version of dissertation). For electronic copies of this data please access the Scholars Archive at Oregon State University; links for this data will be available with an electronic version of this dissertation. Chapter 3 data are summed up thoroughly by Table 3.1.